Design and synthesis of chiral ligands for use in stereoselective atropisomeric biaryl coupling reactions

Mary J. Gresser
University of Wollongong

DESIGN AND SYNTHESIS OF CHIRAL LIGANDS

FOR USE IN

STEREOSELECTIVE ATROPISOMERIC

BIARYL COUPLING REACTIONS

A thesis submitted in fulfilment of the
requirements for the award of the degree

DOCTOR OF PHILOSOPHY

from

THE UNIVERSITY OF WOLLONGONG

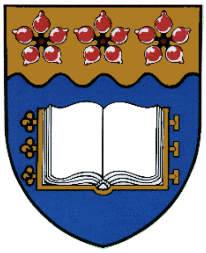

by

Mary J. Gresser, B. Sc. (Adv.) (Hons)

DEPARTMENT OF CHEMISTRY

MARCH 2007

Certification

I, Mary Jacinta Gresser, declare that this thesis, submitted in fulfilment of the requirements for the award of Doctor of Philosophy, in the Department of Chemistry, University of Wollongong, is wholly my own work unless otherwise referenced or acknowledged. This document has not been submitted for qualifications at any other academic institution.

Mary Jacinta Gresser

March 2007

Publications

Gerhard Bringmann, Anne J. Price Mortimer, Paul A. Keller, Mary J. Gresser, James Garner, Matthias Breuning; Atroposelective Synthesis of Axially Chiral Biaryl Compounds, *Angew. Chem. Int. Ed.* **2005**, *44*, 5384-5427.

Acknowledgments

Thank you to everyone who has helped me in any way throughout my PhD.

To **PK**, without your guidance, encouragement and understanding, I would not have finished.

To **Steve P**, for the supervision while PK was away.

To **G. Bringmann** and **M. Breuning** in Würzburg, for help with the graphics used in this thesis.

To **Andrew** and **Mark**, for making me laugh and cry (!) and every emotion in between! Our times here together will stay with me forever.

To **Chris**, thank you so much for being there for me, especially this last year.

To **Jody**, **Sue**, **Dan**, **Bill**, **Neal** and all other members of the **KRG**, past and present.

To my "Team Ligand" counterpart **Walesy**, where would our project be without us???

To **Roger**, **Larry**, **Wilford**, **Karin** and **John**, for having the solutions to all my MS and NMR problems!

To **Glennys** and **Di**, for providing me with the opportunity to do what I love – teaching.

To **Georgia**, for being such a good friend to me the last six years.

Finally, to my family – **Dad**, **Mum**, **Laurence**, **Anne**, **Matt**, **Peter**, **John**, **Jane**, **Bernard**, **Lucy**, **Elizabeth**, and the boys, **Joseph**, **Michael** and **Xavier** – who are always there for me.

Abstract

A new chiral ligand design program was initiated for the stereoselective synthesis of sterically hindered systems, such as atropisomeric biaryls. The concept of helical-sense discrimination was investigated, for use in the Pd-based Suzuki coupling reaction. A new set of design principles was established for chiral ligands for use in these reactions; 1) the ligand must contain a defined helical twist enclosed at each end by donor atoms, 2) the ligand must be bidentate, to best transfer the helical aspect of the ligand to the Pd reaction site, 3) the substituents of the donor atoms should be tied back in ring systems to prevent steric hindrance of the already sterically demanding reaction site and 4) the helical twist should be in close proximity to the Pd reaction site. The first two target scaffolds which would incorporate the above principles were chiral 2,2'-bispyrrolidine and 2,2'-bisindoline.

A new synthetic strategy was devised, which provided both enantiomers of 2,2'-bispyrrolidine and was modified to access 2,2'-bisindoline. The key steps of the synthesis were the metathesis dimerisation and subsequent Sharpless asymmetric dihydroxylation (AD) from achiral starting materials.

(*R*,*R*)-*N*,*N*'-Di-*tert*-butoxycarbonyl-2,2'-bispyrrolidine **92a** was synthesised in 13% yield, over 10 steps, from commercially available 4-penten-1-ol. The metathesis reaction gave the desired benzyl protected alkene as a mixture of geometric isomers (4:1), which were dihydroxylated using AD mix α and standard Sharpless conditions to give the corresponding diol with an *ee* of 80%.

The procedure was repeated using the PMB protected derivatives to give (*R*,*R*)-**92a** in overall 9% yield, with the AD reaction using AD mix α giving the diol in 92% *ee*. The procedure was repeated using AD mix β, which gave the enantiomeric 2,2'-bispyrrolidine (*S*,*S*)-**92b** in 24% overall yield and 88% *ee*.

The synthetic strategy was applied towards the synthesis of chiral 2,2'-bisindoline, for which there is no literature precedent. Benzyl protected 2-allylphenol was dimerised via the metathesis reaction using Grubbs 1st generation catalyst, to give the dimeric aromatic allylic alkene in 81% yield (*E*:*Z* 5.2:1). The geometric ratio could be improved to 9:1 via recrystallisation from DCM/hexanes. Grubbs 2nd generation catalyst was found to increase the geometric ratio, however the alkene could not be separated from the secondary metathesis products. The alkene was dihydroxylated using AD mix α in 15% yield and 64% *ee*. The yield was increased to 60% by using modified Sharpless conditions, however the enantiopurity decreased to 36% *ee*.

The poor outcome of the AD reaction lead to extensive investigations into the Sharpless AD reaction via the modification of the *ortho* substituent of dimeric aromatic allylic alkenes. A variety of dimeric, heterodimeric and monomeric alkenes were synthesised, including seven phenolic based and two nitrogen based dimeric alkenes, via the metathesis reaction using both Grubbs 1st and 2nd generation catalysts. The alkenes were subsequently dihydroxylated using AD mix α and AD mix β. The diols were formed in poor yield (0% to 58%) and poor enantioselectivity (1% to 58%). The AD reaction of the *ortho*-tolyl derivative increased the yield (45-65%) and the *ee* (62-70%) while the unsubstituted derivative gave the corresponding diol in 84-88% yield with excellent stereocontrol (93-95% *ee*).

It was therefore concluded that the presence of *ortho*-substituents in the aromatic rings of dimeric allylic aromatic alkenes prevented access of the substrate to the ligand bound OsO_4, thereby minimising chemical yield and enantioselection.

Abbreviations

Ac	acetyl
AD	asymmetric dihydroxylation
BINAP	2,2'-bis(diphenylphosphino)-1,1'-binaphthyl
Boc	*tert*-butoxycarbonyl
Bn	benzyl
CI	chemical ionisation
CM	cross-metathesis
COSY	correlation spectroscopy
d	day
DCM	dichloromethane
DHQ	dihydroquinine
DHQD	dihydroquinidine
DMF	*N*,*N*'-dimethylformamide
DMSO	dimethylsulfoxide
ee	enantiomeric excess
EI	electron ionisation
ES	electrospray
h	hour
HMBC	heteronuclear multiple bond correlation experiment
HPLC	high performance liquid chromatography
HR	high resolution
HSQC	heteronuclear single quantum correlation
IR	infrared
min	minute
MHz	megahertz
m/z	mass/charge ratio
MS	mass spectrometry
Ms	methanesulfonyl
NMR	nuclear magnetic resonance
PMB	*p*-methoxybenzyl
ppm	parts per million
RCM	ring-closing metathesis
ROMP	ring-opening polymerization
RT	room temperature
SM	self-metathesis
SMPs	side metathesis products
Tf	trifluoromethanesulfonyl (triflate)
THF	tetrahydrofuran
TLC	thin layer chromatography
TBS	*tert*-butyldimethylsilyl
TMS	trimethylsilane
UV	ultraviolet

Table of Contents

CHAPTER 1
Introduction

1.1 Atropisomerism

The development of stereoselective reactions has long been recognised as a key requirement in synthesis and subsequent applications.[1] The ability to isolate only one stereoisomer has typically been investigated with respect to chirality around a stereogenic carbon, or to conformation around a double bond.[2-4] Axial asymmetry is another type of chirality that deserves more attention due to the prevalence of the biaryl axis,[1,5-7] and the difficulty of its enantiomeric discrimination.

Atropisomerism results from restricted rotation around any single bond.[8] When the adjacent substituents are different and the rotation is sufficiently restricted, stereoisomers may be isolated. Although many examples of atropisomeric bonds are known,[9] the focus of this review is that for which the term atropisomerism was originally used to describe[10] – biaryls.

Biaryls are the result of two aryl systems joined by an sp^2-sp^2 carbon bond. When the positions *ortho* to this bond are occupied by three or four bulky substituents, free rotation around the axis may be restricted and the biaryl system is locked into a specific conformation. When these *ortho* substituents A, B, A', B' (**Figure 1.1**) are different, two stereoisomers are possible. In this way, **1** and **2** are enantiomers; they are non-superimposable mirror images. Stereoisomerism arising from axial chirality, as in biaryl compounds, is known as atropisomerism, where **1** and **2** are known as atropisomers (**Figure 1.1**).

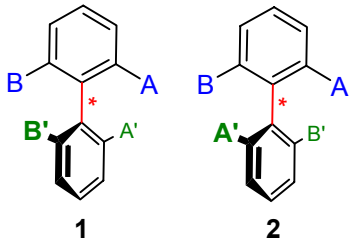

Figure 1.1: Enantiomeric atropisomers arising from; **a)** restricted rotation around the axial C-C bond, and **b)** the presence of different *ortho* substituents, where A ≠ B, A' ≠ B'.

The term atropisomer is derived from the Greek terms 'a' meaning 'not' and 'tropos' meaning 'turn'.[11] The extent to which axial rotation is hindered can be quantified as the barrier to rotation[8] and can be related to; 1) the size and number of substituents and 2) the presence of any bridges connecting the two halves of the molecule. The atropisomerisation barrier in nonbridged biaryl compounds is increased by the steric repulsion of the *ortho* substituents, corresponding to the van der Waals radii of the substituents (I > Br > Me > Cl > NO_2 > CO_2H > OMe > F > H).[12] Tetra-*ortho* substituted biaryls, such as **3** and **4** (**Figure 1.2**), are stable and the two atropisomers can be separated. Tri-*ortho*-substituted biaryls can also form stable atropisomers[13,14] and there are selected examples of di-*ortho*-substituted biaryls with sufficiently high barrier to rotations to permit the formation of stable atropisomers.[15-18]

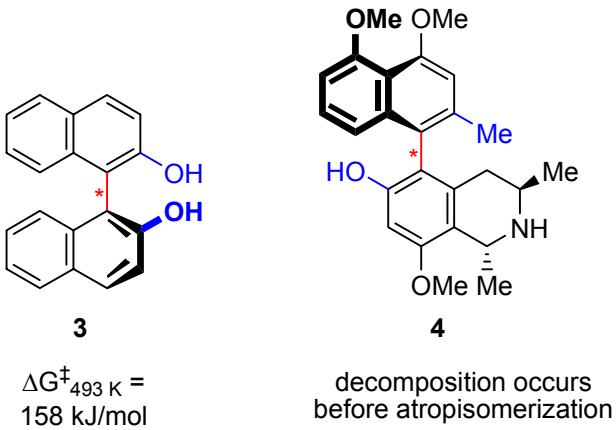

Figure 1.2: Configurational stability of two examples of tetra-*ortho*-substituted biaryl compounds.[19,20]

The stereochemistry of biaryl atropisomers is assigned by viewing a Newmann projection of the molecule, along the biaryl axis from either end. Priority is assigned to the substituents on each of the aryl units separately, and stereochemistry is determined

from the direction of the higher priority substituent on the distal ring, **A'**, from that of the proximal ring, **A**. This direction in **Figure 1.3 (a)** is anti-clockwise, or the minus direction, and is therefore the *M* isomer, where *M* stands for 'minus'. The enantiomer, **Figure 1.3 (b)**, is the plus, or *P* isomer. To relate this to the equally acceptable system of *R* and *S*, the *P* isomer corresponds to the *S* isomer, while *M* is the *R* isomer, sometimes denoted *aR* and *aS*.

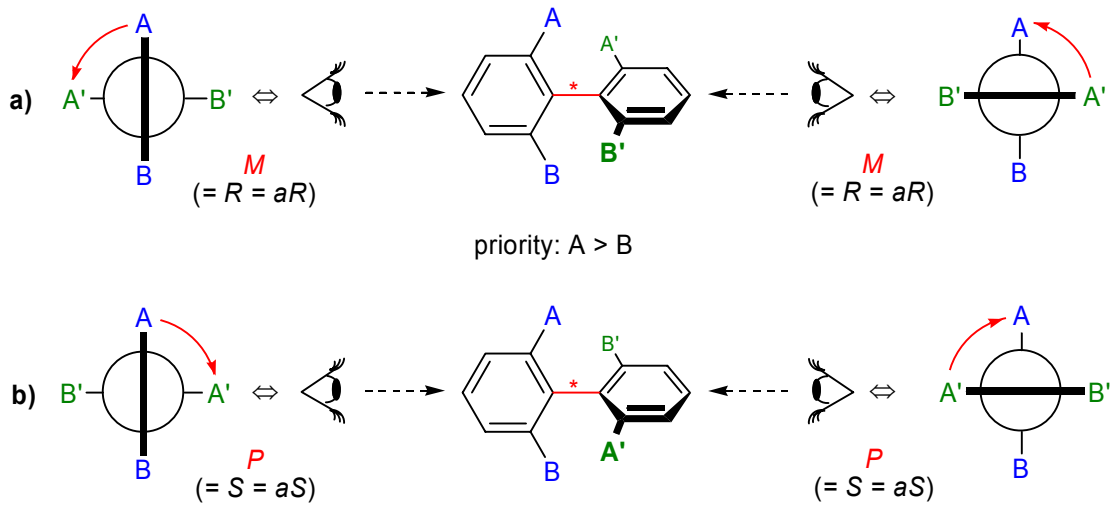

Figure 1.3: Assignment of stereochemistry of two atropisomeric biaryls.

Despite the prevalence of the atropisomeric biaryl bond in a variety of important natural products,[21] this type of stereochemistry is repeatedly ignored in publications. Atropisomeric biaryls are drawn flat, incorrectly indicating a planar conformation,[22] without any reference to $[\alpha]_D$ values.[23] The presence of rotationally hindered axes in natural products[21] is widespread and structurally diverse, e.g. the antibiotic vancomycin (**Figure 1.4**, **5**) contains one atropisomeric biaryl axis, which in conjunction with multiple stereogenic atoms and two biaryl ether linkages gives the molecule a rigid structure which binds to bacterial cell wall peptides.[24-26] Mastigophorene A (**Figure 1.4**, **6**) has been found to stimulate nerve growth.[27] Michellamine B (**Figure 1.4, 7**), which has anti-HIV activity,[28] contains three biaryl axes, two of which are rotationally hindered.[29,30]

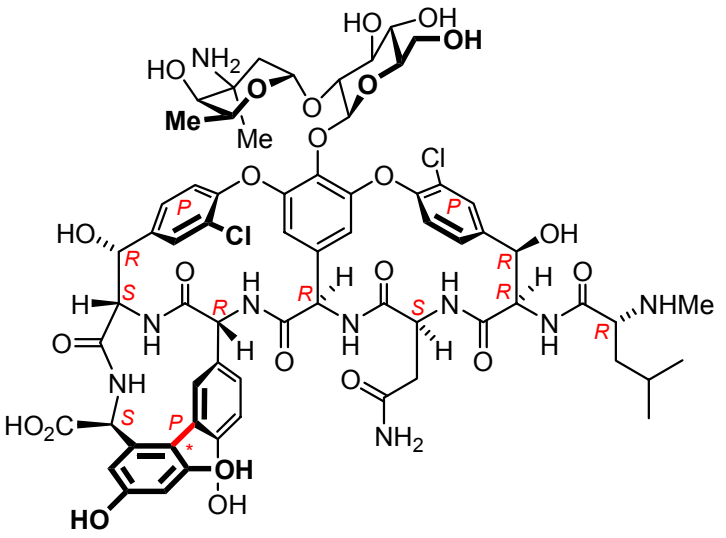

vancomycin

5

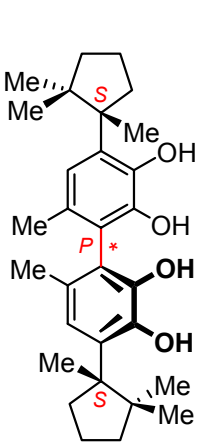

mastigophorene A

6

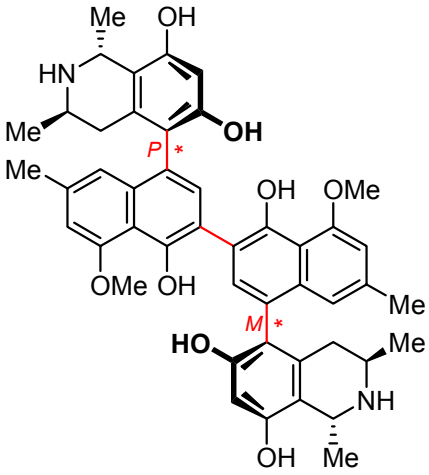

michellamine B

7

Figure 1.4: Selected examples of the natural occurrence of the atropisomeric biaryl.

Chiral catalysts utilise the presence of the atropisomeric biaryl axis for transfer of chirality,[31,32] e.g. the ubiquitously used diphosphine BINAP (**Figure 1.5**, **8**).[33-35] and the epoxidation ligand **9**.[36]

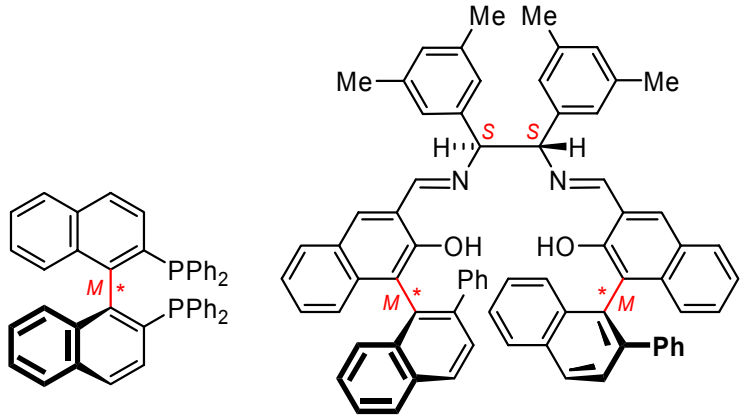

Figure 1.5: Examples of axially chiral ligands.

The development of efficient synthetic methods to select one atropisomer over the other has been limited due to the inherent difficulty in producing such a hindered system, and as such, enantioselection is complicated. A brief account of this development thus far is outlined.

1.2 Chiral biaryl synthesis

The challenge to form atropisomeric biaryls can be divided into two areas. One is the formation of the actual biaryl system and the second is to stereoselectively form one atropisomer over the other. There are three fundamentally different strategies for the atroposelective synthesis of axially chiral biaryls of the type **10** (**Figure 1.6**). The first strategy is the resolution or desymmetrisation of an existing, yet stereochemically undefined, biaryl **11**.[37-42] A contrasting approach is the direct coupling of two aromatic halves, **12** and **13**, to form the biaryl axis stereoselectively, in a single step.[43-45] The third approach is the construction of a chiral biaryl axis from non-aryl substituent attached to an aromatic ring **14**, usually with central-to-axial chirality transfer.[46-53]

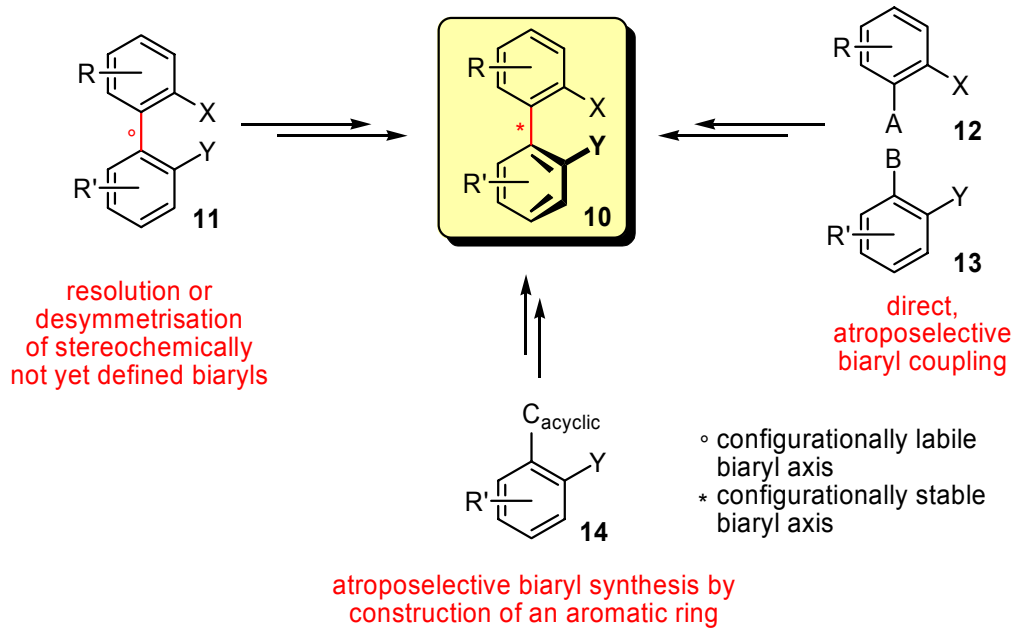

Figure 1.6: Three strategies for the atroposelective synthesis of axially chiral biaryls.

1.2.1 Resolution or desymmetrisation of stereochemically undefined biaryl compounds

The formation of an asymmetric biaryl can be approached via a two step synthesis in which the biaryl axis is formed non-stereoselectively and a second step that establishes the configuration of the biaryl axis.

1.2.1.1 Desymmetrisation of prochiral biaryls

A highly efficient, yet not widely versatile, method is the selective functionalisation of one substituent of a rotationally stable, symmetric biaryl, e.g. **Figure 1.7**.[54-56] The ditriflate **15** is achiral, owing to the presence of two triflate groups on one aryl ring; however the axis is rotationally stable. Reaction with selected Grignard reagents in the presence of chiral Pd^{II} catalyst [$PdCl_2${(*S*)-alaphos}] **16** provided the atropisomers **17** in high yield and enantioselectivity. The remaining triflate substituent can undergo further cross-coupling.

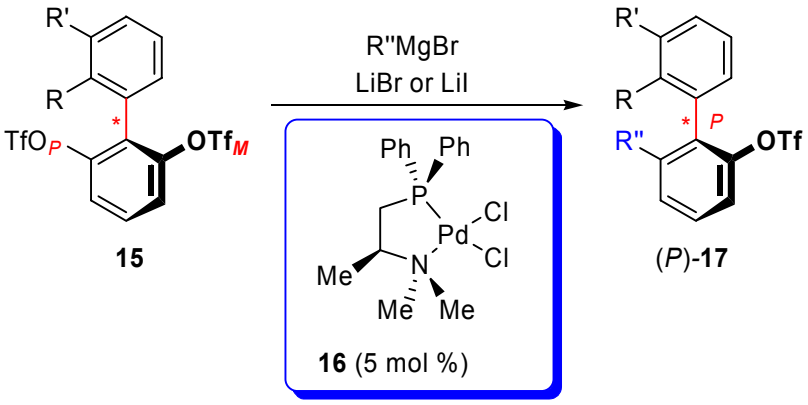

R	R'	R"	Yield [%]	*ee* [%]
benzo		Ph	92	94
benzo		*m*Tol	90	95
benzo		Ph_3Si—≡—	88	92
Ph	H	Ph	80	94
Ph	H	Ph_3Si—≡—	88	99
Me	H	Ph	85	95
Me	H	Ph_3Si—≡—	87	85

Figure 1.7: Desymmetrisation of rotationally stable, achiral biaryl ditriflate **15** via Grignard cross-coupling reaction in the presence of catalytic [$PdCl_2${(*S*)-alaphos}] **16**.

1.2.1.2 Resolution via chiral bridge formation

An alternative approach is the formation of a chiral bridge on a rotationally unstable biaryl compound. The chiral bridge serves two purposes. First, the presence of a bridge hinders rotation around the biaryl axis and second, the chirality of the bridge results in the formation of diastereomers, in which one is more stable and therefore the atropisomer is formed stereoselectively, e.g. **Figure 1.8**.[57] This method is best utilised when the bridge is part of the final target biaryl, otherwise further manipulation is required to ensure atropisomerism is conserved upon removal of the chiral bridge.

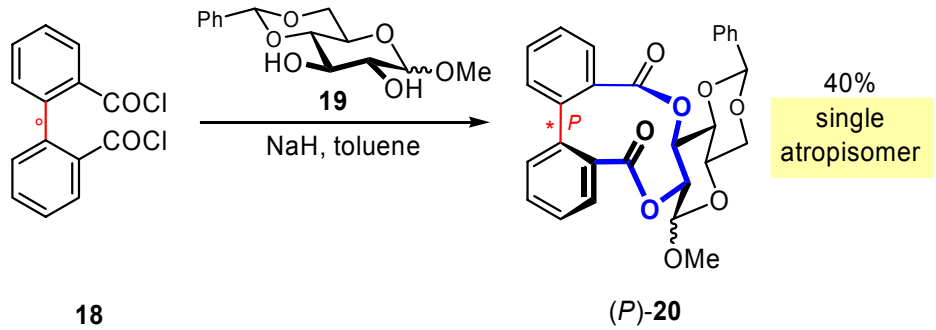

18 (*P*)-**20**

Figure 1.8: Dynamic kinetic resolution of 2,2'-dibenzoyl dichloride **18** by a glucopyranose-based scaffold.

A rotationally labile biaryl compound can be locked into one conformation via chelation with a metal centre. This can be achieved if the biaryl contains chiral auxiliaries which must adopt a conformation which minimises steric effects,[58,59] or, more widely investigated, if the metal is chirally modified by another ligand.[60,61] The chiral environment surrounding the chiral diamine (*S*,*S*)-**22** results in the formation of one atropisomer of the racemic bisphosphine ruthenium complex **21** (**Figure 1.9**).[62,63]

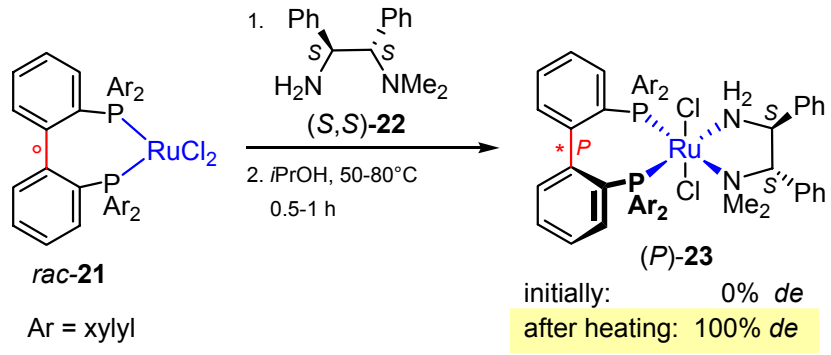

Figure 1.9: Resolution of racemic ruthenium complex **21** in the presence of diamine (*S*,*S*)-**22**.

1.2.1.3 Stereoselective Cleavage of a Bridge

One of the most versatile and applicable methods for the stereoselective formation of atropisomeric biaryls is the stereoselective cleavage of the configurationally unstable biaryl lactone (**Figure 1.10**).[38-42,64,65] Pd^{II} catalysed aryl-aryl coupling of bromoester **26** provides configurationally unstable biaryl lactones **27**. Cleavage of the lactone bridge with chiral nucleophiles establishes the chirality of the rotationally stable biaryl products **28**.[38-42,64,65] An equilibrium exists between the two atropisomeric biaryl lactones (*P*)- and (*M*)-**27**. This, combined with the reactivity of the chiral nucleophile towards only one atropisomer, leads to the formation of only one atropisomeric biaryl.

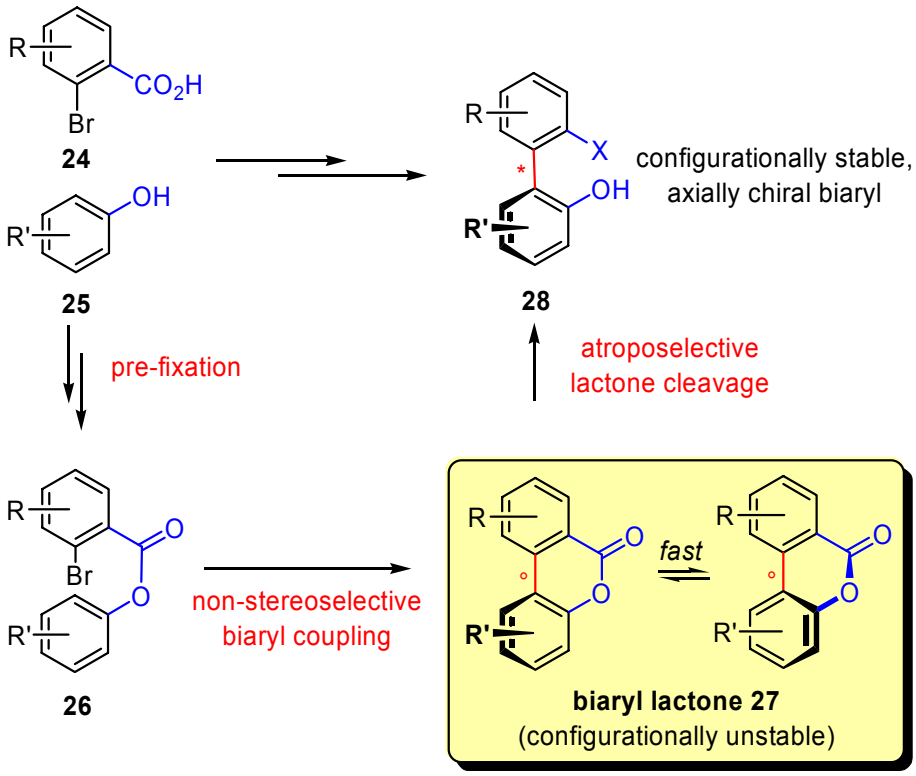

Figure 1.10: The principle of the lactone strategy.

The use of the 'lactone method' has been applied to the synthesis of many natural products and chiral synthesis precursors.[38-42,64-73] The atropodiastereoselective ring opening of biaryl lactone (*M*)-**29** with sodium (*R*)-menthoxide ((*R*)-**31**) as an oxygen nucleophile gave ester **32** in good yield and diastereoselectivity (**Figure 1.11**).[74,75] Almost complete configurational control was obtained via ring opening with the more sterically demanding (*R*)-8-phenylmenthoxide ((*R*)-**33**), delivering the ester (*M*,*R*)-**34** exclusively in 95% yield.[75] A major advantage of the lactone method is its atropodivergent nature, where both atropisomers can be obtained from the same, non-atropisomeric precursor, by using enantiomeric nucleophiles for the ring opening.

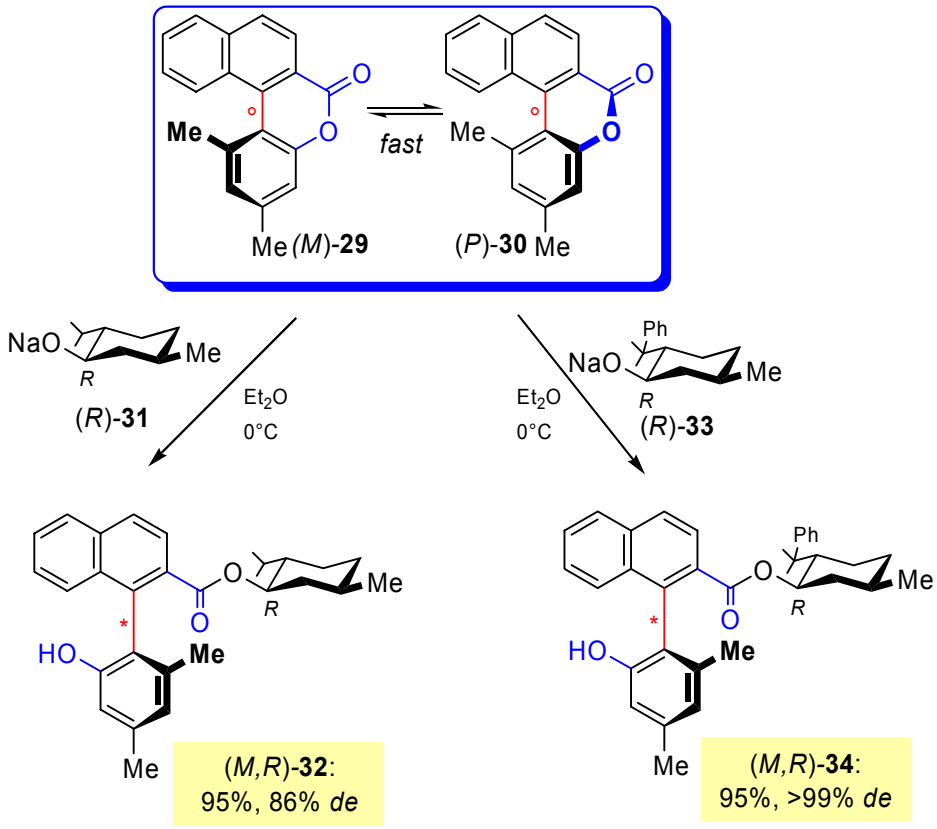

Figure 1.11: Atroposelective ring opening of lactone **29**, with chiral O nucleophiles.

1.2.2 Direct atroposelective biaryl coupling

The classical fundamental approach is the direct atroposelective biaryl coupling, in which the chirality of the biaryl axis is determined simultaneously with biaryl axis formation.[43-45] Depending upon the source of chirality, the resulting atropisomers may form diastereomers or enantiomers (**Figure 1.12**). The diastereomeric strategies are:

1. The use of a chiral tether to link the two aryl precursors (**35** → **10**).[76-82]
2. The inclusion of a chiral auxiliary in the *ortho* position of one of the aromatic precursors (**12** + **36** → **10**).
3. The presence of a removable chiral element, for example, the planar chiral η_6-chromium complexes **37** (**9** + **37** → **10**).

The enantiomeric strategies are:

1. The coupling of two arenes, in which one contains a chiral leaving group (**38** + **39** → **10**).[83-91]

2. Stoichiometric and catalytic oxidative dimerisations with metal based reagents combined with chiral ligands (e.g. Cu**.**amine complexes) (**40** + **41** → **10**).
3. Catalytic 'redox-neutral' couplings (**12** + **13** → **10**, e.g. Suzuki reactions) in which a chiral ligand is employed.

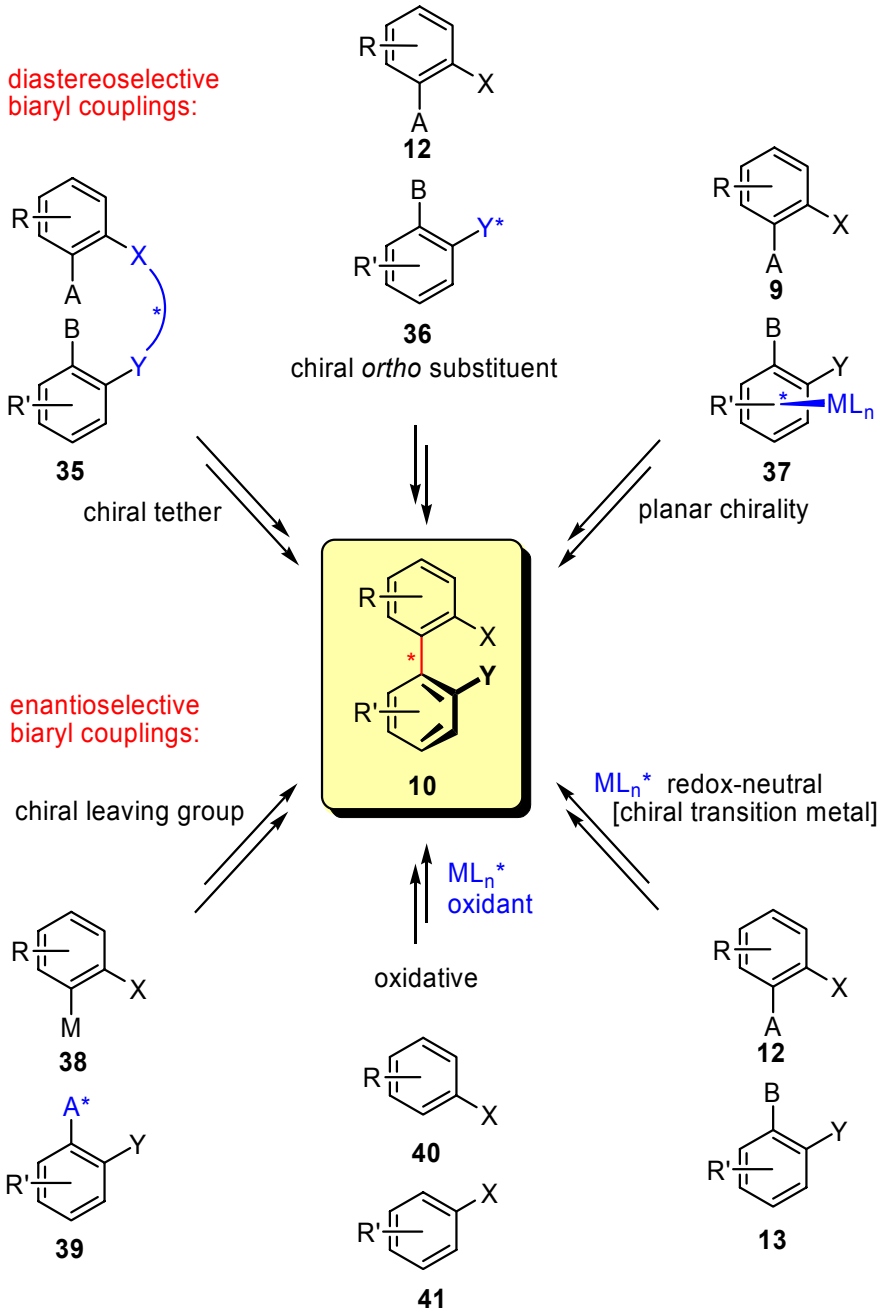

Figure 1.12: Strategies for the direct, atroposelective construction of biaryl axes.

1.2.2.1 Diastereomeric biaryl formation

When the chiral inducing element of the biaryl coupling is a substituent of one of the aryl precursors, the atropisomeric biaryl product is diastereomeric. The chiral source, therefore, is used stoichiometrically. The two most versatile methods are discussed.

1.2.2.1.1 Chiral ortho *substituents*

The biaryl bond can be formed via a Grignard reaction. Through the work of Meyers[83,92-94] an atropisomeric method has been realised via the inclusion of a chiral oxazoline moiety *ortho* to the site of biaryl bond formation (**Figure 1.13**). *Ortho*-methoxy substituted bromide **42** is converted to the Grignard reagent, which upon reaction with chiral *ortho*-methoxy(oxazolinyl) arene **43**, forms biaryls (*P*,*S*)-**44** or (*M*,*S*)-**44**, dependant on the relative electron-donating ability of the *ortho*-substituent of the aryl Grignard, R. Diminishing the chelating ability (e.g. R = CH_2OTBS) results in selective formation of the *P* atropisomer. Increasing the electron donating ability (e.g. R = 1,3-dioxolane-2-yl) gives the *M* atropisomer.

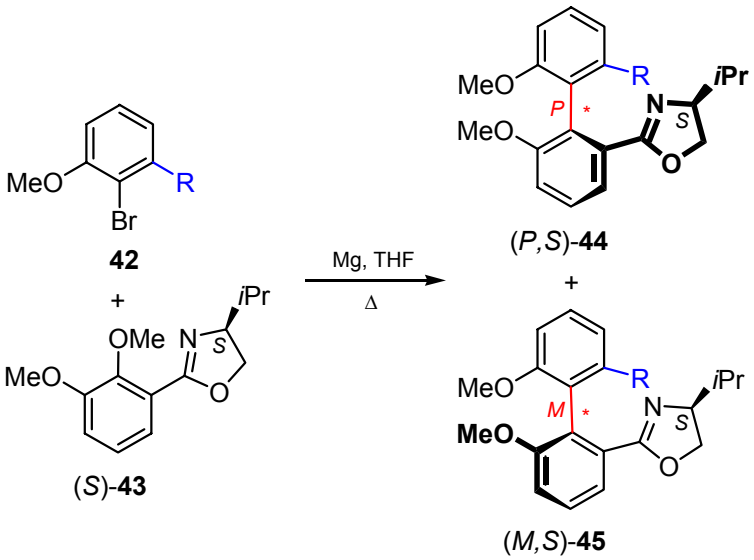

R	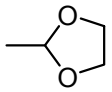	CH_2OMe	CH_2OBn	CH_3	CH_2OTBS
Yield [%]	90	75	80	79	73
(*P*,*S*)-**45**:(*M*,*S*)-**45**	20:80	40:60	42:58	90:10	93:7

electron donating ability of R

Figure 1.13: Synthesis of axially chiral biphenyls **45** by S_N2 Ar reaction of oxazolinylbenzene (*S*)-**43** and the influence of the electron-donating properties of the *ortho* substituents R of the aryl Grignard reagent on the asymmetric induction.

The reaction is believed to proceed via an addition-elimination mechanism (**Figure 1.14**) and diastereoselectivity is determined at both steps.[92,93] Initially, a chelate complex **46** is formed between the aryl Grignard reagent and the *ortho*-methoxy(oxazolinyl) arene. The diastereomer **46B** is favoured over **46A** due to steric interactions between the R substituent of the oxazoline moiety and the *ortho* substituent of the aryl Grignard. Nucleophilic addition of **46B** results in aza-enolates **47A** or **47B**. If the chelating ability of R' is greater than that of OMe, **47A** is favoured, which leads to biaryl **48A** after elimination of Mg(OMe)Br. If the electron donating ability of R' is removed, then **47B** is favoured, leading to biaryl **48B**.

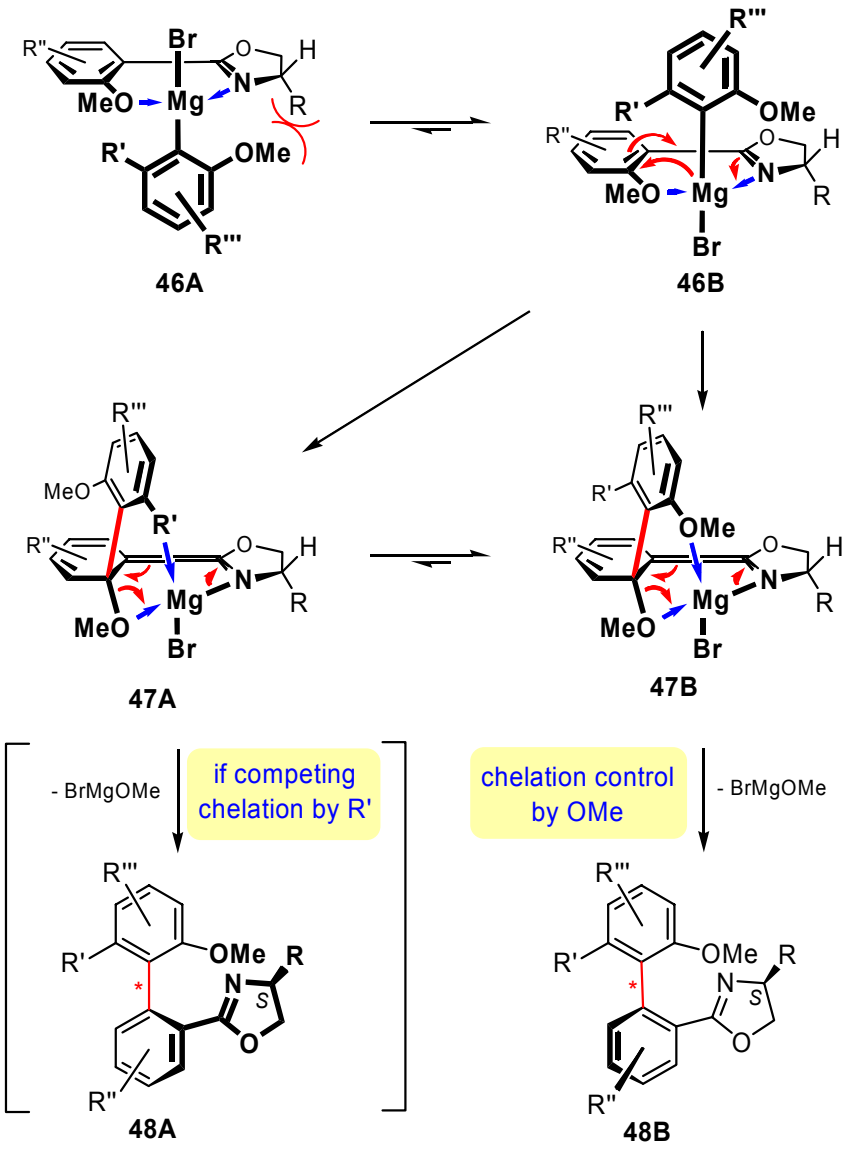

Figure 1.14: The stereochemical course of the S_N2 Ar reaction of aryl Grignard reagents on chiral aryl oxazolines.

The major advantage of this method is the high diastereoselectivities of up to 98%. Since the oxazoline is chiral, the biaryls formed are diastereomers and if present, the minor isomer can be more easily separated. The presence of the oxazoline moiety can be a useful functionality as a precursor to various synthetic products, such as (–)-steganone[95] and (+)-schizandrin.[96] This method, however, is limited in its ability to tolerate a wide range of substitution patterns and sterically hindered substituents, with certain requirements essential for diastereoselectivity. One of the substituents of the incoming Grignard must be a methoxy group, for the most efficient coordination with Mg^{2+}; the other must not compete for chelation with this MeO; and purely chiral

oxazolines are required - rendering the choice of stereochemistry of the resultant atropisomer dependent on the availability of the functionalised aryl substrates, both commercially and synthetically. Furthermore, the removal of the oxazoline and functionalisation of the other substituents must be gentle enough to avoid racemisation of the final biaryl axis.

1.2.2.1.2 Planar chirality

An alternative to chiral *ortho* substituents is the attachment of a chromium moiety, developed by Uemura, giving the aryl precursor and subsequent biaryl product the element of planar chirality. The presence of the chromium moiety directs the formation of the biaryl bond. Pd-catalysed Suzuki coupling of boronic acid **49** and (racemic) complex **50** delivered biaryl complexes *syn*-**51** and *anti*-**51** with excellent atropdiastereoselectivities (**Figure 1.15**).[45,97-99] The more sterically congested product *syn*-**51** was generally formed, where the substituent R is directed toward the $Cr(CO)_3$ fragment (entries 1-3). If an *ortho* carbonyl group is present, the thermodynamically more favoured atropdiastereomer *anti*-**51** is formed (entries 4 and 5), probably due to isomerisation at the biaryl axis under the reaction conditions, as a consequence of the lower rotational barrier. The results are inconsistent however (entries 6 and 7). In general, the electron-withdrawing $Cr(CO)_3$ fragment must be located on the aryl halide as it accelerates the oxidative addition to Pd^0.[45,100] The alternative coupling of an aryl halide with a $[Cr(CO)_3]$-complexed aryl boronic acid resulted in poor coupling yields.[45,101] Extension of the method to di-*ortho*-substituted aryl boronic acids and 2-substituted 1-naphthyl boronic acids led to diminished yields and stereoselectivities.[45,98,102]

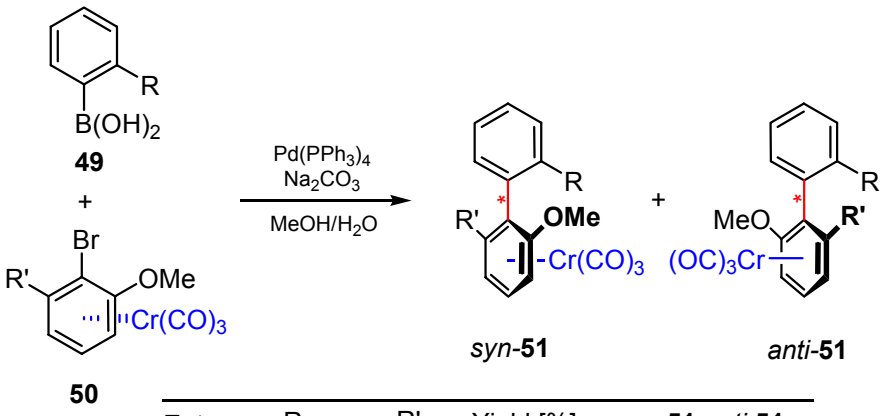

Entry	R	R'	Yield [%]	*syn*-**51**:*anti*-**51**
1	Me	Me	96	100:0
2	Me	CH_2OH	77	100:0
3	OMe	Me	94	97:3
4	CHO	Me	95	0:100
5	CHO	CHO	43	0:100
6	OMe	CHO	85	4:96
7	Me	CHO	82	100:0

Figure 1.15: Highly atropdiastereoselective Suzuki cross-couplings of phenyl boronic acids **49** with planar-chiral [(arene)$Cr(CO)_3$] **50** (all compounds racemic with respect to planar chirality).

The initial formation of the thermodynamically less stable *syn* product is proposed to be caused by steric repulsions in the two diastereomeric *cis*-diorganopalladium intermediates **52A** and **52B** (**Figure 1.16**).[45,98] The chromium fragment is directed towards the other arene moiety to avoid severe steric interactions with the bulky PPh_3 ligands, but **52A** is thermodynamically more favourable due to the weaker steric repulsions between H and R_L relative to those between R and R_L in **52B**. Reductive elimination in **52A** leads, under kinetic control, to the chromium biaryl complex *syn*-**53** as the simultaneous rotation around the forming biaryl axis proceeds in a way that minimises the steric interactions. The kinetic product can be converted to the thermodynamically more favourable atropdiastereomer via heating in an aromatic solvent,[98,103,104] or via functionalisation of one of the *ortho* substituents,[98,103,105,106] in which rotation of the biaryl axis is allowed.

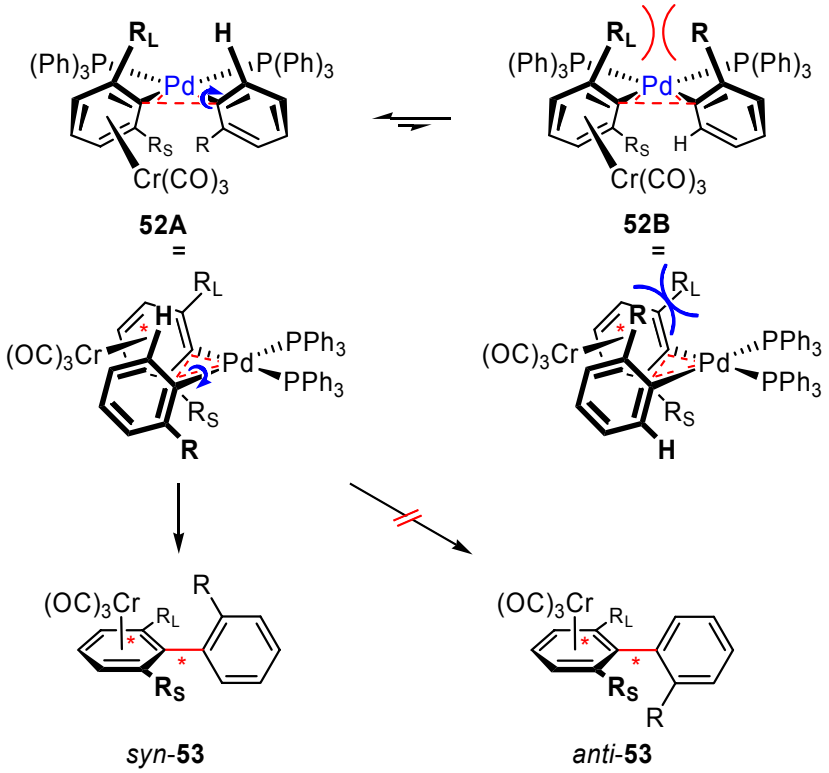

Figure 1.16: Stereochemical origin of the observed formation of thermodynamically less favourable [(biaryl)Cr(CO)$_3$] complexes *syn*-**53**. The blue arrow indicates the rotation that occurs upon biaryl-bond formation.

The major advantages of this method are the high yields and the excellent stereoselectivities obtained in the aryl-aryl coupling step. The [Cr(CO)$_3$] fragment can be removed by photooxidative demetallation (*hv*, O_2) with yields between 50 and 90%. Besides the toxicity of the chromium compounds, the most problematic limitation is the restricted and laborious access to the enantiomerically pure [(arylhalide)Cr(CO)$_3$] complexes.[107-109] The otherwise excellent coupling yields and diastereoselectivities decrease with increasing steric hindrance at the coupling sites, thus hampering the atroposelective synthesis of, for example, tetra-*ortho*-substituted biaryl compounds.

1.2.3 Enantioselective biaryl formation

Where the chiral element is present as either a leaving group or as a chiral ligand, the resulting biaryl contains only the element of axial chirality, and as such forms two possible atropenantiomers.

1.2.3.1 Oxidative couplings in the presence of a chiral additive

The use of chiral amines as ligands for use in metal catalysed oxidative couplings to form atropisomeric biaryls is widespread. Chiral C_2-symmetric (*S*,*S*)-1,5-diazadecalin ligands (*S*,*S*)-**56** were used with catalytic Cu^I in the presence of O_2 as the oxidant to dimerise 2-naphthol derivatives **55** to give (*M*)-**57** in good yields with up to 92% *ee* (**Figure 1.17**).[110,111] A coordinating substituent at C3 (carboxylic, phosphonate ester, benzoyl) is crucial for attaining high atroposelectivities (c.f. coupling of 2-binaphthol **54**). The stereochemical outcome is rationalised by bidentate coordination of the substrate to the chiral amine-copper complex.[110-112] For example, for the coupling of substrate **55a**, electron transfer should lead to the formation of the tetrahedral Cu^I complex **58**, which carries a C-centred radical.[110,111] The second substrate approaches from the less-hindered top face to give **59** stereoselectively, leading to atropisomer (*M*)-**57a**.

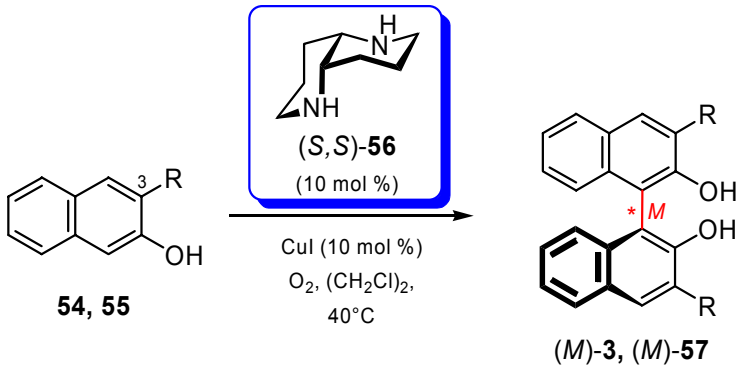

Substrate	Product	R	Yield [%]	*ee* [%]
54	**3**	H	81	16 [a]
55a	**57a**	CO_2Me	85	91
55b	**57b**	CO_2Bn	79	90
55c	**57c**	COPh	88	89
55d	**57d**	$P(O)(OMe)_2$	76	92

[a] The *P*-atropisomer was obtained.

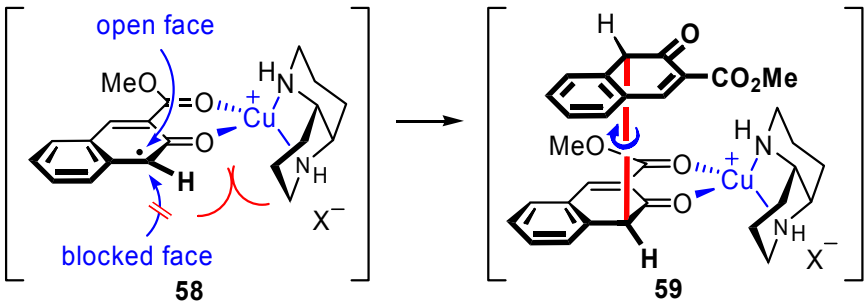

Figure 1.17: Cu^I catalysed oxidative homo-coupling of 2-naphthols of type **55** in the presence of chiral diamine (*S*,*S*)-**57** and O_2.

Other chiral ligand-metal complexes that have been used for the oxidative homo-couplings of 2-naphthols include the Cu^{I} complexes of chiral pyrrolidine **60**,[113,114] ruthenium^{II} complex (*P*,*P*)-**61**[115] and oxovanadium^{IV} complexes (*M*,*S*,*S*)-**62** and (*S*,*S*)-**63** (**Figure 1.18**).[116-121]

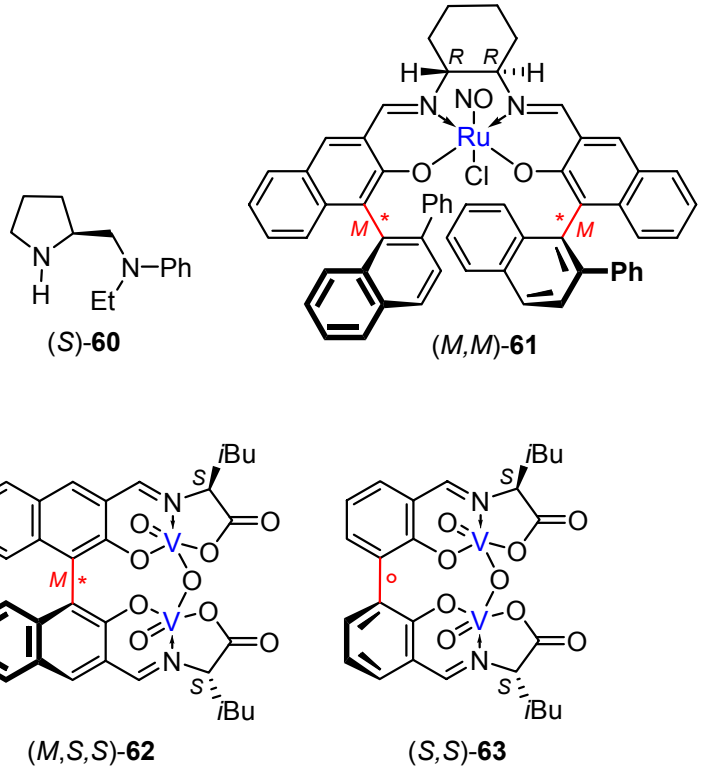

Figure 1.18: Chiral ligand-metal complexes used for the stereoselective homo-couplings of 2-naphthol derivatives.

1.2.3.2 Redox-neutral couplings in the presence of a chiral additive

Redox-neutral biaryl couplings (e.g. Grignard and Suzuki reactions) are widely used in the preparation of non-atropisomeric biaryl compounds. Extension to the synthesis of hindered biaryl systems has been limited.

1.2.3.2.1 Atroposelective Grignard reactions

Axially chiral binaphthalenes (*M*)-**68** and (*M*)-**69** were obtained in excellent yields and enantiopurities via the atropoenantioselective cross-coupling (Kumada coupling)[122,123] of aryl halide **64** or **65** with aryl Grignard reagent **66** in the presence of ≤ 5 mol % of $NiBr_2$, chirally modified with the ferrocenylphosphine ($_P$*S*,*S*)-**67b** (**Figure 1.19**).[109,124,125] The methoxy group in the ligand ($_P$*S*,*S*)-**67b** is crucial for good chirality transfer (c.f. the use of ($_P$*S*)-**67a**), proposed to function as a coordination site for the

magnesium cation of the incoming Grignard reagent in the transmetallation step.[125] While high enantioselectivities were achieved via this method, application as a general method is limited by the intolerance of several usual functional groups due to the use of a Grignard reagent, and as such this method has not been developed further.

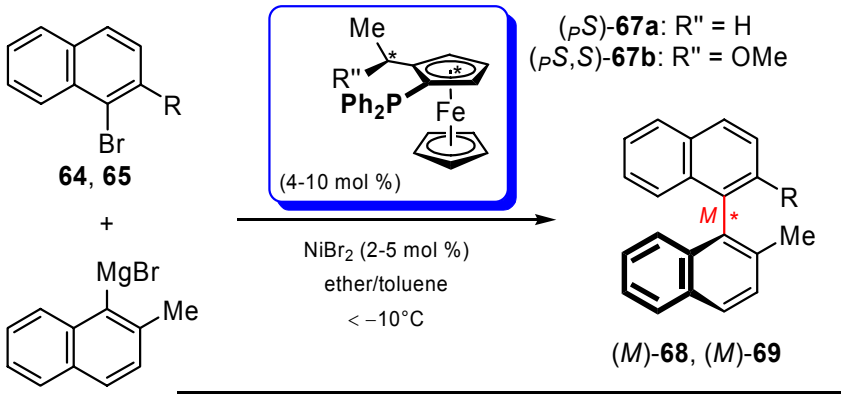

Substrate	Product	R	Ligand*	Yield [%]	*ee* [%]
64	(*M*)-**68**	H	(*pS*)-**67a**	81	1
64	(*M*)-**68**	H	(*pS*,*S*)-**67b**	92	83
65	(*M*)-**69**	Me	(*pS*,*S*)-**67b**	69	95

Figure 1.19: Nickel catalysed atropoenantioselective Kumada cross-coupling of 1-bromonaphthalenes with the 2-methyl-1-naphthyl Grignard reagent **66** in the presence of the chiral ferrocenylphosphine (*pS*,*S*)-**67b**.

1.2.3.2.2 The Suzuki reaction

One of the most common methods of forming biaryl systems is the Suzuki cross-coupling reaction.[126,127] The aryl boronic acids or esters used as the nucleophilic arene species are more stable and storable than Grignard reagents[128] and are therefore easier to handle, and are tolerant of a wide range of other functional groups. The high temperatures usually required to overcome steric hindrance at the reaction site has hampered its application in asymmetric biaryl synthesis. Recent solutions to these problems however,[129-133] have triggered research towards asymmetric Suzuki cross-couplings.

The Suzuki reaction involves the coupling of an arylboronic acid or ester **12** with an aryl halide **13** in the presence of a palladium catalyst (**Figure 1.20**). The reduced nucleophilicity of the boronic acid metalloid compared to the Grignard reagent results in a reduced quantity of side reactions.[6]

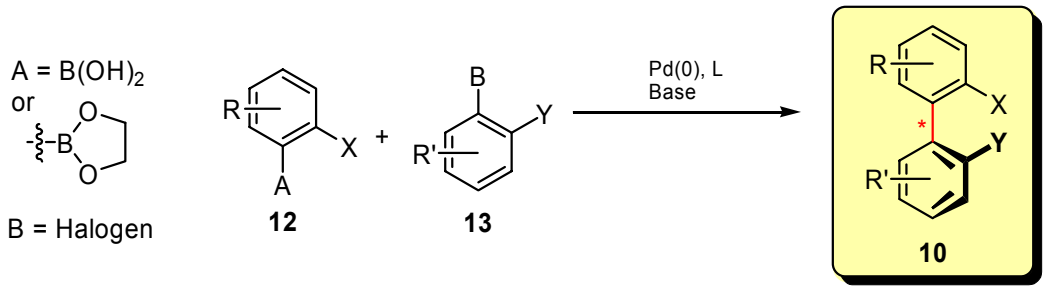

Figure 1.20: The Suzuki reaction.

The use of the Suzuki reaction, widely used in non-stereoselective biaryl synthesis, provides several benefits.

1. They proceed under relatively mild conditions; they are not restricted to a specific substitution pattern.
2. They allow regioselective cross-coupling of two different aromatic moieties (in contrast to the oxidative homocouplings previously discussed.)

The catalytic enantioselective version offers two additional advantages, providing a nearly ideal method:

3. The target biaryls are accessible with all the substituents required already in place, avoiding any subsequent modification (in contrast with the diastereoselective couplings with a chiral auxiliary.)
4. Most importantly, a chirally modified transition metal is the carrier of asymmetric information which is used catalytically – allowing highly economical use of the chiral information.

Despite the advantages of this method, there has been, as yet, only limited research activity in the field. Pd-based coupling reactions have generally been limited when the C_{ipso} carbon is sterically hindered by bulky *ortho*-substituents. These bulky groups tend to block the approach of the aryl substrates to the metal binding site, requiring rigorous reaction conditions. Resolvable atropisomers at room temperature may not be so at higher temperatures since the barrier to rotation[8] may be reached thereby resulting in racemisation.[126] This presents a two-fold problem when coupling sterically hindered substrates via Suzuki conditions. Elevated temperatures are required to enhance the coupling of such hindered substrates, but as a consequence, any atropisomeric biaryl

formed may racemise[5] thereby negating any attempt at stereoselectivity. Development of the Suzuki reaction with the aim to provide conditions for successful coupling at ambient temperature has been undertaken. This resulted in a thorough analysis of all parts of the reaction. The strength and amount of base required for optimisation has been examined.[132] Comparison of the form in which the substrates are added to the reaction has also been studied. Aryl triflates have extensively been used[134] over aryl bromides and the typically inactive aryl chlorides. The success and subsequent use of the more available aryl chloride has increased due to the work of Buchwald.[132,133] The development of the arylboronic acid component has resulted in the use of arylboronic esters being used, with encouraging yields.[135]

However, the success of the Suzuki coupling has increased substantially due to the development of the ligand catalyst. Traditionally, triphenylphosphine has been used as the ligand. When this ligand is used in sterically demanding couplings the chemical yield is low, if successfully forming the coupling product at all. Buchwald and others have developed a wider range of ligands for use in Suzuki couplings.

The catalytic cycle for the coupling of the two aryl systems with palladium involves three primary steps; oxidative addition, transmetallation and reductive elimination (**Figure 1.21**).[126]

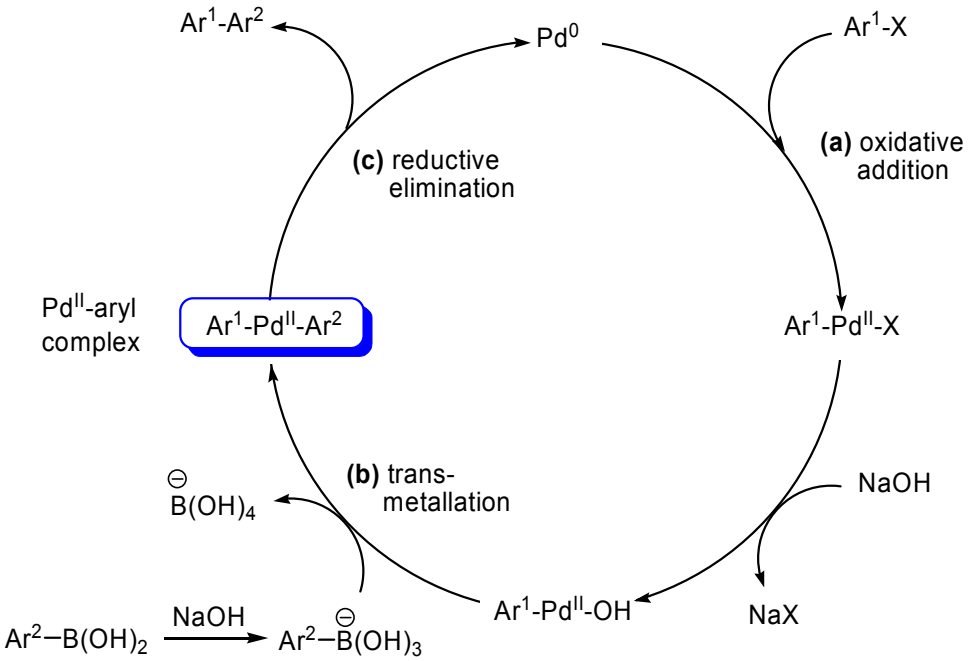

Figure 1.21: The catalytic cycle of palladium-based cross-coupling reactions.

The first step **(a)** involves oxidative addition of the palladium catalyst to the aryl halide, resulting in two of the coordination sites on palladium being occupied by the first aryl substrate and a halide. This halide is replaced with a hydroxyl group, which in turn is replaced by the second aryl group as it approaches the palladium centre in the transmetallation step **(b)**, generating a diaryl palladium species, as indicated in **Figure 1.21**. Reduction of the palladium in this complex **(c)** produces the biaryl compound, and releases the palladium^0 catalyst to be reused in the next cycle.

The Suzuki reaction requires the presence of a base (**Figure 1.21**, **(b)**).[128,135] The carbanion character of the organic group on the boron must be increased, as it is not nucleophilic enough to transfer from the boron to the palladium, due to the strong covalent character of the B-C bond. It does this by the formation of an organoborate with a tetravalent boron atom.

Since the development of the use of ligands in these couplings, the scope of aryl systems able to be coupled has expanded greatly, with the formation of tetra-*ortho*-substituted biaryls possible.[131] This leads to the need for stereoselective control, of which there are limited examples.

The catalytic system of the ferrocenylphosphine ligands ($_P$*S*,*S*)-**67** (6 mol %) with $PdCl_2$ (3 mol %) was applied to the cross-coupling of 1-iodonaphthalene **70** and 2-methylnaphthalene-1-boronic acid **71** (**Figure 1.22**).[136,137] The use of the methoxy substituted ligand ($_P$*S*,*S*)-**67b** gave the binaphthyl (*M*)-**68** in good yield, but poor *ee*. The use of the P,N-derivative ($_P$*S*,*S*)-**67c** increased the enantioselectivity, but decreased the yield. Suzuki coupling of the sterically more demanding aryl iodide **72** with the cyclic boronic ester **73** delivered the tetra-*ortho*-substituted binaphthyl derivative (*M*)-**69** with good enantioselectivity (**Figure 1.22**).[136,137]

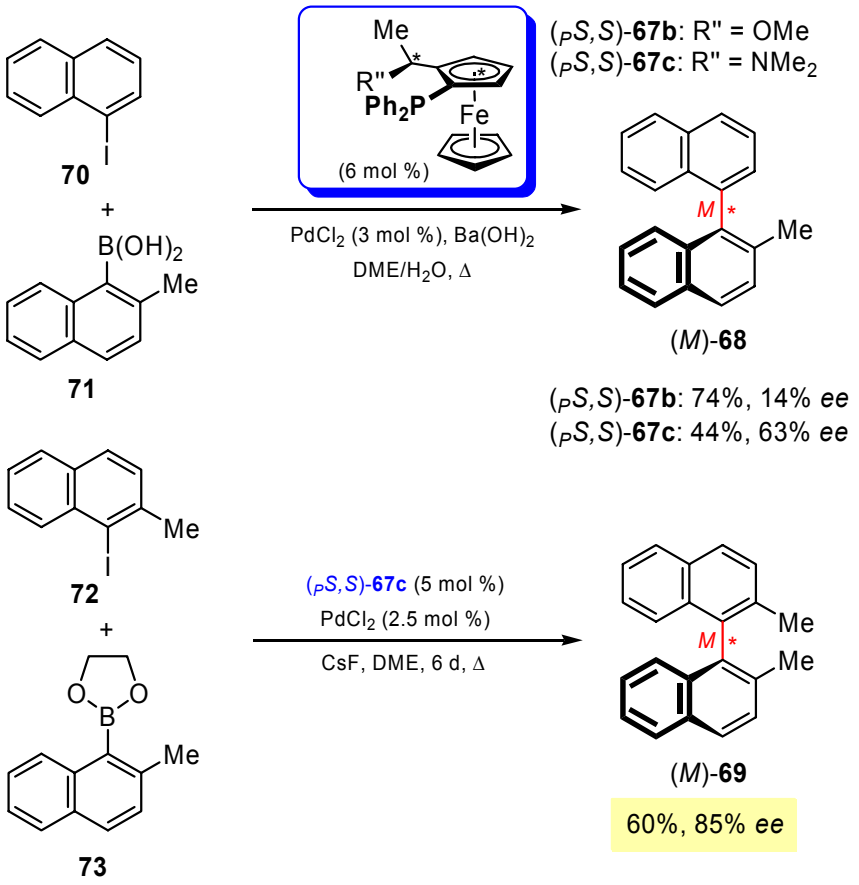

Figure 1.22: Atropoenantioselective Suzuki couplings with the bidentate ferrocenylphosphines (*P*S,*S*)-**67** as the chiral ligands.

The use of aryl substituted ferrocenylmonophosphines (*P*R)-**74** with $Pd_2(dba)_3$ under Suzuki conditions provided (*M*)-**69** with stereoselectivities of 43-54% (**Figure 1.23**).[138]

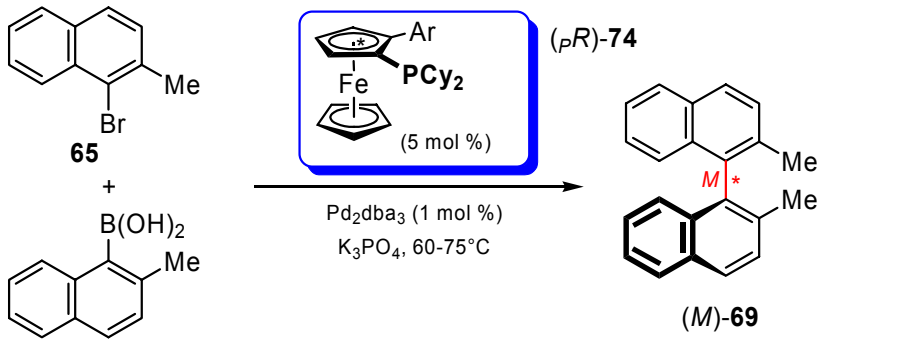

(*P*R)-**74**: Ar	Solvent	Yield [%]	*ee* [%]
2-anisyl	toluene/H_2O	62	43
1-naphthyl	toluene/H_2O	65	54
9-phenanthryl	THF/H_2O [a]	32	45

[a] No reaction occurred in toluene/H_2O.

Figure 1.23: Asymmetric synthesis of the dinaphthalene (*M*)-**69** in the presence of planar chiral ferrocenyl monophosphine (*P*R)-**74**.

The most successful asymmetric Suzuki couplings so far have been published by Buchwald et al.[139] Initial screening showed that $Pd_2(dba)_3$ and the electron rich biaryl aminophosphine (*P*)-**76** were the catalytic system of choice. Cross-coupling of the naphthyl phosphonate **75** with several phenyl boronic acids **49** delivered the tri-*ortho*-substituted axially chiral biaryls (+)-**77** in excellent yields (up to 98%) with up to 92% *ee* (**Figure 1.24**). The amount of Pd/(*P*)-**76** (ratio 1.2:1) can be lowered to as little as 0.2 mol % without any decrease in optical purity.

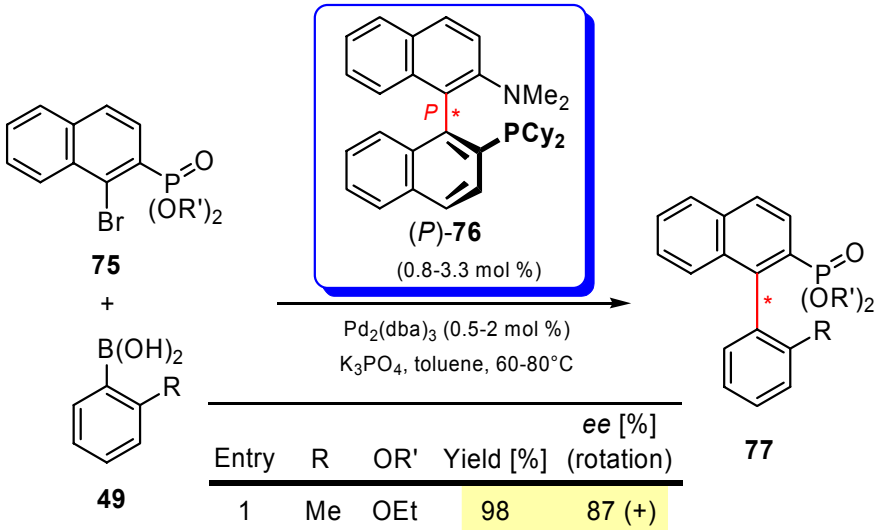

Entry	R	OR'	Yield [%]	*ee* [%] (rotation)
1	Me	OEt	98	87 (+)
2	Et	OEt	96	92 (+)
3	*i*Pr	OEt	89	85 (+)
4	Ph	OEt	74	74 (+)
5	Me	OMe	91	84 (+)
6[a]	Me	OMe	95	86 (+)

[a] 0.1 mol % $Pd_2(dba)_3$ were used.

Figure 1.24: Selected examples of the asymmetric Suzuki cross-coupling of **75** with different phenyl boronic acids **49** in the presence of the biaryl aminophosphine (*P*)-**76**.

The ligand **76** was not applied to the synthesis of tetra-*ortho*-substituted axially chiral biaryls. The coupling reaction to form such hindered systems was performed using biaryl mono-phosphine ligands in good yields, however no *ee* data was reported.[140] No further development of these ligands for the stereoselective synthesis of axially chiral biaryls has been reported in the last 7 years. Ligand **76** (and those used in **Figures 1.22-1.24**) was encountered as the result of ligand screening studies, without a general ligand design program. The lack of further development may perhaps be attributed to the absence of such a ligand design program.

Only recent improvements have allowed the application of the Suzuki reaction in stereoselective biaryl synthesis, and there are, as yet, no standard procedures available. Each new catalyst and substrate still requires time-consuming optimisation of the particular reaction conditions, including; catalyst loading, base, solvent, choice of substrate (boronic acids or esters, aryl bromides or iodides) and substitution patterns (tetra-substituted or tri-substituted). For examples of the possible variations of reaction conditions, see **Figures 1.22-1.24**. The stereoselectivities obtained thus far are not sufficient for incorporation of this method into enantioselective syntheses. However, the easy handling of the aryl precursors, the lack of dependence on particular substitution patterns, the relatively mild reaction conditions and the catalytic nature of the reaction with regard to the chiral ligands make the asymmetric Suzuki coupling an attractive reaction strategy.

New, more effective ligands that deliver good and reliable chemical yields and optical purities under standard conditions for a broad variety of substrates need to be designed. The Suzuki cross-coupling could then become one of the most important methods for atroposelective biaryl couplings. A new strategy for the development of such ligands must be devised, which accommodates the requirements of sterically hindered substrates. For this to occur, a ligand design program must be initiated.

1.3 Project aims

Despite the lack of a general method for applying the Suzuki reaction to the stereoselective synthesis of axially chiral biaryls and the limited success thus far, this method presents the most potential for fulfilling the requirements of a general method. The development of such a general method lies in the design of the chiral ligand catalyst. Therefore, the aims of the project are;

1. To devise a design strategy for new ligands for use in the stereoselective synthesis of sterically hindered systems, specifically, axially chiral biaryls.

2. To design new chiral ligand scaffolds for use in metal catalysed biaryl couplings.

3. To develop an efficient stereoselective synthetic strategy which provides access to the new target scaffold, and derivatives thereof.

4. To couple a range of hindered aryl groups under Suzuki conditions, to form atropisomeric biaryls, using the new chiral ligand and derivatives, and to ascertain the stereoselectivity of these reactions.

CHAPTER 2
Ligand Design and Synthetic Strategy

The incorporation of a chiral ligand as part of catalytic stereoselective syntheses is well documented.[3,141-144] A plethora of chiral ligand-metal complexes have been developed for use in catalytic enantioselective synthesis.[3,5,145] The major advantages are the economic use of the chiral ligand, catalyst recovery and proximity of the chiral information to the reaction site. The chiral ligand itself is often laboriously obtained, so use in catalytic quantities is desirable. The application of chiral ligands for use in asymmetric Suzuki cross-coupling reactions for the synthesis of sterically hindered, atropisomeric biaryl systems is not, as yet, general. In order to develop a ligand design protocol, an understanding of the catalytic cycle of the Suzuki coupling is required.

Each of the palladium complexes formed throughout the catalytic cycle (see **Figure 1.21**) requires stabilisation, which is provided by the coordination of a ligand to the unfilled sites on the palladium. The presence of phosphorous, nitrogen or arsenic donor atoms in the ligand is necessary for coordination to the palladium. Either can be used, although the P-Pd or As-Pd bond offers greater stability than the N-Pd bond.[146] One of the most common ligands used is triphenylphosphine, forming the complex tetrakis(triphenylphosphine)palladium(0), $Pd(PPh_3)_4$. Variations on this phosphine ligand have been developed to increase the electron donating ability of the P donor atom, to increase the stability of the ligand-Pd complex.[147] The formation of a more stable transition state results in a better yield of the biaryl system under milder conditions.[148] Therefore, the development of better coordinating ligands has been a key step in the broadening of the functional groups allowed on the aryl substrates.

2.1 Ligand function

The importance of the Pd-ligand intermediate on yield can be utilised to enhance the stereoselectivity of the atropisomer formed. The use of a bidentate ligand will coordinate to two of the unfilled palladium sites, resulting in a more stable Pd-complex intermediate. This will also leave two sites unoccupied with which the incoming aryl substrates can coordinate. The use of a *chiral* bidentate ligand in this transition state will result in a chiral environment surrounding the palladium, giving rise to the possibility of a selective approach to the palladium coordination sphere by the substrates (**Figure 2.1**).

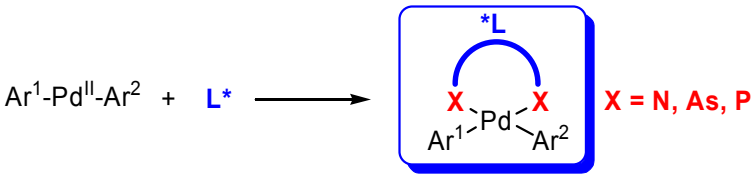

Figure 2.1: The ligand-Pd-substrate complex.

This will force the incoming aryl groups to coordinate into a specific orientation. The use of non-chiral ligands, such as the commonly used PPh_3, does not produce this selective approach of the aryl substrates,[149] required for the generation of axial chirality. While the use of chiral ligands will, in principal, result in stereoselectivity, there is to date no established set of requirements or conditions which control the stereochemistry of the atropisomeric biaryl bond. Design and development of chiral ligands would therefore improve the use of palladium-based reactions enormously.

2.2 Design of a chiral ligand for stereoselective atropisomeric biaryl couplings

There are many chiral auxiliary ligands available, designed for a variety of different types of reactions. Ligands such as BINAP, **8**, and its analogues are commonly used,[7,147,150] containing a large chiral backbone[76] that induces the desired chiral twist[151] at the metal binding site. Chiral ligands are often designed so as to have the effect of blocking one approach for the incoming aryl substrates resulting in the desired conformation of the product. By definition however, the asymmetric biaryl axis is formed as a result of the restriction around the axis by the presence of bulky *ortho* substituents. Difficulties arise therefore, since the bulky ligand not only blocks the

approach of the aryl substrates into the undesired conformation, but it also stops the formation of the desired atropisomer.

An alternate method of designing a chiral ligand is to utilise the helicity of the biaryl axis. The axis of a rotationally hindered biaryl system can be viewed as having a helical sense or a twist (**Figure 2.2**). In fact, the assignment of *P* and *M* stereochemistry to the biaryl, as outlined in ***Section 1.1***, is the same assignment given to helices.

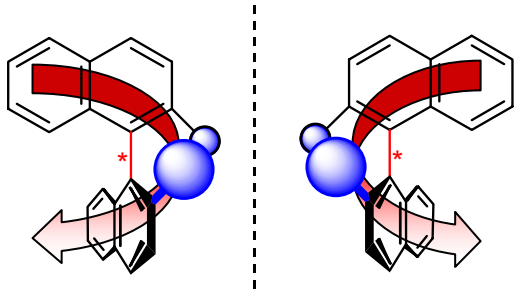

Figure 2.2: The biaryl system illustrating helicity.

Therefore, helices can exist in two forms of handedness, depending on the direction of the helical twist. The tongue-in-groove intermeshing of helices is a manifestation of chiral discrimination, e.g. the helical axes of an intermeshing right- and left-handed helix lie parallel to each other because the interactions occur in equal measure along the entire length of each helix. Therefore, the most efficient way of building a rigid one-handed helix (e.g. biaryl) would be to construct an intermeshing helix of the opposite handedness as a guiding template. The resulting transfer of (inverted) chirality to the new helix is of great significance in chemistry, e.g. it is seen in many products of stereoselective chemical reactions performed on C_2-chiral templates. As such, atropisomeric biaryls should be ideally constructed using helix-sense selective discrimination reactions.

This design principle can be incorporated into the formation of atropisomeric biaryls via the use of Pd-based coupling reactions. The 'guiding template' would be the Pd-ligand catalyst which will have the complementary helicity to that of the desired atropisomer. The two aryl substrates will coordinate in a more stable conformation with the Pd-ligand complex if the *ortho* substituents on each substrate are oriented to interact least with the helical conformation of the Pd-ligand complex, thereby selectively forming one

atropisomer over the other. To illustrate this, **Figure 2.3(a)** displays a biaryl inserted into the groove of a helix. The larger *ortho* groups of the biaryl are directed outwards of the helical groove. In order to fit into the groove, the smaller substituents are directed inwards. The opposite atropisomer is unable to fit into the groove of the same helix (**Figure 2.3(b)**), since both larger substituents are not able to point outwards without clashing with the helix. As is shown by the red ring in **Figure 2.3(b)**, there are unfavourable interactions between these substituents with the helix. Therefore, the atropisomer shown in **Figure 2.3(a)** will be selected if the intermediate adopted by the Pd-ligand complex can be designed to have the conformation represented by the gold helix. This helical-sense discrimination represents a new approach to the design of chiral ligands for use in the stereoselective synthesis of axially chiral biaryls.

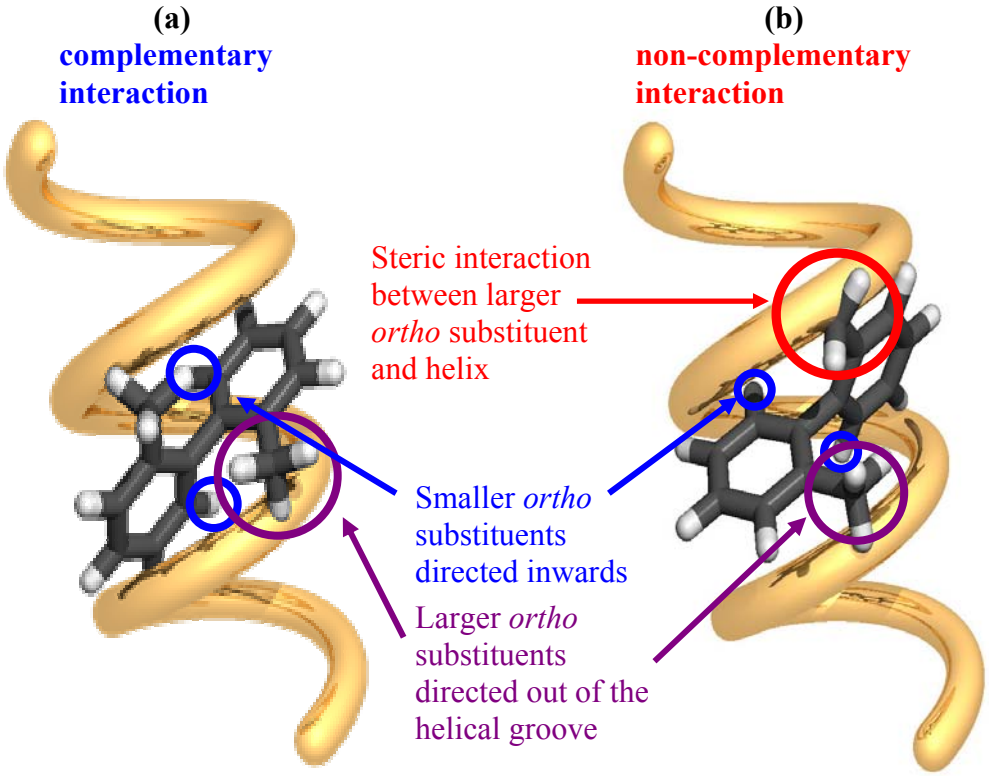

Figure 2.3: The interaction of enantiomeric atropisomers with the same helical structure.

A ligand must therefore contain features that best transfers the helicity of the ligand to the Pd-ligand complex. This can most effectively be achieved when the helical twist in the ligand is in close proximity to the Pd-binding site. The Pd binds through the donor atoms of the ligand, so the most obvious feature, aside from incorporating chirality into the donor atoms, would be to place the chiral element of the ligand in close proximity to

the donor atoms. The general principles for the design of such a Pd-ligand template are shown in **Figure 2.4**.

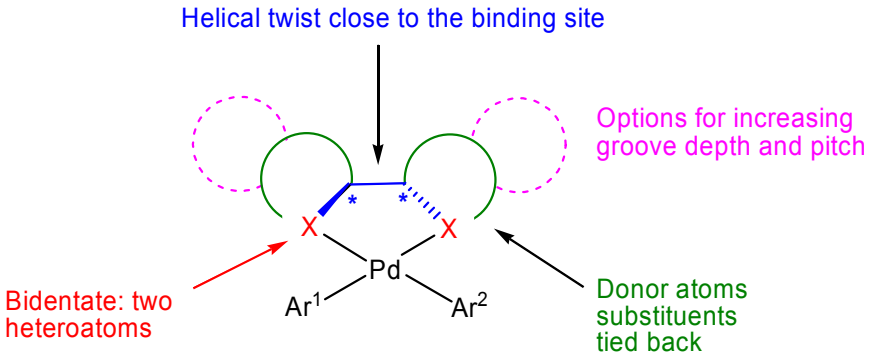

Figure 2.4: Template for the new ligand scaffold design.

If two stereogenic carbons are attached to one another, then the helical aspect of the first carbon is continued in the second, forming a more visible helical twist.[152] Therefore, in achieving this desired helical twist, two attached stereogenic carbons should be present, and in order for this helicity to be in close proximity to the palladium coordination site, the donor atoms should themselves be attached to either side of the two stereogenic carbons.

The chiral ligand must not create any further steric crowding around the Pd-coordination site, since the highly hindered aryl substrates already impose steric demand on the Pd reaction site. Therefore, for the donor atoms to be best coordinated to the palladium, there should be minimal steric hindrance surrounding the donor atom, so the substituents of the donor atoms should be tied back. In principal, using a non-bulky ligand would not block the approach of the aryl substrates to any of the unfilled coordination sites.

The ligand design must be able to incorporate modifiable helical aspects depending on the type of biaryl being synthesised, for example groove pitch or depth. A higher pitched helix has a shorter distance between successive turns, or whorls (**Figure 2.5**, **(a)**), whereas a lower pitched helix has a larger distance (**Figure 2.5**, **(b)**). It is predicted that if the desired biaryl is highly pitched, then a ligand which has a similar pitch should be used, to maximise the complementary interactions. Similarly, if the biaryl has a deep, well-defined groove, then the ligand should have a groove of similar depth and width. In order to examine this theory, a range of ligands must be modelled, designed and

synthesised, and their effectiveness in the enantioselective formation of these biaryls determined. More information must be gained on the environment surrounding the Pd in the ligand-Pd-substrate intermediate; therefore a range of Pd-ligand systems must be synthesised and trialled. Therefore, the ligand design program must incorporate a scaffold which is easily derivatised and substituted, in order to trial a range of ligands.

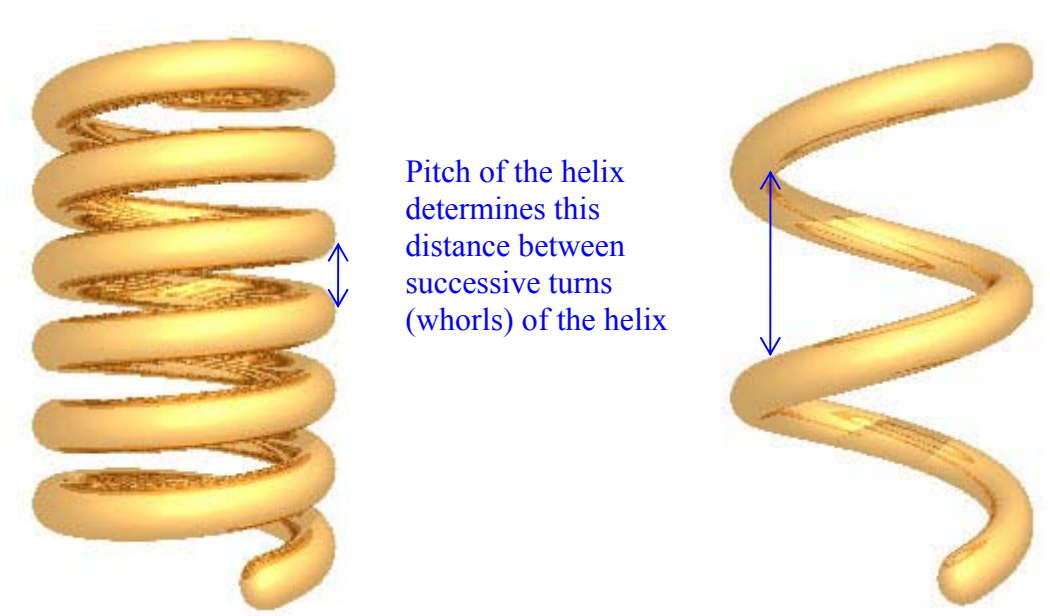

(a) High pitch helix:
shorter distance between turns

(b) Low pitch helix:
larger distance between turns

Figure 2.5: Helices of different pitches will be important in the design of ligands for a range of biaryl systems.

The concepts outlined above would be realised by designing a chiral ligand that incorporates the following features;

1. A defined helical twist in the ligand-palladium complex – to ensure that the incoming substrates coordinate in the complimentary helix,
2. Bidentate – to create a rigid intermediate complex and ensure the helical twist is around the reaction centre,
3. The donor atoms should be tied back in ring systems – to minimise steric hindrance of the coordination sites and decrease ligand flexibility,
4. The helical twist should be in close proximity to the Pd binding site – to maximise the effect of the twist on the Pd-ligand intermediate complex and hence aryl-aryl coupling.

The currently available ligands ($_PS,S$)-**67**, ($_PR$)-**74** and (*P*)-**76** do not contain all of these design features. For example, the axially chiral aminophosphine (*P*)-**76** does contain a defined helical twist, however the substituents of the donor atoms are not tied back in ring systems.

Three suitable ligands that fit these design principals are illustrated in **Figure 2.6**.

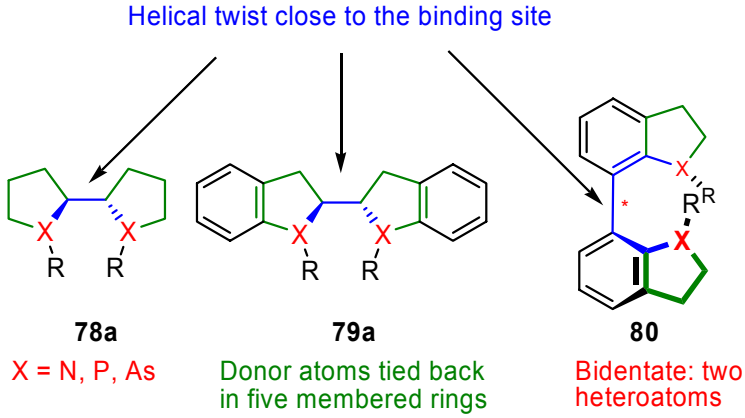

Figure 2.6: Features of target molecules as helical ligands.

This thesis will concentrate on the development of ligands **78** and **79**. Possible modifications of the target scaffold include;

1. Donor atoms – dinitrogen, diarsine, diphosphine and mixed versions of each.
2. Heteroatom substitution – where the size of the substituent is modified (e.g. R = H, Me, Ph, Bn).
3. Further substitution around the stereogenic atoms (**Figure 2.7**, e.g. R' = Me) – to enhance the helical twist.
4. Aromatic ring substitution (**Figure 2.7**, R" = Br) – to increase the depth or pitch of the helical groove.

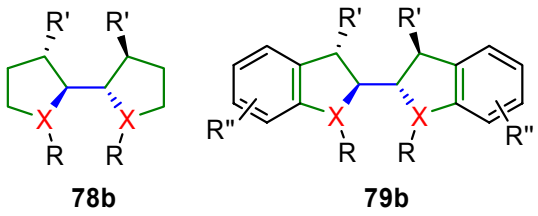

Figure 2.7: Further possible modifications of the target scaffold.

Therefore, a synthetic strategy must be devised in which the target scaffold and its derivatives can be accessed in both enantiomeric forms from simple starting materials and reliable chemistry. Modifications such as aromatic ring substitution to form **79** must

be possible from the established synthetic strategy. Application of the strategy towards the dinitrogen, diarsine, diphosphine and mixed heteroatom versions thereof is desirable. Due to the easier handling of such substrates, the dinitrogen ligands will be synthesised initially, in order to establish the chemistry towards these C_2 symmetrical ligands.

2.3 Synthetic strategy

2.3.1 Chiral diamines

Chiral diamines with C_2 symmetry have been widely used as chiral auxiliaries in asymmetric transformations due to the bidentate chelating nature of the nitrogen donor atoms, and the chiral environment created in close proximity to the metal reaction centre.[3,141-144] For example, chiral 2,2'-bispyrrolidines **81** and **82** have been used as ligands for osmium tetroxide in asymmetric dihydroxylations (**Figure 2.8**).[153-155]

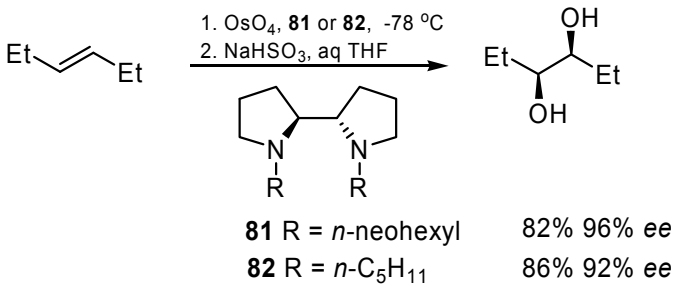

Figure 2.8: The use of chiral 2,2'-bispyrrolidines as chiral ligands in asymmetric dihydroxylation reactions.[154,155]

The published procedures for the synthesis of the 2,2'-bispyrrolidine scaffold were examined to determine if any fulfilled our requirements of a synthetic strategy which could be modified to provide all variations of the target scaffold (e.g. different heteroatoms, mixed heteroatoms, fused aromatic systems).

2.3.2 Diastereomeric strategies towards the 2,2-bispyrrolidine scaffold

The first reported synthesis of 2,2'-bispyrrolidine **86**[156] included a two-step synthesis (**Figure 2.9**) including condensation of pyrrole **83** with 2-pyrrolidinone **84** under the action of phosphorous oxychloride which gave **85**. Subsequent hydrogenation with rhodium on alumina provided the diastereomeric mixture of (*R*,*R*)- and (*S*,*S*)-chiral and

meso isomers of **86**. Resolution with tartaric acid provided the enantiopure bispyrrolidines. Repetition of this procedure however,[157] found the hydrogenation step sluggish, with a significantly diminished yield when the scale of the reaction was increased, with reaction times of up to 30 days.

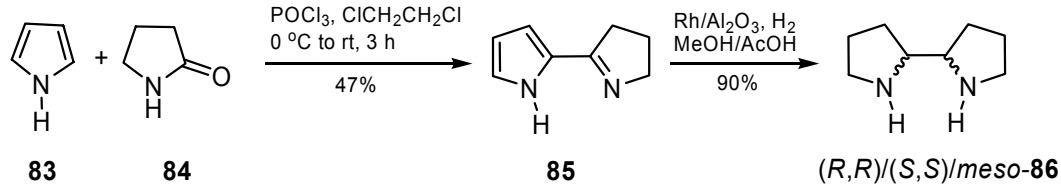

Figure 2.9: Reaction conditions for the synthesis of bispyrrolidine **86**.[156]

An alternative approach to the diastereomeric mixture of 2,2'-bispyrrolidine **86** is the photodimerisation of pyrrolidine **87** in the presence of trace mercury (**Figure 2.10**).[142,157,158] After 10 days at reflux under irradiation, followed by resolution with tartaric acid, the chiral bispyrrolidines (*R*,*R*)- and (*S*,*S*)-**86** were isolated.

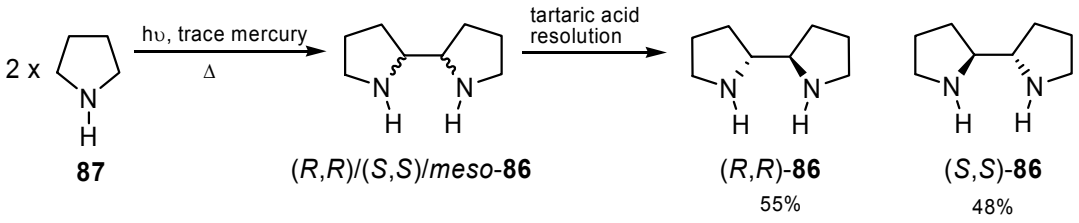

Figure 2.10: Reaction conditions for the photodimerisation of pyrrolidine to form bispyrrolidine **86**. The yields reported in the literature[142,157,158] are presumably based on the maximum possible return of each enantiomer from the diastereomeric mixture.

A diastereomeric synthesis for the dicarbamate *N*,*N*-diBoc-2,2'-bispyrrolidine **92** was developed following the formation of the dimer as a byproduct in the reaction between α-(*N*-carbamoyl)alkylcuprates with aromatic triflates (**Figure 2.11**).[159] The reaction with non-aromatic enol triflates e.g. **89** with Boc-pyrrolidine **88** proceeded smoothly with yields of up to 93% (**Figure 2.11**, **a**). The same reaction conditions however, could not be extended to aromatic triflates **91**, with the major product being the homocoupled bispyrrolidine **92**, as a mixture of diastereomers (**Figure 2.11**, **b**).

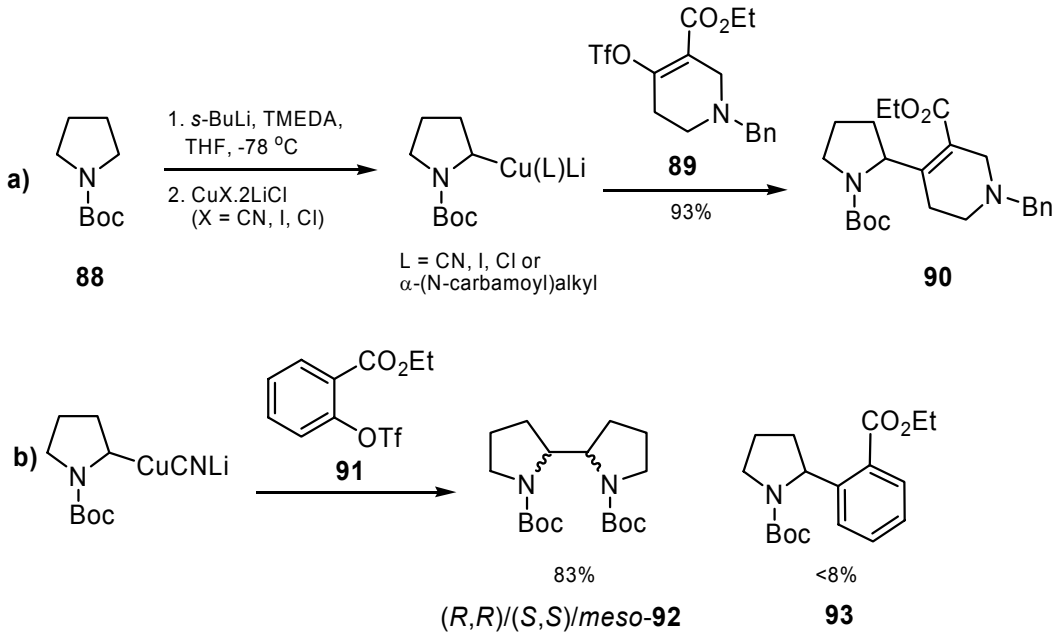

Figure 2.11: Reaction conditions for the coupling of α-(*N*-carbamoyl)alkylcuprates with **a)** enol triflates **b)** aromatic triflates.

This lead to an investigation into the oxidative homo-coupling of α-(*N*-carbamoyl)-alkylcuprates **88**.[160] Depending on the source of Cu^{I} (CuCN, CuI) and the oxidant (I_2, Br_2, NBS), the dimer **92** was formed in up to 98% yield, in ratios of chiral to *meso* diastereomers near unity. The addition of (–)-sparteine provided the α-lithiocarbamate **94** scalemically, which subsequently provided the dimer **92** in enantiomerically enriched form, dependant upon the source of copper (**Table 2.1**).

Table 2.1: Conditions for the copper-mediated oxidative homo-coupling of Boc-protected pyrrolidine **88**, to form a diastereomeric mixture of bispyrrolidine **92**, in enantiomerically enriched form.

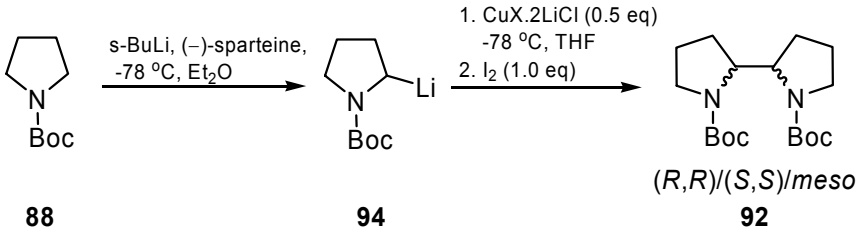

	CuX	yield (%)[a]	*ee* (%)
1	CuCN	60	0
2	CuI	67	8
3	CuBr	50	30

[a]Yield of chiral and *meso* diastereomers.

2.3.3 Enantiospecific strategies towards the 2,2'-bispyrrolidine scaffold

Currently available efficient strategies towards the enantiomeric synthesis of chiral 2,2-bispyrrolidine rely upon chemical manipulation of enantiomerically pure starting materials which provides the bispyrrolidine in high enantiopurity. The disadvantage of such methods is the stoichiometric use of the chiral source, and in the case of the synthetic procedure from chiral amine **95** (**Figure 2.12**) the chiral element is removed at the end. Despite these disadvantages, this method provided (*R*,*R*)-2,2'-bispyrrolidine **86a** in high yield and high enantiopurity.[141] Chiral amine **95** is converted to diamine **96** via reaction with oxalaldehyde, with subsequent allylation occurring diastereoselectively to form *N*,*N*-bis[(*S*)-1-phenylethyl]-(*R*,*R*)-4,5-diamino-1,7-octadiene **97**.[161-163] Double hydroboration gave **98** which cyclised to bispyrrolidine **99** upon addition of mesyl chloride in the presence of triethylamine. Debenzylation using Pearlmann's catalyst and ammonium formate as a hydrogen source, gave the desired (*R*,*R*)-bispyrrolidine **86a** in high enantiopurity (>99% *ee*). The same procedure was not reported for the synthesis of the enantiomeric bispyrrolidine.

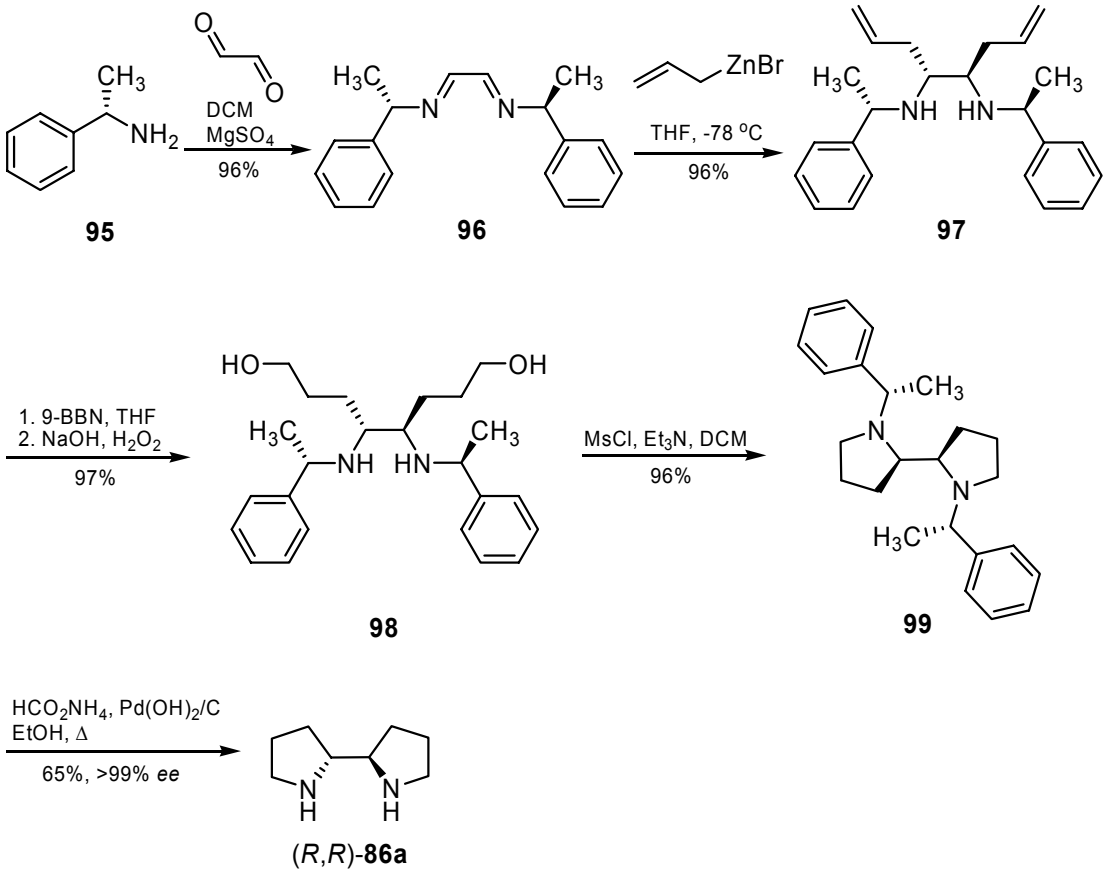

Figure 2.12: Total synthesis of (*R*,*R*)-bispyrrolidine **86a** from chiral amine **95**.

In an alternate procedure, the enantiomerically pure bispyrrolidines (*S*,*S*)- and (*R*,*R*)-**86** were obtained from D- and L-tartaric acid **100** (**Figure 2.13**).[164,165] D-Tartaric is converted to the protected diol **102**, with subsequent triflation providing an appropriate leaving group for the chain-elongation step via reaction with the *tert*-butyl acetate anion, to form the diester **104**. Reduction with lithium aluminium hydride provides the diol **105**. The terminal hydroxy groups were benzyl-protected, and the internal diol was revealed via deprotection under acidic conditions, which were converted to good leaving groups via mesylation. Displacement of the mesylate groups with the azide anion N_3^- under S_N2 conditions provided chiral diazido **108b**, with inversion of stereochemistry. The corresponding Boc-protected amine **109b** was obtained via reduction of the azido groups under a hydrogen atmosphere in the presence of Pd on carbon, and subsequent Boc-protection using Boc anhydride. The terminal hydroxy functionalities were deprotected and mesylated, to provide good leaving groups for the subsequent cyclisation to form Boc-protected 2,2-bispyrrolidine (*S*,*S*)-**92b** in enantiopure form. Removal of the Boc-groups yields the bispyrrolidine (*S*,*S*)-**86b**. Repetition of the entire sequence from L-tartaric acid provides the enantiomeric bispyrrolidine (*R*,*R*)-**86a**.

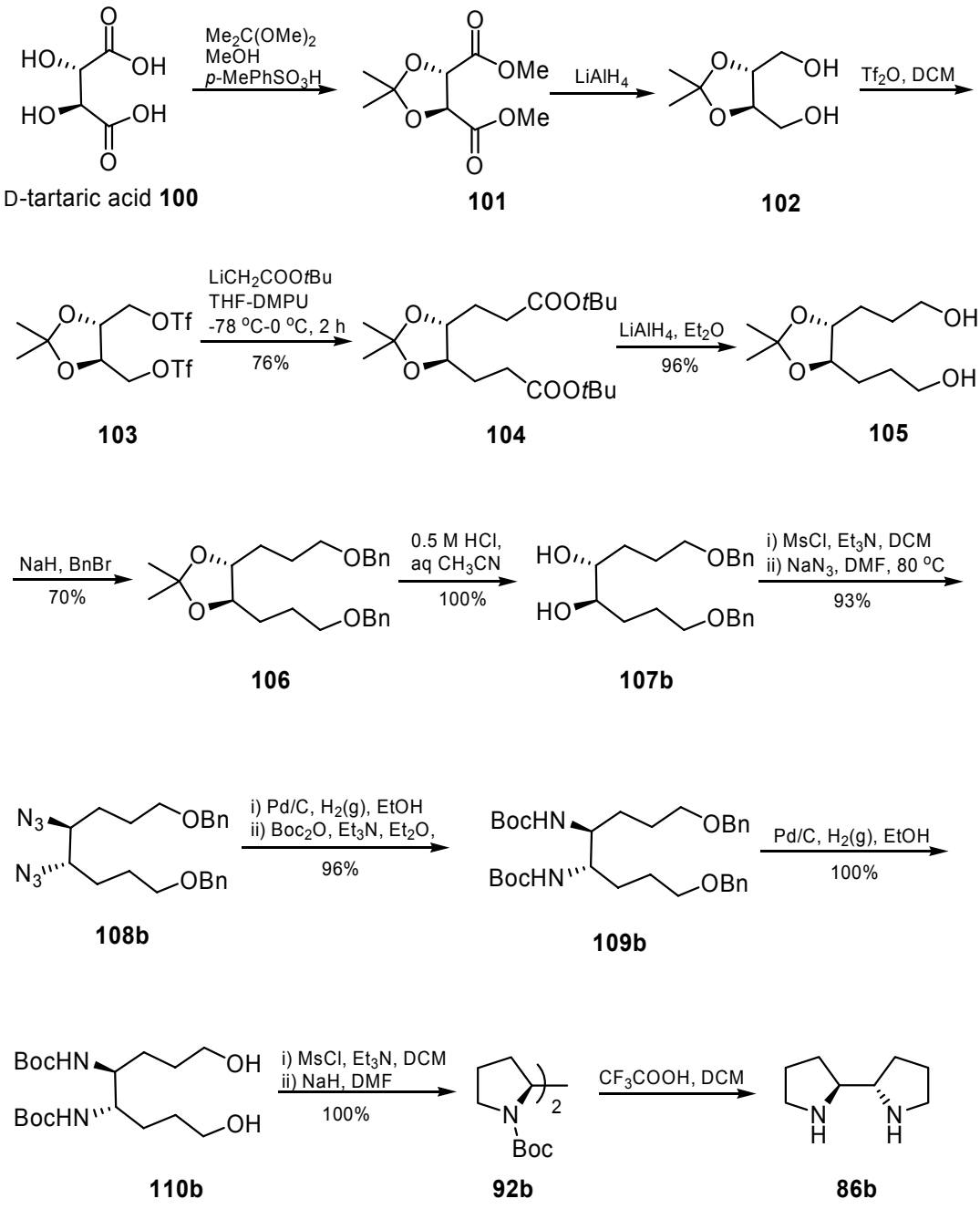

Figure 2.13: Total synthesis of (*S*,*S*)-bispyrrolidine **86b**, from D-tartaric acid.[164,165]

Attempts to synthesise bispyrrolidine **86** via this procedure in our laboratories were unsuccessful.[166] The LDA reaction with *tert*-butyl acetate to provide the corresponding anion for subsequent nucleophilic attack on the ditriflate **103** was unreliable. A success rate of 6% was achieved after 55 attempts. The best results were achieved when the ditriflate **103** was purified via neutral alumina gel column chromatography rather than the slightly acidic silica gel column chromatography reported.

2.3.4 Synthesis of 2,2'-bisindoline

The second target scaffold is chiral 2,2'-bisindoline **112**, which to date has not been used as a chiral ligand. There are no reported enantioselective syntheses to the bisindoline, with only one procedure reported for the formation of a diastereomeric mixture, although the ratios were not reported (**Figure 2.14**).[167] The bisindoline **112** was formed via a radical dimerisation of indoline **111**, in the presence of di-*tert*-butyl peroxide (20 mol %), in 72% yield. Inspection of the reaction mechanism however, reveals that the *t*BuO$^{\bullet}$ radical is required in stoichiometric quantities to indoline; therefore 50 mol % of di-*tert*-butyl peroxide should be used. This leads to doubt over the yield of 72% reported.

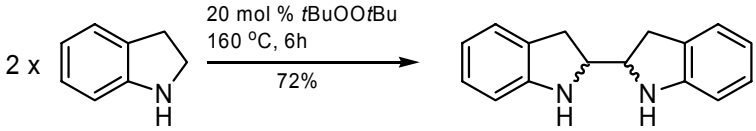

111 (*S*,*S*)/(*R*,*R*)/*meso*-**112**

Figure 2.14: Dimerisation of indoline **111** to form bisindoline **112**.

2.4 Proposed enantioselective synthesis of chiral 2,2'-bis-pyrrolidine and 2,2'-bisindoline

We required a synthetic approach that would satisfy the following criteria:

1. Access to both enantiomers of C_2 symmetric 2,2'-bispyrrolidine **86** from a cheap, achiral starting material.
2. The formation of the stereogenic carbons via a catalytic method.
3. Flexibility of the established procedure to incorporate pyrrolidine ring substitution including the fused aromatic ring system 2,2'-bisindoline **111**.
4. Modification to incorporate alternate heteroatoms to synthesise the diarsine and diphosphine analogues, and the mixed heteroatom systems.

Other than the problems associated with repetition of the procedure experienced in our laboratories, the major disadvantage of the reported synthesis from D- or L-tartaric acid is that the stereogenic carbons in the final product are defined from the use of enantiomerically pure starting material. The entire procedure must be repeated with the alternate enantiomer, to achieve the enantiomeric bispyrrolidine **86**. Despite the

unreliable nature of the preliminary steps of the reported synthesis the chemical manipulations used to complete the synthesis are well known, widely used and high yielding. Therefore, the synthesis proposed for this study would combine modern techniques to establish the chirality of the molecule with subsequent adaptation of the published methodology to complete the synthesis.

The proposed synthesis of chiral (*S*,*S*)- and (*R*,*R*)-2,2'-bispyrrolidine **86** is summarised in **Figure 2.15**. The cheap and readily available 4-penten-1-ol **113** would be protected and dimerised via an **olefin metathesis reaction** using Grubbs 1st or 2nd generation catalyst to form the *trans* octene **115**. Subsequent **asymmetric dihydroxylation (AD)** under Sharpless conditions would yield stereoselectively either enantiomeric chiral diol **123**, which can be converted to the bispyrrolidine **86** via known methodology.[164] The hydroxy groups are converted to a good leaving group via mesylation, and S_N2 displacement with azide forms the diazido compound **117**. The diazido compound is reduced to the amine, followed by Boc-protection. The terminal hydroxyl groups are deprotected and converted to the mesylate leaving group for the final cyclisation step to form the Boc-protected bispyrrolidine **92**. *N*-Deprotection would yield the desired ligand **86**, which can be further functionalised and complexed with palladium or copper for biaryl coupling trials.

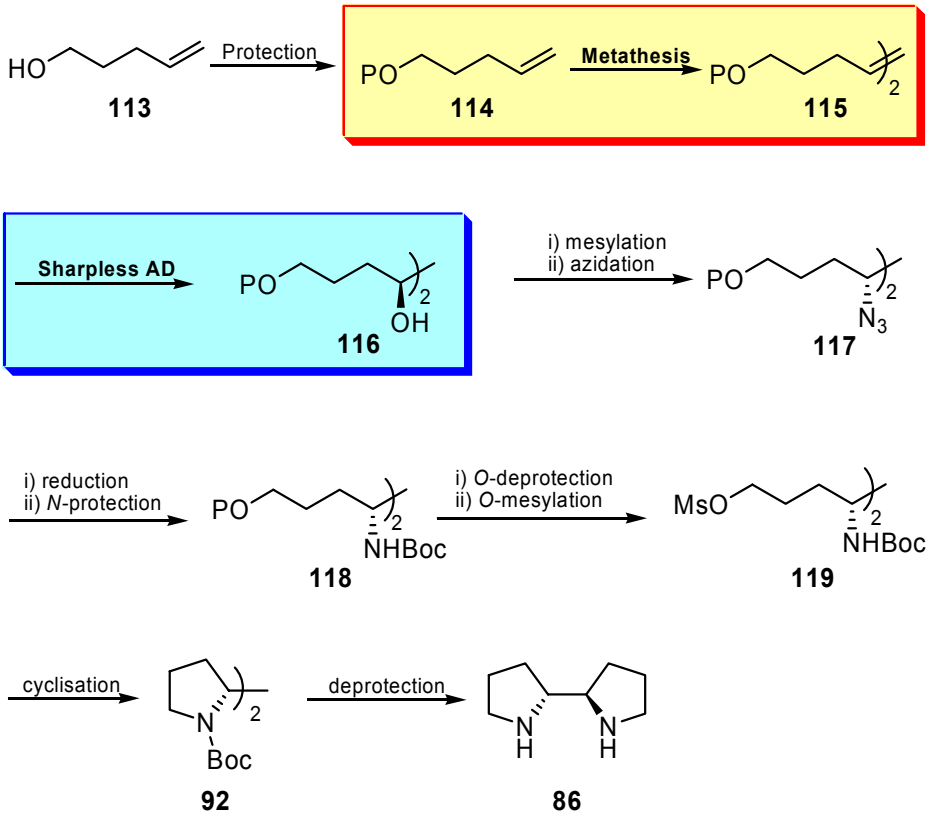

Figure 2.15: The proposed synthesis of the chiral bispyrrolidine ligand **86**.

The key steps are the reliable **metathesis** and **asymmetric dihydroxylation** reactions. The thermodynamically favourable *trans* alkene is formed in the intermolecular self-metathesis (SM) reaction. The two stereogenic carbons can be formed selectively via the ubiquitously used Sharpless asymmetric dihydroxylation (AD). Two preformed AD mixes (α and β) are commercially available, with each one yielding enantiomeric forms of the diol, which in turn will provide the enantiomeric forms of the bispyrrolidine ligand.

The introduction of the heteroatom occurs via an S_N2 mechanism, which conserves the enantiomeric purity obtained from the AD reaction. The incorporation of the heteroatom is part way through the synthesis. Other nucleophiles (e.g. As or P) can potentially be introduced to obtain alternative ligands, for example the arsine and phosphine analogues.

One of the advantages of the synthetic route to the bispyrrolidine scaffold is the ability to alter the substituents on the pyrrolidine rings, by selecting the appropriate substrate for the metathesis dimerisation. For example, to synthesise the fused ring bisindoline

system **112** (**Figure 2.16**), the synthesis could be performed via the self-metathesis of protected 2-allylphenol **121**, to form the homodimer **122**. Subsequent asymmetric dihydroxylation (AD) under Sharpless conditions would yield the chiral diol **123**. The nitrogen heteroatom would be introduced in an analogous method to that of the bispyrrolidine synthesis, to form the diazido compound **124**. With the Boc-protected derivative **125** in hand, the protected phenolic OH could be converted to the triflate **126**, with subsequent amination[168,169] yielding the cyclised bisindoline **127**. Deprotection would provide the chiral 2,2-bisindoline **112**. The similarity in chemistry to the established bispyrrolidine **92** synthesis would render this a suitably efficient synthesis. This would represent the first stereoselective synthesis of chiral (*S*,*S*)- or (*R*,*R*)-2,2'-bisindoline **112**.

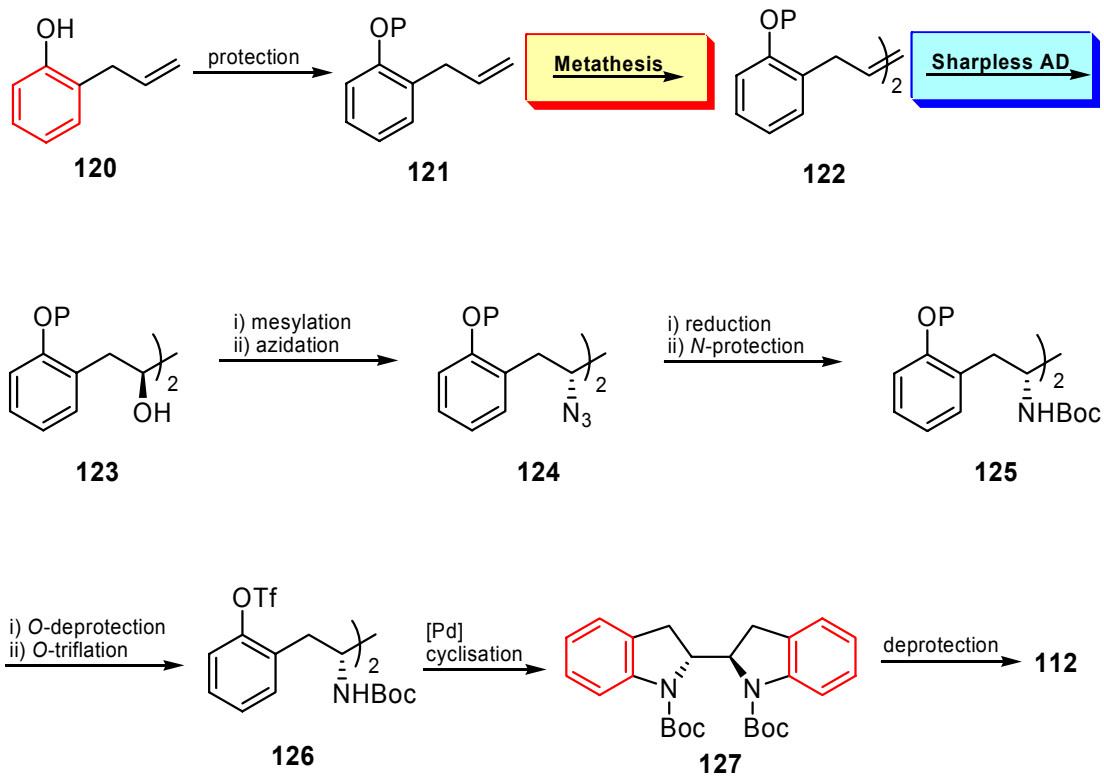

Figure 2.16: Proposed synthesis of 2,2'-bisindoline **112**.

CHAPTER 3
The Synthesis of Chiral 2,2'-Bispyrrolidine

The first target was 2,2'-bispyrrolidine **86** for which the strategy is outlined in **Figure 2.15**, where P = Bn.

3.1 Protection of 4-penten-1-ol

One of the advantages of the first key step of the synthesis, the metathesis reaction, is high functional group tolerance. There is conflicting evidence however, of metathesis reactions where a free hydroxy group is present.[170-172] This, combined with the intolerance of free hydroxy groups to subsequent reaction steps, lead to the necessity of *O*-protection as the first step. The choice of protecting group was limited to those that would be stable to the basic conditions of the AD reaction, stable to the reductive conditions of the azidation, and could be selectively removed in preference to the nitrogen protecting group. A simple benzyl ether fulfils such criteria and additionally provides a UV active marker, contributing to reaction monitoring and product purification.

Therefore, benzyl protection of 4-penten-1-ol **113** (**Scheme 3.1**) was achieved by deprotonation of the alcohol using NaH, followed by addition of benzyl bromide, in a typical S_N2 reaction. The converse reaction, in which benzyl alcohol is deprotonated and reacted with 5-bromo-1-pentene, was also successful, however yields not greater than 60% were obtained.

Scheme 3.1: Benzyl protection of 4-penten-1-ol **113**.

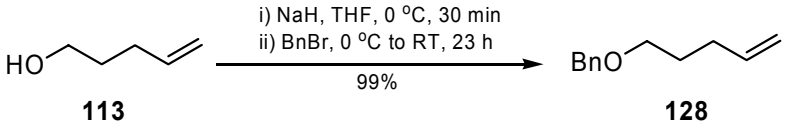

The ^{1}H NMR spectrum of **128** showed a peak at 4.50 ppm of integral 2H assigned to the benzylic CH_2 protons and a multiplet of integral 5H in the aromatic region, assigned to the monosubstituted benzene ring, which was a recurring marker throughout the synthesis. Three sets of peaks at 4.93-4.98, 4.99-5.05 and 5.82 ppm were present in the ^{1}H NMR spectrum, assigned to H_Z, H_E and H_A, characteristic of a terminal alkene. Although a characteristic splitting pattern for allylic systems, the peaks are generally reported as multiplets without any reference to coupling constants. Owing to the high use of such systems in this thesis, the peaks assigned to the allylic protons are described in greater detail.

The sp^2 hybridised methine proton H_A exhibits three sets of coupling, giving a ddt splitting pattern (**Figure 3.1**), which result in a characteristic set of peaks in the ^{1}H NMR spectrum.

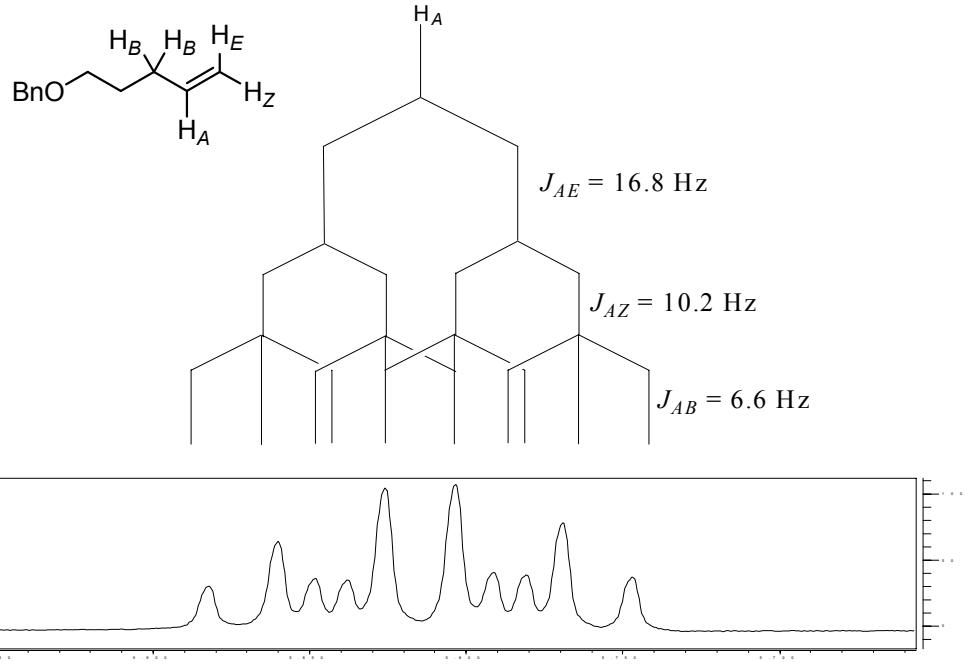

Figure 3.1: Tree-diagram showing the splitting pattern of the sp^2 hybridised methine proton characteristic of mono-substituted terminal alkenes, and the resultant peak in the ^{1}H NMR spectrum, at 5.82 ppm.

The coupling experienced by the two terminal protons H_E and H_Z also gives rise to a characteristic set of peaks in the ^{1}H NMR. The proton H_E *trans* to the methine proton H_A exhibits a larger coupling constant (16.9 Hz) than the corresponding *cis* coupling (10.2 Hz) (**Figure 3.2**) allowing the assignment of H_E to the multiplet further downfield. Analysis of the gHSQC NMR spectrum confirms the assignment of these protons to the two terminal protons, since both sets of peaks show a correlation to a single carbon.

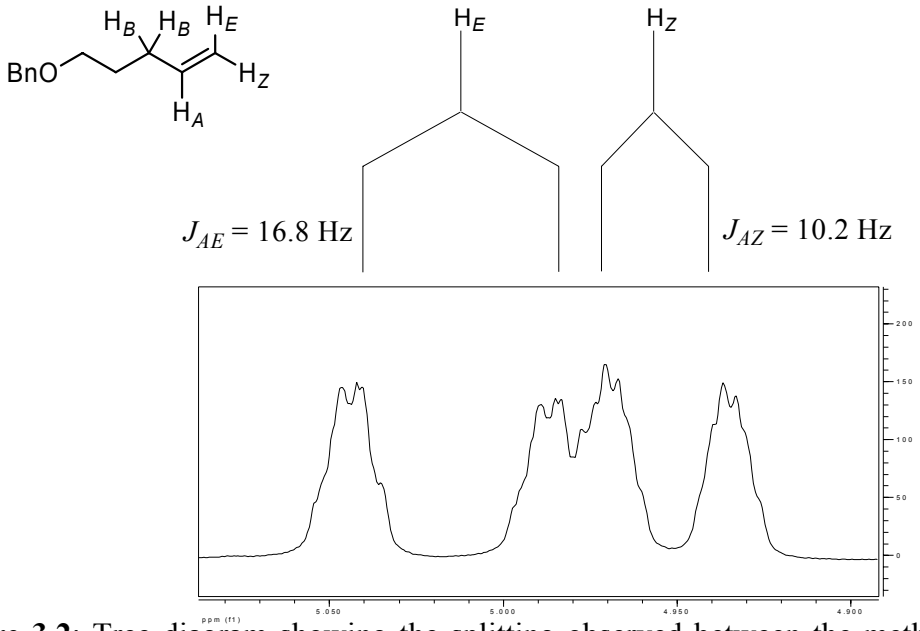

Figure 3.2: Tree diagram showing the splitting observed between the methine proton and the two terminal protons, with both *E* and *Z* coupling constants, and the resultant peaks in the ^{1}H NMR spectrum.

3.2 Metathesis of protected 4-penten-1-ol (Key Step 1)

With the pentenol suitably protected, dimerisation to the protected 4-octenol **129** could be attempted. Therefore, Grubbs 1st generation catalyst was added to a solution of protected alkene **128** in DCM under a N_2(g) atmosphere, and the reaction mixture was heated at reflux for 5 hours (**Scheme 3.2**). The solvent was removed *in vacuo* and the crude mixture was adsorbed onto silica gel. Subsequent column chromatography gave **129** in 75% yield, and the metathesis side product **130** in 5% yield.

Scheme 3.2: The self-metathesis of protected pentenol **128** to form the homo-dimerised product **129** and the cross-metathesis by-product **130**, with evolution of ethene gas. Selected chemical shifts are quoted in ppm.

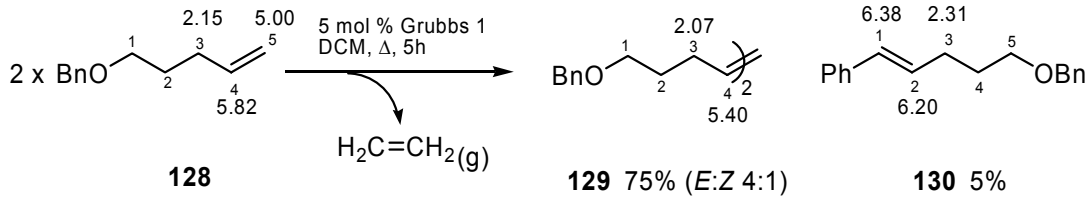

128 **129** 75% (*E*:*Z* 4:1) **130** 5%

The multiplet at 5.38-5.41 ppm in the ^{1}H NMR spectrum of the dimer **129** was assigned to the methine H4 proton, shifted upfield from 5.82 ppm in the ^{1}H NMR of the starting material **128**. The peaks assigned to the terminal CH_2 protons H5 and the corresponding carbon C5 in the NMR spectra of the monomer **128** were absent from that of the dimer **129**. The peak at 130.0 ppm in the ^{13}C NMR of the dimer **129** was assigned to the methine carbon C4. The simplicity of both the ^{1}H and ^{13}C NMR spectra supported the formation of a symmetrical molecule. Further evidence was provided by CI-MS, which contained a peak at *m/z* 325 assigned to the M+H ion.

Inspection of both the ^{1}H and ^{13}C NMR spectra highlighted the presence of both geometric isomers, in a ratio of 5:1, determined by integration of the peaks at 2.10-3.04 ppm corresponding to the methylene protons H3 adjacent to the double bond, which partially resolved. ^{1}H NMR analysis could not identify which isomer was in excess, due to the overlapping of peaks assigned to the methine protons H4 from each isomer, although it was assumed that the thermodynamically more stable *trans* geometry would be favoured. Analysis of TLC using a range of solvent systems could not resolve the two isomers. Owing to the large number of alkenes as mixtures of geometric isomers synthesised in this thesis, a definitive method for the identification of the *cis* and *trans* isomers was required. This was achieved via ^{13}C NMR analysis. The chemical shifts of methylene carbons adjacent to the double bond in *cis* and *trans* isomers of disubstituted alkenes are different.[173,174] Application of this phenomenon to **129** shows that the C3 carbon in the *cis* isomer is slightly shielded relative to C3 in the *trans* isomer, due to the γ effect from the protons H3 on the alternate side of the double bond, and therefore is shifted further upfield (**Figure 3.3**). Therefore, the peak at 23.7 ppm in the ^{13}C NMR spectrum is assigned to C3 of the *cis* isomer; the peak at 29.0 ppm is assigned to C3 of the *trans* isomer. Subsequently, the assignment of H3 of the *cis* and *trans* isomers was

determined through gHSQC ^{13}C-^{1}H correlations. Hence, the ratio of *trans*:*cis* isomers was determined.

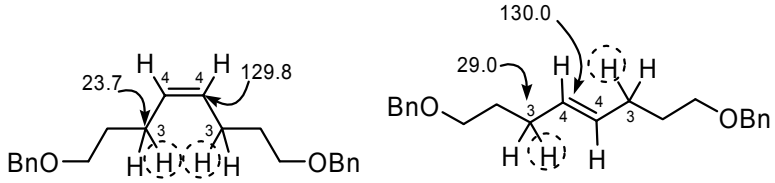

Figure 3.3: ^{13}C NMR chemical shifts (in ppm) exhibited by the methine C4 and adjacent methylene carbons C3 in the *cis* and *trans* isomers of **129**.

The ^{1}H NMR spectrum of pentene **130** (**Scheme 3.2**) showed a doublet at 6.38 ppm of integration 1H, with a coupling constant of 15.8 Hz, assigned to the vinylic proton H1. A peak at 6.20 ppm of integration 1H exhibited a coupling constant of 15.8 Hz, and was assigned to the H2 proton. This substitution pattern and coupling constants are typical of a *trans* vinylic aromatic system.[175] A singlet at 4.51 ppm of integration 2H was assigned to the benzylic protons and a peak at 2.31 was assigned to the H3 protons, adjacent to the double bond. A peak at 3.48 ppm was assigned to the H5 protons, adjacent to the ether oxygen, and a multiplet at 1.75-1.84 ppm was assigned to the H4 protons.

Alkene metathesis, or redistribution of carbon-carbon double bonds, has become a viable and widely used method in organic synthesis, due mainly to the commercial availability of highly active, yet air and moisture stable catalysts, such as Grubbs 1st **131** and 2nd **132** generation ruthenium catalysts (**Figure 3.4**), replacing molybdenum ligands which require inert atmospheres and rigorously purified, dried and degassed solvents and reagents.[176] These ligands show a high functional group tolerance, including alcohols, acids, aldehydes, ketones, esters and amides, resulting from the higher reactivity of ruthenium to the alkene double bond.[176] The most commonly used types of metathesis reactions include ring closing metathesis (RCM) and ring opening metathesis polymerisation (ROMP). The use of the intermolecular metathesis reactions, such as cross-metathesis (CM) and self-metathesis (SM) is less common, as general reaction conditions giving high yield and good *trans*/*cis* selectivity have yet to be developed.[170,172,177]

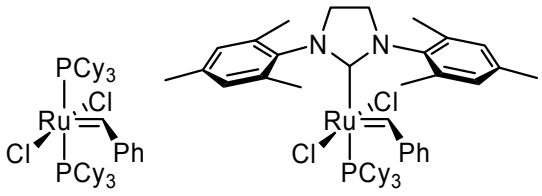

131 **132**

Figure 3.4: Structure of the ubiquitously used Grubbs 1st **131** and 2nd **132** generation catalysts.

The metathesis reaction involves a series of reversible [2+2] cycloadditions and cycloreversion steps, resulting in a complex set of intermediates in equilibrium. The self-metathesis reaction mechanism for terminal alkene **128** is outlined in **Figure 3.5**. The first step of the cycle [not drawn] is the dissociation of PCy_3.[178] This yields the active form of the catalyst **G*** that can coordinate to the alkene to form either of the isomeric forms of the corresponding ruthenacyclobutane intermediate **133** or **138**. The isomeric conformation (**133** or **138**) determines at which point the primary catalytic cycle is entered. The *cis* isomer **133** leads to **Entry Pathway 1**, in which by-product **130** is released, and the highly activated carbene complex **134** is formed. Subsequent [2+2] addition of the terminal alkene **128** provides ruthenacyclobutane **136**, which upon release of ethene gas gives the new carbene complex **137**. [2+2] Cycloaddition of a second molecule of terminal alkene **128** provides the 'dimeric' ruthenacyclobutane **135**, which upon reverse cycloaddition releases the desired dimer **129** and the active carbene complex **134**. The formation of the *trans* ruthenacyclobutane isomer **138** enters the catalytic cycle via **Entry Pathway 2**, through the release of styrene. The equilibrium of the catalytic cycle is shifted towards the formation of the homodimer **129** by the evolution of ethene gas.

Mono and disubstituted terminal alkenes undergo SM readily, due to the high reactivity of the ruthenium-carbene complexes. Sterically encumbered substrates cannot undergo SM, but can undergo cross-metathesis (CM) with simpler terminal alkenes.

The initiation step – the dissociation of the PCy_3 ligand to form the active form of the catalyst – is dependent upon the solvent. The rate is increased by 30% by using DCM as the solvent instead of toluene.[171] Therefore, all metathesis reactions were performed in halogenated solvents.

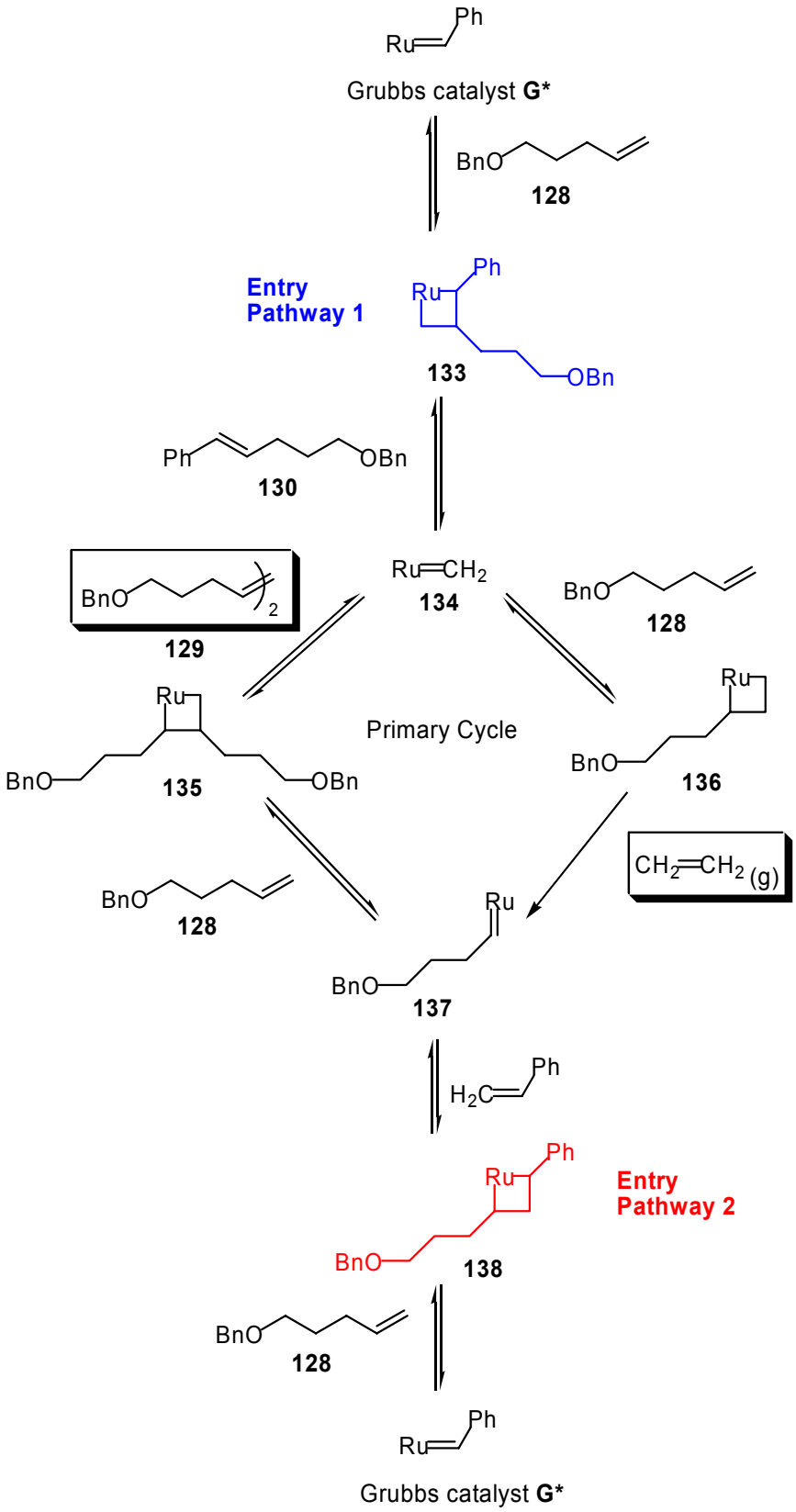

Figure 3.5: The catalytic cycle of the self-metathesis reaction of **128**, showing the entry pathways of the activated Grubbs catalyst **G***, into the catalytic cycle. Ligands of the Ru complexes are omitted for clarity.

In an effort to optimise the *E*:*Z* ratio, a series of reaction conditions were trialled (**Table 3.1**).

Table 3.1: Optimisation of the self-metathesis of **128** to form the dimer **129**. Reactions are performed in DCM at 40 °C, with 5 mol % Grubbs 1 catalyst, under a N_2(g) atmosphere.

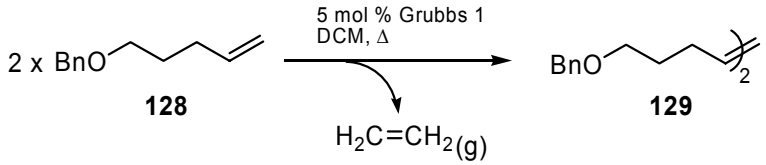

	Reaction time (h)	**129** yield (%)[a]	*E*:*Z*[b]
1	45	58	4.4:1
2	28	68	n.m.[d]
3	24	79	4.5:1
4	17	72	n.m.[d]
5	7	85	3.7:1
6	5	75	4:1
7	28[c]	74	4:1

[a]Isolated yield. [b]Determined by ^{1}H NMR. [c]3.5 mol % Grubbs 1 catalyst was used. [d]Not measured.

An increase in reaction time resulted in a slight increase of the *trans*:*cis* ratio of **129** (entry 1 vs. 5). Although an increase in reaction temperature would intuitively increase the amount of the more thermodynamically stable isomer, it is known that Grubbs 1 is intolerant to temperatures of higher than 50 °C, and as such an increase in temperature was not trialled as a method for increasing the ratio of geometric isomers. Studies into the decomposition rate of the catalyst[171] has shown that monitoring the *trans*:*cis* ratio of the self-metathesis product is an indication of the rate of catalyst decomposition, since as long as the catalyst is active the more sterically accessible *cis* product will be converted to the *trans* product. As can be seen from the table, the *trans*:*cis* ratio did not substantially increase with time, indicating that the catalyst had decomposed.

Interestingly, the chemical yield significantly decreased with time (entries 1 and 2 vs. 5 and 6), resulting from the formation of unwanted secondary metathesis products, such as the CM between either the monomer **128** or the dimer **129** with the styrene from the

Grubbs catalyst, to form **130** (**Figure 3.5**). Since only 5 mol % of catalyst was used, the maximum amount of styrene available for this side product to form was 5 mol %. Documented side products from the metathesis reaction include double bond migration.[171,172,179,180] Many other unidentified side products were obtained. Although not characterised, ^{1}H NMR analysis showed many peaks, indicating the formation of unsymmetrical side products. A decrease in catalyst loading (entry 7) gave the same chemical and stereochemical result as the reaction with 5 mol % catalyst for a shorter time.

The mixture of geometric isomers was taken through to the next step of the reaction sequence, with the anticipation that separation of isomers could be easier upon functionalisation of the double bond.

3.3 Sharpless asymmetric dihydroxylation (Key Step 2)

The dihydroxylation of olefins by osmium tetroxide is widely accepted as one of the most versatile methods for functionalisation of organic molecules.[181] The development of a catalytic and asymmetric methodology by Sharpless and coworkers has lead to the efficient and reliable synthesis of chiral 1,2-diols.[3] The extensive work on the Sharpless asymmetric dihydroxylation (AD) has produced a protocol using two commercially available premixes, AD mix α and β, which both contain $K_2OsO_2(OH)_4$ as a non-volatile source of OsO_4, $K_3Fe(CN)_6/K_2CO_3$ as the stoichiometric reoxidant and a biscinchona alkaloid moiety as the chiral ligand, $(DHQ)_2PHAL$ (α) and $(DHQD)_2PHAL$ (β). The biscinchona alkaloid moieties consist of two dihydroquinoline (DHQ) or the diastereomeric dihydroquinidine (DHQD) based subunits, separated by a phthalazine linker (PHAL). The Sharpless protocol is performed under biphasic conditions (*t*BuOH/H_2O), with the addition of methanesulfonamide for more sterically demanding substrates, e.g. 1,2-disubstituted alkenes, to increase the hydrolysis of the osmate (VI) ester and therefore, increasing the catalytic turnover. Despite the mechanistic uncertainties, under these standard conditions, the stereochemistry of the resultant chiral diol can be predicted using a reliable mnemonic, as depicted in **Figure 3.6**.

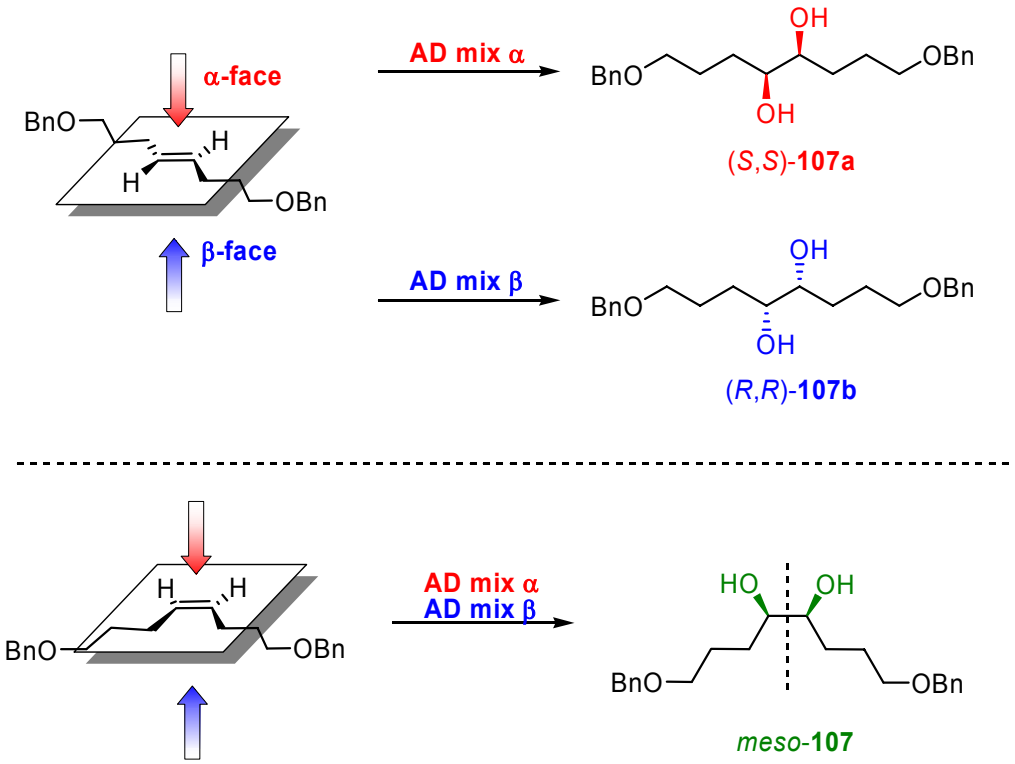

Figure 3.6: Predicted outcome of the Sharpless asymmetric dihydroxylation of alkene **129** using either AD mix α or AD mix β.

The OsO_4 bound DHQ based ligand, present in AD mix α, will bind to the *trans* olefin **129** from the top face as drawn, resulting in the (*S*,*S*)-**107a** diol. The use of AD mix β will result in the enantiomeric diol (*R*,*R*)-**107b** diol, via dihydroxylation of the bottom enantioface. Due to its symmetrical nature, the dihydroxylation of the *cis* alkene from either face will result in the optically inactive *meso*-**107** diastereomer.

Therefore, a mixture of alkene **129** (*E*:*Z*, 4.4:1) was reacted under Sharpless AD conditions, using AD mix α and methanesulfonamide in a 1:1 mixture of *t*BuOH and water, for 24 hours (**Scheme 3.3**). The reaction was quenched with sodium sulfite, and following a workup of 2M KOH (to remove the methanesulfonamide),[3] and sat. NaCl, the crude oil was subjected to gravity silica gel column chromatography to yield the (*S*,*S*)-diol as a mixture of chiral and *meso* diastereomers (4.9:1), in overall 86% yield and 80% *ee*.[†] The optical rotation of a 3.4:1 chiral:*meso* diastereomeric mixture was –13.8° (*c* 0.08, $CHCl_3$). The presence of the optically inactive *meso* isomer decreases

[†] Enantiomeric excess was determined via chiral HPLC analysis. The areas of peaks assigned to the (*S*,*S*)- and (*R*,*R*)-diols were compared, i.e. disregarding the peak assigned to the *meso*-diol. This is discussed in detail in *Section 3.3.1*.

the rotation obtained from the mixture, and hence cannot confirm the *ee* by comparison with the literature.[164] It does however confirm the formation of the (*S*,*S*) enantiomer, which has a negative optical rotation.

Scheme 3.3: Asymmetric dihydroxylation under Sharpless conditions of the 4-octene **129** to form the chiral diol (*S*,*S*)-**107a**.

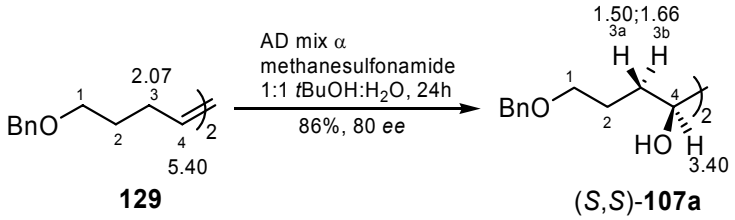

129 (*S*,*S*)-**107a**

The multiplet assigned to the vinylic protons H4 at 5.38-5.41 ppm in the ^{1}H NMR and the peak at 130.0 ppm assigned to the corresponding carbon C4 in the ^{13}C NMR of the alkene **129** had shifted upfield to 3.40 ppm and 74.1 ppm respectively, indicating a change in hybridisation from sp^2 to sp^3. A broad singlet with a relative integration of 2H in the ^{1}H NMR at 3.07 ppm was assigned to the two hydroxy substituents. The relatively simple spectra obtained confirmed the retention of symmetry. The formation of stereogenic atoms was clear from the appearance of two sets of peaks in the ^{1}H NMR at 1.44-1.56 and 1.60-1.73 ppm, which correlated to a single carbon peak at 30.8 ppm in the ^{13}C NMR. This occurrence is characteristic of diastereotopic protons adjacent to a stereogenic carbon.

Similarly, alkene **129** (*E*:*Z*, 4:1) was reacted with the alternate chiral ligand in AD mix β to yield the enantiomeric diol (*R*,*R*)-**107b** in 80% yield, as a mixture of chiral:*meso* diastereomers (4:1), with an *ee* of 98% (**Scheme 3.4**). As expected, the spectral properties of the enantiomer were identical to that of (*S*,*S*)-**107a**. The fact that the chiral:*meso* ratio was identical to the *E*:*Z* ratio of the starting alkene **129** indicates a lack of preference for the *trans* or *cis* isomer in the active site of the AD reaction, with this particular system.

Scheme 3.4: Asymmetric dihydroxylation under Sharpless conditions of the 4-octene **129** to form the chiral diol (*R*,*R*)-**107b**.

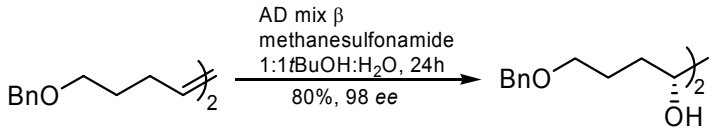

129 (*R*,*R*)-**107b**

3.3.1 Determination of enantiomeric excess via HPLC analysis

Direct comparison of reported optical rotations could not be made, due to the presence of the optically inactive *meso* diol **107** in samples of the chiral diols (*S*,*S*)-**107a** and (*R*,*R*)-**107b**. Therefore, the enantiomeric purity of the chiral diols (*S*,*S*)-**107a** and (*R*,*R*)-**107b** was determined via chiral HPLC analysis, although the presence of the *meso* isomer resulted in three peaks in the resultant chromatograms.

HPLC analysis of **107a** (3.4:1, chiral:*meso*) showed peaks at t_R 20.4 min, 21.4 min and 23.3 min assigned to (*R*,*R*)-**107b**, *meso*-**107** and (*S*,*S*)-**107a** respectively (**Figure 3.7**, **a**). Comparison of the analyte peak areas of the peaks assigned to (*R*,*R*)-**107b** and (*S*,*S*)-**107a** showed a ratio of 10:90, corresponding to an enantiomeric excess of 80% of the (*S*,*S*)-diol **107a**.

A second sample of **107a** (14:1, chiral:*meso*) was analysed via HPLC analysis under the same conditions (**Figure 3.7**, **b**), which displayed three peaks with identical retention times of 20.4, 21.5, 23.3 min, assigned to the (*R*,*R*)-, *meso*- and (*S*,*S*)-diols. Again, comparison of the analyte peak areas revealed the *ee* of (*S*,*S*)-**107a** to be 80%. As expected, the relative area of the peak at t_R 21.5 min assigned to *meso*-**107** was significantly reduced, due to the increased ratio of chiral:*meso* **107** (3.4:1 to 14:1).

A third sample, which contained only chiral **107** as determined by ^{1}H NMR analysis was analysed via HPLC (**Figure 3.7**, **c**). The chromatogram revealed two peaks, at t_R 20.4 and 23.2 min assigned to the (*R*,*R*) and (*S*,*S*) chiral diols. The absence of a peak at t_R 21.4 min confirmed the assignment of this peak in the previous chromatograms to the *meso*-diol. The ratio of the remaining two peaks confirmed the *ee* of the (*S*,*S*)-diol to be 80%. The isolation of chiral **107** required three successive columns, with only 1 mg of

chiral **107** obtained from a 60 mg sample. As baseline separation was achieved between the chiral and *meso* diols the time consuming removal of the *meso* impurity was not pursued for subsequent AD reactions, since the *ee* could be determined from the HPLC analysis of the diastereomeric mixture.

a) 107 (chiral:*meso*, 3.4:1)

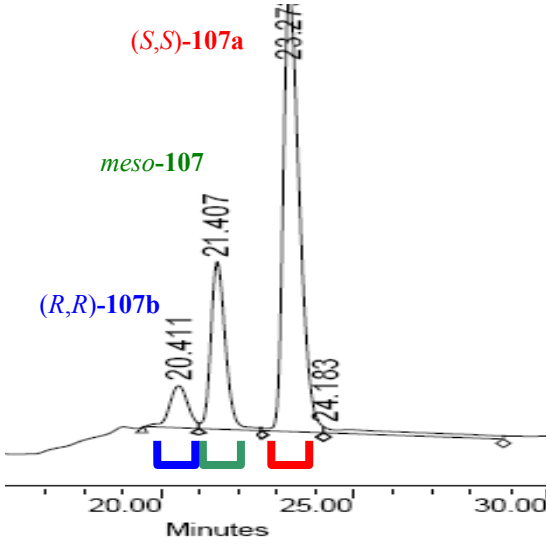

b) 107 (chiral:*meso*, 14:1)

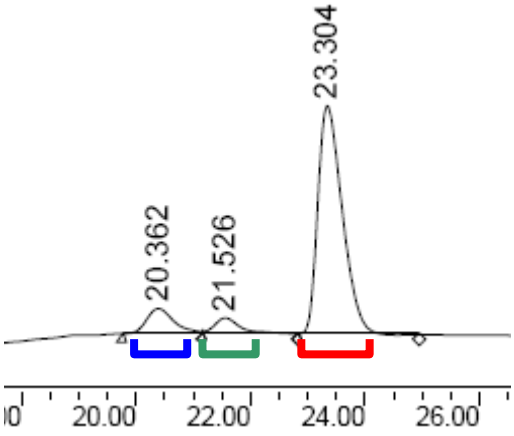

c) 107 (chiral only)

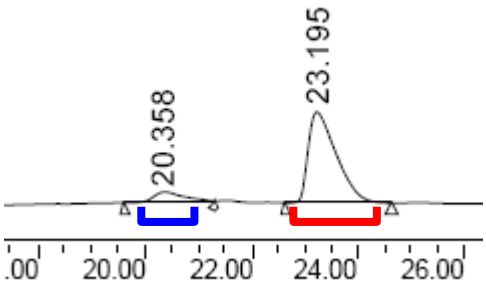

Figure 3.7: HPLC traces obtained from diastereomeric mixtures of diol **107a**. Traces were obtained on a Daicel Chiralcel OD-H chiral column (4.6 x 250 mm) using a gradient elution system (20% to 40% isopropanol:hexane, flow rate 0.5 mL/min) and a UV detector (254 nm). The horizontal scale (minutes) is displayed.

Therefore, the outcome of these HPLC experiments showed that the second peak could be assigned to the *meso* isomer, while further evidence was required to confirm the assignment of the first and third peaks to (*R*,*R*)- and (*S*,*S*)-**107** respectively. Injection of a sample of diol (*R*,*R*)-**107b** obtained from the AD reaction using AD mix β, should show an increase in the area of the peak assigned to (*R*,*R*)-**107b** and a decrease in the peak assigned to (*S*,*S*)-**107a**. The same solvent system used in **Figure 3.7** was not sufficient for the analysis of this alternate sample, as the area of the peak corresponding to (*S*,*S*)-**107a** was so small (due to a large *ee*), that further optimisation of the solvent system was required for determination of the *ee*.

Therefore, HPLC analysis of (*S*,*S*)-**107a** (chiral:*meso*, 3.4:1) was repeated using a less polar gradient elution (10% to 40% isopropanol:hexane), to increase separation between the peaks assigned to the (*R*,*R*)- and *meso*-diols (**Figure 3.8, a**). The peaks at t_R 30.8, 32.1 and 33.9 min were assigned to (*R*,*R*)-, *meso*- and (*S*,*S*)-**107**, respectively. Comparison of the peaks assigned to the chiral diols confirmed the *ee* of (*S*,*S*)-**107a** was 80%.

HPLC analysis of the enantiomeric diol (*R*,*R*)-**107b** (15:1, chiral:*meso*) using the same conditions indicated the presence of three peaks, at t_R 30.5, 32.8 and 34.7 min assigned to (*R*,*R*)-, *meso*- and (*S*,*S*)-**107** (**Figure 3.8, b**). The major peak, as expected, was the peak at 30.5 min, assigned to (*R*,*R*)-**107b**. Comparison of the peaks assigned to the two chiral diols showed that the *ee* of (*R*,*R*)-**107b** was 98%.

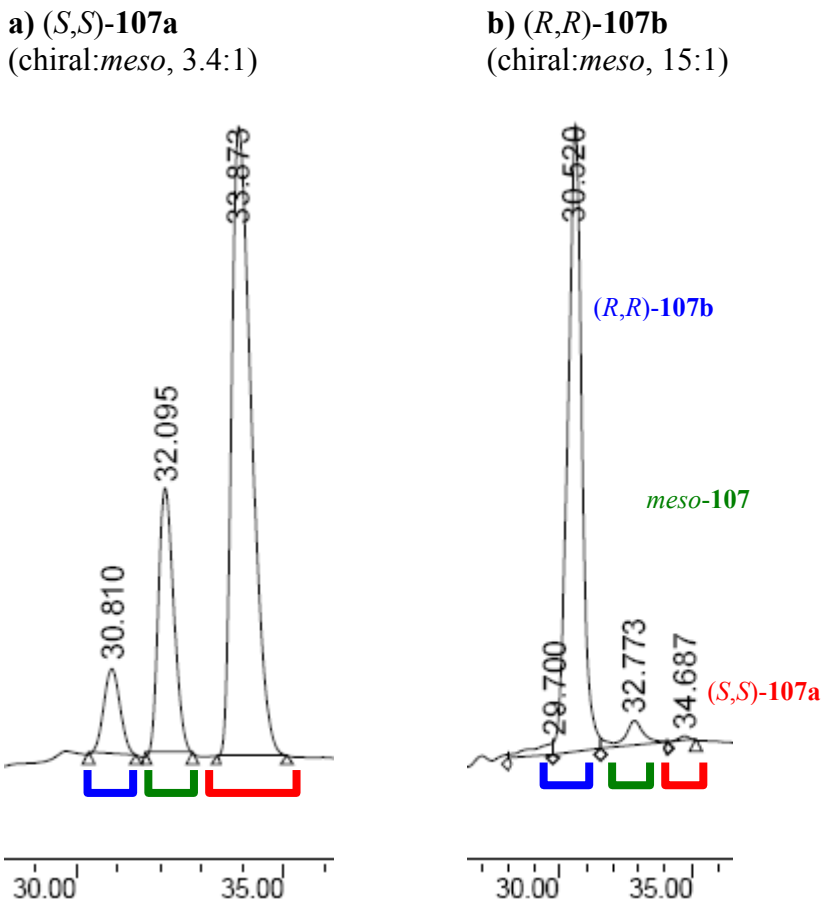

Figure 3.8: HPLC traces (10% to 40% isopropanol:hexane, flow rate 0.5 mL/min) obtained from diastereomeric mixtures of **a)** diol (*S*,*S*)-**107a** and **b)** diol (*R*,*R*)-**107b**.

Attempts to separate the chiral and *meso* isomers on a preparatively useful scale were unsuccessful, either by TLC or column chromatography. Therefore, the reaction sequence was continued with the diastereomeric mixture, until separation was possible.

3.3.2 Mechanism of the Sharpless AD

The Sharpless AD protocol has been extensively and successfully applied to the synthesis of many synthetic targets.[3,153] The versatility results from the selectivity of OsO_4 towards olefins with a range of additional functional groups, the ease of experimental procedure as a result of the AD premixes and the predictability of the stereochemical outcome. The development of biphasic conditions was pivotal in the realisation of high enantioselectivity, by preventing entry into the second catalytic cycle. The mechanism of biphasic catalytic dihydroxylation developed by Sharpless is outlined in **Figure 3.9**. OsO_4 is released into the organic layer from the inorganic

osmium(VIII) complex **141**, and binds to the olefin *E*-**129** and the chiral ligand **L*** to form the osmium(VI) glycolate ester **139**. The osmate is hydrolysed to release the chiral diol (*R*,*R*)-**107b** and the ligand, while the inorganic osmium(VI) complex **140** is released into the aqueous layer. Hydrolysis is accelerated through the use of one equivalent of methanesulfonamide, for sterically congested substrates, which acts a nucleophile towards the ester. The inorganic osmium(VI) complex **140** is oxidised by $K_3Fe(CN)_6$ to regenerate the osmium(VIII) complex, thereby generating a cycle, catalytic with respect to osmium. The hydrolysis of the osmate **139** into the aqueous layer prevents the addition of a second olefin molecule, thereby preventing entry into the second, less enantioselective, cycle.

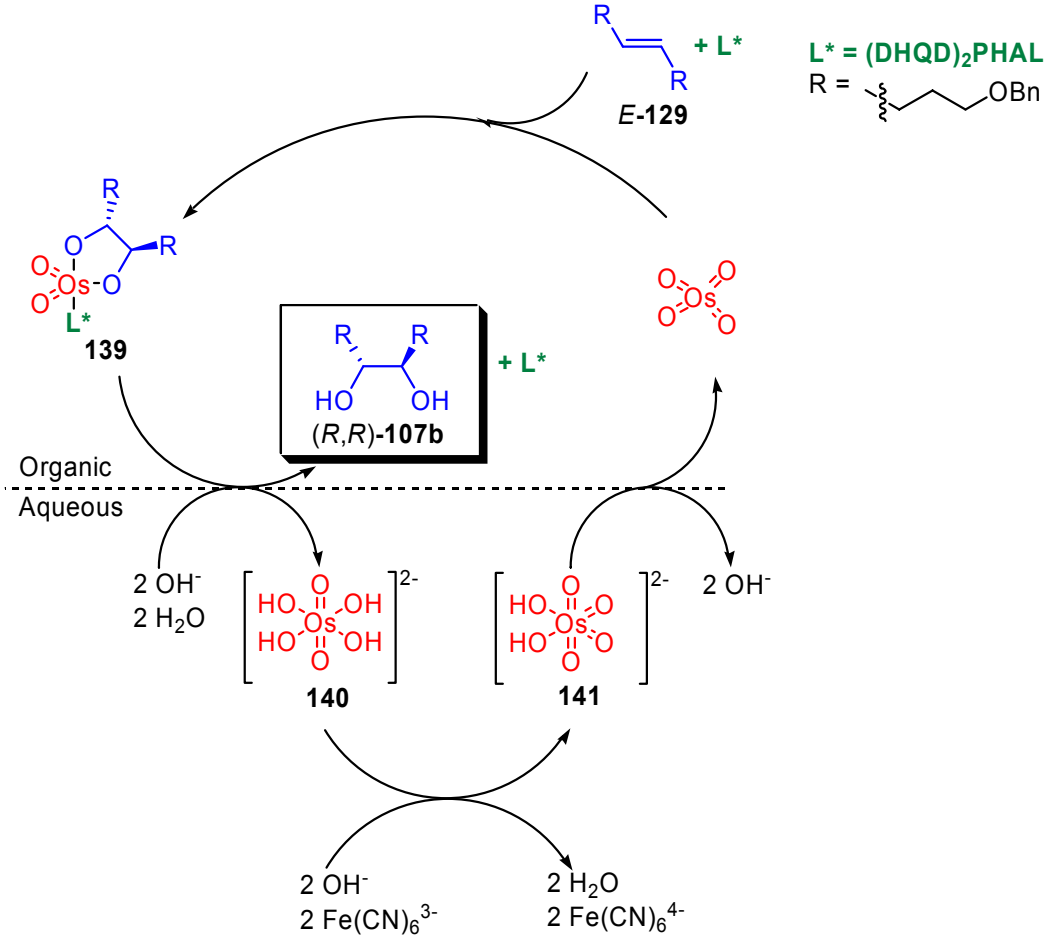

Figure 3.9: The catalytic cycle of the biphasic asymmetric dihydroxylation under Sharpless conditions, using AD mix β and $K_3Fe(CN)_6$ as the cooxidant.

Despite the vast number of studies, the mechanism of stereoselectivity has long been debated, with two models being presented: the Sharpless model, in which a metallacyclo complex is formed via a [2+2] cycloaddition followed by rearrangement to form the osmium(VI) complex **139**; and the Creigee-Corey-Noe (CCN) model in which

the complex **139** is formed directly in a concerted [3+2] cycloaddition. The dispute is in the formation of the osmium(VI) complex **139** and the structure of the binding pocket created by the biscinchona ligand, however both agree that it is the stability of the two diastereomeric forms of the transition states leading to this complex that provides the enantiomeric outcome. Although further evidence for the [2+2] model has recently been reported,[182] consensus towards the CCN [3+2] model is being reached[153] and will therefore be assumed throughout this thesis. The structures of the two diastereomeric biscinchona alkaloid ligands present in the AD premixes are shown in **Figure 3.10**. A rigid U-shaped binding pocket is formed in which the phthalazine linker forms the base and the methoxyquinoline units form two parallel walls. OsO_4 binds to one of the tertiary nitrogens in the quinuclidine subunits, and as such a chiral environment is created around the osmium.

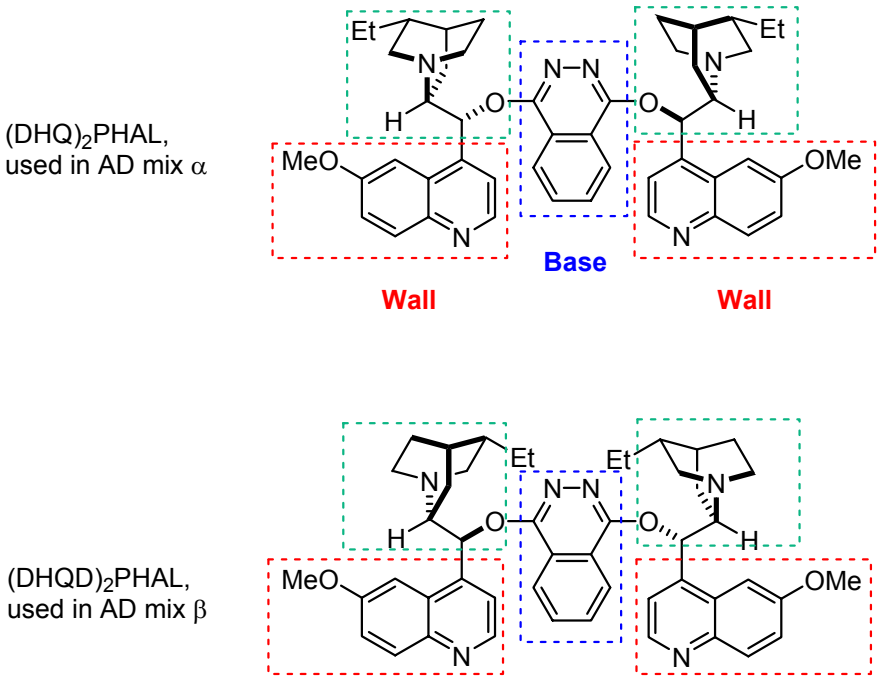

Figure 3.10: Structure of the biscinchona ligands used in the AD premixes. AD mix α contains two dihydroquinine (DHQ) units connected via a phthalazine (PHAL) linker. AD mix β contains two dihydroquinidine (DHQD) units connected via a PHAL linker. Both contain two methoxyquinoline units, which form the walls of a rigid U-shaped binding pocket, while the phthalazine linker forms the base of the pocket.

The approach of the olefin to the bound OsO_4 via one axial and one equatorial oxygen allows entry of the substrate into the binding pocket, forming one of two possible diastereomeric transition states, as depicted in **Figure 3.11**. Diastereomer **142** is oriented such that one of the olefin substituents is directed away from the binding

pocket. In this orientation, the other substituent experiences unfavourable steric interactions with the floor of the binding pocket, leading to destabilisation of the transition state. The diastereomeric transition state **143** places the substituent within the binding pocket, which is stabilised via favourable van der Waals interactions and, substrate dependant, aromatic π-stacking interactions. This stabilisation leads to the [3+2] cycloaddition of the olefin to form the osmium(VI) complex **139**, which following hydrolysis, yields the desired chiral diol.

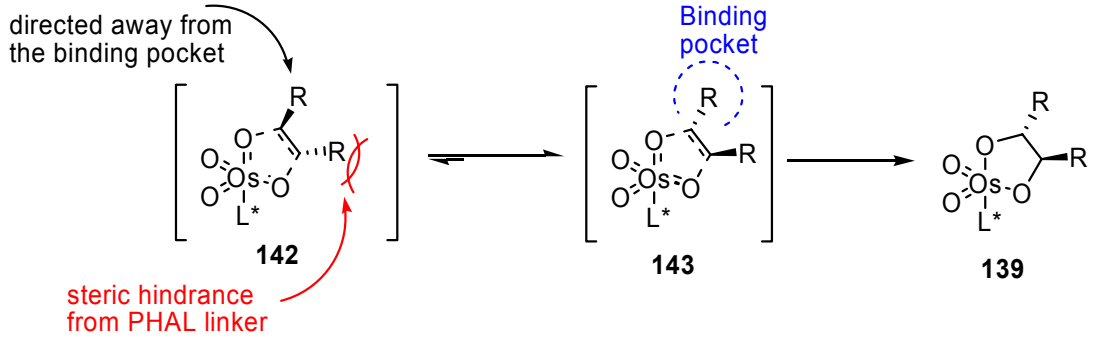

Figure 3.11: Two diastereomeric transition states leading to the stable osmium(VI) glycolate ester **139**. Diastereomer **142** is not stabilised due to steric interactions between one of the double bond substituents and the floor of the binding pocket, while diastereomer **143** is stabilised by favourable interactions with the walls and floor of the binding pocket.

The discrepancy (80% vs. 98%) in the stereochemical induction between the two diastereomeric biscinchona ligands is in agreement with the literature, with AD mix β usually resulting in better enantioselectivities.[3,153] The difference, however, is much larger than that expected. The diastereomeric nature of the two biscinchona alkaloid moieties results in a better fit of the substrate into the binding pocket of the DHQD based ligand than the DHQ based diastereomer, and as such the differentiation between the transition states **142** and **143** is more pronounced, leading to a better stereochemical outcome.

3.4 Synthesis of chiral (2*R*,2'*R*)-2,2'-bispyrrolidine

The final steps in the strategy utilised reported reactions,[164] and in order to finalise the synthesis of bispyrrolidine **92**, the chiral diol (*S*,*S*)-**107**, although a mixture of diastereomers, was used.

A summary of results of this sequence from diol (*S*,*S*)-**107a** to diBoc (*R*,*R*)-**109a** is shown in **Scheme 3.5**. Spectral evidence for the formation of each of the compounds is summarised in **Table 3.2**. In particular, the chemical shifts of the stereogenic methine proton and carbon confirmed the nature of the substituent attached to the stereogenic carbon.

Scheme 3.5: The optimised synthesis and separation of (*R*,*R*)- and *meso*-**109** from diol (*S*,*S*)-**107a** via the literature procedure.[164]

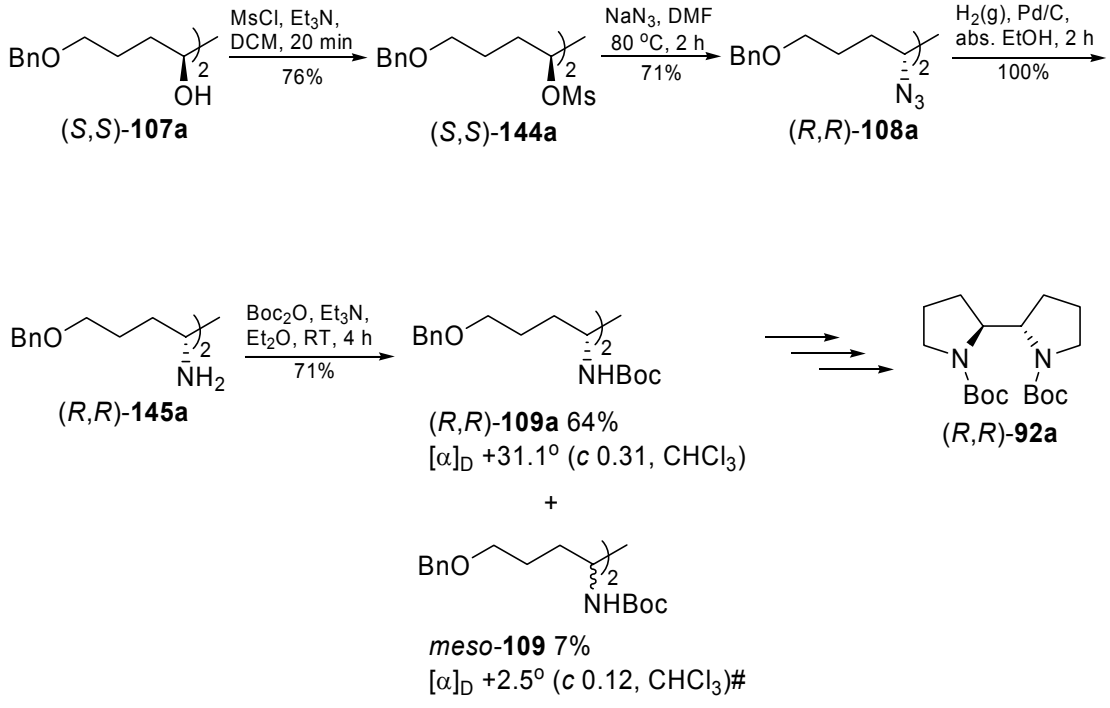

#The optical rotation of *meso*-**109a** was presumably due to instrumental variation, and possible contamination with chiral (*R*,*R*)-**109a**. The rotation however, was considered negligible.

Table 3.2: Spectral evidence used for the confirmation of the synthesis of each of the derivatives from **107a** to **109a**. The ^{1}H and ^{13}C NMR shifts (in ppm) are indicated for the sp^3 hybridised methine carbon (and corresponding proton) and the functional group (**X**) attached to the same carbon, where applicable. The M+H ion is quoted for the CI-MS (*m/z*).

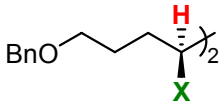

Compound	X	CH		X		CI-MS (*m/z*)
		^{1}H (ppm)	^{13}C (ppm)	^{1}H (ppm)	^{13}C (ppm)	
(*S*,*S*)-**107a**	**OH**	3.07	74.1	3.40	-	359
(*S*,*S*)-**144a**	**OMs**	4.86	80.6	3.02	38.7	515
(*R*,*R*)-**108a**	**N_3**	3.30	65.0	-	-	409
(*R*,*R*)-**145a**	**NH_2**	2.55	55.0	1.35	-	357
(*R*,*R*)-**109a**	**NHBoc**	3.54	54.3	NH 4.65 *t*Bu 1.42	C=O 156.4 *t*Bu 28.3, 79.1	557

Diol (*S*,*S*)-**107a** was converted to the corresponding dimesylate (*S*,*S*)-**144a** by reaction with methanesulfonyl chloride in the presence of the triethylamine in dichloromethane. The reaction was instantaneous, and work up after 20 minutes revealed no remaining starting material. Silica gel column chromatography afforded the chiral dimesylate as a viscous oil in 76% yield, as a mixture of chiral:*meso* diastereomers (7:1), which could not be separated by column chromatography. Triethylamine is required for the elimination of HCl from methanesulfonyl chloride to produce the sulfene (**Figure 3.12**).[183] The sulfene is highly electrophilic and as such is susceptible to nucleophilic attack by the secondary alcohol **107a**. Proton transfer generates the desired dimesylate **144a**.

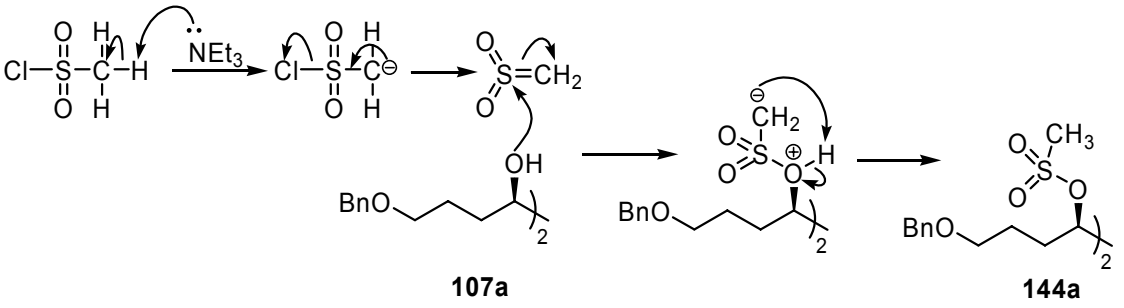

Figure 3.12: Mechanism for the mesylation of diol **107a**.[183]

Subsequent reaction with sodium azide in *N*,*N*-dimethylformamide at 80 °C resulted in the S_N2 displacement of the mesylate groups by the negatively charged nucleophile N_3^-, to yield the diazido compound (*R*,*R*)-**108a** in 71% yield, with inversion of stereochemistry at both stereogenic carbons.

Reduction of the azido group to the amine was performed by stirring the diazido compound (*R*,*R*)-**108a** in absolute ethanol, with a catalytic amount of Pd/C, and excess H_2(g) as the reductant. Filtration of the reaction mixture through Celite to remove the catalyst and subsequent removal of the reaction solvent yielded the chiral diamine (*R*,*R*)-**145a** in quantitative yield. The ^{1}H NMR spectrum displayed a broad singlet of integration 6H at 1.35 ppm, assigned to the NH_2 protons and two of the adjacent diastereotopic methylene protons. Deuteriated water (D_2O) was added to the NMR solvent, and as expected, the broad singlet assigned to the exchangeable protons disappeared. This revealed a multiplet of integration 2H, assigned to the methylene CH_2 protons.

The amine was Boc-protected by stirring a solution of the crude diamine (*R*,*R*)-**145a** in diethyl ether at reflux with Boc_2O, and triethylamine as a proton scavenger for 15 hours, to yield the desired diBoc **109a** as a mixture of diastereomers, in 40% yield over two steps, based on diazido compound **108a**. The two diastereomers were separated via column chromatography, to give the chiral (*R*,*R*)-**109a** in 26% yield, and the corresponding *meso*-**109m** in 14% yield, as white solids, m.p. 78-80 °C and 126 °C, respectively.

The ^{1}H and ^{13}C NMR spectra of the chiral and *meso* forms of the diBoc **109** were almost identical. In the ^{1}H NMR, the chemical shift of the signal assigned to the methine **CH** proton is slightly more upfield (**Figure 3.13**). The peak assigned to the corresponding carbon showed no difference in chemical shift in the ^{13}C NMR, while the adjacent methylene carbon experienced an upfield shift in the *meso* isomer, from 29.6 ppm to 28.2 ppm. As expected, MS (ES, +ve) of each isomer displayed a base peak at *m/z* 579 assigned to the M+Na ion. The optical rotation of the optically active (*R*,*R*)-diBoc was +31.1° (*c* 0.31, $CHCl_3$). The optical rotation of the optically inactive *meso* isomer was negligible (+2.5°; *c* 0.12, $CHCl_3$).

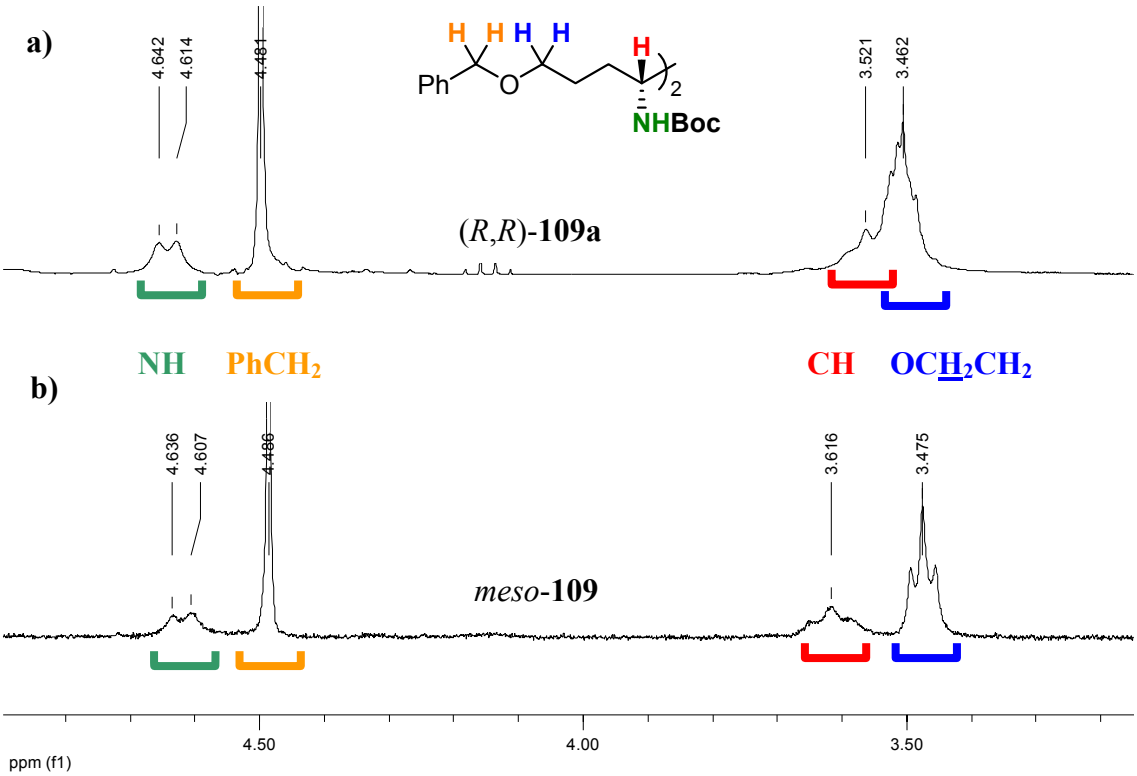

Figure 3.13: Expansion of the ^{1}H NMR of **a)** chiral (*R*,*R*)-**109a** and **b)** *meso*-**109**, showing the difference between shifts of the methine proton **CH** geminal to the NHBoc substituent, relative to the peaks assigned to the alkoxy **CH_2** protons. The peaks assigned to the **NH** (δ 4.6 ppm) and benzylic **CH_2** (δ 4.5 ppm) protons are shown for comparison. Spectra were recorded at 300 MHz, in $CDCl_3$, at 25 ^oC.

A third product, tentatively assigned to cyclic urea **147**, was isolated as a colourless oil, in 12% yield (**Figure 3.14**). The ^{1}H NMR spectrum showed a singlet of integration 9H at 1.42 ppm, assigned to the Boc protons, two multiplets as 3.48 and 4.50 ppm assigned to the methine protons. The MS (CI, +ve) showed a peak at *m/z* 483, assigned to the M+H ion.

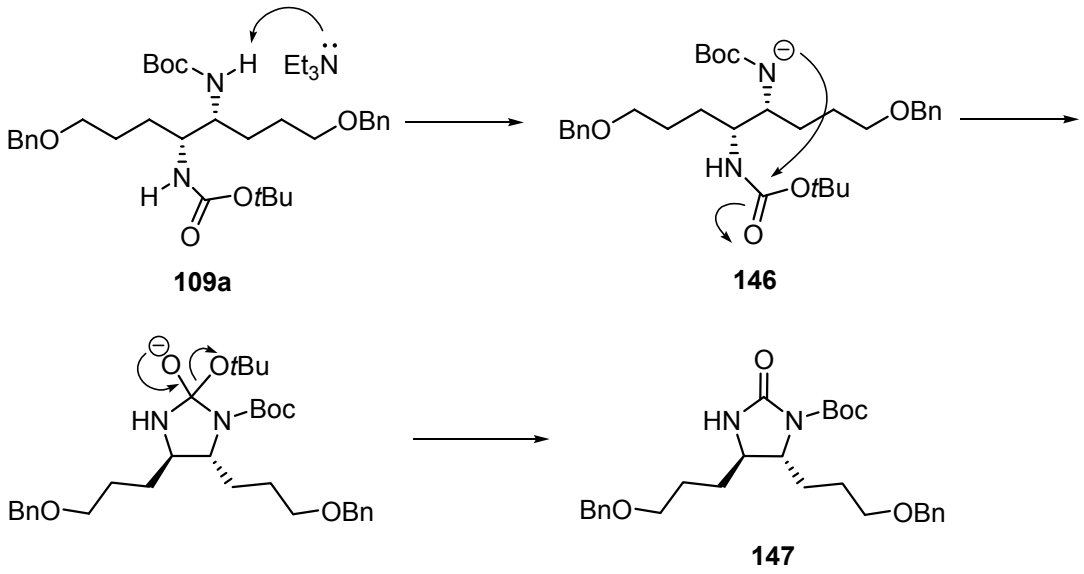

Figure 3.14: The proposed mechanism for the formation of the cyclic urea **147** from diBoc **109a**.

The degradation of **109** to the cyclic urea **147** is proposed to involve deprotonation of one of the amide protons by triethylamine and subsequent nucleophilic addition of the carbamate nitrogen atom of **146** onto the amide carbon of the Boc group on the adjacent N atom. The carbonyl bond is reformed with the *t*BuO$^-$ group leaving to form the cyclic urea **147**. The poor nucleophilicity of the deprotonated amide proton is overcome by the proximity of the electrophilic carbamate.

The reported literature yield for the synthesis of **109** was 96% over two steps,[164] from the diazido compound **108a**, much higher than the obtained 40% yield (of both chiral and *meso* diastereomers). The conditions used for the optimisation of the Boc protection are shown in **Table 3.3**.

Table 3.3: Optimisation of the Boc-protection of chiral diamine (*R*,*R*)-**145a** to form diBoc (*R*,*R*)-**109a**.

	Time (h)	Temp. (^{o}C)	**109** yield (%)[a]
1	15	35	40[b]
2	24	35	51
3	8	RT	65
4	4	RT	71

[a]Total isolated yield of both *meso* and chiral diastereomers. [b]Isolated yield over two steps, based on diazido **108a**.

The first attempt involved increasing the time of reaction to 24 hours (**Table 3.3**, entry 2). This did increase the yield of diBoc **109a** to 51%, but TLC analysis indicated the amount of degradation product **147** also increased with reaction time. Therefore it was hypothesised that a shorter reaction time would decrease the amount of degradation. A decrease in temperature was also trialled, to provide less energy for the deprotonation of the amide nitrogen and subsequent nucleophilic substitution to form the cyclic urea. Hence, the reaction was repeated, at RT, and stopped after 8 h (entry 3). Column chromatography afforded the mixture of diastereomers in overall 65% yield. The reaction was repeated, and stopped after only 4 hours (entry 4). A shorter reaction time decreased the amount of product degradation, yielding the diBoc **109** in 71% yield. Column chromatography afforded chiral diBoc (*R*,*R*)-**109a** (168 mg, 64%) and *meso*-**109** (19 mg, 7%) (**Scheme 3.5**).

The protection of the amine allowed for the selective deprotection of the alcohol moiety, using hydrogenation with H_2(g), in the presence of Pd/C in abs. ethanol which gave the deprotected diBoc (*R*,*R*)-**110a** as a white solid in 85% yield (**Scheme 3.6**). Significantly, a broad singlet at 1.96 ppm was observed in the ^{1}H NMR spectrum of (*R*,*R*)-**110a** when acquired in $CDCl_3$, and was assigned to the OH proton. When CD_3OD was the solvent, the broad singlet was not present, due to proton exchange with the deuteriated solvent. Mesylation of the free hydroxy groups using standard conditions gave the dimesylate (*R*,*R*)-**119a** in 86% yield as a viscous oil.

Scheme 3.6: Optimised reaction conditions for the synthesis of chiral 2,2'-bispyrrolidine (*R*,*R*)-**92a** from diBoc (*R*,*R*)-**109a**.

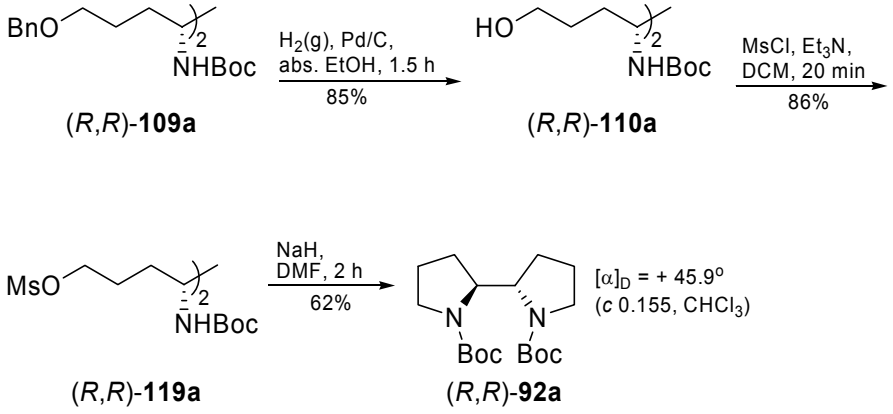

The cyclisation step was achieved by slow addition of a solution of the dimesylate (*R*,*R*)-**119a** in DMF to a suspension of sodium hydride in DMF, at 0 ^{o}C. Silica gel column chromatography isolated the bispyrrolidine (*R*,*R*)-**92a** as a colourless oil. CI-MS analysis showed a peak at *m/z* 341 assigned to the M+H ion. ^{1}H NMR spectrum showed two singlets, each of integral 9H, at 1.44 and 1.47 ppm, assigned to two non-equivalent Boc peaks and the peaks assigned to the remaining protons were broadened (**Figure 3.15**, **a**). The chiral 2,2'-bispyrrolidine scaffold contains C_2 symmetry, therefore the Boc groups in the structure of (*R*,*R*)-**92a** should be chemically equivalent. However, restricted rotation of the N-C bond caused by the sterically bulky Boc groups result in four possible conformations, or rotamers.[160] The ^{13}C NMR spectrum also showed splitting due to rotamers (**Figure 3.15**, **b**). Therefore, the temperature at which the ^{1}H NMR was acquired was increased. At 37 ^{o}C, the methyl protons of the Boc group resonated as a single peak of integral 18H at 1.46 ppm, indicating that the barrier to rotation of the N-C bond had been reached.

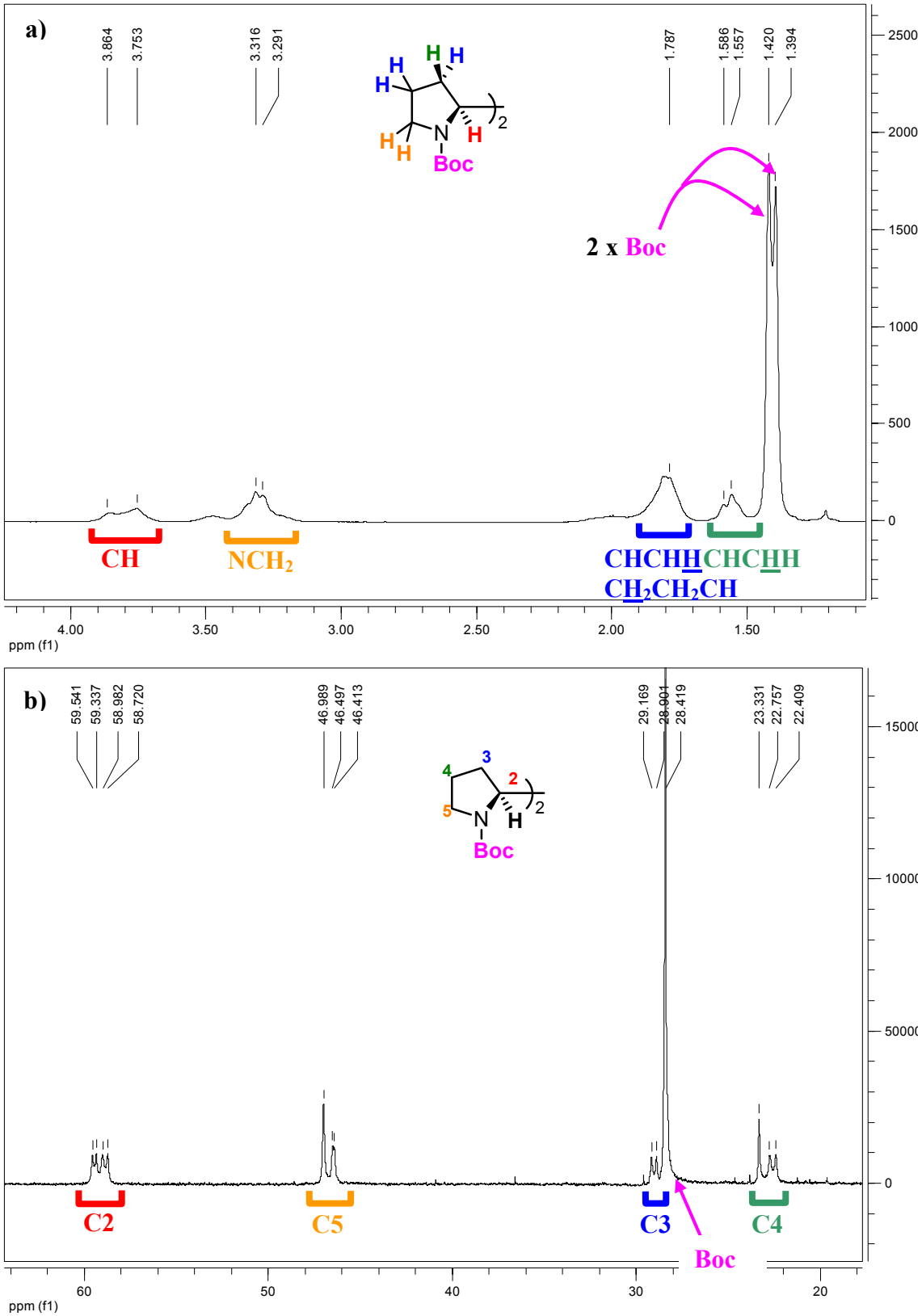

Figure 3.15: Expansion of the **a)** ^{1}H NMR spectrum (300 MHz) and **b)** ^{13}C NMR spectrum (75 MHz) of (*R*,*R*)-**92a** showing the broadening of each of the peaks as a result of restricted rotation of the N-C bond to the Boc protecting group. The NMR spectra were acquired in $CDCl_3$, at 25 ^{o}C.

The reaction mixture was contained in an ice bath for the addition of the dimesylate, to promote the formation of the bispyrrolidine **92**, rather than the sterically less accessible 6,6'-fused ring system **148** (**Figure 3.16**). Literature precedent indicates that the 2,2'-bispyrrolidine **92** is the only isomer formed under these conditions.[164,184,185]

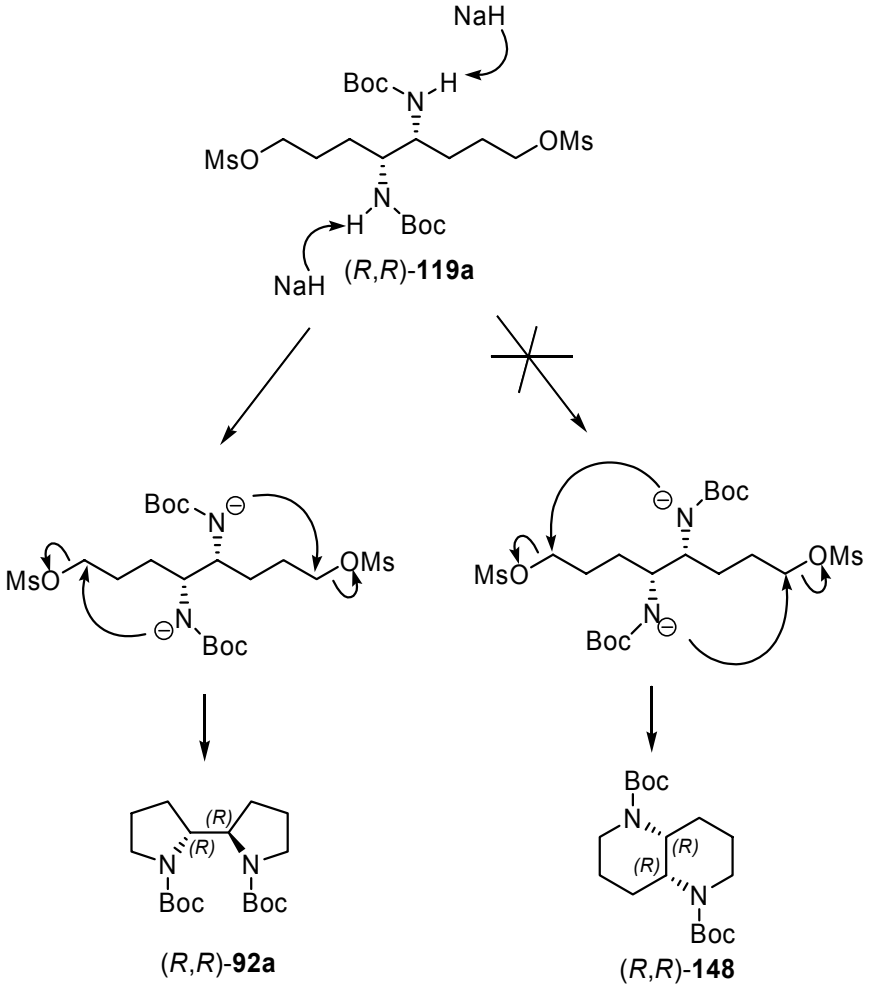

Figure 3.16: Two possible pathways for the intramolecular dicyclisation of **119a**, to form either the desired (*R*,*R*)-2,2'-bispyrrolidine **92a** or the fused bicyclic structure, Boc-protected (4a*R*,8a*R*)-decahydro-1,5-naphthyridine (*R*,*R*)-**148**.

Therefore, the synthesis of the Boc-protected bispyrrolidine (*R*,*R*)-**92a** was completed from the chiral diol (*S*,*S*)-**107a** (**Scheme 3.5**). The enantiomeric version of the bispyrrolidine (*S*,*S*)-**92b** could be accessed using the same chemistry on the chiral diol (*R*,*R*)-**107b**, however optimisation of the stereochemical aspects of the synthetic strategy was sought. For example, the quantity of the *meso* isomer could be reduced by an increase in *trans*:*cis* ratio of **129** in the metathesis reaction. The modifications made to the synthesis, and subsequent synthesis of both enantiomeric forms of **92**, are outlined in the following section.

3.5 Optimisation of the stereochemical yield of chiral 2,2'-bispyrrolidine 92

The synthesis of the enantiomeric bispyrrolidine (*S*,*S*)-**92b** required large scale synthesis of the chiral diol (*R*,*R*)-**107b**, and therefore the *trans* alkene **129**. The benzyl ethers **128** and **129** are both non-polar compounds, with R_f values >0.9 in hexanes as the developing solvent. Separation via column chromatography was laborious and only partially successful, with the problem exacerbated as the scale of the reaction was increased due to increased quantities of side products. An opportunity was sought to increase the polarity of the molecules in order to increase the retention to silica, so a more discriminating elution solvent could be used. As such, the benzyl ether protecting group was replaced with the *p*-methoxybenzyl ether derivative. The slight modification would not affect the synthetic strategy, since the two protecting groups have similar chemical properties. It was anticipated that the increase in polarity might even affect the stereochemical outcome of the asymmetric dihydroxylation reaction, by increasing the solubility of the alkene in the polar reaction solvent (*t*BuOH/H_2O).

The first step required the *p*-methoxybenzyl (PMB) protection of 4-penten-1-ol (**Scheme 3.7**).

Scheme 3.7: The synthesis of the PMB protected 4-penten-1-ol **149**.

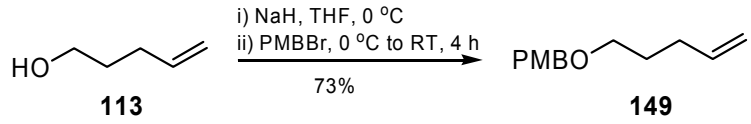

p-Methoxybenzyl bromide was freshly prepared by reaction of *p*-methoxybenzyl alcohol in 40% HBr in glacial acetic acid. The crude bromide (following workup with sat. $NaHCO_3$) was added to a suspension of 4-penten-1-ol and sodium hydride in THF. The deprotonated alcohol underwent an S_N2 displacement of the bromide of the *p*-methoxybenzyl bromide, to yield the protected alcohol **149** in 73% yield.

The optimised reaction conditions for the formation of the dimer **150** from **149** are shown in **Scheme 3.8**. TLC analysis indicated the disappearance of the monomer **149** after 20 hours, therefore the reaction was stopped, and subsequent column chromatography gave the 4-octene **150** as a 3.5:1 mixture of geometric isomers in 86%

yield. Separation from the side metathesis products proved to be simpler than with the corresponding benzyl protected alkenes, due to the greater difference in polarity of the dimer resulting from the presence of two methoxy groups, compared to one in the starting material and the styrene by-product.

Scheme 3.8: The self-metathesis of PMB-protected pentenol **149** to form the homo-dimerised product **150**, with evolution of ethene gas.

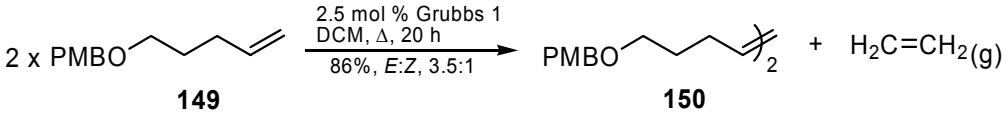

149 **150**

Table 3.4 shows the reaction conditions for the optimisation of this dimerisation. Shorter reaction times provided the best yields (e.g. entry 1 vs. 5), as explained in *Section 3.2*. A decrease in catalyst loading (entries 3-5) did not greatly affect the stereochemical outcome, and minimised the quantity of side products formed.

Table 3.4: The self-metathesis reaction of **149** to form the dimer **150**, at varying reaction times, in the presence of Grubbs 1 catalyst **131**. Reactions performed in DCM at 40 ^{o}C, under a N_2(g) atmosphere.

	Reaction time (h)	Catalyst loading (mol %)	**150** yield (%)[a]	*E*:*Z*[b]
1	72	5	61	n.m.[c]
2	48	5	78	3.5:1
3	24	2.5	80	4:1
4	20	2.5	83	3.4:1
5	20	2.5	86	3.5:1

[a]Isolated yield. [b]Determined by ^{1}H NMR. [c]Not measured.

Grubbs 2nd generation catalyst **132** (**Figure 3.4**) has enhanced catalytic performance and the sterically demanding carbene ligand increases the lifetime of the ligand, compared to Grubbs 1.[186] The catalytic activity of Grubbs 2 is comparable to that of the molybdenum catalysts, however the ruthenium catalyst is air and water tolerant, stable in high temperatures and has much higher functional group tolerance.[187] The use of Grubbs 2 catalyst has been reported to increase the geometric purity of the resulting dimer, due to increased activity of the active ruthenium catalyst to the sterically accessible *cis* isomer.[187] The *cis* isomer, therefore, continues to react in the catalytic

cycle, and is converted to the *trans* isomer. This higher activity however, can also be detrimental to the total yield of desired product, since the ruthenium catalyst is more active towards *all* double bonds in each intermediary step of the catalytic cycle, resulting in loss of product to the formation of undesired side metathesis products (SMPs), usually resulting in double bond migration,[188] and cross-metathesis products thereof.[171] Yields of up to 30% of undesired side metathesis products have been reported.[171] Despite the possible complications, the monomer **149** was heated at reflux in the presence of 5 mol % of Grubbs 2nd generation catalyst **132** for 72 hours (**Scheme 3.8**).

Scheme 3.9: Attempted self-metathesis of PMB-protected pentenol **149** to form the homo-dimerised product **150**, with evolution of ethene gas, in the presence of Grubbs 2nd generation catalyst **132**. Possible side products formed from the reaction, **151** and **152**.

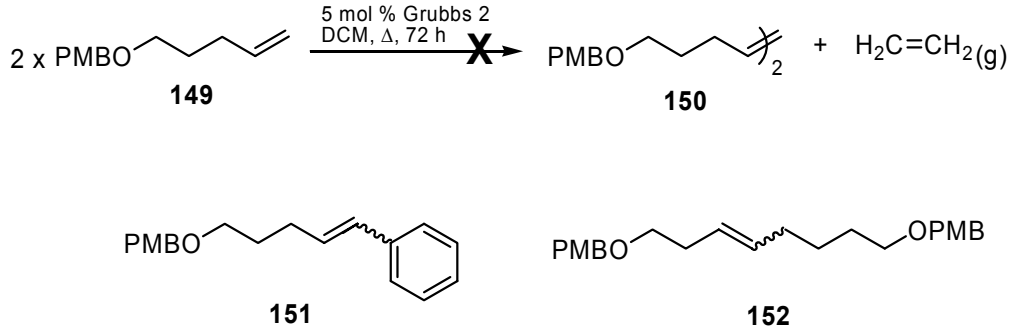

The crude reaction mixture was subjected to silica gel column chromatography, and although no starting material was recovered, no desired dimer **150** was isolated. ^{1}H NMR analysis showed a mixture of unsymmetrical, undesired products were formed, including the *cis* and *trans* cross-metathesis products **151** between styrene and the monomer **149**, and a product tentatively assigned to **152**, an isomer of **150**, with the double bond migrated to the 3-position (**Scheme 3.9**).

Therefore, the optimal conditions for the conversion of the monomer **149** to the dimer **150** were using Grubbs 1st generation catalyst, and a shorter reaction time. Using shorter reaction times and trialling the reaction at RT to minimise the continued reaction of the desired dimer **150**, could increase the yield even further. The presence of the PMB protecting group increased the ease of purification from the side metathesis products remarkably. Attempts to isolate the *E* and *Z* isomers via column chromatography or

semi-preparative HPLC (silica, normal phase) however, were not successful, as a discriminating elution system was not found.

The dihydroxylation of the PMB protected alkene **150** was performed using AD mix α and AD mix β (**Scheme 3.10**). The enantiomeric diols (*S*,*S*)-**153a** and (*R*,*R*)-**153b** were isolated as mixtures of chiral:*meso* diastereomers. The diastereomeric purity could be improved via recrystallisation of the white solid from DCM/hexanes. The *meso* isomer was less soluble in DCM/hexane, and as such could be removed, although complete separation was not achieved.

Scheme 3.10: The asymmetric dihydroxylation of **150** to form the chiral diols (*S*,*S*)-**153a** and (*R*,*R*)-**153b**, under standard Sharpless conditions.[3]

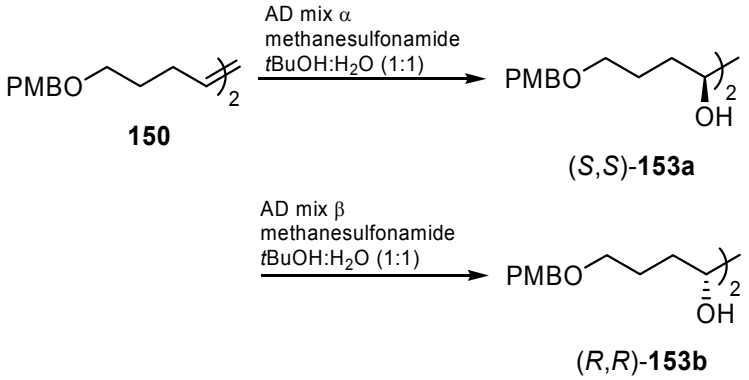

	AD mix	Reaction time (h)	**153** yield (%)[a]	*ee*[b]
1	α	24	69	98
2	α	20	90	92
3	β	65	98	88
4	β	24	93	70

[a]Isolated yield of **153** as a mixture of chiral:*meso* diastereomers. [b]Determined by chiral HPLC.

Analysis of the results shown in **Scheme 3.10** indicates the inconsistencies in both chemical and stereochemical yield, with longer reaction times providing a higher yield and stereoselectivity using AD mix β (entries 3 and 4), while the opposite effect was observed when using AD mix α (entries 1 and 2). In general, the use of AD mix α resulted in better enantioselectivity, which is contrary to literature precedent.[3]

In general, the results of the AD reactions of the PMB protected derivative were better than that of the benzyl protected derivative. The increased yield was assumed to be as a result of the higher solubility of the alkene **150** in *t*BuOH, than the corresponding OBn protected alkene **129**.

The synthesis of both isomers of the chiral 2,2'-bispyrrolidine was completed from the PMB protected diol **153**, using the same reaction conditions as those outlined in **Section 3.4**. The results for the synthesis of (*R*,*R*)-**92** are outlined in **Scheme 3.11**. The *O*-deprotection of (*R*,*R*)-**157a** yields the diol (*R*,*R*)-**110a**, which in turn provides access to the bispyrrolidine (*R*,*R*)-**92a**, which has been outlined in **Scheme 3.6**. The results from the complete synthesis of the enantiomeric bispyrrolidine (*S*,*S*)-**92b** is summarised in **Scheme 3.12**.

Scheme 3.11: The synthesis of (*R*,*R*)-**92a** from the PMB protected diol (*S*,*S*)-**153a**.

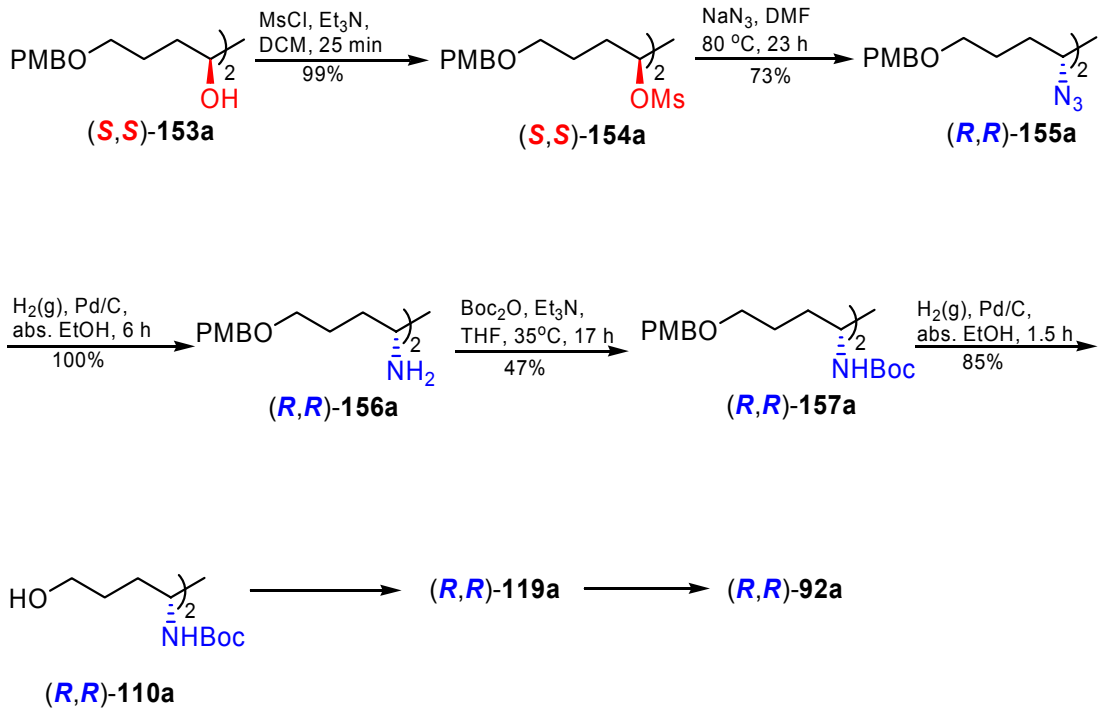

Scheme 3.12: The synthesis of (*S*,*S*)-**92b** from the PMB protected diol (*R*,*R*)-**153b**.

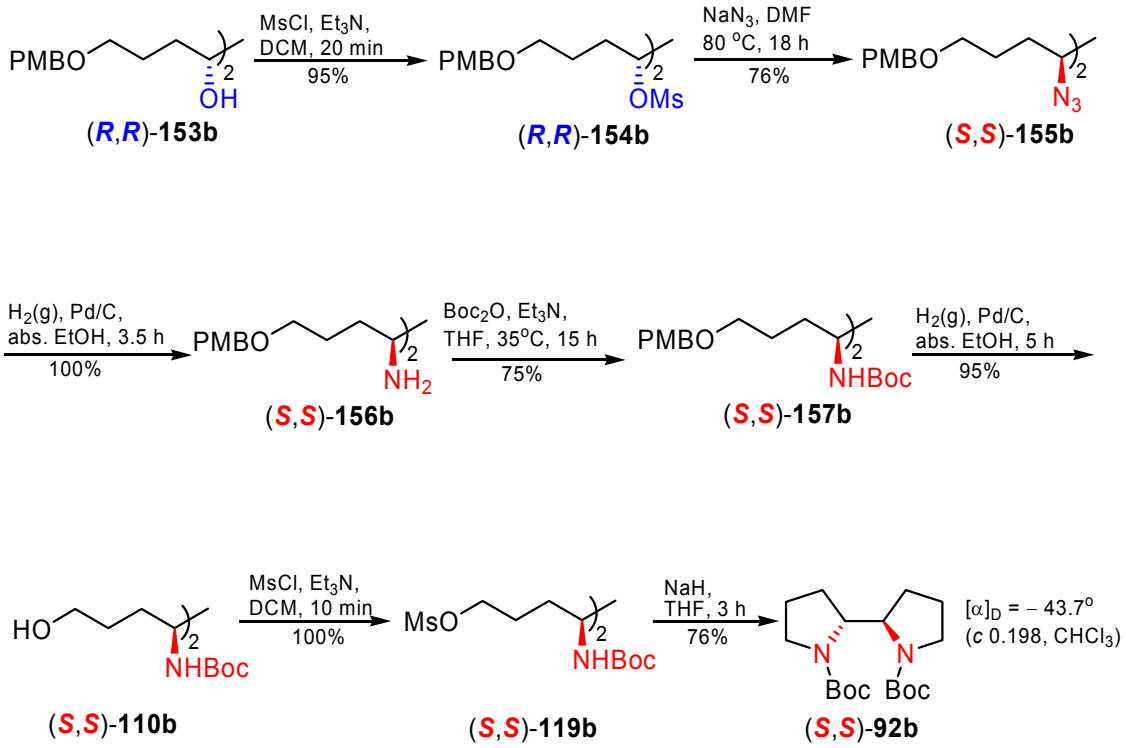

The synthesis of the OPMB protected derivatives proved to be similar, as expected, to the OBn derivatives. Partial separation of the chiral and *meso* diazido compound **155** was achieved via column chromatography, although samples containing a mixture of diastereomers could be separated more easily after Boc-protection to form **157**. Deprotection of the diBoc (*S*,*S*)-**157b** yielded the diol (*S*,*S*)-**110b**, which exhibited identical physical and spectral properties to the enantiomer (*R*,*R*)-**110a** formed from the synthesis outlined in **Section 3.5**. Mesylation and subsequent cyclisation afforded the enantiomeric Boc-protected (*S*,*S*)-2,2'-bispyrrolidine **92b**.

3.6 Attempted strategy optimisation

*3.6.1 Separation of chiral (*R,R*)-**153b** and* meso-***153** via derivatisation*

One of the disadvantages of the synthetic strategy is the formation of the *meso* diastereomers, which were not separable from the chiral derivatives until 3-5 steps through the synthesis. In an attempt to remove the *meso* impurity by replacing a synthetic step, an alternative synthesis was proposed as outlined in **Figure 3.17**.

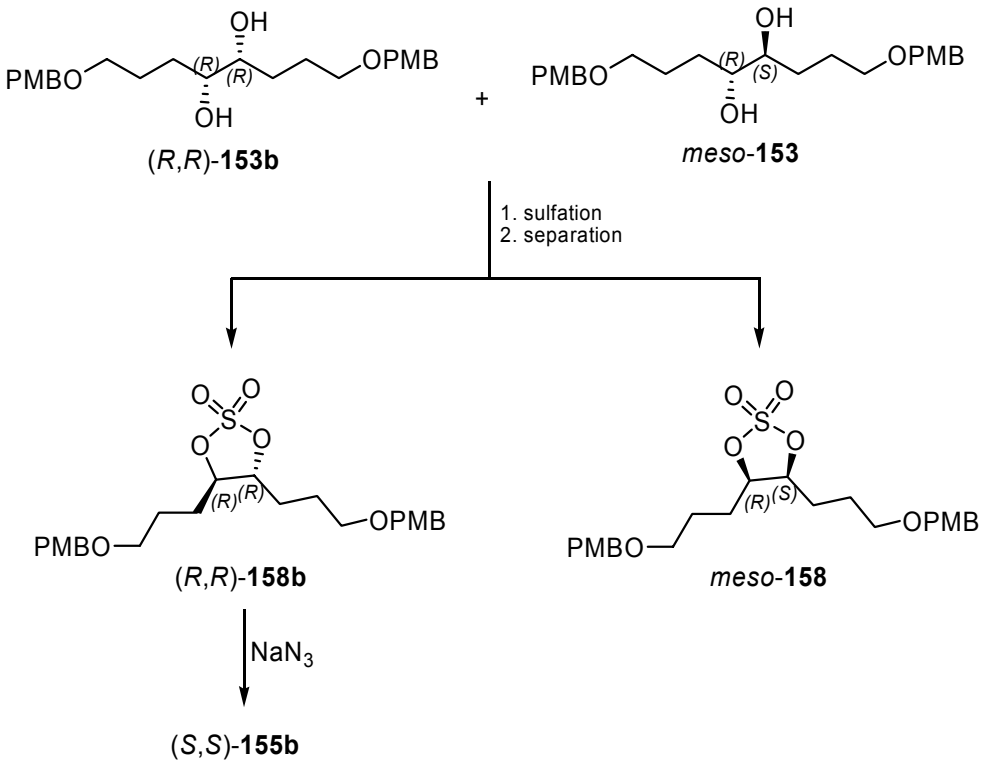

Figure 3.17: Proposed synthesis for the separation of the chiral and *meso* diastereomers of diol **153**, via formation of the cyclic sulfate **158**.

The conversion of the mixture of diastereomeric diols **153** to the corresponding sulfates **158** was anticipated to provide sufficient restrictions in bond rotation resulting in differences in the molecular shape of the two diastereomers. This would lead to increased differences in physical properties such as polarity or solubility which could be manipulated for easier separation via column chromatography or recrystallisation. As such, a mixture of chiral and *meso* diol **153** was reacted in a two step procedure as outlined in **Scheme 3.13**.[3,189]

Scheme 3.13: Attempted synthesis of the cyclic sulfate **158** from the diol **153** (as a mixture of diastereomers).

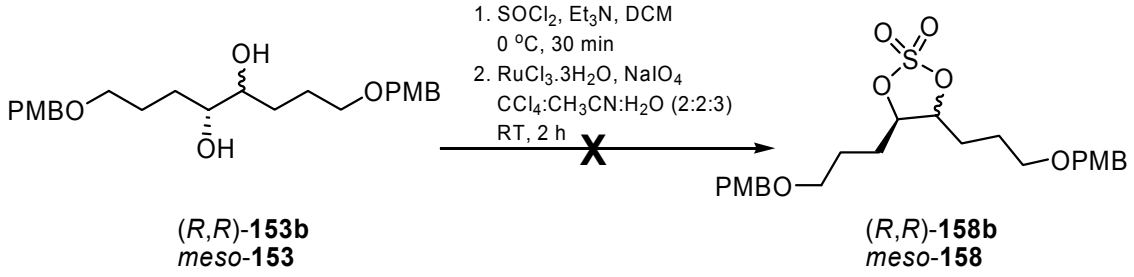

A mixture of the chiral diol (*R*,*R*)-**153b** and the *meso* diastereomer was reacted with thionyl chloride in the presence triethylamine, in dichloromethane, at 0 ^{o}C. After 30 minutes TLC analysis indicated loss of starting material and the formation of two products, and the reaction was quenched with water. The cyclic sulfite intermediate was extracted with dichloromethane, and the solvent was removed *in vacuo*. The crude sulfite was dissolved in a 2:2:3 mixture of carbon tetrachloride, acetonitrile and water, hydrated ruthenium (III) chloride and sodium periodate was added. The reaction mixture was stirred for 2.5 hours at RT. After an aqueous work up with water, sodium bicarbonate and brine, the crude mixture was subjected to flash silica gel column chromatography. Multiple products were formed; none of which could be identified as the cyclic sulfate **158**.

In order to more carefully monitor the progress of the oxidation from the sulfite to the sulfate, the reaction was repeated; however the sulfite was purified before the oxidation step. Therefore, the crude sulfite was subjected to silica gel column chromatography, which provided partial separation of the chiral and *meso* cyclic sulfites **159** (**Scheme 3.14**), to give an overall yield of 70%.

Scheme 3.14: The synthesis of the cyclic sulfite **159** from the diol **153** (as a mixture of diastereomers).

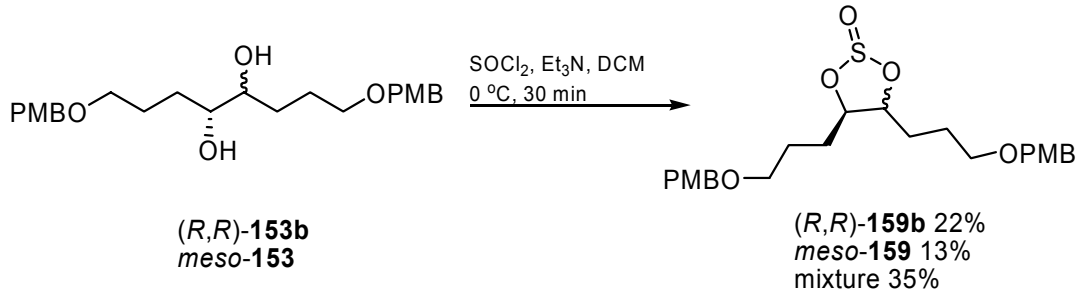

(*R*,*R*)-**153b**
meso-**153**

(*R*,*R*)-**159b** 22%
meso-**159** 13%
mixture 35%

The chiral cyclic sulfite eluted first, and was isolated in 22% yield. Analysis of the ^{1}H and ^{13}C NMR indicated the presence of an unsymmetrical molecule. The lone pair of electrons on the tetrahedral sulfur atom creates an uneven distribution of electrons and therefore a non-equivalent chemical environment for the two halves of the molecule. This effect is most strongly exhibited by the methine protons (**Figure 3.18, a**). The chiral molecule loses its C_2 symmetry while the corresponding *meso* compound retains

a plane of symmetry (**Figure 3.18, b**), and was therefore distinguished from the chiral version.

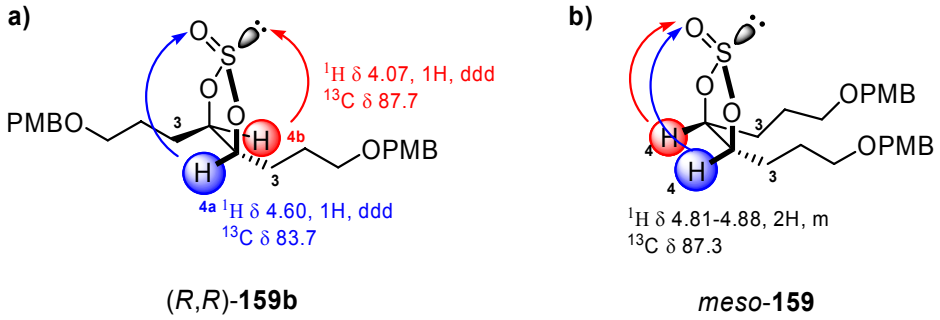

(*R*,*R*)-**159b** *meso*-**159**

Figure 3.18: **a)** The chemical inequivalence of the two methine protons and carbons in the chiral (*R*,*R*)-**159b**, resulting from the lone pairs of electrons of the tetrahedral sulfur atom of the sulfite. **b)** The chemical equivalence of the two methine protons and carbons in the corresponding *meso* compound. Chemical shifts (δ) of the methine protons and carbons are quoted in ppm. Integration and multiplicity for the methine protons are labelled.

Two sets of ddd peaks in the ^{1}H NMR of the chiral (*R*,*R*)-**159b**, at 4.07 and 4.60 ppm, each of relative integration 1H were assigned to the non-equivalent methine protons, **H4a** and **H4b**. Both sets of peaks correlated, in the gCOSY spectrum, to the multiplet from 1.67-1.95 ppm corresponding to the adjacent methylene protons H3. The peak assigned to the benzylic protons showed partial splitting. The ^{13}C NMR spectrum shows further evidence of an unsymmetrical structure via a doubling of each of the peaks, with the exception of those peaks assigned to the aryl group and methoxy substituent, which are sufficiently remote from the sulfur atom to show any significant difference in chemical shift. Confirmation of the cyclic sulfite structure **159** was provided by ES-MS (+ve) analysis, which showed a base peak at *m/z* 487 assigned to the M+Na ion.

The peaks in the ^{1}H and ^{13}C NMR spectra of the *meso* sulfite were observed at similar chemical shifts to the corresponding peaks in the chiral sulfite. Significantly, a single multiplet of integration 2H at 4.81-4.88 ppm in the ^{1}H NMR was assigned to the methine protons; the peak at 87.3 ppm in the ^{13}C NMR was assigned to the methine carbon, in contrast to the two carbon peaks at 83.2 and 87.7 ppm for the chiral derivative (**Figure 3.18**).

With the pure chiral sulfite (*R*,*R*)-**159b** in hand, the oxidation to the cyclic sulfate **158b** was attempted. Therefore, chiral sulfite (*R*,*R*)-**159b** was dissolved in a 2:2:3 mixture of

carbon tetrachloride, acetonitrile and water (**Scheme 3.15**). Hydrated ruthenium (III) chloride and sodium periodate were added and the reaction was stirred at RT for 2.5 hours. TLC analysis indicated full conversion of the sulfite **159b** and multiple products formation. Work up and subsequent column chromatography isolated the chiral sulfate (*R*,*R*)-**158b** in only 3% yield. The remaining products could not be identified.

Scheme 3.15: The oxidation of the cyclic sulfite (*R*,*R*)-**159b** to the cyclic sulfate (*R*,*R*)-**158b**.

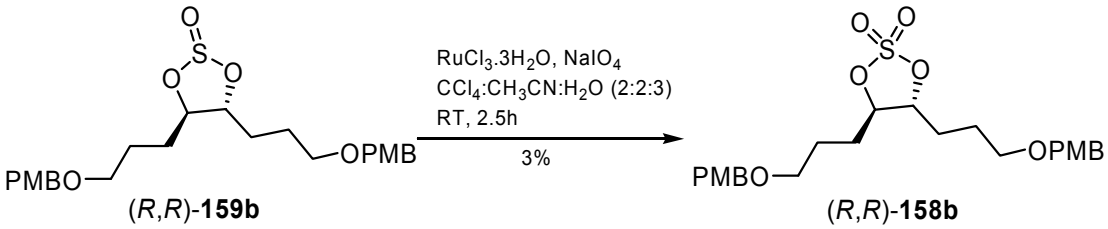

The oxidation to the cyclic sulfate re-establishes C_2 symmetry to the molecule, and as such less complicated ^{1}H and ^{13}C NMR spectra were obtained. A multiplet as 4.57-4.59 ppm in the ^{1}H NMR was assigned to the methine protons and a single peak at 4.42 ppm was assigned to the benzylic protons. The ^{13}C NMR displayed a peak at 87.3 ppm assigned to the methine carbon. All other carbons in the molecule were assigned to a single carbon peak. Although the ^{1}H and ^{13}C NMR spectra both look similar to that of the *meso* sulfite *meso*-**159**, comparative TLC analysis indicated a difference in R_f between the two. The ES-MS (+ve) displayed a base peak at *m/z* 503, assigned to the M+Na ion of (*R*,*R*)-**158b**. Although the structure was confirmed, 3% yield was insufficient to continue this reaction sequence.

3.6.2 Potential alternate N nucleophiles

The Boc protected bispyrrolidine **92** does not fulfil the requirements of a ligand, due to the non-chelating nature of the amide nitrogen. The diBoc **92** requires deprotection to form the bispyrrolidine **86**, and subsequent derivatisation, to form e.g. dibenzyl **160** (**Figure 3.19**). Of note is the instability and volatility of the bispyrrolidine **86**.

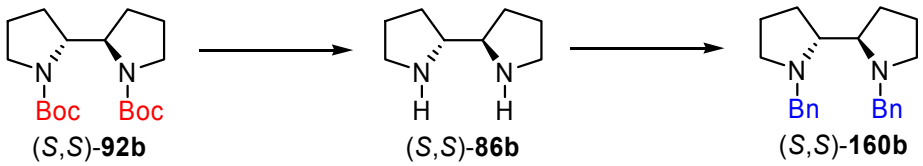

Figure 3.19: The proposed synthesis of the *N*,*N*'-dibenzyl bispyrrolidine **160b** from the *N*,*N*'-diBoc **92b**, via bispyrrolidine **86**.

To shorten the number of steps to the desired dibenzyl **160**, an alternative synthesis from dimesylate **154b** was proposed (**Figure 3.20**, **Route 2**). Nucleophilic substitution of the mesylate groups with benzylamine via an S_N2 mechanism should provide the *N*,*N*-dibenzylated diamine **161b**. Selective removal of the benzyloxy ether should give the diol **162b**, mesylation of the free hydroxy groups render the adjacent carbon amenable to nucleophilic attack by the *N*-benzyl nitrogen during the cyclisation to form *N*,*N*'-benzyl bispyrrolidine **160b**. Comparison with the established procedure (**Figure 3.20**, **Route 1**) highlights the advantage of the introduction of the N in the desired form for the final ligand – the number of protections and deprotections is significantly reduced.

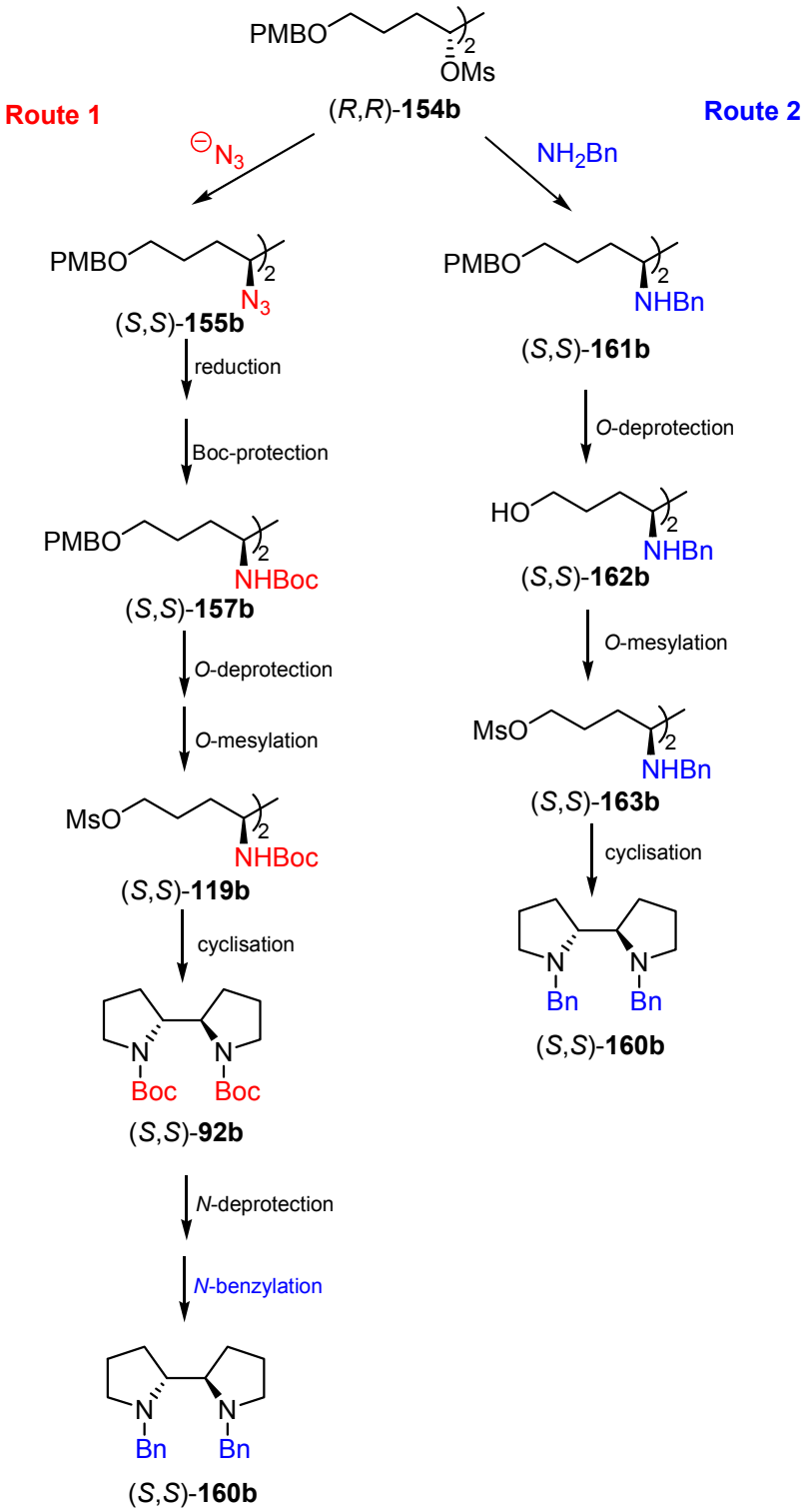

Figure 3.20: The synthesis of diBoc **92b** from dimesylate **154b**, and subsequent deprotection and *N*-benzylation to form *N*,*N'*-dibenzyl **160b** (**Route 1**). The proposed synthesis of the *N*,*N'*-dibenzyl bispyrrolidine **160b** via reaction of dimesylate **154b** with benzylamine (**Route 2**).

Therefore, to a suspension of sodium hydride in THF containing benzylamine was added (*R*,*R*)-**154b** (**Scheme 3.16**). After stirring for 15 hours only starting material was

recovered. A second attempt using potassium carbonate as a proton scavenger also resulted in only starting material being recovered. Increasing the reaction temperature by heating benzylamine and (*R*,*R*)-**154b** in DMSO for 2.5 days resulted in multiple products. Column chromatography isolated four different products, although the structure of each could not be elucidated, and confirmation could not be made that any of the products was the desired benzylated diamine.

Scheme 3.16: Attempted synthesis of the benzylated diamine (*S*,*S*)-**161b** via nucleophilic substitution of benzylamine to dimesylate (*R*,*R*)-**154b**.

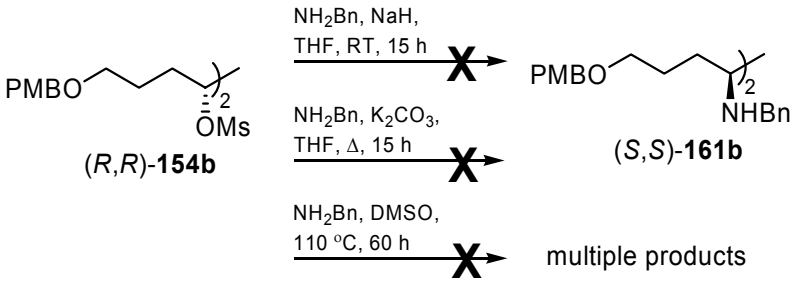

Therefore, the synthesis of **161b** was not attained. The nucleophilicity of the benzylamine could be increased by deprotonation with a stronger base, e.g. *n*BuLi. The advantages of the proposed synthesis warrant further investigation into the synthesis of dibenzyl **161b**.

3.7 Derivatisation of the bispyrrolidine scaffold

The dibenzyl protected bispyrrolidine (*S*,*S*)-**160** was accessed via **Route 1** (**Figure 3.19)**, and the non-optimised reactions conditions are shown in **Scheme 3.17**. Boc-protected bispyrrolidine (*S*,*S*)-**92** was subjected to acidic conditions in the presence of trifluoroacetic acid.[164] The crude bispyrrolidine (*S*,*S*)-**86** was obtained after basic work-up and was benzylated using triethylamine and benzyl bromide in DCM to give (*S*,*S*)-**160b** in 28% yield, over two steps. The reaction required aqueous work up to remove $Et_3BnN^+Br^-$ formed as a byproduct.

^{1}H NMR analysis showed two doublets (J = 13 Hz) at 3.98 and 4.26 ppm, assigned to the two diastereotopic benzylic CH_2 protons. This phenomenon had previously been observed in the ^{1}H NMR of the corresponding 2,2'-bisindoline analogue.[185] The peak at

3.35-3.38 ppm was assigned to the CH proton, and two peaks at 2.68-2.72 and 3.29-3.33 ppm were assigned to the diastereotopic CH_2 protons adjacent to the nitrogen. MS (ES, +ve) analysis showed a base peak at *m/z* 321, assigned to the M+H ion.

Scheme 3.17: Non-optimised reaction conditions for the synthesis of (*S*,*S*)-**160b** from (*S*,*S*)-**92**, via 2,2'-bispyrrolidine **86b**.

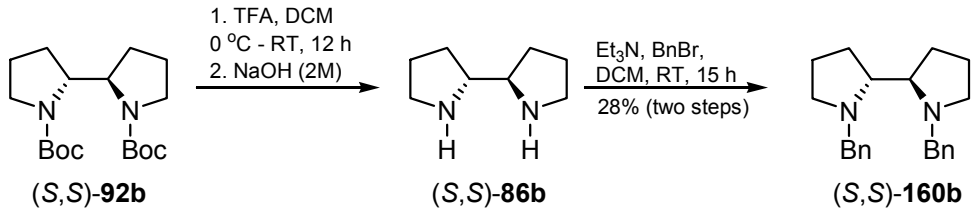

2,2'-Bispyrrolidine (*S*,*S*)-**86b** is a volatile, colourless oil which is unstable.[164] The work up procedure involved concentration under reduced pressure, which may have resulted in loss of product, which would have decreased the yield of (*S*,*S*)-**160b**. Distillation should be attempted as the method of purification in future. The conditions for the benzylation of (*S*,*S*)-**86b** should be modified, to include a base that is unreactive towards benzyl bromide. The large quantity of byproduct generated masked reaction monitoring, making TLC analysis difficult. The use of NaH in THF would be excessive, but would not react with benzyl bromide. Potassium carbonate could also be an appropriate alternative.

3.8 Conclusion

The key steps of **metathesis dimerisation** and **Sharpless AD** provided access to the previously reported[164] enantiomeric diols (*S*,*S*)- and (*R*,*R*)-**107** in 80% and 98% *ee* respectively, determined by chiral HPLC analysis, as mixtures of chiral and *meso* diastereomers. The literature procedure was repeated on the diol (*S*,*S*)-**107a**, to give the chiral Boc-protected 2,2'-bispyrrolidine (*R*,*R*)-**92a**, with the *meso* diastereomer being removed partway through the synthesis.

The reaction sequence was modified by the inclusion of the PMB protecting group, in place of the Bn group, to increase the possibility of separation of *E* and *Z* or chiral and *meso* diastereomers. While the *E* and *Z* isomers of the PMB protected 4-octene **150** were not isolated using column chromatography or semi-preparative HPLC techniques,

the ease with which the isomers could be separated from the side metathesis products was improved.

The results of the AD reaction were the reverse of those achieved from the Bn protected alkenes; AD mix α gave higher *ee* than AD mix β. The diastereomeric purity of the diol could be increased by recrystallisation, however the chiral diols were not isolated from the *meso*. Therefore the diastereomeric mixtures of each enantiomeric diols (*S*,*S*)-**153a** and (*R*,*R*)-**153b** was taken through to the Boc-pyrrolidines (*R*,*R*)-**92a** and (*S*,*S*)-**92b**, with the *meso* isomer being removed most successfully at the diBoc derivative **157**.

Attempted derivatisation of the diol (*R*,*R*)-**153b** via the cyclic sulfate (*R*,*R*)-**158b** was not successful, however separation of the chiral and *meso* sulfites **159** was possible via column chromatography.

Nucleophilic substitution of dimesylate (*R*,*R*)-**154b** with benzylamine was attempted using three different reaction conditions, however the desired dibenzyl derivative (*R*,*R*)-**161b** was not synthesised. Further study into alternate N-nucleophiles would be advantageous, as the number of steps to the final derivatised 2,2'-bispyrrolidine ligand would be significantly reduced.

Finally, the Boc-protected bispyrrolidine (*S*,*S*)-**92b** was deprotected, with subsequent benzylation giving the dibenzyl ligand (*S*,*S*)-**160b**, although the reaction conditions were not optimised.

CHAPTER 4

Towards the Synthesis of 2,2'-Bisindoline

The modification of the synthetic procedure that yielded the bispyrrolidine **92** to access 2,2'-bisindoline **112** is outlined in **Figure 4.1**. Benzyl protection of 2-allylphenol **120** gives **164**, which is dimerised via the metathesis reaction to give alkene **165**. Subsequent AD using AD mix α gives diol (*S*,*S*)-**166a** or alternatively, AD mix β gives diol (*R*,*R*)-**166b**. Using the same chemical manipulations as those used for the synthesis of 2,2'-bispyrrolidine would give phenol **169**. *O*-Triflation, Pd catalysed cyclisation and *N*-deprotection would give 2,2'-bisindoline **112**.

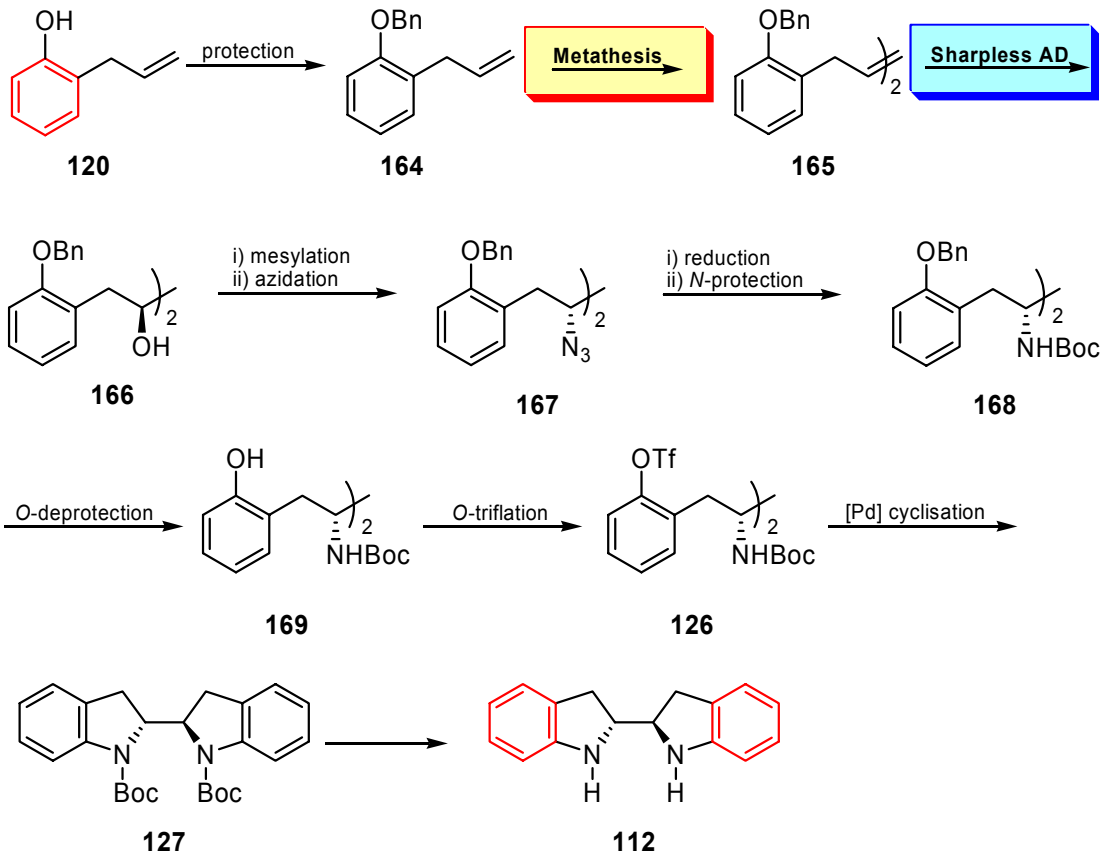

Figure 4.1: Proposed synthesis of chiral 2,2'-bisindoline **112**.

4.1 Protection of 2-allylphenol

The first step of the synthesis towards 2,2'-bisindoline **112** was the benzyl protection of 2-allylphenol **120**, under typical conditions to give the benzyl ether **164** in 99% yield, as a colourless, volatile liquid (**Scheme 4.1**). The literature procedure reported **164** in 78% yield however, the product was not spectroscopically characterised.[190] The ^{1}H NMR spectrum showed peaks of total integration 9H in the aromatic region assigned to the four protons of the disubstituted aromatic ring and the five protons of the benzene ring in the benzyl ether moiety. A singlet of integral 2H at 5.07 ppm was assigned to the benzylic CH_2 protons. The characteristic ddt at 6.02 ppm was assigned to the sp^2 hybridised methine proton of the allyl substituent. The MS (CI, +ve) showed a peak at *m/z* 225 assigned to the M+H ion.

Scheme 4.1: Benzyl protection of 2-allylphenol.

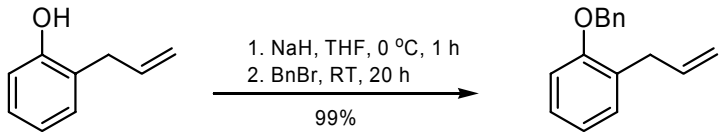

120 **164**

4.2 Dimerisation via the metathesis reaction (Key Step 1)

The dimerisation of the suitably protected allylphenol was performed via the metathesis reaction. A solution of the allylic benzylic ether **164** in dichloromethane was heated at reflux for 45 hours, in the presence of 5 mol % Grubbs 1st generation catalyst **131** (**Scheme 4.2**). After subjecting the crude reaction mixture to silica gel column chromatography, the desired dimer **165** was obtained in 51% yield, as a 3:1 mixture of *E*:*Z* diastereomers. The simplicity of the ^{1}H and ^{13}C NMR spectra indicated the formation of a symmetrical molecule. The peaks at 5.02-5.06 ppm assigned to the two terminal sp^2 hybridised protons in the ^{1}H NMR of the monomer **164** were absent. The peak at 5.68-5.71 ppm in the ^{1}H NMR of the dimer **165** was assigned to the sp^2 hybridised methine proton, shifted upfield from 6.02 ppm in the monomer. The ratio of *E*:*Z* isomers was determined by comparison of the integration of the two doublets at 3.43 and 3.54 ppm, assigned to the methylene protons H1/H4 adjacent to the double

bond in the *trans* and *cis* isomers, respectively. MS (CI, +ve) analysis showed a peak at *m/z* 421 assigned to the M+H ion of the dimer **165**.

Scheme 4.2: Self-metathesis of benzyl ether **164** to form the *trans* and *cis* homodimer **165**. Chemical shifts in the ^{1}H and ^{13}C NMR spectra assigned to the methylene protons H1 (and H4) and corresponding carbons C1 (and C4) adjacent to the double bond are quoted in ppm.

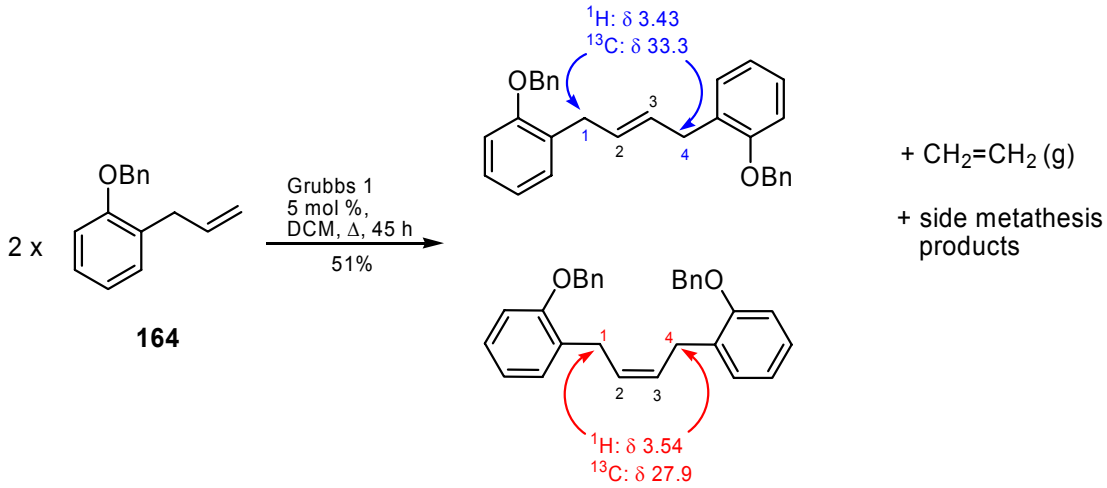

TLC analysis of the reaction indicated the formation of unidentified side metathesis products, presumably resulting from double bond migration. The similar R_f values exhibited by the starting material **164**, the desired product **165** and the side products rendered purification difficult. The reaction mixture was subjected to three successive columns, using 1% EtOAc:hexanes as the eluting solvent, which resulted in isolation of alkenes *E*- and *Z*-**165** from the side metathesis products. TLC analysis using DCM/hexanes, Et_2O/hexanes, $CHCl_3$/hexanes, and mixtures thereof, as the developing solvent showed no separation of the two isomers. The geometric mixture was then subjected to radial chromatography (hexanes to 1% EtOAc:hexanes), however the ^{1}H NMR analysis of the collected fractions showed only partial improvement in the ratio of isomers.

As the mixture of geometric isomers could not be separated, optimisation of both the chemical and geometric stereochemical yield of **165** was undertaken and is summarised in **Table 4.1**.

Table 4.1: Optimisation of the self-metathesis reaction of **164** to form the dimer **165**. Reactions were heated at reflux, under a N_2(g) atmosphere in the presence of Grubbs 1st or 2nd generation catalyst. Note that the conditions presented in entry 1 are those outlined in **Scheme 4.1**.

	Grubbs catalyst (mol %)	Solvent	Reaction time (h)	**165** yield (%)[a]	*E*:*Z*[b]
1	1 (5)	DCM	45	51	3:1
2	1 (5)	$CHCl_3$	19	62	5:1
3	1 (6.7)	DCM	4.5	81	5.2:1
4	2 (5)	DCM	26	93[c]	7:1

[a]Isolated yield. [b]Determined by ^{1}H NMR. [c]Final yield determined by ^{1}H NMR.

A decrease in reaction time resulted in better yields (entries 2 and 3). Longer reaction times increase the amount of secondary metathesis reactions, thereby decreasing the yield. Using chloroform as the reaction solvent increased the yield and the geometric selectivity of the homodimerisation (entry 2). A slight increase in catalyst and a much shorter reaction time afforded the dimer in good yield (entry 3). Following column chromatography, slow recrystallisation of the dimer **165** increased the geometric ratio from 5.2:1 to 9:1; however the quantity of enriched isomers was small. The use of Grubbs 2nd generation catalyst gave the highest yield (entry 4); however the dimer could not be separated from the side metathesis products. The mixture was subjected to two successive columns, but the dimer could only be purified to within 96% purity, as determined by ^{1}H NMR. The impurity was attributed to at least two olefinic side metathesis products resulting from isomerisation of the double bond and metathesis products thereof. Although only a minor impurity, the presence of two additional alkenes to *E*- and *Z*-**165**, resulted in a possible seven isomeric diols from the AD reaction. Chiral HPLC analysis of a mixture of isomers with similar properties was not possible, without extensive attempts to isolate the desired diols. So although the geometric ratio was increased substantially by the use of the more active catalyst; the amount of side products was also substantially increased.

Therefore, the most synthetically useful reaction conditions was the use of Grubbs 1 and shorter reaction times (entry 3). The *trans* isomer could not be isolated from the *cis* isomer in large quantities. Therefore a mixture of geometric isomers was taken through to the next step of the synthesis.

4.3 Asymmetric dihydroxylation (Key Step 2)

A diastereomeric mixture (*E*:*Z* 3.8:1) of alkene **165** was reacted under typical Sharpless conditions using AD mix α and methanesulfonamide in *t*BuOH and water (**Scheme 4.3**). The reaction was quenched with sodium sulfite after 24 hours, and after a basic aqueous workup, the crude mixture was subjected to silica gel column chromatography to afford the chiral diol (*S*,*S*)-**166a** as a white solid in 15% yield, with an *ee* of 64%.

Scheme 4.3: Asymmetric dihydroxylation under typical Sharpless conditions to form the chiral diol (*S*,*S*)-**166a**.

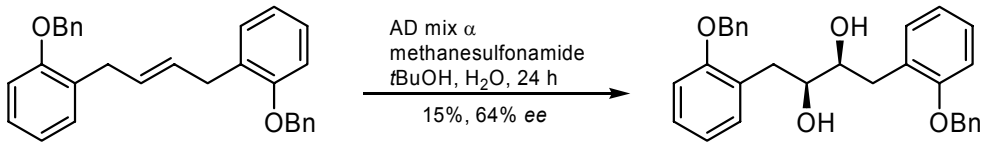

165 (*S*,*S*)-**166a**

The ^{1}H NMR spectrum showed a peak at 3.66 ppm assigned to the sp^{3} CH protons attached to the hydroxy group, shifted upfield from the peak at 5.68 ppm in the ^{1}H NMR of the alkene **165**, assigned to the sp^{2} CH protons. The characteristic splitting pattern observed for the two sets of diastereotopic methylene protons confirmed the presence of a stereogenic atom in the molecule. The ^{13}C NMR spectra contained a peak at 73.1 ppm assigned to the sp^{3} hybridised methine carbon, and a peak at 35.1 ppm assigned to the methylene protons adjacent to the hydroxylated carbon. The MS (ES, +ve) displayed a base peak at *m/z* 477, assigned to the M+Na ion.

Silica gel column chromatography of the diastereomeric mixture did not separate the chiral diol from the *meso* diol. Recrystallisation from DCM/hexanes increased the diastereomeric purity of the filtrate, by partially removing the *meso* isomer; however the chiral diol also crystallised. Preparative TLC of a 10 mg sample of the mixture isolated <1 mg of chiral diol for HPLC analysis. This could not be performed on a large scale; therefore the chiral diol could not be isolated from the *meso* diol in synthetically useful quantities.

The poor yield of 15% was attributed to the poor solubility of the alkene **165** in the reaction mixture (*t*BuOH/H_2O). Attempts to increase the solubility of the alkene by modifying reaction conditions are summarised in **Table 4.2**. In order to increase its

solubility, the alkene was dissolved in THF before addition to the reaction mixture (entry 2). The yield doubled, however a significant decrease in enantioselectivity was observed. THF is miscible with water, so although the alkene has increased solubility, a significant amount of the alkene is likely to be dihydroxylated in the aqueous phase, in the absence of the chiral ligand. This results in an increase in yield of the diol with poor enantioselectivity. Generally, extended reaction times provided a higher yield of diol (*S*,*S*)-**166a**, however inconsistency in the results was evident. The quantity of THF added had a dramatic effect on the enantioselectivity, with the minimal amount required for dissolution (entries 3 and 4) resulting in a higher stereochemical outcome, than when equal parts of *t*BuOH, water and THF were used (entry 2). Increased reaction time increased the chemical yield; however the enantiopurity of the resulting diol was decreased. The increased reaction time may allow entry of the monoglycolate into the second, less enantioselective, catalytic cycle.

Table 4.2: The optimisation of the asymmetric dihydroxylation of **165** to form the chiral diol (*S*,*S*)-**166a** under standard Sharpless conditions, using AD mix α.[3] Note that the conditions described in entry 1 are those outlined in **Scheme 4.3**.

	Reaction time (h)	*t*BuOH:H_2O:THF	**166a** yield (%)[a]	*ee*[b]
1	24	1:1:0	15	64
2	23	1:1:1	30	11
3	91	1:1:0.25	64	33
4	37	1:1:0.25	60	36

[a]Isolated yield of **166a** as a mixture of chiral:*meso* diastereomers. [b]Determined by chiral HPLC.

Therefore, the asymmetric dihydroxylation of the alkene **165** under Sharpless conditions, or modified Sharpless conditions, did not provide the chiral diol (*S*,*S*)-**166a** in sufficient chemical and stereochemical yield. The sacrifice in enantioselectivity was too significant in order to obtain a synthetically useful chemical yield.

The reaction was repeated with the alternate AD mix, in order to provide confirmation of HPLC interpretation. The alkene was subjected to Sharpless conditions using AD mix β, which yielded the chiral diol in 69% yield, and a much higher enantiopurity of

91% *ee* (**Scheme 4.4**). It is known[3] that the AD mix β generally results in higher enantioselectivity, but the degree of the increase to 91% was unexpected.

Scheme 4.4: Asymmetric dihydroxylation under Sharpless conditions using AD mix β to form the chiral diol (*R*,*R*)-**166b**.

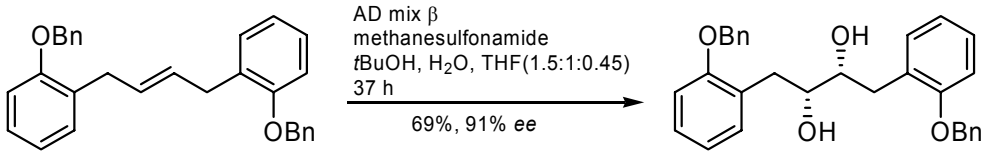

165 (*R*,*R*)-**166b**

Although the results were varied, even the highest *ee*s obtained were not sufficient for a chiral synthesis. Literature examples of ADs on dimeric aromatic allylic-type systems are shown in **Figure 4.2**. The AD reaction using AD mix β of the disubstituted dimeric aromatic alkene **170** gave the diol (*R*,*R*)-**171b** in 84% yield, although no stereochemical yield was reported (**Figure 4.2**, **a**).[191] The tetrasubstituted alkene **172** was dihydroxylated using AD mix β under modified Sharpless conditions (increased Os, ligand and methanesulfonamide) to give the diol (*R*,*R*)-**173** in 85-87% yield and 29% *ee* (**Figure 4.2**, **b**).[3]

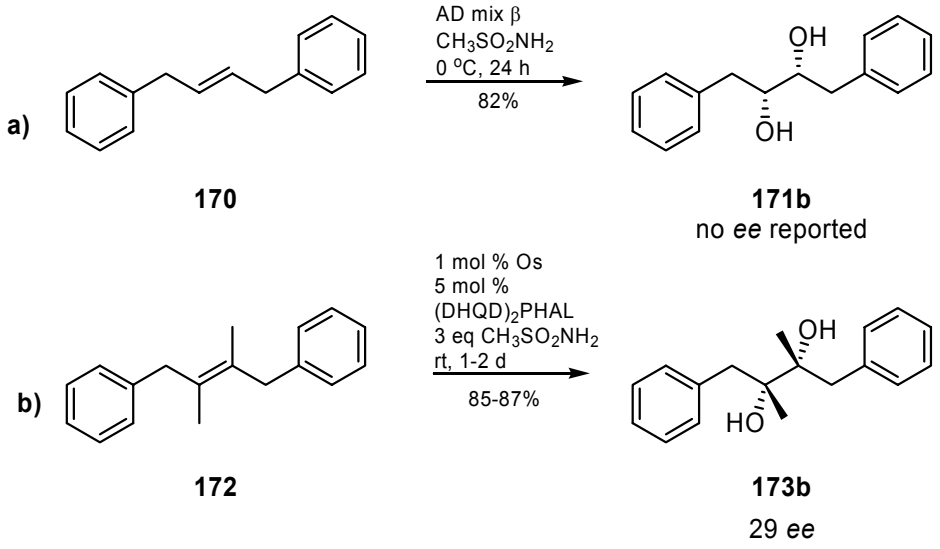

Figure 4.2: AD reactions of disubstituted aromatic allylic-type systems reported in the literature.[3,191]

Comparison of the reported reactions with the AD reaction of **165** gave some points for consideration. The yield of the AD reaction of the alkene **170** was much higher than with alkene **165**, although no comparison could be made with respect to the stereochemical outcome. Although a tetrasubstituted alkene, the AD reaction of **172** gave the diol **173b** in high yield, albeit in poor *ee*. The source of the poor stereoselectivity was presumably the tetrasubstitution of the double bond, which is known to hamper the AD reaction due to steric hindrance. Direct comparison of the structures **170** and **172** with alkene **165** indicates that the presence of the *ortho*-benzyloxy substituents on the aromatic rings has a detrimental effect on the yield of diol. Whether the benzyloxy substituent was causing a steric effect or decreasing solubility of the alkene in the organic layer was unknown.

Therefore, in a separate, extensive study, the nature of the *ortho*-substituent was examined. The solubility of the alkene in the *t*BuOH layer was increased in an attempt to maximise contact with the OsO_4 bound ligand. The size of the *ortho* substituent was decreased to ensure inclusion of the alkene into the binding cavity of the ligand. The biscinchona ligands typically favour aromatic or long alkyl chain substrates; therefore the electronic nature of the *ortho*-substituent was modified to determine if there were any unfavourable interactions between the alkene and the hydrophobic pocket. The results of the study are presented in **Chapter 5**.

It was expected that an appropriate alternative to the benzyloxy could be found and therefore the remaining steps towards the synthesis of 2,2'-bisindoline **112** were attempted to demonstrate proof of concept for the strategy.

4.4 Towards the synthesis of 2,2'-bisindoline

*4.4.1 Mesylation of diol (*S,S*)-**166a***

In order to establish the chemistry of the new system, the synthesis of 2,2'-bisindoline was attempted using samples of the diol **166a** that contained stereochemical mixtures. Therefore, diol (*S*,*S*)-**166a** (chiral:*meso* 14:1) was subjected to typical conditions for mesylation (**Scheme 4.5**). The crude dimesylate (*S*,*S*)-**174a** was isolated as a white solid, as a 14:1 mixture of chiral:*meso* diastereomers in quantitative yield. The chiral

isomer was isolated from the diastereomeric mixture via recrystallisation from DCM/hexanes.

Scheme 4.5: Mesylation of the chiral diol (*S*,*S*)-**166a**.

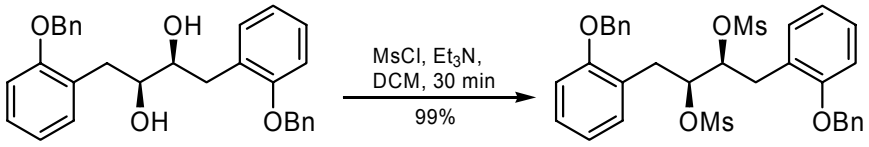

(*S*,*S*)-**166a** (*S*,*S*)-**174a**

The MS (ES, +ve) displayed a peak at *m/z* 633 assigned to the M+Na ion. A singlet at 2.22 ppm of integration 6H in the ^{1}H NMR spectrum and a peak at 37.5 ppm in the ^{13}C NMR spectrum were assigned to the methyl protons and carbons of the sulfonyl substituent, respectively. The difference in chemical shifts in the ^{1}H NMR spectra between the peaks assigned to the two diastereotopic methylene protons of the dimesylate (*S*,*S*)-**174a** (2.98 and 3.26 ppm) was much larger compared to the shifts between the peaks assigned to the corresponding protons in the diol **166a** (2.75 and 2.87 ppm), highlighting the greater difference in chemical environment between the two diastereotopic protons. The peak assigned to the methine proton also experienced a downfield shift, from 3.66 to 5.23 ppm, due to the increased electronegativity of the mesylate group compared to the hydroxy substituent.

*4.4.2 Attempted azidation of dimesylate (*S,S*)-174a*

An S_N2 displacement reaction of the mesylate groups of (*S*,*S*)-**174a** with N_3 was attempted in an analogous method to the azidation of the dimesylates (*S*,*S*)-**144a** and (*S*,*S*)-**154a** (**Chapter 3**). A solution of dimesylate (*S*,*S*)-**174a** in DMF was treated with 6 equivalents of sodium azide, and the reaction mixture was stirred 50 ^{o}C for 3 hours. TLC analysis indicated the presence of starting material only, and therefore the temperature was increased to 80 ^{o}C for 13 hours. TLC analysis indicated the presence of two products, and starting material. An additional 6 equivalents of sodium azide were added and after a further 7 hours of heating, the reaction was quenched, even though the starting material was not consumed. After aqueous workup and column chromatography the starting material was recovered (29%), and alkene **175** and azide **176** were isolated in 20% and 15% yields, respectively (**Scheme 4.6**).

Scheme 4.6: Attempted azidation of dimesylate (*S*,*S*)-**174a** to form diazido (*R*,*R*)-**167a**. Two major products were isolated, **175** and **176**. The chemical shifts of peaks in the ^{1}H NMR spectra assigned to the alkyl protons of **175** and **176** are quoted in ppm, and multiplicities are indicated.

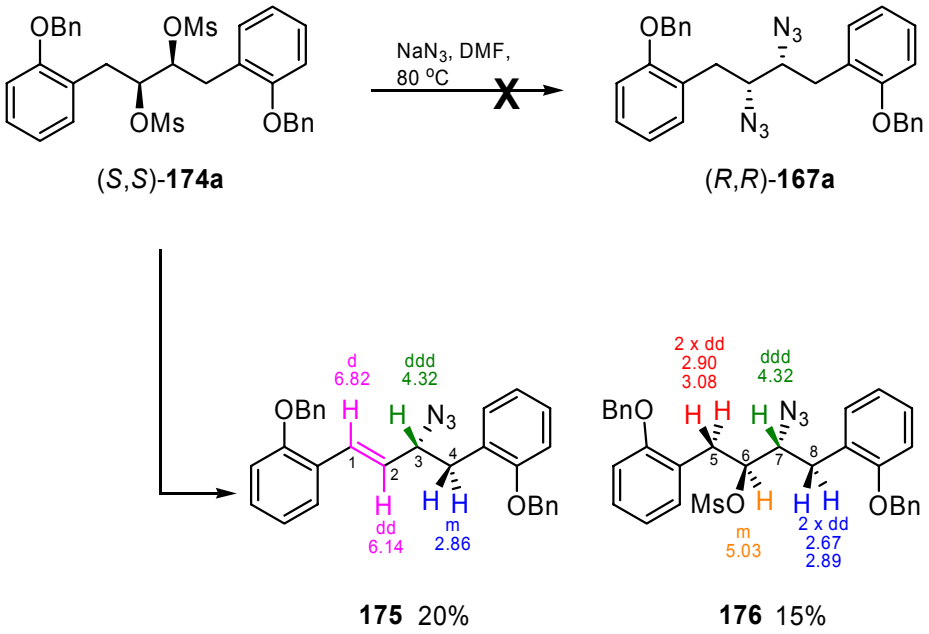

Two peaks in the ^{1}H NMR spectrum of **175** at 6.82 and 6.14 ppm were assigned to the sp^2 hybridised alkenyl protons **H1** and **H2**. The protons exhibited a coupling of 16 Hz, indicative of a *trans* configuration. A ddd peak at 4.32 ppm was assigned to **H3** and a multiplet at 2.86 ppm was assigned to the diastereotopic **H4** protons. Two sets of dd peaks at 2.90 and 3.08 ppm in the ^{1}H NMR of the azido compound **176** were assigned to the **H5** protons, and another two sets of dd at 2.67 and 2.89 ppm were assigned to the alternate diastereotopic protons **H8**. A multiplet at 5.03 ppm was assigned to the **H6** proton geminal to the mesylate group, and a ddd at 4.32 ppm was assigned to the **H7** proton geminal to the azido functionality.

Despite the presence of excess sodium azide (six equivalents per mesylate group), the desired nucleophilic substitution reaction did not go to completion. Good S_N2 reaction conditions are promoted by the presence of a) a strong nucleophile in the negatively charged azide anion N_3^- and b) a good leaving group in the mesylate substituent, which provides an electrophilic carbon via its electron-withdrawing effect. Despite favourable conditions for the desired S_N2 reaction, 29% of the unreacted starting material **174** was recovered and the 15% mono-substituted azido **176** was isolated, indicating that the structure of the molecule was not susceptible to two S_N2 reactions possibly due to steric

effects imposed by the neighbouring *ortho*-substituted aromatic rings. Although a good nucleophile, the azido anion is unable to access the electrophilic carbon.

Following mono-substitution via an S_N2 mechanism, the competing reaction to form the alkene **175** prevents the formation of the diazido **167**. The formation of **175** is proposed to occur via the E1 reaction of mono-azido **176** (**Figure 4.3**). The remaining mesylate group dissociates leaving a secondary carbocation **177**, which is followed by hydride transfer to form **178**, promoted by the stability of the resulting benzylic carbocation. The azide anion removes the proton to generate the double bond. The driving force for the elimination is the establishment of a conjugated system combined with the stability of the benzylic carbocation. An alternative mechanism for the formation of the benzylic carbocation **178** from **176** involves the hydride transfer and loss of the mesylate anion occurring in concert.

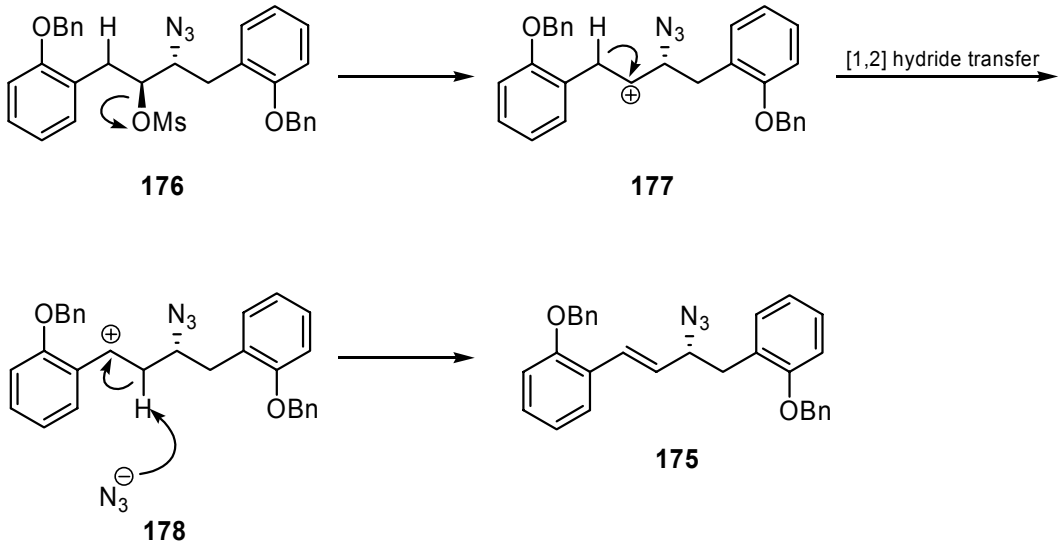

Figure 4.3: Proposed E1/hydride transfer mechanism for the formation of azido compound **175**.

Further examples of this reaction were observed in two analogous systems, shown in **Figure 4.4**.[192] The azidation was performed on dimesylates **179** (R = Br) and **180** (R = OMe), to yield the desired diazidos **181** and **182** and the elimination products **183** and **184**. Optimisation of the reaction provided the desired diazidos via longer reaction times; however the reaction remained poor yielding.

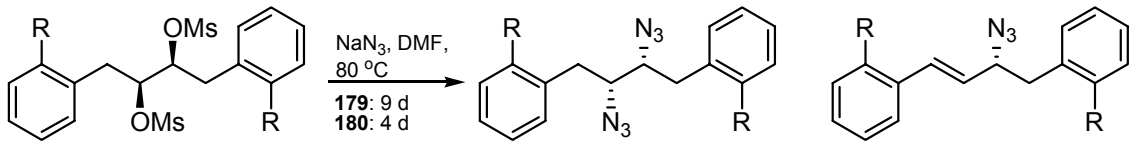

179 R = Br
180 R = OMe

181 R = Br 53%#
182 R = OMe 29%*

183 R = Br 19%#
184 R = OMe 15%*

Figure 4.4: Outcomes of the azidation of dimesylates **179** and **180**.[192] #The bromo derivatives **181** and **183** were inseparable via column chromatography; therefore the yield was determined via ^{1}H NMR analysis. *Isolated yield.

The analogous elimination products **185a** and **186a** were identified, although not isolated and characterised, from the azidation of dimesylates **144a** and **154a** (**Scheme 4.7**). The minimal quantity of this side product supports the mechanism proposed in **Figure 4.3**, since the initial carbocation formed in the first step of the E1 mechanism is not as stabilised as the benzylic cation, and therefore results in a lower yield.

Scheme 4.7: The azidation of dimesylates **144a** and **154a** to give diazidos **108a** and **155a** with the elimination side products **185a** and **186a**.

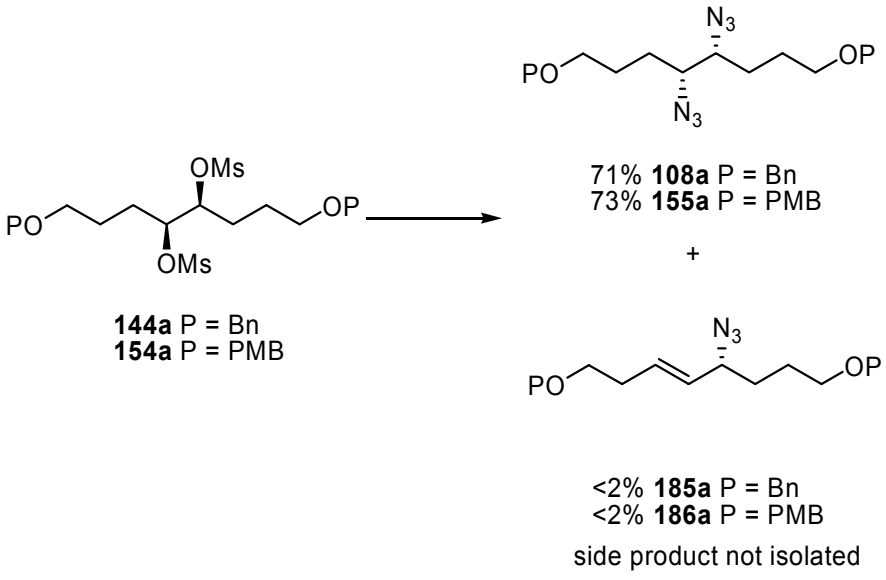

144a P = Bn
154a P = PMB

<2% **185a** P = Bn
<2% **186a** P = PMB
side product not isolated

4.4.3 Alternative strategy towards 2,2'-bisindoline[185]

The synthesis of 2,2'-bisindoline via the key steps of metathesis dimerisation and subsequent AD had been realised in concurrent studies[185] whereby the nitrogen heteroatom was incorporated into the synthesis from the beginning (**Figure 4.5**).[185] Protected 2-allylaniline **187** was subjected to metathesis dimerisation followed by AD

to give diols **189**. The chemical (31-34%) and stereochemical results (50-56% *ee*) of the AD reaction were poor, which was proposed to be due to the poor solubility of the alkene **188** in the *t*BuOH/H_2O reaction mixture. Large amounts of *t*BuOH were required to dissolve the alkene, and longer reaction times were required. These deviations from the general protocol for the AD reaction had a detrimental effect on the enantioselectivity.

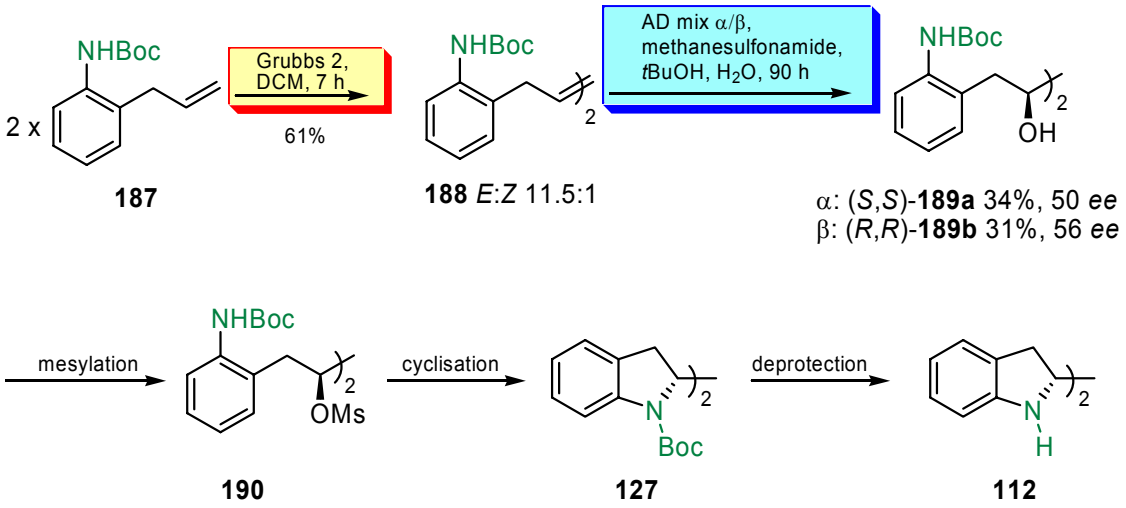

Figure 4.5: Alternative synthesis of bisindoline **112**, from Boc-protected 2-allylaniline.[185]

Although this alternate strategy did provide the desired 2,2'-bisindoline, the enantiopurity obtained was poor. In an effort to improve the outcome of the AD reaction, alternate N-protecting groups were proposed to replace the Boc group.

4.4.4 Conclusion

The preliminary results of the synthesis towards 2,2'-bisindoline in this thesis, in combination with the results from the alternate strategy used in concurrent studies,[185] indicated that the while the concept succeeded, the major setbacks were the poor results obtained from the normally reliable Sharpless AD. It was expected that an appropriate alternative to the protecting group of either the phenolic-based or anilino-based derivatives would provide the necessary modification to improve the stereochemical and chemical outcome of the AD and, in turn, the synthesis of 2,2'-bisindoline.

CHAPTER 5

The Asymmetric Dihydroxylation of Dimeric Aromatic Allylic Alkenes

The asymmetric dihydroxylation using Sharpless conditions of the dimeric aromatic allylic alkenes **165** and **188** gave poor yields and stereochemical yields of the diols **166** and **189**. Analysis of the reaction outcome provides two sources of information regarding the mechanism of reaction.

1. The **poor chemical yield** indicates that the alkene is prevented from accessing the ligand bound OsO_4 and therefore cannot undergo dihydroxylation.
2. The **poor enantioselectivity** indicates that the differentiation in stability between the two diastereomeric transition states is minimal (**Figure 5.1**), leading to the formation of the undesired enantiomer.

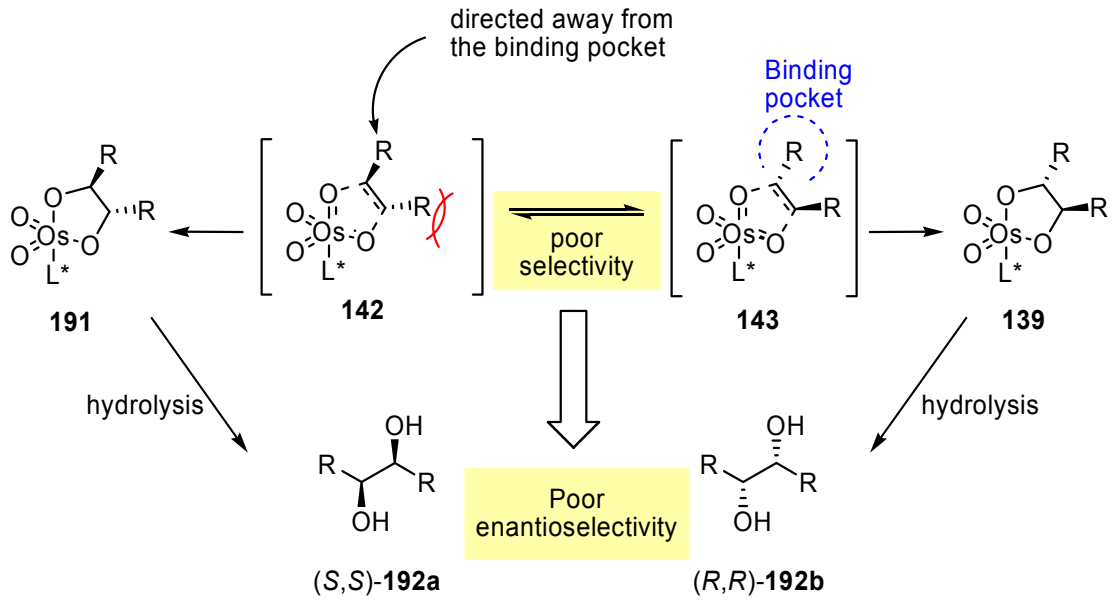

Figure 5.1: The transition states leading to the formation of diols (*S*,*S*)-**192a** and (*R*,*R*)-**192b**. When the stability of **142** and **143** are similar resulting from destabilising effects between the substrate and the chiral ligand, the diols will be formed with poor enantioselection.

The reason for the inability of the alkene to access the ligand bound OsO_4 could be due to;

1. steric interactions between the substrate and the binding pocket,
2. poor solubility of the substrate, or
3. an unfavourable electronic interaction between the substrate and the phthalazine linker or methoxyquinoline walls of the ligand.

Therefore, a study was undertaken to improve the outcome of the AD reaction, via the modification of the nature of the protecting group of the phenol-based and nitrogen-based alkenes.

5.1 Phenol-based derivatives

The phenol-based derivatives were first examined, due to the increased potential of the synthetic route to access alternate derivatives of the final bisindoline ligand. It was proposed that the protecting group could be modified to determine the effect of substituent polarity, size, solubility and electronic nature on the outcome of the asymmetric dihydroxylation (**Figure 5.2**). Initially, the protecting groups were chosen for the simplicity of the synthesis of the precursors; additionally, those chosen would give a range of information regarding the nature of the substituent.

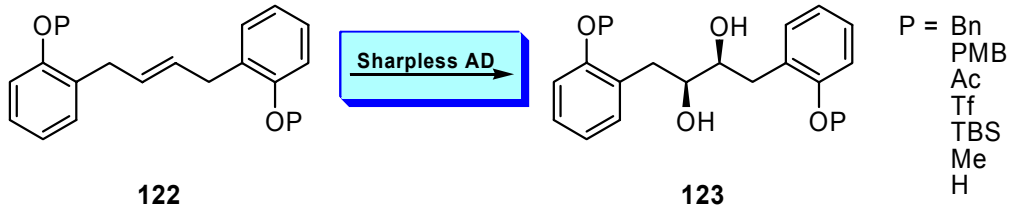

Figure 5.2: Proposed optimisation of the asymmetric dihydroxylation of dimeric aromatic allylic alkenes of the type **122** to form the diols **123**. Examination of the AD reaction was performed via modification of the O-protecting group, to determine the effect of the nature of the substituent on the chemical and stereochemical outcome of the reaction.

Therefore, dimeric alkenes of the type **122** (P = PMB, Ac, Tf, TBS, Me, H) were required. Due to the lack of literature precedent for these systems, the proposed synthesis of the dimers was via the self-metathesis reaction of monomeric *ortho*-allylphenolic precursors of the type **121** (**Figure 5.3**), themselves generated from 2-allylphenol **120** using standard protection procedures.

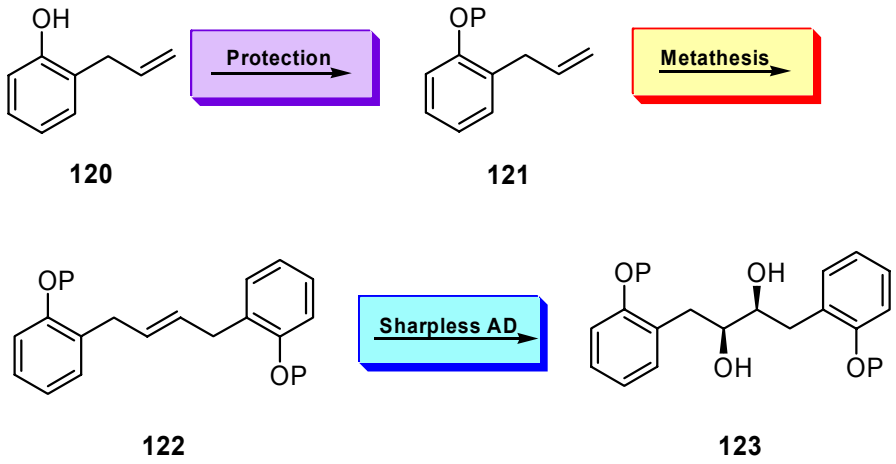

Figure 5.3: Synthesis of the monomeric aromatic allylic alkenes **121**, dimerisation via self-metathesis to form dimeric alkenes **122** and asymmetric dihydroxylation to form chiral diols **123**.

5.1.1 Synthesis of the phenol-based monomers

Commercially available 2-allylphenol **120** was protected using standard conditions, as outlined in **Table 5.1**.

Table 5.1: Conditions for the *O*-protection of 2-allylphenol **120**, and relevant spectral evidence. ^{1}H and ^{13}C NMR peaks are quoted in ppm, and the peak assigned to the M^{+} ion in the EI-MS is quoted.

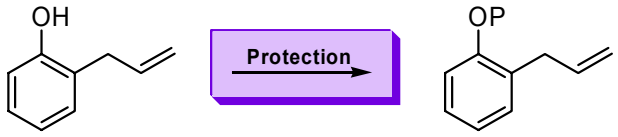

	P	Conditions	121	Yield[a] (%)	NMR evidence			EI-MS (*m/z*)
					^{1}H (ppm)	^{13}C (ppm)	Assign-ment	
1	PMB	1. NaH, THF, 0 °C 2. PMBBr, 0 °C to RT, 23 h.	**193**[193]	90	3.81, 3*H* 5.00, 2*H*	55.3 69.7	O<u>C</u>H$_3$ <u>C</u>H$_2$Ph	254
2	Ac	Acetic anhydride, Et_3N, RT, 25 h.	**194**[194]	99	2.30, 3*H* -	20.9 169.3	<u>C</u>H$_3$ <u>C</u>=O	176
3	Tf	*N*-Phenyl-triflimide, K_2CO_3, THF, Δ, 48 h.	**195**[195]	83	-	118.6, q, *J* = 320 Hz	<u>C</u>F$_3$	266
4	TBS	Imidazole, TBSCl, RT, 18 h.	**196**[196]	99	0.24, 6*H* 1.02, 9*H* -	-4.1 25.8 18.3	Si(<u>C</u>H$_3$)$_2$ C(<u>C</u>H$_3$)$_3$ <u>C</u>(CH$_3$)$_3$	247[b]
5	Me	MeI, K_2CO_3, acetone, water (cat.), 40 °C, 20 h.	**197**[197]	87	3.81, 3*H*	55.3	O<u>C</u>H$_3$	148

[a]Isolated yield after purification via silica gel column chromatography. [b]M-H ion.

5.1.2 Metathesis reaction of phenol-based monomers

The protected phenol based monomers **121** were dimerised via the metathesis reaction to form dimeric disubstituted aromatic allylic alkenes of the type **122**, using Grubbs 1st and 2nd generation catalysts, as summarised in **Table 5.2**.

Table 5.2: Homo-dimerisation of monomeric phenol-based derivatives **121**, via self-metathesis to form the dimers **122**. Reaction conditions were standard involving heating at reflux in DCM with Grubbs 1st or 2nd generation catalysts.

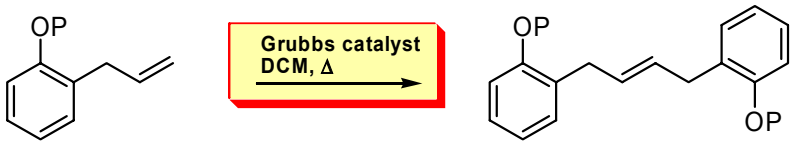

121 **122**

	P	121	122	Grubbs 1				Grubbs 2			
				mol %	time (h)	yield (%)[a]	*E*:*Z*[b]	mol %	time (h)	yield (%)[a]	*E*:*Z*[b]
1	Bn[c]	**164**	**165**	6.7	4.5	81	5.2:1	5	26	93[d]	7:1
2	PMB	**193**	**198**	5	23	51	5:1	5	23	71	7.1:1
3	Ac	**194**	**199**	5	15	85	4:1	5	66	77	8:1
4	Tf	**195**	**200**	5	15	88	3.8:1	5	66	75	9:1
5	TBS	**196**	**201**	5	66	85	4.3:1	5	66	95[d]	8.4:1
				-	-	-	-	5	7.5	95[d]	7:1
6	Me	**197**	**202**	5	19	81	4.4:1	5	19	60[d]	5.6:1
				5	7	91	4.5:1	5	24	73[d]	5.5:1
7	H	**120**	**203**	10	25	50	9:1	-	-	-	-

[a]Isolated yield. [b]Determined by ^{1}H NMR. [c]Discussed in **Chapter 4**. [d]Final yield determined by ^{1}H NMR.

The self-metathesis reaction in the presence of the more active Grubbs 2 catalyst generally resulted in higher *trans* selectivity and although the chemical yield also increased in most cases, the desired alkene could not be isolated from the secondary metathesis products. The bulkier benzyl groups (entries 1 and 2, P = Bn, PMB) resulted in higher *trans* selectivity than substitution with smaller groups (entries 3-6, P = Ac, Tf, TBS, Me), when using Grubbs 1, however the opposite effect was observed with Grubbs 2. No differentiation was found when using the acetate or triflate (entry 3 and 4) with the same reaction times. The use of Grubbs 2 decreased the yield despite the apparent full conversion of the starting material as determined by TLC analysis. The extended reaction time (66 hours) lead to degradation of the desired alkenes via secondary

metathesis reactions. Interestingly, the longer reaction time (66 hours) in the presence of Grubbs 1 provided the silyl derivative **201** in similar chemical and stereochemical yields (entry 5, P = TBS) to the acetate and triflate derivatives after 15 hours. Grubbs 1 catalyst becomes inactive after short reaction times; therefore the desired product does not undergo further reaction during extended reaction times. The Grubbs 2 catalyst is, by design, more active[186] and retains activity; therefore extending reaction time is detrimental to overall yield. The results obtained from the use of Grubbs 2 catalyst with the silyl protecting group are anomalous (entry 5, P = TBS). The same chemical yield was obtained from the reaction after 66 hours and 7.5 hours, and both yields were high (95%). The remaining 5% yield was attributed to the cross-metathesis of the monomer with the styrene from the catalyst, which could not be separated from the desired alkene by silica gel column chromatography. The extended reaction time provided a higher *E*:*Z* ratio (from 7:1 to 8.4:1). The *cis* isomer is less sterically hindered, and as such is more accessible by the catalyst to under go further reaction to the *trans* isomer. The only possible explanation for the lack of any secondary metathesis products is that the catalyst was rendered inactive shortly into the reaction, however this does not explain the increase in the *E*:*Z* ratio.

The self-metathesis of the free phenol **120** was trialled as a possible alternative to the protected phenol (entry 7, P = H). Grubbs 1 catalyst (10 mol %) was added in two portions, and the desired alkene was isolated in 50% yield, in higher selectivity (9:1), comparable to the selectivity when using Grubbs 2 catalyst with protected phenolic derivatives. There is evidence[171] that the addition of phenol (5 mol %) to the self-metathesis reaction of terminal alkenes improves the efficiency of the first generation catalyst, by extending the lifetime of the catalyst, with minimal formation of undesired secondary metathesis products. The more accessible *cis* isomer can therefore undergo conversion to the *trans* product. The higher selectivity (9:1) obtained in the dimerisation of 2-allylphenol indicates that this effect is occurring. The quantity of side products however, was not minimised. ^{1}H NMR analysis of the crude product indicated the presence of multiple unidentified side products. Following isolation, confirmation of the structure of **203** was made via comparison with the product obtained via deprotection of TBS protected dimer **201** (**Scheme 5.1**).

Scheme 5.1: Deprotection of TBS protected dimer **201** using standard conditions, to give diphenol **203**.

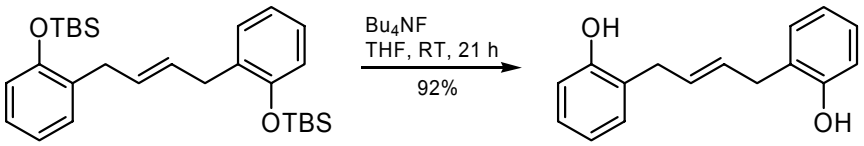

201 **203**

5.1.3 Asymmetric dihydroxylation of phenol-based dimers

The asymmetric dihydroxylation of the phenol-based dimers **122** gave the chiral diols **123**, as summarised in **Table 5.3**, using both AD mix α and AD mix β. Enantiomeric excesses were determined using HPLC analysis; therefore both isomers were required for confirmation of the assignments of peaks.

Table 5.3: Asymmetric dihydroxylation of the phenol-based dimeric aromatic allylic alkenes **122** under standard Sharpless conditions. Reaction with AD mix α provided the diols (*S*,*S*)-**123**; AD mix β gave the diols (*R*,*R*)-**123**.

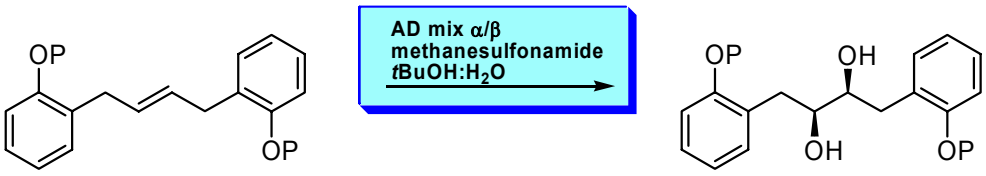

122 **123**

	P	122	123	AD mix α (*S*,*S*)-123a			AD mix β (*R*,*R*)-123b		
				time (h)	yield (%)[a]	*ee* (%)[b]	time (h)	yield (%)[a]	*ee* (%)[b]
1	Bn[c]	**165**	**166**	91	64	30	37	69	91
2	PMB	**198**	**204**	40	trace	-	40	trace	-
3	Ac	**199**	**205**	24	0	-	24	0	-
4	Tf	**200**	**206**	24	25	1.4	24	58	8
5	TBS	**201**	**207**	24	13	23	24	31	14
6	Me	**202**	**208**	24	52	34	24	37	40
7	H	**203**	**209**	24	0	-	24	0	-

[a]Isolated yield. [b]Determined by chiral HPLC. [c]Discussed in **Chapter 4**.

The PMB protecting group was trialled, due to the improvement in the result of the AD reaction of the PMB protected alkene **150** discussed in **Chapter 3**. The use of the PMB group in the aromatic derivative **198** (entry 2, P = PMB) was proposed to either increase the solubility of the diol in the *t*BuOH/H_2O reaction solvent or increase hydrophobic

interactions within the binding pocket of the ligand. However, only trace amounts of diol **204** were obtained. The alkene **198** was less soluble in *t*BuOH than alkene **165**, therefore, more information was required as to whether the poor result was due to unfavourable interactions within the binding pocket or a simple solubility issue. The acetyl protecting group (entry 3, P = Ac) was trialled to reduce the size of the substituent, with a slight increase in polarity. The AD of alkene **199** however, did not yield the corresponding diol, using either AD mix. Concurrently, in an attempt to increase the solubility of the alkene, the AD of alkene **200** (entry 4, P = Tf) with AD mixes α and β gave the corresponding diols **206** in almost racemic form. The ditriflate **200** was able to undergo dihydroxylation in the aqueous layer due to its water solubility. The dihydroxylation cycle occurring in the aqueous layer is in the absence of the chiral ligand, therefore enantioselectivity cannot be induced. TLC analysis of the reaction mixture indicated 100% conversion of the alkene **200**, however the isolated yields were low (25% and 58%). The poor isolated yield can be attributed to the water-solubility of the diol **206**, resulting in its poor recovery from the reaction mixture and subsequent aqueous workup.

Information regarding possible interactions between the alkene substrate and the chiral ligand could still not be ascertained, since the dihydroxylation reaction of the ditriflate **206** did not occur in the presence of the chiral ligand. Therefore, an alkene substrate was required that was more soluble than the benzylic ethers **165** and **198**, but less soluble than the ditriflate **206**. Alkenes **201** (P = TBS) and **202** (P = Me) fulfilled this requirement; in addition, the size and electronic effects of the *ortho* substituent could be determined. The diols **207** (entry 5, P = TBS) were obtained in poor chemical and stereochemical yield, while the reaction of the anisole derivative **202** (entry 6, P = Me) gave the diols (*S*,*S*)- and (*R*,*R*)-**208** in higher yield and *ee*. The OMe substituent is smaller than the OTBS and OPMB substituent, and presumably poses less steric hindrance with the chiral ligands; hence the alkene can access the ligand-bound OsO_4.

The reaction of the free phenolic derivative **203** (entry 7, P = H) was trialled in an effort to remove any steric interaction between the protecting group and the chiral ligand. However upon addition of the alkene to the AD mixture, the reaction immediately turned black, and did not provide the corresponding diol. In the basic conditions of the

reaction mixture (K_2CO_3) the phenolic proton is deprotonated, and presumably deactivates the catalyst.

5.2 Nitrogen-based derivatives

Improvement of the nitrogen-based synthetic strategy (see **Figure 4.5**) was envisaged through two methods of modification, demonstrated in **Figure 5.4**. The first was the use of an alternate protecting group to Boc, while the second utilises the nitro substituent in place of the protected anilino group. Following metathesis and AD, reduction of the nitro substituent and subsequent N-protection would provide dimesylate **213**, which would be converted to 2,2'-bisindoline **214**. In addition to providing an alternate strategy to 2,2'-bisindoline **112**, further information would be gained regarding the problems associated with the AD reaction of dimeric allylic aromatic alkenes.

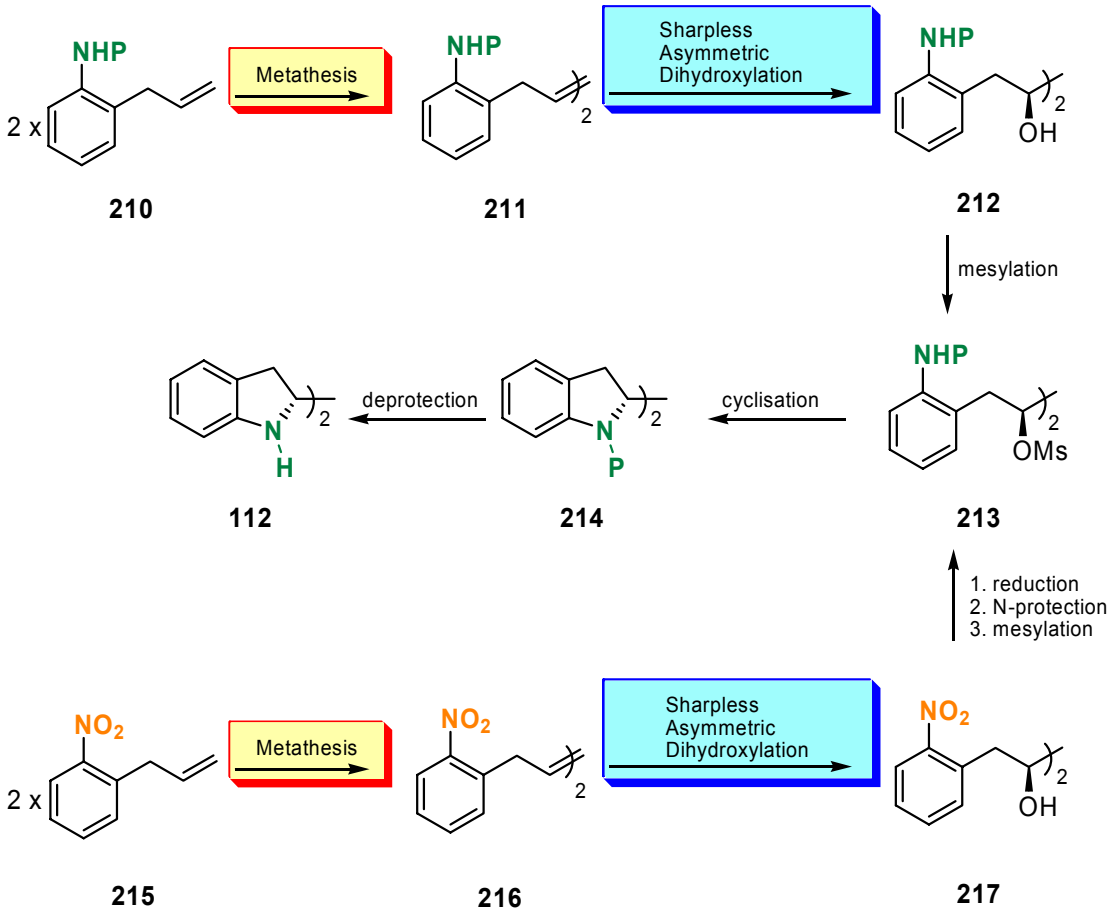

Figure 5.4: Two alternative strategies for the synthesis of 2,2'-bisindoline **112**, using nitrogen-based derivatives.

Therefore, the monomers **210** and **215** were required.

5.2.1 Synthesis of the nitrogen-based monomers

The synthesis of monomeric *N*-protected 2-allylanilines required the formation of 2-allylaniline via the Claisen rearrangement of *N*-allylaniline **218** (**Scheme 5.2**). *N*-Allylaniline **218** was heated at reflux in the presence of boron trifluoride diethyl etherate in xylenes. Basic (NaOH) workup followed by silica gel column chromatography afforded the rearranged product **219** in low yield (32%), which was spectroscopically identical to that reported in the literature,[185,198] and degraded upon exposure to light, air and NMR solvent.

Scheme 5.2: The synthesis of 2-allylaniline **219** via the [3,3]-sigmatropic or Claisen rearrangement of *N*-allylaniline **218**.

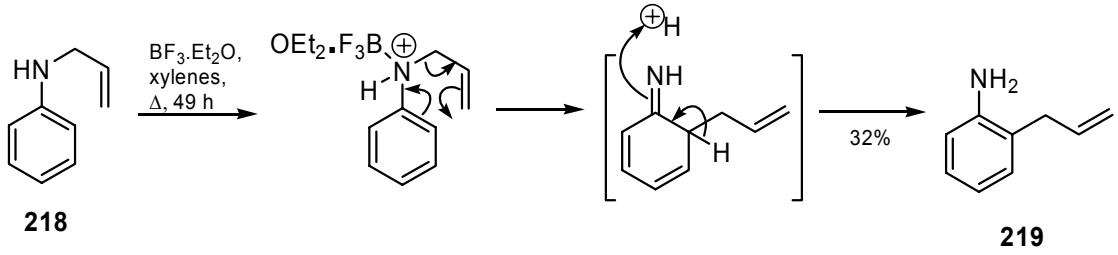

The isomerisation occurs via a [3,3]-sigmatropic rearrangement and subsequent rearomatisation. The Lewis acid coordinates to the nitrogen by accepting a pair of electrons into the vacant orbital of the boron. The rearrangement is performed under thermal conditions. Aromaticity is regained via protonation to form the aniline **219**.

The protection of 2-allylaniline **219** was attempted with three different protecting groups, with limited success (**Scheme 5.3**). The PMB protection (**Scheme 5.3, a**) utilised the same procedure as that for the phenolic derivative **193**, where PMBBr was generated *in situ*, and added to a suspension of 2-allylaniline **219** and sodium hydride in THF. The reaction failed to provide any of the desired PMB protected aniline **220**, giving only an inseparable mixture of unidentified products.

Scheme 5.3: Protection of 2-allylaniline **219** using **a)** *p*-methoxybenzyl bromide, **b)** *N*-phenyltriflimide and **c)** acetic anhydride.

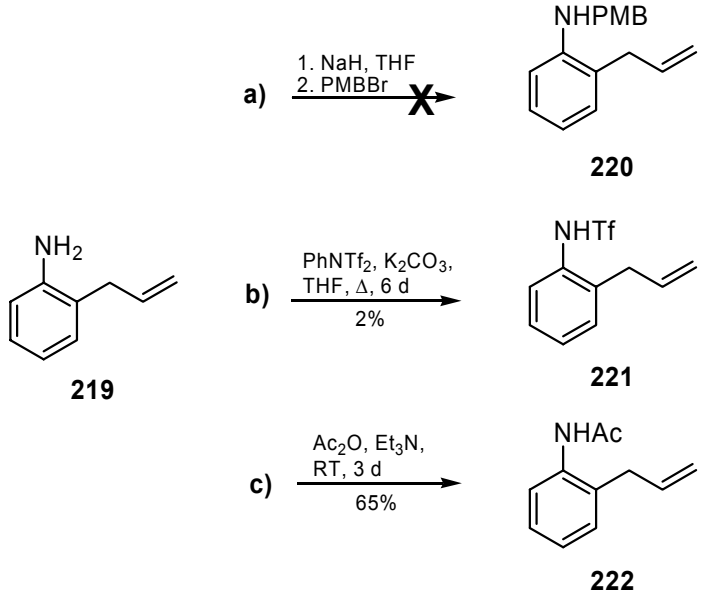

Aniline **219** was heated in the presence of *N*,*N*-bis(trifluoromethylsulfonyl)aniline, or *N*-phenyltriflimide, with potassium carbonate in THF as solvent (**Scheme 5.3, b**). After 6 days of heating at reflux, the reaction was stopped, and purification via silica gel column chromatography afforded the desired triflate **221** as a white solid, in 2% yield. The ^{1}H NMR spectrum showed a broad singlet with an integration of 1H at 6.25 ppm, a downfield shift of the broad singlet of integration 2H at 3.63 ppm in the ^{1}H NMR spectra of **219** assigned to the anilino protons, due to the deshielding effect of the adjacent triflate group. The use of the more reactive triflating agent triflic anhydride, Tf_2O, did not afford any of the desired triflate.

The poor results from attempted protection of 2-allylaniline **219** cannot be explained. Literature precedent shows that 2-allylaniline **219** and its derivatives have been protected using acetyl chlorides,[198,199] sulfonyl chlorides[200-202] and Boc_2O[203,204] in good yields, using standard procedures.

The protection of 2-allylaniline **219** as the acetanilide **222** was performed by reaction with acetic anhydride in the presence of triethylamine as a scavenger base (**Scheme 5.3, c**). After 3 days at RT and subsequent work up and silica gel column chromatography,

the acetanilide was isolated as a white solid in 65% yield which was spectroscopically identical to that reported in the literature.[199]

The alternate strategy required the synthesis of 1-allyl-2-nitrobenzene **215**. Typical methods for the aromatic allylation reactions include Pd catalysed Stille[205,206] and Suzuki[207] reactions and Grignard reactions.[208-211] Owing to the easier handling of Pd based reagents, the allylation of 1-iodo-2-nitrobenzene **223** was initially attempted using the generally reliable, standard Stille conditions (**Scheme 5.4**). A mixture of palladium (II) acetate, triphenyl phosphine, potassium carbonate, 1-iodo-2-nitrobenzene **223** and tributyl tin **224** was **a)** heated at reflux in THF and **b)** heated in a sealed tube at 130 ^{o}C, however the desired allylated product **215** was not formed.

Scheme 5.4: Attempted allylation of 1-iodo-2-nitrobenzene **223** using Stille conditions.

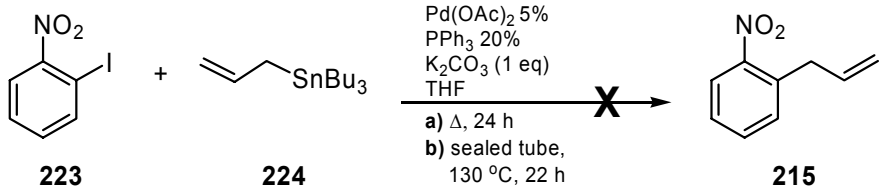

Therefore, the synthesis of the desired allylated product **215** via the recently reported Grignard-transmetallation reaction sequence[209,210] was attempted (**Scheme 5.5**).[209,211] A solution of 1-iodo-2-nitrobenzene was cooled to –40 ^{o}C and a solution of phenyl magnesium bromide was added. After 10 minutes, a solution of copper (I) cyanide (1 eq) and lithium chloride (2 eq)[212] in THF was added and after a further 10 min, allyl bromide was added neat. The reaction was continued for 2 hours. Purification via silica gel chromatography afforded the desired allylation product **215** in 82% yield, which was spectroscopically identical to that reported in the literature.[210]

Scheme 5.5: Conditions for the allylation of 1-iodo-2-nitrobenzene **223** to provide 1-allyl-2-nitrobenzene **215**.[210]

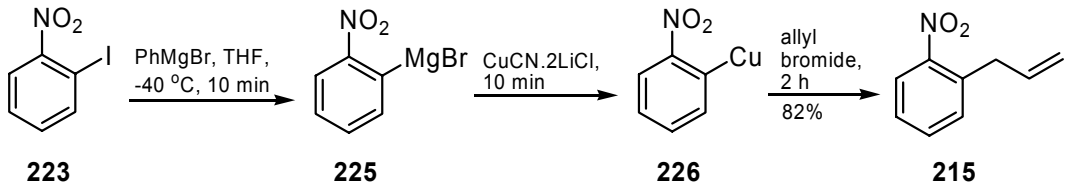

The Grignard reagent **225** was formed via an iodine-magnesium exchange between 1-iodo-2-nitrobenzene **223** and phenyl magnesium bromide. The low temperature of the exchange minimises possible unwanted side reactions between the Grignard and the nitro substituent. A number of derivatives have been formed[210] by reaction of the nitro substituted aryl Grignard **225** with a range of aldehydes, with excellent functional group tolerance. The magnesium-iodine exchange will only occur when a nitro or ester group is *ortho* to the iodine, since coordination between the *ortho* substituent and the magnesium centre is required. For the reaction to proceed smoothly with soft electrophiles, such as allyl bromide, the arylmagnesium species requires conversion to the aryl copper reagent **226** via transmetallation with CuCN.2LiCl.

5.2.2 Metathesis reaction of nitrogen-based monomers

The metathesis reaction was performed on the nitrogen-based monomers in the presence of Grubbs 1st and 2nd generation catalysts, as shown in **Table 5.4**.

Table 5.4: Homo-dimerisation of nitrogen-based monomeric aromatic allylic alkenes **227**, via self-metathesis to form the dimers **228**. Reaction conditions were standard involving heating at reflux in DCM with Grubbs 1st or 2nd generation catalysts.

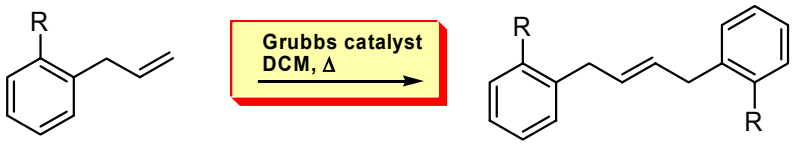

227 **228**

	R	227	228	Grubbs 1				Grubbs 2			
				mol %	time (h)	yield (%)[a]	*E*:*Z*[b]	mol %	time (h)	yield (%)[a]	*E*:*Z*[b]
1	NHBoc[c]	**187**	**188**	10	3	76	1.6:1	10	7	61	11.5:1
2	NHAc	**222**	**229**	-	-	-	-	10	17	73	*E* only
3	NO_2	**215**	**216**	-	-	-	-	5	7	26	43:1
				-	-	-	-	5	20	23	10:1

[a]Isolated yield. [b]Determined by ^{1}H NMR. [c]S. M. Wales, *Honours Thesis*, University of Wollongong, **2004**.[185]

The dimerisation of the N-Boc derivative **187** had previously been optimised to 10 mol % of Grubbs 2 catalyst (entry 1, R = NHBoc).[185] Therefore, the same conditions were applied to the *N*-acetyl derivative **222** (entry 2, R = NHAc). Immediately after addition

of the catalyst to the reaction mixture, a white precipitate formed. The reaction was continued for a further 17 hours, and the mixture was filtered to yield the desired dimer **229** as an insoluble white solid, in 73% yield, exclusively in the *trans* configuration. Although a promising result for the metathesis reaction, the alkene **229** obtained was not useful for further reaction, due to its excessively poor solubility in e.g. hexane, DCM, Et_2O, $CHCl_3$, DMSO, MeOH, acetone, water and the AD reaction solvent *t*BuOH.

The dimerisation of the nitro derivative **215** provided excellent stereoselectivity (43:1), 7 hours reaction time (entry 3, R = NO_2), although in poor yield (26%). Extending the reaction time to 20 hours decreased the yield slightly (23%), and decreased the stereoselectivity significantly (10:1). The poor yield can be attributed to the quantity of side products formed via undesired secondary metathesis reactions (**Scheme 5.6**). The desired self-metathesis of 2-allylnitrobenzene **215** yielded the symmetrical dimer **216**, in *E* or *Z* conformation. The monomer **215** or the dimer **216** underwent cross-metathesis with the styrene from the catalyst to form the unsymmetrical vinyl benzene **230**, which following double bond-migration gave **231** (2%). Alternatively, the dimer **216** underwent isomerisation, in which the double bond migrates from the allylic position to the vinylic position, forming the 1,4-disubstituted 1-butene **232** (3%). The isomerisations to form **231** and **232** are catalysed by Ru, with the formation of a highly conjugated system being the driving force. The cross-metathesis between the **232** and the monomer **215** (or **216** or **231**) gave the 1,5-disubstituted 2-pentene **233** (2%). Column chromatography isolated a 6.6:1 mixture of **216**:**233**. TLC analysis (mixtures of EtOAc and hexanes) did not resolve the alkenes. Further elution of the column yielded a mixture of all products outlined in **Scheme 5.6**. Both mixtures were subjected to column chromatography, and multiple recrystallisations using DCM/hexanes, DCM/Et_2O and DCM/ethanol, which did not purify the products any further. Therefore, the final yields of each were determined via comparative integration of the peaks assigned to protons of each of the byproducts in the ^{1}H NMR spectra. The peaks observed in the ^{1}H NMR were assigned, as shown in **Scheme 5.6**.

Scheme 5.6: The self-metathesis of 2-allylnitrobenzene **215** using Grubbs 2nd generation catalyst to form dimer **216**, and subsequent undesired secondary metathesis reactions, to form side products **231**, **232** and **233**. Chemical shifts and multiplicities of peaks in the ^{1}H NMR assigned to the protons in the alkenyl chain are quoted in ppm. Partial separation was achieved via column chromatography; however final yields were determined by ^{1}H NMR.

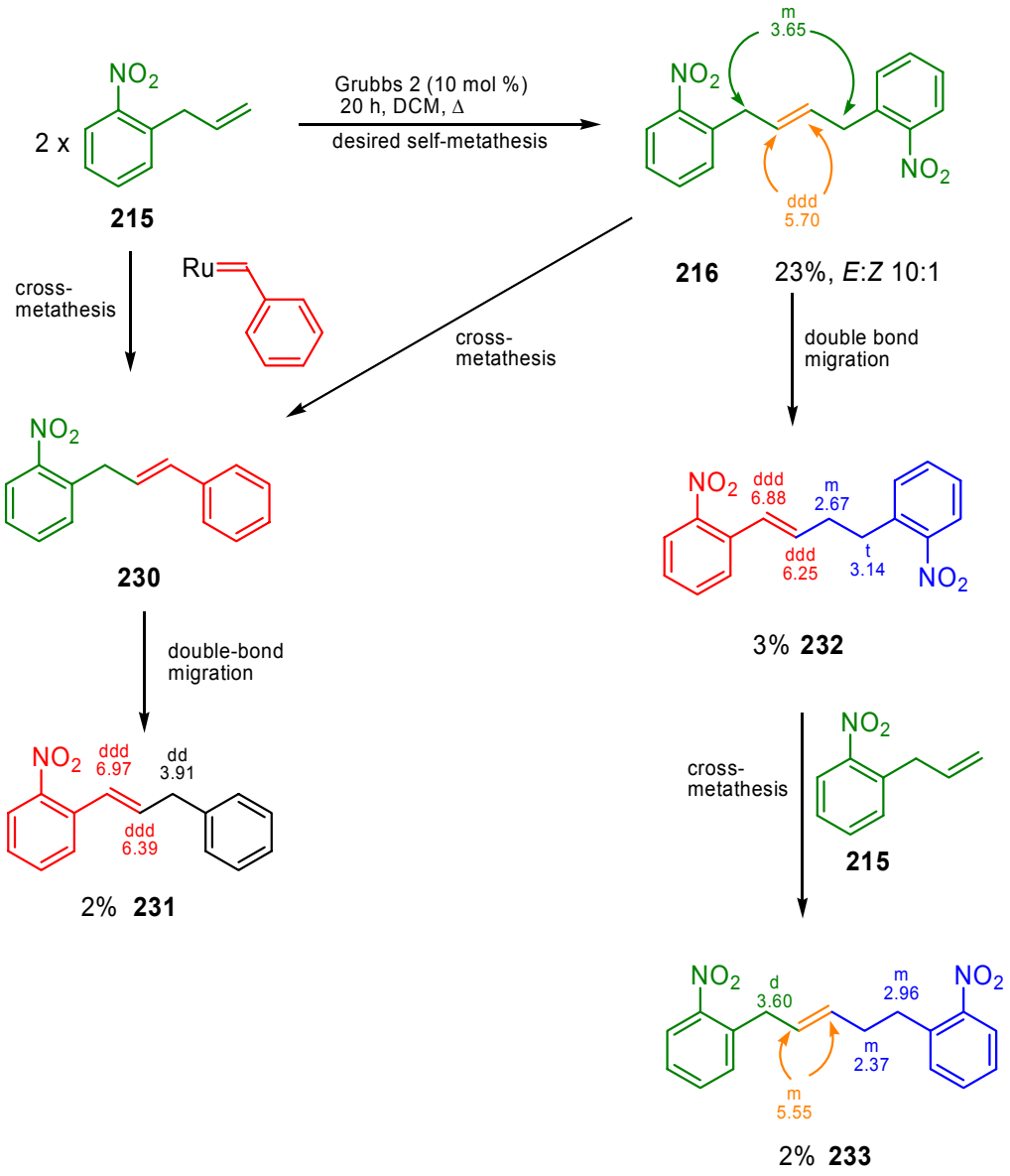

Although only partially characterised, the structures of the secondary metathesis products **231**, **232** and **233** were identified via ^{1}H NMR and gCOSY analysis of mixtures of the products. The ^{1}H NMR spectrum of a mixture of **a)** *E*- and *Z*-**216** and pentene **233** and **b)** butene **232** and propene **231** (and *E*- and *Z*-**216**) are shown in **Figure 5.5**. The gCOSY ^{1}H-^{1}H correlations are marked.

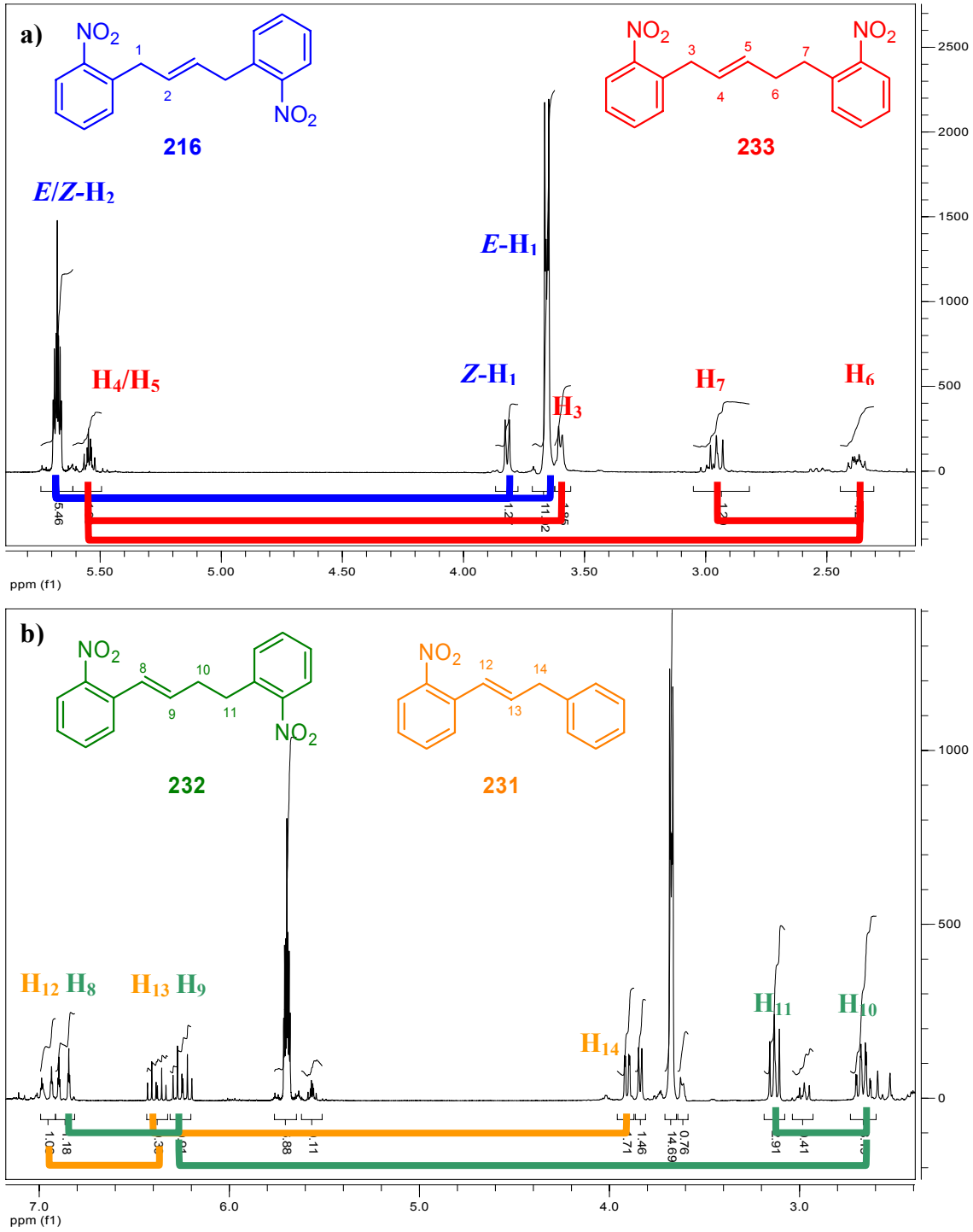

Figure 5.5: ^{1}H NMR of **a)** a mixture of alkenes **216** and **233**, and **b)** a mixture of alkenes **232** and **231** (and *E*- and *Z*-**216**). Spectra were obtained at 300 MHz at 25 ^{o}C.

Analysis of the ^{1}H NMR obtained from the mixture of **216** and **233** showed similar chemical shifts in the peaks assigned to the methine protons **H2** and **H4**/**H5**, and methylene protons **H1** and **H3**, adjacent to both the phenyl ring and the olefinic bond. gCOSY analysis shows a correlation between the peak assigned to **H5** in the ^{1}H NMR of **233** and the peak upfield at 2.37 ppm, assigned to **H6**, which in turn is correlated to

the peak at 2.96 ppm, assigned to **H7**. Two similar peaks are observed in the ^{1}H NMR spectrum of the mixture of **232** and **231** (and *E*- and *Z*-**216**) assigned to **H10** and **H11** (**Figure 5.5**, **b**; for expansion see **Figure 5.6**), which are in a similar chemical environment to **H6** and **H7**.

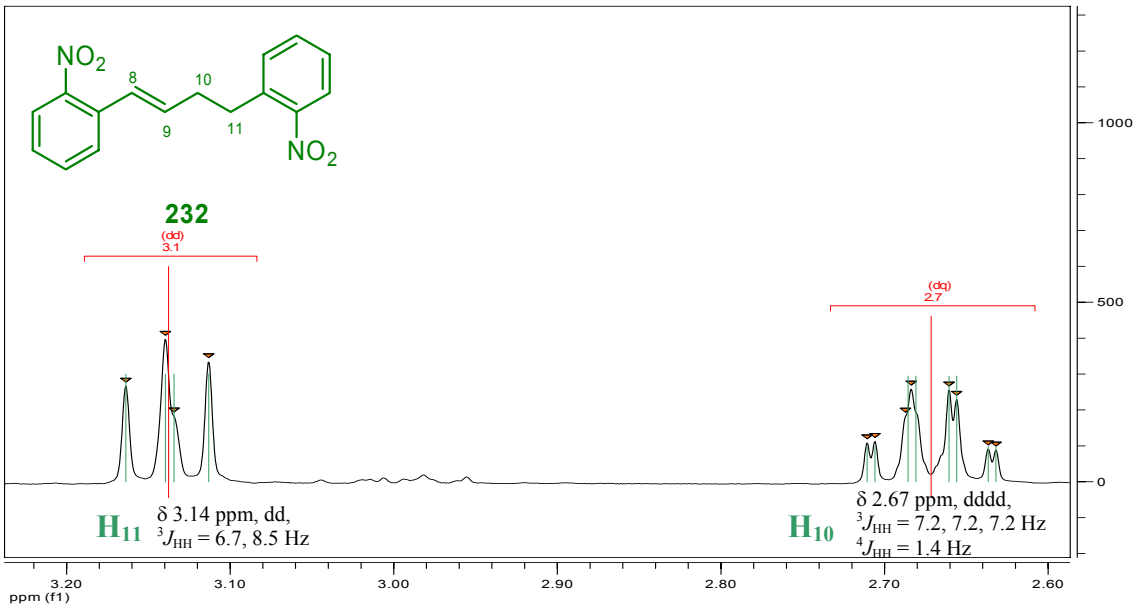

Figure 5.6: Expansion of the ^{1}H NMR of **232**, showing the peaks assigned to **H10** and **H11**.

The peak assigned to **H10** showed a gCOSY correlation to the peak at 6.25 ppm, assigned to **H9** (**Figure 5.5**, **b**; for expansion see **Figure 5.7**, **a**), which showed a correlation to the peak at 6.88 ppm, assigned to **H8** (**Figure 5.7**, **b**) characteristic of vinylic protons adjacent to an aromatic ring. Similarly, the peaks at 6.39 ppm (**Figure 5.7**, **a**) and 6.97 ppm (**Figure 5.7**, **b**) were assigned to the vinylic protons **H13** and **H12** respectively. The assignment of the double bond adjacent to the nitro-substituted aromatic ring (rather than the unsubstituted benzene ring) was verified by comparison of the reported ^{1}H NMR shifts of the vinylic peaks of an *ortho*-nitro substituted benzene ring.[213] The peak assigned to **H13** showed a ^{1}H-^{1}H correlation to the peak at 3.91 ppm (**Figure 5.7**, **c**), assigned to **H14**, which exhibits a similar chemical shift to the methylene protons *E*- and *Z*-**H1**.

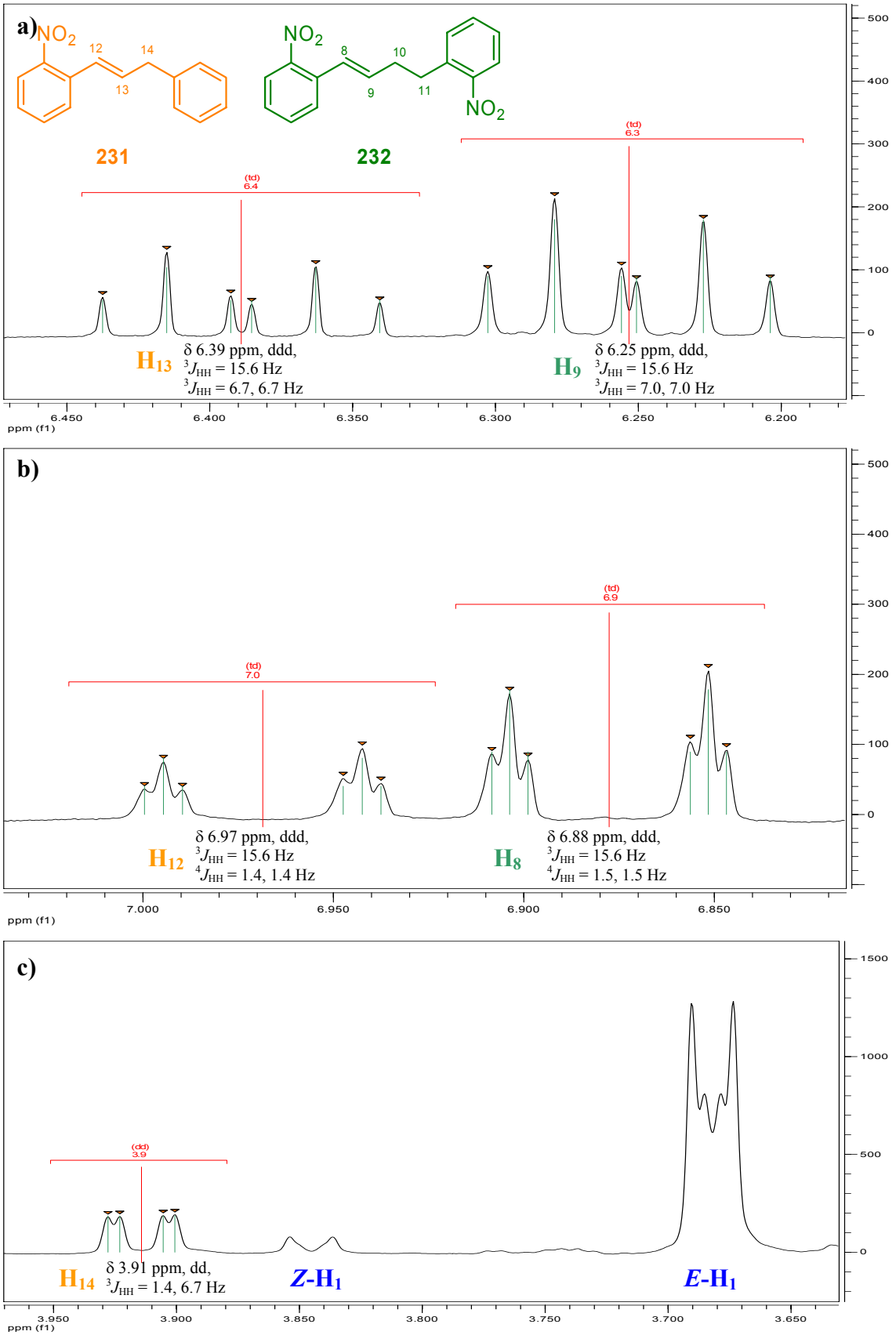

Figure 5.7: Expansions of the ^{1}H NMR spectrum of the mixture of **232** and **231** (and *E*- and *Z*-**216**) showing the peaks assigned to; **a)** **H13** and **H9**, **b)** **H12** and **H8** and **c)** **H14** and *Z*- and *E*-**H1**.

5.2.3 Asymmetric dihydroxylation of nitrogen-based dimers

The results of the asymmetric dihydroxylations using AD mix α and AD mix β of the nitrogen-based dimers **228** are summarised in **Table 5.5**.

Table 5.5: Asymmetric dihydroxylation of nitrogen-based dimeric aromatic allylic alkenes **228** under standard Sharpless conditions. Reaction with AD mix α provided the diols (*S*,*S*)-**234**; AD mix β gave the diols (*R*,*R*)-**234**.

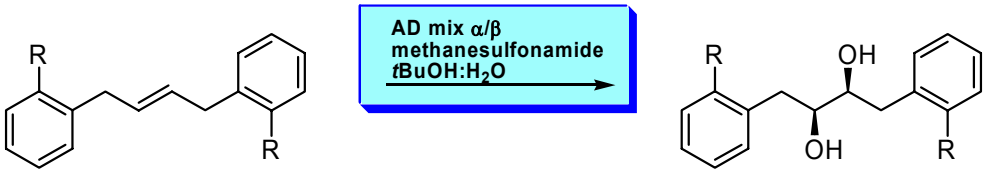

228 **234**

	R	228	234	AD mix α (*S*,*S*)-234			AD mix β (*R*,*R*)-234		
				time (h)	yield (%)[a]	*ee* (%)[b]	time (h)	yield (%)[a]	*ee* (%)[b]
1	NHBoc[c]	**188**	**189**	90	34	31	90	31	56
2	NHAc	**229**	**235**	24	0	-	24	0	-
3	NO_2	**216**	**217**	24	18	44	24	45	58

[a]Isolated yield. [b]Determined by chiral HPLC. [c]S. M. Wales, *Honours Thesis*, University of Wollongong, **2004**.[185]

As discussed in *Section 4.4.3*, the enantiomeric forms of Boc-protected aniline diol **189** (entry 1, R = NHBoc) were obtained in poor yield and enantiopurity via the AD reaction.[185] The acetylated analogue **235** was not formed from the AD reaction of alkene **229** (entry 2, R = NHAc) using either chiral ligand, presumably due to the excessively poor solubility of the alkene **229** in the reaction solvent.

Replacing the amine functionality with a nitro substituent was expected to improve the result of the AD reaction by; 1) reducing the size of the *ortho* substituent and 2) increasing the solubility of alkene substrate in the reaction mixture. In addition, the nitro group represents a strongly withdrawing substituent - the effects of which had not yet been investigated. The AD reaction of the nitro-substituted alkene **216** again gave a poor outcome (entry 3, R = NO_2).

A mixture of alkenes *E*- and *Z*-**216** and *E*-**233** (8.5:1:1.4, not resolvable via TLC development) was reacted under modified Sharpless conditions using AD mix α (**Scheme 5.7**), in a 1:1:0.1 mixture of *t*BuOH:H_2O:THF for 24 hours.

Scheme 5.7: The asymmetric dihydroxylation of a mixture of alkenes **216** and **233**, using AD mix α.

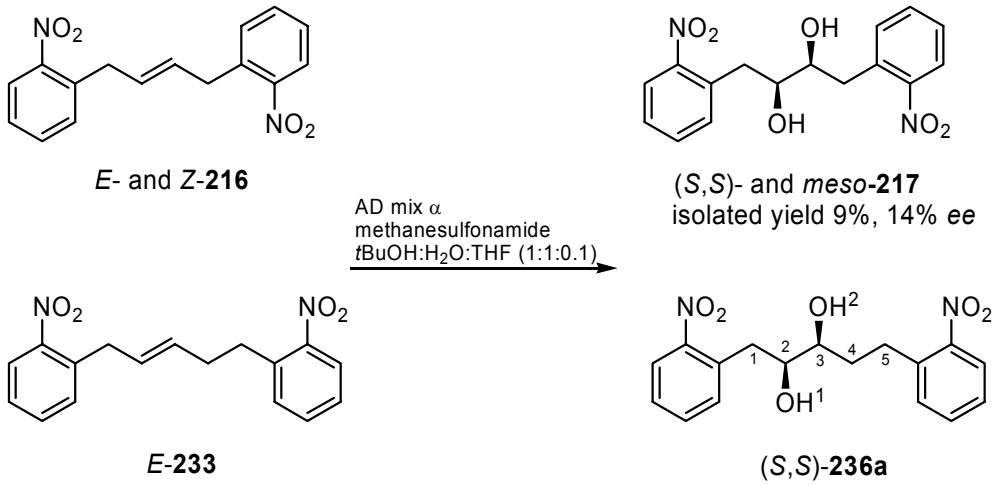

^{1}H	δ (ppm)	*J* (Hz)
1a	2.99	9.7, 13.2
1b	3.22	3.8, 13.6
2	3.83	9.4, 4.2
3	3.59	4.3, 8.6, 10.2
4a	3.03	9.2, 13.8
4b	3.13	5.5, 9.9, 13.7
5a/b	1.89-2.02	-
OH^1	2.31	4.7
OH^2	2.03	5.4

TLC analysis of the reaction mixture indicated that the spot assigned to the starting alkenes **216** and **233** was present, and two polar products. The crude mixture was subjected to column chromatography, giving the starting material and a mixture of diols **217** and **236**. ^{1}H NMR analysis of the starting material showed that the peaks assigned to the alkene **233** were absent, indicating full conversion of the pentene **233**. The mixture of diols was recrystallised (DCM/hexanes) giving the diol (*S*,*S*)-**236a** in 30% yield and 94% *ee*. The filtrate was reduced to give the diol (*S*,*S*)-**217** (9% yield, 14% *ee*) as a mixture of chiral and *meso* diastereomers. The discrepancy in isolated yield (30%) of the diol **236** and conversion (100%) of the alkene **233** can be attributed to the small scale of the reaction. ^{1}H NMR analysis of the diol **236a** showed a more complicated

spectrum, confirming the unsymmetrical nature of the molecule. The peaks were assigned as outlined in **Scheme 5.7**. The MS (ES, +ve) displayed a peak at *m/z* 369 assigned to the M+Na ion.

The chemical and stereochemical outcome of the AD reaction of the pentene **233** provide two points of discussion (**Figure 5.8**).

1. The apparent full conversion of the alkene indicated that the substrate was able to adopt a conformation such that the double bond could be situated at one equatorial and one axial oxygen atom of the bound OsO_4, with minimal steric interactions with the chiral catalyst, allowing the catalytic dihydroxylation to occur.
2. The high stereoselectivity of the reaction is attributed to the stability of one diastereomeric transition state **143** over the other **142**. The higher stability comes from the increase in favourable van der Waals or aromatic π-stacking interactions between the substrate and the PHAL linker of the binding pocket.

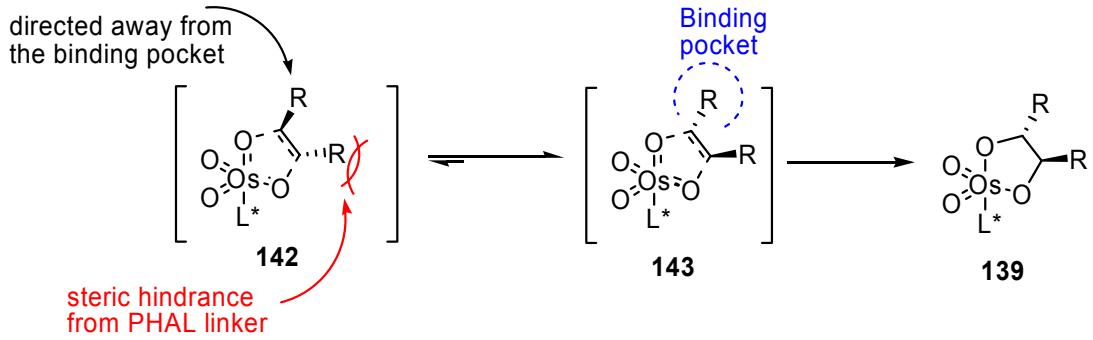

Figure 5.8: Two diastereomeric transition states leading to the stable osmium(VI) glycolate ester **139**. Diastereomer **142** is not stabilised due to steric interactions between one of the double bond substituents and the floor of the binding pocket, while diastereomer **143** is stabilised by favourable interactions with the walls and floor of the binding pocket.

The increased flexibility of the substrate within the binding pocket must be a result of the increased chain length so that the aromatic ring can be positioned so as to have π-stacking interactions, or so that the aromatic ring is oriented out of the pocket so that the favourable interactions are only van der Waals forces between the alkyl chain and the PHAL linker. An alternate explanation could be the reduced steric hindrance surrounding the double bond, allowing access to the ligand bound OsO_4.

5.3 Derivatives not containing a heteroatom

Another possible cause of the poor outcome of the AD reaction was the presence of a heteroatom at the *ortho* position. The presence of the oxygen or nitrogen could be interacting repulsively with the methoxy group of the methoxyquinoline units of the biscinchona ligand (see **Figure 3.10**). This effect could be tested by performing the AD reaction on derivatives not containing a heteroatom, such as the tolyl (R = Me) or bromine (R = Br) analogues, or removing the *ortho* substituent completely (R = H). Although these substrates will not necessarily provide access to 2,2'-bisindoline **112**, the information gained from these investigations would help to solve the problems currently being experienced in the proposed synthesis.

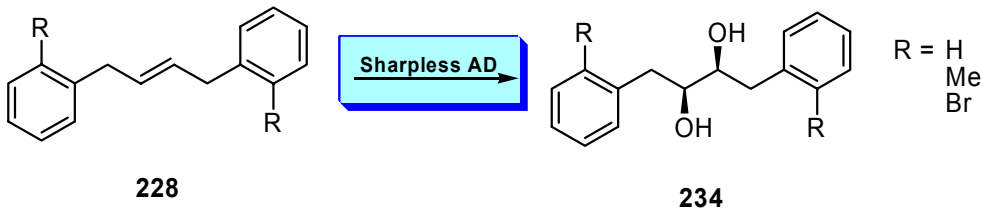

228 **234**

Figure 5.9: Proposed optimisation of the Sharpless AD reaction of dimeric aromatic allylic alkenes of the type **228**, by removal of the coordinating ability of the *ortho* substituent.

5.3.1 Synthesis of the non-coordinating monomers

The monomers required for the formation of dimeric alkenes **228** (where R = Me, Br) were synthesised, while allylbenzene **237** which would provide **228** (where R = H) is commercially available.

1-Allyl-2-bromobenzene **239** was synthesised according to the literature procedure, via an iodine-magnesium exchange reaction.[214] A solution 1-bromo-2-iodobenzene **238** in THF was equilibrated to –25 °C, and freshly prepared *i*PrMgBr (via addition of magnesium turnings to *i*PrBr) was added (**Scheme 5.8**). Allyl bromide was added after 30 mins and the mixture was stirred at RT (18 °C) for 23 hours, to give the desired allylated product **239** in 94% yield, which was spectroscopically identical to that reported in the literature. The lower temperature at which the iodine-magnesium exchange occurs prevents halogen displacement at the less reactive bromide position.

The formation of the same Grignard reagent by reaction with Mg turnings would not be selective.

Scheme 5.8: Reaction conditions for the synthesis of 1-allyl-2-bromobenzene **239** from 1-bromo-2-iodobenzene **238**.[214]

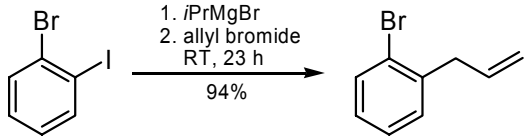

238 **239**

The synthesis of 2-allyltoluene was performed via the Grignard reaction of 2-bromo-toluene with allyl bromide, using the literature procedure (**Scheme 5.9**).[206] Purification via silica gel column chromatography gave the desired allylated product **241** in 35% yield, which was spectroscopically identical to that reported in the literature.[206]

Scheme 5.9: Reaction conditions for the allylation of 2-bromotoluene **240** to form 2-allyltoluene **241**.

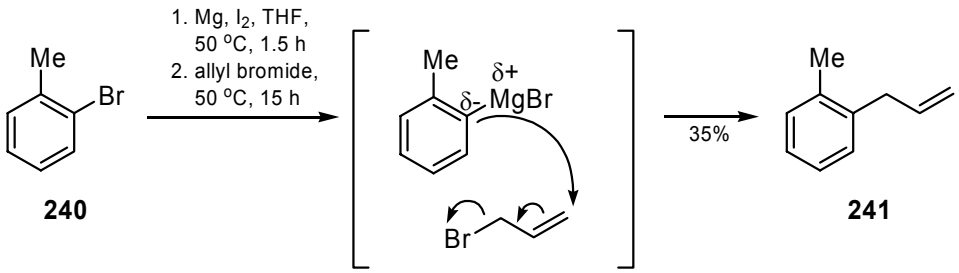

240 **241**

Although the yield obtained was much lower than that reported in the literature, a sufficient quantity of the desired product was synthesised, and as such repetition of the reaction was unnecessary.

5.3.2 Metathesis reaction of non-coordinating monomers

The metathesis reaction was performed on the non-coordinating monomers **227** and are summarised in **Table 5.6**.

Table 5.6: Homo-dimerisation of non-coordinating monomeric aromatic allylic alkenes **227**, via self-metathesis to form the dimers **228**. Reaction conditions were standard involving heating at reflux in DCM with Grubbs 1st or 2nd generation catalysts.

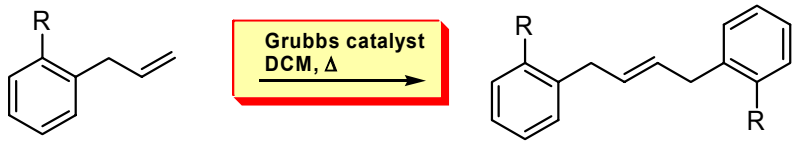

227 **228**

	R	227	228	Grubbs 1				Grubbs 2			
				mol %	time (h)	yield (%)[a]	*E*:*Z*[b]	mol %	time (h)	yield (%)[a]	*E*:*Z*[b]
1	H	**237**	**170**	5	24	69	4.8:1	3	25	0	-
				2.5	18	89	4.7:1	-	-	-	-
2	Me	**241**	**242**	2.5	27	77	4.5:1	-	-	-	-
3	Br	**239**	**234**	-	-	-	-	5	23	16[d]	6.2:1

[a]Isolated yield. [b]Determined by ^{1}H NMR.

The dimerisation of allyl benzene **237** in the presence of Grubbs 1 gave the dimer **170** (entry 1, R = H). The catalyst loading did not affect the stereochemical outcome, however 2.5 mol % and a shorter reaction time (18 h) gave a higher yield. The tolyl derivative **241** (entry 2, R = Me) gave almost the same chemical and stereochemical yield as the *ortho* methoxy derivative (see **Table 5.2**, entry 6), and only a slightly poorer outcome than the allyl benzene reaction (entry 1). The use of Grubbs 2 for the dimerisation of allyl benzene **237** (entry 1, R = H) did not provide the desired alkene **170**, and only an inseparable mixture of unidentified products. The same reaction for the bromo substituted derivative **239** (entry 3, R = Br) yielded the desired alkene **234** in poor yield, which again could not be isolated from the side metathesis products using column chromatography, analogous to those obtained from the self-metathesis of the nitro derivative. The structures were again elucidated via ^{1}H NMR and gCOSY analysis of a mixture of *E*- and *Z*-**234**, **244**, **245**, **246** and **247** (**Figure 5.10**, c.f. **Scheme 5.6**). Therefore the AD reaction was not attempted on the bromo derivative.

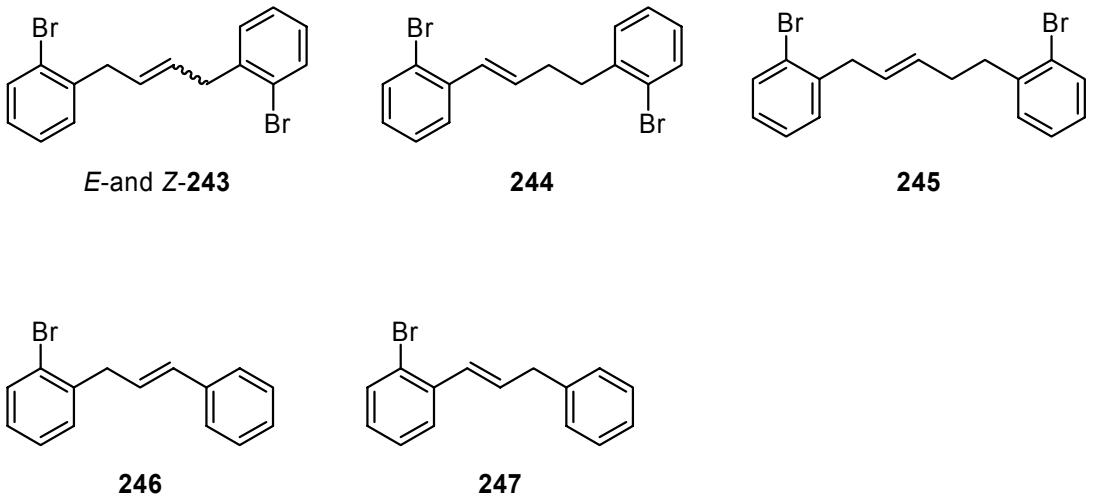

Figure 5.10: Products obtained from the self-metathesis of **239**.

5.3.3 Asymmetric dihydroxylation of non-coordinating dimers

The AD reaction was performed on the dimeric alkenes **228**, where R = Me and H, and the results are summarised in **Table 5.7**.

Table 5.7: Asymmetric dihydroxylation of non-coordinating dimeric aromatic allylic alkenes **228** under standard Sharpless conditions. Reaction with AD mix α provided the diols (*S*,*S*)-**234**; AD mix β gave the diols (*R*,*R*)-**234**.

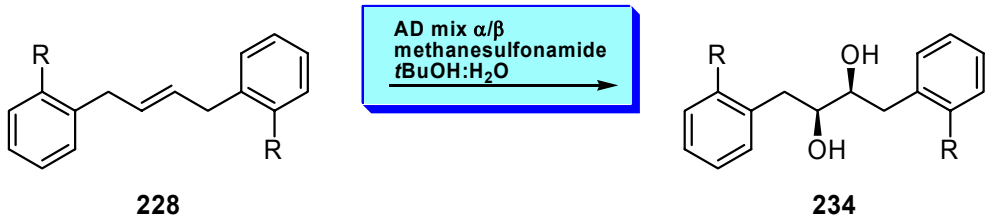

	R	228	234	AD mix α (*S*,*S*)-234			AD mix β (*R*,*R*)-234		
				time (h)	yield (%)[a]	*ee* (%)[b]	time (h)	yield (%)[a]	*ee* (%)[b]
1	H	**170**	**171**	24	88	93	24	84	95
2	Me	**242**	**248**	24	65	62	24	45	70

[a]Isolated yield. [b]Determined by chiral HPLC.

The AD reaction was performed on the unsubstituted alkene **170** (entry 13, R = H) to remove any possible steric or coordinating effects from aromatic substitution. The enantiomeric diols (*S*,*S*)- and (*R*,*R*)-**171** were formed in excellent enantiopurity and high yield, indicating that favourable stabilising interactions were occurring between the

substrate and the binding pocket. This leads to the observation that removal of the *ortho* substituent eliminates the destabilising effect imposed by the presence of a substituent on the aromatic ring. The AD reaction was performed on the tolyl substituted alkene **242** (entry 2, R = Me) using AD mix α and β. The diols (*S*,*S*)- and (*R*,*R*)-**248** were obtained in moderate yield and *ee*. While the outcome was worse than for the AD reaction of the unsubstituted derivative **170**, the chemical and stereochemical yield was higher than that obtained for the AD reaction of phenol- and nitrogen-based dimers (c.f. **Table 5.3** and **Table 5.5**). This indicates that there could be a repulsive electronic effect or the outcome could simply be as a result of the reduction in effective bulk of the entire *ortho* substituent, or most probably a combination of both.

5.4 *Ortho*, *meta* and *para* substituted derivatives

The results obtained thus far indicated that the *ortho*-substituted dimeric aromatic allylic alkenes of the type **228** were providing unfavourable steric interactions between the substrate and the chiral ligand, summarised as follows (**Figure 5.11**);

1. The extension of the butenyl chain of the dimeric scaffold to the pentene **233** resulted in high conversion and excellent stereoselectivity (94% *ee*) of the AD reaction.

2. Removal of the *ortho* substituent gave the corresponding diols **171** in excellent yield (84-88%) and stereoselectivity (93-95% *ee*).

3. Reduction of the effective bulk and coordinating ability of the *ortho* substituent (R = Me) resulted in moderate yield (45-65%) and reduced stereoselectivity (62-70% *ee*), albeit higher than the stereoselectivities obtained from the AD reaction of phenol- and nitrogen-based derivatives.

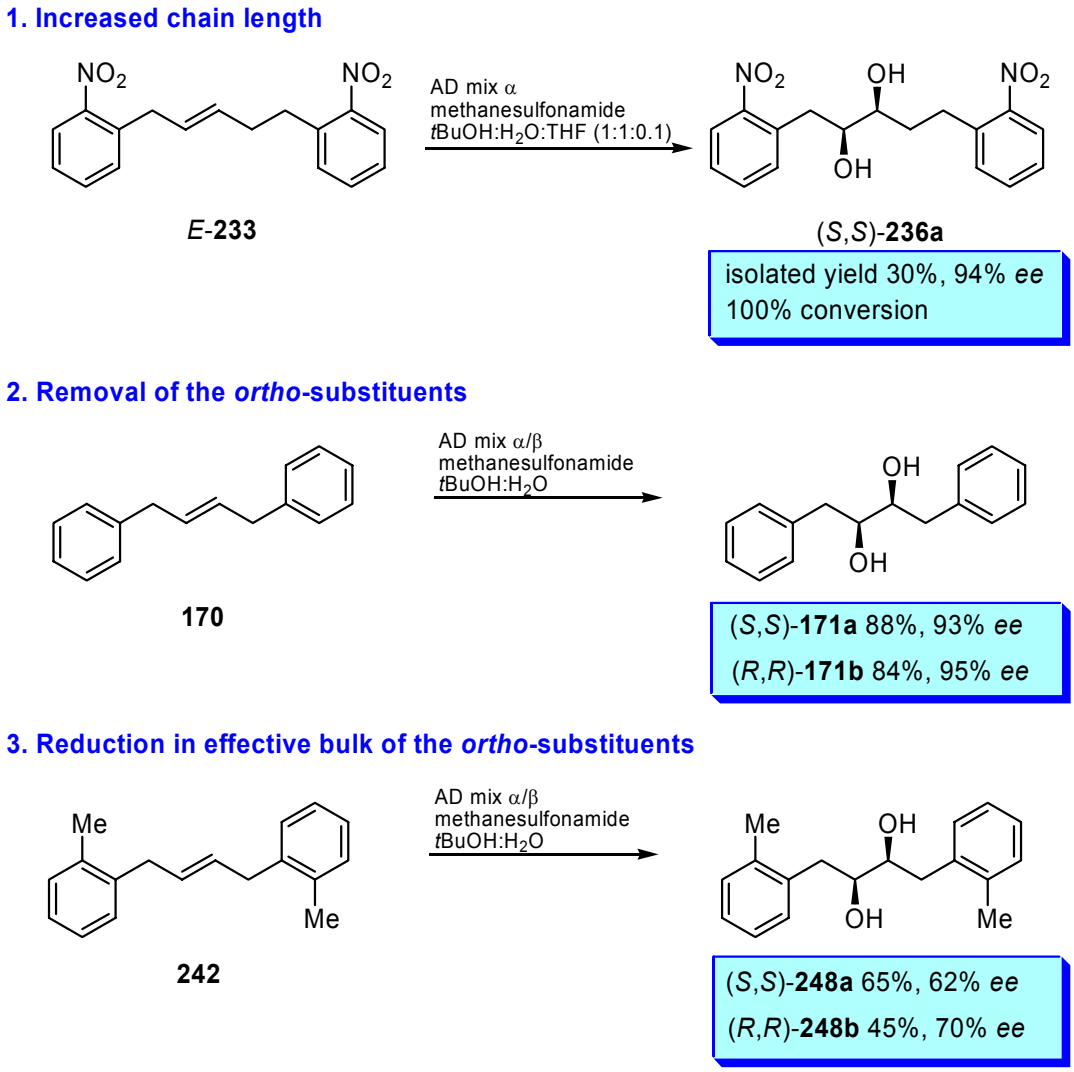

Figure 5.11: The AD reaction of alkenes in which; **1.** The chain length is increased, **2.** The *ortho* substituents are removed and **3.** Methyl groups are present in the *ortho* positions.

To determine if the *ortho* substituent was blocking the approach of the substrate to the OsO_4, the position of the aromatic substituent was investigated. The ease with which the *meta*- and *para*-substituted anisole alkenes could be prepared lead to a comparison of the AD reaction of *o*-, *m*- and *p*-**249** (**Figure 5.12**).

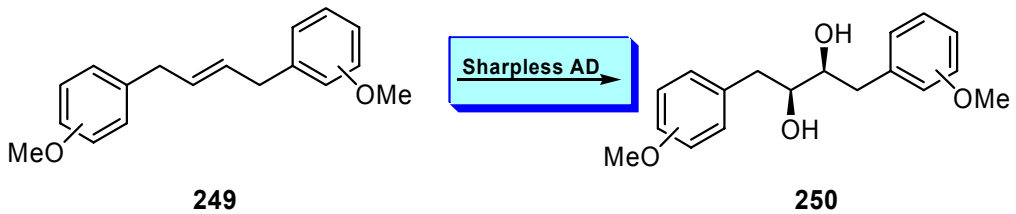

249 **250**

Figure 5.12: Proposed optimisation of the AD reaction, via comparison of the *ortho*, *meta* and *para* substituted alkenes **249**.

5.4.1 *Synthesis of the* ortho, meta *and* para *substituted monomers*

The monomers required for the synthesis of the *ortho*, *meta* and *para* dimers are the corresponding anisole derivatives **197**, **251** and **252** (**Figure 5.13**).

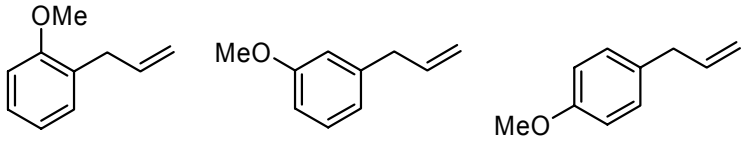

197 **251** **252**

Figure 5.13: *Ortho*, *meta* and *para* substituted allylanisoles.

Synthesis of 2-allylanisole **197** is described in *Section 5.1.1*, and 4-allylanisole (**252**) is commercially available. 3-Allylanisole **251** was prepared, using a literature procedure, via formation of the Grignard reagent of 3-bromoanisole **253**,[215] followed by reaction with allyl bromide,[216] in an analogous manner to that used to form 2-allyltoluene **241** (see **Scheme 5.10**). The desired allylated product **251** was isolated in 58% yield and was spectroscopically identical to that reported in the literature.[216]

Scheme 5.10: Reaction conditions for the Grignard reaction for the allylation of 3-bromoanisole **253** to form 3-allylanisole **251**.

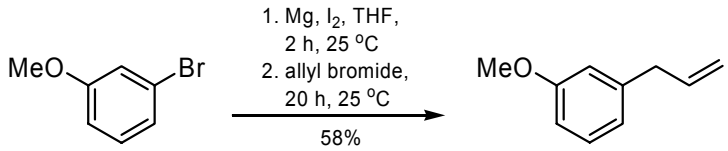

253 **251**

5.4.2 *Metathesis reaction of* ortho, meta *and* para *substituted monomers*

The dimerisation of the *ortho*, *meta* and *para* substituted derivatives was performed via the metathesis reaction, and is summarised in **Table 5.8**.

Table 5.8: Homo-dimerisation of *ortho*, *meta* and *para* substituted monomeric aromatic allylic alkenes **254**, via self-metathesis to form the dimers **249**. Reaction conditions were standard involving heating at reflux in DCM with Grubbs 1st or 2nd generation catalysts.

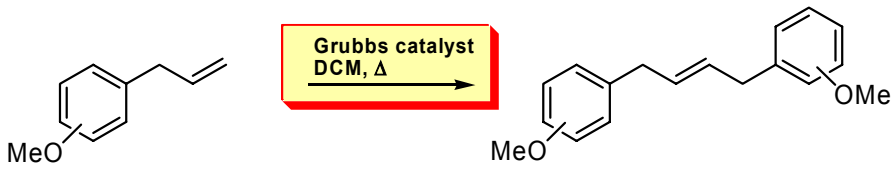

254 **249**

	R	254	249	Grubbs 1				Grubbs 2			
				mol %	time (h)	yield (%)[a]	*E*:*Z*[b]	mol %	time (h)	yield (%)[a]	*E*:*Z*[b]
1	*o*-OMe[c]	**197**	**202**	5	19	81	4.4:1	5	19	60[d]	5.6:1
				5	7	91	4.5:1	5	24	73[d]	5.5:1
2	*m*-OMe	**251**	**255**	2.5	15	63	4.5:1	-	-	-	-
3	*p*-OMe	**252**	**256**	2.5	4.5	97	6.2:1	-	-	-	-

[a]Isolated yield. [b]Determined by ^{1}H NMR. [c]Discussed in *Section 5.1.2*. [d]Final yield determined by ^{1}H NMR.

The dimerisation of *meta* and *para* allylanisoles were performed using a reduced catalyst loading (2.5 mol %, entries 2 and 3). While the *meta* derivative **255** was formed in moderate yield (63%) and similar stereochemical yield (4.5:1) to the *ortho*-methoxy dimer **202** (entry 1), the *para* derivative **256** was isolated in excellent yield (97%) and improved stereochemical yield (6.2:1). A possible explanation is that the removal of the *ortho* substituent, removes the steric hindrance surrounding the double bond. This provides access to the double bond by the catalyst, so the double bond can undergo [2+2] addition to the ruthenium preferentially. Dimerisation using Grubbs 2 was not attempted since the alkene was synthesised in sufficient quantities for trialling the AD reaction, in combination with the poor outcome previously observed using Grubbs 2 (see **Scheme 5.6**; R = NO_2 and **Figure 5.10**; R = Br).

5.4.3 *Asymmetric dihydroxylation of* ortho, meta *and* para *substituted dimers*

The results for the AD reaction of the *ortho*, *meta* and *para* substituted dimers **249** using AD mix α and β are summarised in **Table 5.9**.

Table 5.9: Asymmetric dihydroxylation of *ortho*, *meta* and *para* substituted dimeric aromatic allylic alkenes **249** under standard Sharpless conditions. Reaction with AD mix α provided the diols (*S*,*S*)-**250a**; AD mix β gave the diols (*R*,*R*)-**250b**.

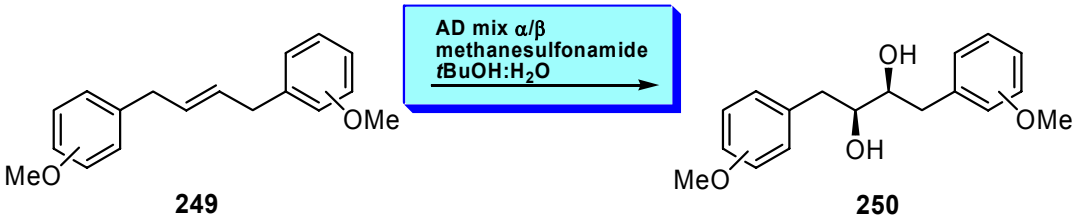

249 **250**

	R	249	250	AD mix α (*S*,*S*)-250a			AD mix β (*R*,*R*)-250b		
				time (h)	yield (%)[a]	*ee* (%)[b]	time (h)	yield (%)[a]	*ee* (%)[b]
1	*o*-OMe[c]	**202**	**208**	24	52	34	24	37	40
2	*m*-OMe	**255**	**257**	24	77	73	24	86	76
3	*p*-OMe	**256**	**258**	24	90	85	24	96	87

[a]Isolated yield. [b]Determined by chiral HPLC. [c]Discussed in *Section 5.1.3*.

The AD reaction of the *meta* substituted alkene **255** (entry 2) increased the yield and *ee* significantly, when compared to the *ortho* analogue (entry 1). The *para* substituted diol **258** was obtained in both enantiomeric forms in excellent chemical yield and significantly improved stereochemical yield (entry 3). These results confirmed that *ortho* substitution did indeed have a detrimental effect on the outcome of the AD reaction on these dimeric aromatic allylic systems.

5.5 Metathesis and AD summary

5.5.1 Metathesis of dimeric aromatic allylic alkenes

The metathesis reaction was performed using Grubbs 1 or 2 on a total of 14 dimeric aromatic allylic alkenes, and the results are summarised in **Table 5.10**.

Table 5.10: Homo-dimerisation of monomeric aromatic allylic alkenes **227**, via self-metathesis to form the dimers **228**. Reaction conditions were standard involving heating at reflux in DCM with Grubbs 1st or 2nd generation catalysts.

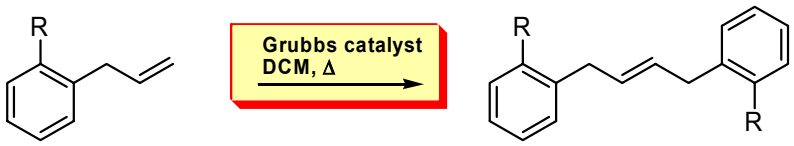

227 **228**

	R	227	228	Grubbs 1				Grubbs 2			
				mol %	time (h)	yield (%)[a]	*E*:*Z*[b]	mol %	time (h)	yield (%)[a]	*E*:*Z*[b]
1	OBn[c]	**164**	**165**	6.7	4.5	81	5.2:1	5	26	93[d]	7:1
2	OPMB	**193**	**198**	5	23	51	5:1	5	23	71	7.1:1
3	OAc	**194**	**199**	5	15	85	4:1	5	66	77	8:1
4	OTf	**195**	**200**	5	15	88	3.8:1	5	66	75	9:1
5	OTBS	**196**	**201**	5	66	85	4.3:1	5	66	95[d]	8.4:1
				-	-	-	-	5	7.5	95[d]	7:1
6	OH	**120**	**203**	10	25	50	9:1	-	-	-	-
7	NHBoc[e]	**187**	**188**	10	3	76	1.6:1	10	7	61	11.5:1
8	NHAc	**222**	**229**	-	-	-	-	10	17	73	*E* only
9	NO_2	**215**	**216**	-	-	-	-	5	7	26	43:1
				-	-	-	-	5	20	23	10:1
10	*o*-OMe	**197**	**202**	5	19	81	4.4:1	5	19	60[d]	5.6:1
				5	7	91	4.5:1	5	24	73[d]	5.5:1
11	*m*-OMe	**251**	**255**	2.5	15	63	4.5:1	-	-	-	-
12	*p*-OMe	**252**	**256**	2.5	4.5	97	6.2:1	-	-	-	-
13	H	**237**	**170**	5	24	69	4.8:1	3	25	0	-
				2.5	18	89	4.7:1	-	-	-	-
14	Me	**241**	**242**	2.5	27	77	4.5:1	-	-	-	-
15	Br	**239**	**234**	-	-	-	-	5	23	16[d]	6.2:1

[a]Isolated yield. [b]Determined by ^{1}H NMR. [c]Discussed in **Chapter 4**. [d]Final yield determined by ^{1}H NMR. [e]S. M. Wales, *Honours Thesis*, University of Wollongong, **2004**.[185]

In summary, the use of Grubbs 2nd generation catalyst for the dimerisation of aromatic allylic alkenes provides the desired alkene in higher *E*:*Z* ratio, however, isolation from the undesired products from secondary metathesis reactions is difficult, and sometimes not possible via column chromatography. The major side products result from isomerisation of the double bond from the allylic position to the vinylic position, and cross-metathesis products thereof. In comparison, the use of Grubbs 1st generation catalyst provides the dimers in moderate yield, with minimal side products albeit in lower stereochemical purity. The geometric purity can be increased by column chromatography or recrystallisation.

Shorter reaction times provide the desired products in higher yields, without affecting the stereochemical outcome. Longer reaction times decrease the yield, as the desired alkene undergoes secondary metathesis reactions.

5.5.2 Asymmetric dihydroxylation of dimeric aromatic allylic alkenes

Asymmetric dihydroxylation was attempted on 13 dimeric aromatic allylic alkenes, using AD mix α or β, under standard Sharpless conditions,[3] and the results are summarised in **Table 5.11**. Generally, the chemical and stereochemical outcome was poor. It can be seen that the best results are obtained when the *ortho*-substituent is removed or the size is reduced.

Table 5.11: Asymmetric dihydroxylation of dimeric aromatic allylic alkenes **228** under standard Sharpless conditions. Reaction with AD mix α provided the diols (*S*,*S*)-**234a**; AD mix β gave the diols (*R*,*R*)-**234b**.

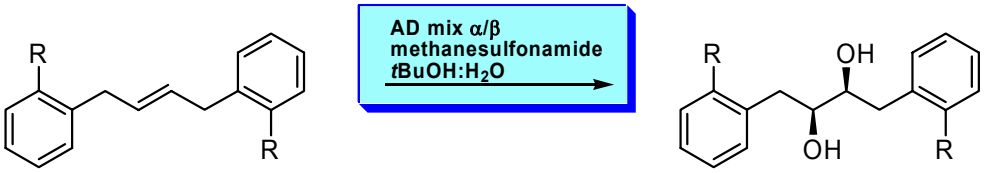

228 **234**

	R	228	234	AD mix α (*S*,*S*)-234a			AD mix β (*R*,*R*)-234b		
				time (h)	yield (%)[a]	*ee* (%)[b]	time (h)	yield (%)[a]	*ee* (%)[b]
1	OBn[c]	**165**	**166**	91	64	30	37	69	91
2	OPMB	**198**	**204**	40	trace	-	40	trace	-
3	OAc	**199**	**205**	24	0	-	24	0	-
4	OTf	**200**	**206**	24	25	1.4	24	58	8
5	OTBS	**201**	**207**	24	13	23	24	31	14
6	OH	**203**	**209**	24	0	-	24	0	-
7	NHBoc[e]	**188**	**189**	90	34	31	90	31	56
8	NHAc	**229**	**235**	24	0	-	24	0	-
9	NO_2	**216**	**217**	24	18	44	24	45	58
10	*o*-OMe	**202**	**208**	24	52	34	24	37	40
11	*m*-OMe	**255**	**257**	24	77	73	24	86	76
12	*p*-OMe	**256**	**258**	24	90	85	24	96	87
13	H	**170**	**171**	24	88	**93**	24	84	**95**
14	Me	**242**	**248**	24	65	**62**	24	45	**70**

[a]Isolated yield. [b]Determined by chiral HPLC. [c]Discussed in **Chapter 4**. [d]Final yield determined by ^{1}H NMR. [e]S. M. Wales, *Honours Thesis*, University of Wollongong, **2004**.[185]

5.6 *ortho*-Substituted monomeric aromatic allylic alkenes

In the transition state of the [3+2] cycloaddition of the olefin substrate to the bound OsO_4 of 1,2-disubstituted alkenes, one R group is directed into the binding pocket of the ligand, while the other is directed away from the pocket. High enantioselectivity is achieved when one R substituent experiences favourable van der Waal interactions within the binding pocket. In an effort to determine if removal of one of the *ortho*-substituted aromatic rings would result in a better outcome, the AD reaction was performed on the monomeric aromatic alkenes **194** and **197**, using both AD mixes α and β (**Scheme 5.11**) under standard Sharpless conditions for terminal alkenes.[3]

Scheme 5.11: **a)** Conditions for the asymmetric dihydroxylation of monomeric aromatic allylic alkenes **197** (R = OMe) and **194** (R = OAc), using standard Sharpless conditions for the reaction of terminal alkenes using AD mixes α and β. Note that methanesulfonamide is not required for the AD reaction of terminal alkenes.[3] **b)** For comparison, the results of the AD reaction on the dimeric analogous discussed in *Section 5.1.3* (R = OMe and OAc) and *Section 5.2.3* (R = NHAc) are given.

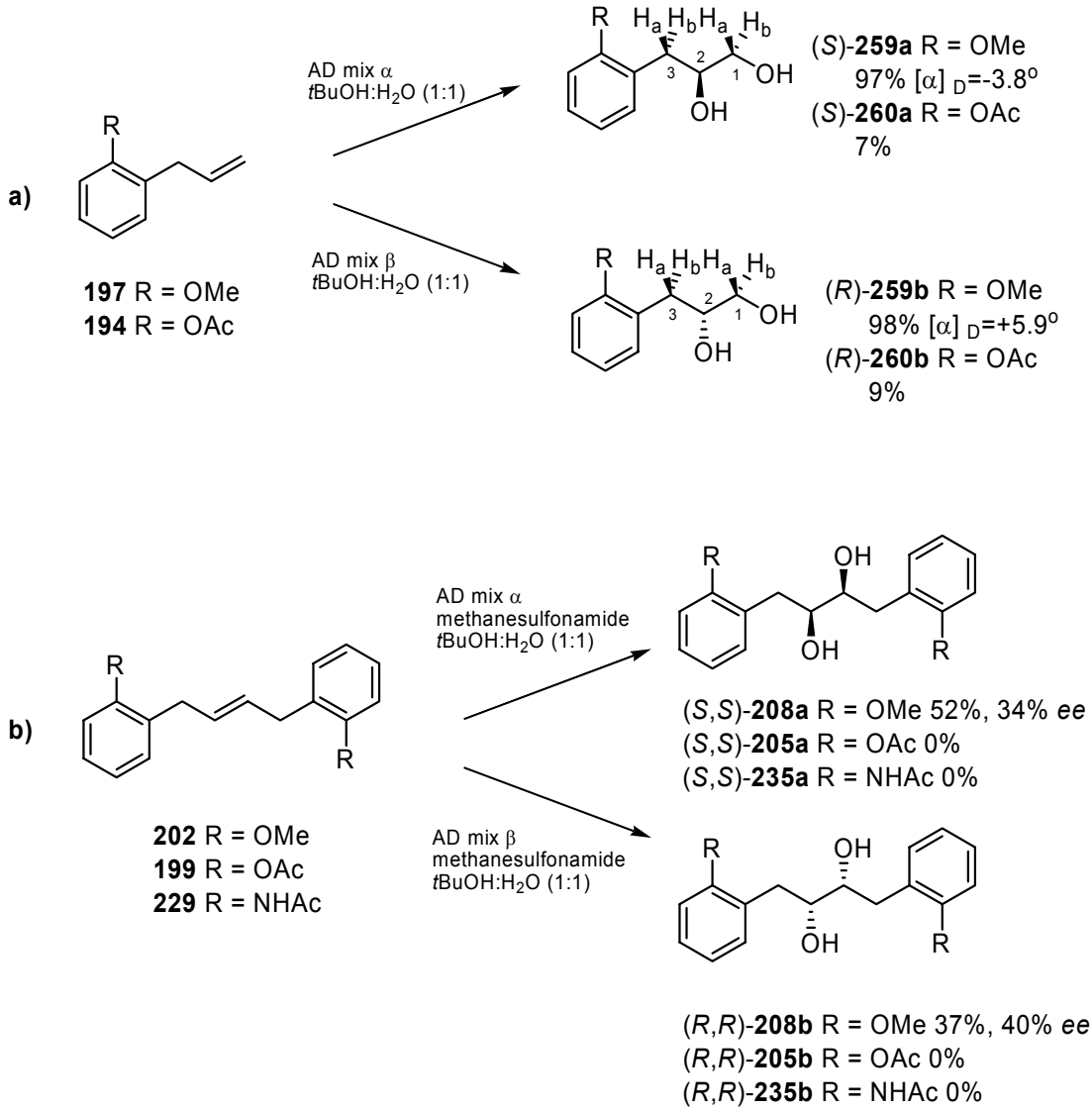

Aqueous workup of the AD reaction of **197** (R = OMe) and column chromatography afforded the diols (*S*)-**259a** in 97% yield and the enantiomer (*R*)-**259b** in 98% yield. The synthesis of the racemic diol **259** has been reported,[217] without spectral data, while synthesis of the (*R*)-diol was reported using a chiral starting material, with minimal spectral data.[218] Therefore, analysis of the spectra of the diols (*S*)- and (*R*)-**259** was necessary. Two broad singlets at 2.75 and 2.80 ppm were assigned to the two hydroxy protons. Two sets of dd peaks at 2.78 and 2.84 ppm were assigned to the diastereotopic

protons H3a and H3b adjacent to the aromatic ring, while the two dd peaks further downfield at 3.46 and 3.59 ppm were assigned to the two terminal diastereotopic methylene protons H1a and H1b. The singlet at 3.82 ppm was assigned to the methoxy protons and the multiplet at 3.92-3.93 ppm was assigned to the methine proton H2 attached to the stereogenic carbon. The methylene carbon C3 adjacent to the aromatic ring was assigned to the peak at 34.4 ppm in the ^{13}C NMR spectrum, and the peak at 66.0 ppm was assigned to the terminal CH_2, C1. The peak at 72.2 ppm was assigned to the stereogenic CH carbon C2, and the peak at 55.3 ppm was assigned to the methoxy carbon. MS (ES, +ve) analysis displayed a peak at *m/z* 200 assigned to the $M+NH_4$ ion. The diols were stored under argon at -15 ^{o}C, to avoid the rapid degradation observed at room temperature.

The optical rotation of (*S*)-**259a** was -3.8^{o} (*c* 0.045, $CHCl_3$), while the optical rotation of enantiomer (*R*)-**259b** was +5.9^{o} (*c* 0.045, $CHCl_3$). Chiral HPLC analysis was attempted, in order to determine the *ee* of the diols. Samples of each enantiomer were subjected to chiral HPLC, using 40% *i*PrOH:hexane (flow rate 0.5 mL/min) however only one peak was observed in the chromatograms from each sample, with the same retention time (20 min). The samples were mixed and reanalysed under the same conditions, which confirmed that the single peak observed in each chromatogram was assigned to both enantiomers. A gradient eluting system was attempted, in which the polarity changed from 20% to 40% *i*PrOH:hexane over 15 min; again resulting in a single peak at 20 min, assigned to both enantiomers. Reduction of the polarity of the eluting solvent (10% to 20% *i*PrOH:hexane over 20 min) showed a single peak at 30 min for both isomers, without any indication of partial resolution. Therefore, it was unlikely that a further reduction in polarity or increase in time of the gradient would provide a useful elution system for analysis of the *ee*.

Comparison of the two optical rotations confirmed the formation of the each enantiomer, therefore NMR analysis using the chiral shift reagent europium tris[3-(heptafluoropropylhydroxymethylene)-(+)-camphorate (**261**) was attempted.[219] Dropwise addition of a solution of **261** (10 mg/mL) followed by ^{1}H NMR analysis, did not produce the desired resolution of any of the peaks. The peaks broadened and did not resolve.

Therefore, the *ee* however, could not be ascertained. The near quantitative yield however, indicated that the diol was able to come into proximity to the ligand bound OsO_4, allowing dihydroxylation to occur.

Reaction of the alkene **194** (R = OAc) under the same conditions gave the corresponding diols (*S*,*S*)- and (*R*,*R*)-**260** in poor yield. The ^{1}H NMR spectrum was similar to that obtained from the diol **259**, with the exception of a singlet at 2.10 ppm in the ^{1}H NMR spectrum and peaks at 20.8 and 171.4 ppm in the ^{13}C NMR spectrum assigned to the acetyl group, in place of the peaks assigned to the methoxy substituent in the NMR spectra of **259**. MS (ES, +ve) analysis showed a peak at *m/z* 211 assigned to the M+H ion. The *ee* could not be determined via HPLC analysis, and the samples had degraded before an optical rotation could be obtained. The poor yield however, showed that although a terminal alkene, the double bond was unable to satisfactorily access the ligand bound OsO_4.

The monomeric methoxy derivatives (*S*,*S*)- and (*R*,*R*)-**259** were obtained in excellent yield (97% and 98%), compared to the dimeric derivatives (*S*,*S*)- and (*R*,*R*)-**208** (52% and 37%, **Scheme 5.11**, **b**). This indicates that the increased steric hindrance of the dimeric alkene **208**, compared to **197**, was preventing access to the OsO_4. Although it could not be determined, the *ee* would probably still be poor, as the removal of one of the *ortho*-substituted aromatic rings would result in the remaining aromatic system being directed away from the binding pocket. Stereoselectivity in the AD reaction for this alkene would only be achieved if the aromatic substituent were directed into the binding pocket. The steric hindrance experienced between the *ortho* substituent and the binding pocket in the dimers would also be experienced by the monomer, resulting in the substrate being directed away from the binding pocket and therefore poor stereoselectivity.

Interestingly, the AD reaction of the monomeric acetyloxy derivative **194** gave the diols (*S*,*S*)- and (*R*,*R*)-**260** in poor yield (7% and 9%), compared to dimeric **199** which failed to give the corresponding diols **205**. It should be highlighted that the AD reaction of the acetanilide **222** (R = NHAc) also did not provide the corresponding diols. This indicates that the presence of the acetyl group has an additional destabilising interaction with the binding pocket of the biscinchona ligands.

5.7 Heterodimeric 1,2-disubstituted aromatic allylic alkenes

Analysis of all the AD results obtained thus far indicates that the limited access of the ligand bound OsO_4 can be attributed to, most predominantly, steric interactions between the *ortho* substituents of the aromatic rings and the binding cavity of the chiral ligand. The removal of the *ortho* substituents from both aromatic rings (**170**, **Table 5.7**, entry 1) resulted in excellent chemical (84-88%) and stereochemical yield (93-95% *ee*). Whether removal of only one of the *ortho* substituents would sufficiently remove the steric effect was unknown, therefore the outcome of the AD reaction on the unsymmetrical system **262** (**Figure 5.14**) was determined.

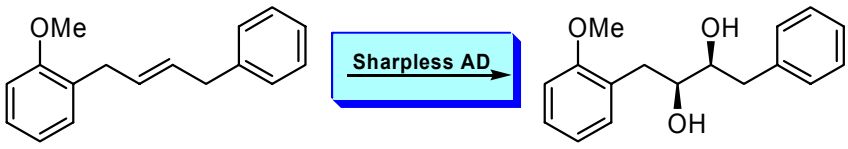

262 **263**

Figure 5.14: Proposed investigation into the determination of the effect of the AD reaction on the unsymmetrical alkene **262**.

5.7.1 Cross-metathesis reaction

The synthesis of the heterodimer **262** was performed via the cross-metathesis reaction[172] of *ortho*-allylanisole **197** and allylbenzene **237** (**Scheme 5.12**).

Scheme 5.12: The cross-metathesis of *ortho*-allylanisole **197** and allylbenzene **237** in the presence of Grubbs 1st generation catalyst, to form the unsymmetrical dimer **262**.

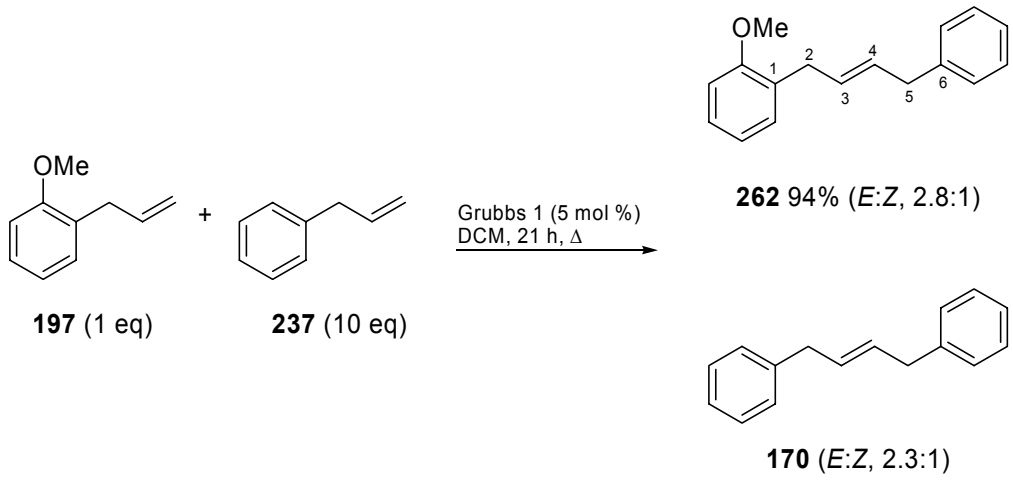

197 (1 eq) **237** (10 eq)

262 94% (*E*:*Z*, 2.8:1)

170 (*E*:*Z*, 2.3:1)

The reaction was heated at reflux in DCM for 21 hours. After removal of the solvent and subsequent column chromatography, the homo-dimer **170** was isolated as a mixture of geometric isomers (2.3:1). Further elution yielded the desired cross-metathesis product **262** in 94% yield, based on **197**, as a 2.8:1 mixture of *E*:*Z* geometric isomers. The EI-MS (+ve) displayed a peak at *m/z* 238 assigned to the molecular ion of the heterodimer **262**. Due to the unsymmetrical nature of the alkene **197**, assignment of the peaks in the NMR spectra required detailed analysis. The ^{1}H NMR showed a peak at 3.81 ppm of integration 3H, assigned to the methoxy protons. A multiplet at 5.58-5.67 ppm was assigned to both methine protons H3 and H4 of the *cis* and *trans* isomers. A multiplet upfield at 3.35-3.37 ppm was assigned to both methylene protons H2 and H5 of the *trans* isomer; the multiplet further downfield at 3.49-3.54 ppm was assigned to the corresponding methylene protons in the *cis* isomer. Peaks in the aromatic region with a relative integration of 9H were assigned to the 9 aromatic protons of the heterodimer. The ^{13}C NMR contains a peak at 55.3 ppm assigned to the methoxy carbon. The peak assigned to the methoxy protons in the ^{1}H NMR showed a two bond C-C-H correlation in the gHMBC 2D-spectrum to a peak at 157.2 ppm in the ^{13}C NMR, assigned to quaternary C1. The peak at 141.0 ppm was assigned to quaternary C6. Further analysis of the two bond C-C-H correlations displayed by the gHMBC spectrum allowed assignment of the peak at 33.0 ppm to CH_2 C2 adjacent to the anisole, and the peak at 39.0 ppm to CH_2 C5 adjacent to the phenyl group.

The use of the intermolecular metathesis reactions, such as cross-metathesis (CM) and self-metathesis (SM) is less common than intramolecular versions (e.g. ROMP and RCM), as general reaction conditions giving high yield and good *trans*/*cis* selectivity have yet to be developed.[170,172,177] The driving force for ROMP is ring strain release, and for RCM the intramolecular metathesis is driven by the proximity of the two double bonds and the entropy gained in the formation of the ring. CM has no such driving force, so product yield can be poor, and coupled with low chemoselectivity and stereoselectivity; the reaction is clearly not as useful as the intramolecular versions.[172]

Terminal alkenes (known as Type I alkenes), however, are highly reactive to cross-metathesis.[220] 1,2-Disubstituted alkenes are less active due to increased substitution around the double bond. Olefins containing adjacent electron withdrawing groups have reduced activity due to the electron deficiency of the double bond. In order for selective

cross-metathesis to occur, the quantity of homo-dimerisation must be minimised. This can be achieved by coupling two alkenes of different reactivity – for example, an electron deficient alkene with a terminal alkene. The homodimerisation of the electron deficient alkene will be slow, and will preferentially undergo cross-metathesis with the terminal alkene. Similarly, in the reaction of a terminal alkene with a 1,2-disubstituted alkene, the internal alkene will not undergo SM, and will preferentially undergo CM with the terminal alkene.

Early methods established for cross-coupling reactions of two terminal alkenes involved a two-step process (e.g. **Figure 5.15**).[221] Firstly, one coupling partner **237** is dimerised via a self-metathesis reaction to form a symmetrical 1,2-disubstituted homodimer **170**. Secondly, the CM is performed between a terminal alkene **197** and the internal alkene **170**, to yield the desired heterodimer **262**.

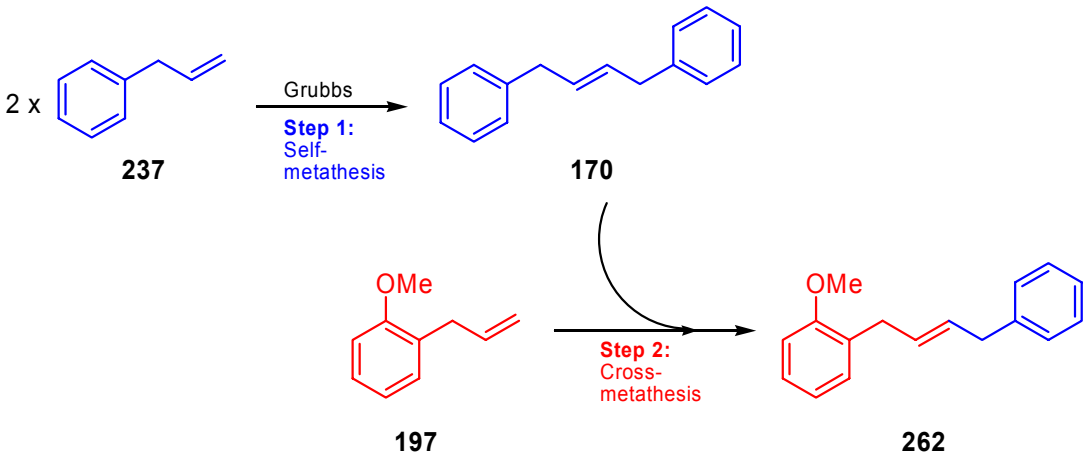

Figure 5.15: The two-step process for the CM of two terminal alkenes. **Step 1:** one coupling partner **237** is subjected to SM to form the homodimer **170**. **Step 2:** the internal alkene undergoes CM with the terminal alkene **197** to yield the heterodimer **262**.

Recently, the approach has been modified to a one-step process.[170] Essentially the same mechanism occurs for the cross coupling, however one coupling partner **237** is added in up to 10 equivalents excess. The resultant homodimer **170**, although not isolated, still undergoes CM with the terminal alkene **197**.

Although the cross-metathesis reaction of two Type I alkenes is not efficient, the goal was to obtain the desired heterodimer **262** in sufficient quantity for testing the AD

reaction. The commercial availability of allylbenzene **237**, to be used in such large excess, rendered this a viable method for the formation of the desired heterodimer.

The separation of *E* and *Z* isomers was attempted using column chromatography combined with semi-preparative HPLC. A sample of isolated alkene **262** (105 mg, *E*:*Z* 2.2:1) was subjected to silica gel column chromatography (1% EtOAc:hexanes) which provided two portions of alkene **262**; **A**: 36 mg, *E*:*Z* 2:1 and **B**: 13 mg, *E*:*Z* 4:1). Sample **A** was subjected to semi-preparative HPLC (normal phase, 100% hexanes to 10% EtOAc:hexanes over 20 min, flow rate 10 mL/min). A single peak which eluted at 11 min was collected and concentrated; however ^{1}H NMR analysis indicated that *E*-**262** had not been isolated, as the geometric ratio of isomers was 5.5:1. Further separation could not be attempted, since the alkene was found to degrade (*vide infra*). Therefore, the cross-metathesis reaction was repeated, and the crude mixture was subjected to silica gel column chromatography (1% EtOAc:hexanes) to give the heterodimer **262** as a 2.4:1 of geometric isomers. The sample was subjected to two successive columns, which increased the ratio of isomers to 4:1. Due to the instability of alkene **262**, further attempts to increase the geometric ratio could not be made; however, the results obtained would indicate that the isolation of pure *E*-**262** was unlikely.

The heterodimer **262** degraded quickly. Column chromatography isolated the major degradation product, which was speculated to be alkenol **264** (**Scheme 5.13**).

Scheme 5.13: The degradation of **262** to form the alkenol **264**.

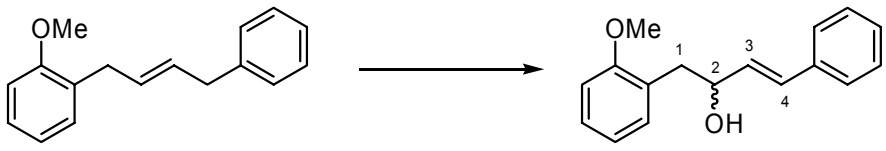

262 **264**

The ^{1}H NMR spectra showed a doublet of integration 1H at 6.62 ppm (J = 16.0 Hz) assigned to H4, and a ddd peak of integration 1H at 6.25 (J = 1.6, 7.5, 16.1 Hz) assigned to H3, characteristic of a vinylic alkene. Two peaks at 3.07 ppm and 3.09 ppm were assigned to the diastereotopic protons H1, and a peak at 4.78 ppm was assigned to the sp^{3} methine proton H2. A doublet of integration 3H at 3.89ppm was assigned to the

methoxy protons. Interestingly, the broad singlet assigned to the hydroxyl proton was observed at 8.78 ppm, indicating hydrogen bonding. A peak in the ^{13}C NMR spectrum at 33.3 ppm was assigned to the methylene carbon C1, and the peak at 86.0 was assigned to the methine carbon C2. ^{13}C NMR analysis displayed a single peak at 55.7 ppm assigned to the methoxy carbon, which showed a two-bond C-C-H correlation in the gHMBC 2D-spectrum to a peak at 157.5 ppm, assigned to the methoxy substituted quaternary carbon. Further analysis of the gHMBC spectrum provided the assignments of each of the carbons of the anisole ring. The peaks at 127.3 and 133.6 ppm were assigned to C3 and C4, respectively. The peaks assigned to the corresponding protons H3 and H4 in the ^{1}H NMR showed a two bond C-C-H correlation in the gHMBC spectrum to the carbons assigned to the unsubstituted phenyl ring. This confirms unequivocally the presence of the double bond in the vinylic position of the unsubstituted phenyl ring, as opposed to the anisole ring.

Degradation to the alkenol was exacerbated by exposure to air, moisture, NMR solvent and silica gel. TLC analysis of the alkene **262** which had been stored at −10 ^{o}C (freezer) under Ar(g) for 4 days indicated the presence of the degradation product **264**. The mechanism by which the alkene degraded is unknown, although water is presumably the source of the hydroxy group. The analogous product was not observed for the dimeric alkenes previously described, indicating that the difference in the electron-withdrawing ability between the two aromatic rings was probably a driving force for the degradation. The reaction could have been catalysed by residual acid from the silica gel, or possibly residual Ru from the Grubbs catalyst.

5.7.2 The AD reaction of heterodimeric 1,2-disubstituted aromatic allylic alkenes

Owing to its instability, the heterodimer **262** was therefore prepared and isolated as a mixture of geometric isomers, and subjected to AD conditions without improvement of the isomeric ratio. A mixture of *E* and *Z*-**262** (1.4:1) was reacted under standard Sharpless conditions using AD mix α (**Scheme 5.14**). Due to the unsymmetrical nature of the *Z* isomer, the dihydroxylation produced two possible enantiomeric diols (*S*,*R*)- and (*R*,*S*)-**263**, rather than the *meso* diol resulting from all previous alkenes. Therefore, the result of the AD reaction was a diastereomeric mixture (1.6:1) of diols (*S*,*S*)-**263a**

and (*S*,*R*)-**263c** in 98% yield. The diastereomeric mixture was subjected to extensive silica gel column chromatography to give partial separation of the (*S*,*S*)-**263a** isomer in 18% yield. Chiral HPLC analysis of the isolated sample indicated that the *ee* was 84%.

Scheme 5.14: Conditions for the asymmetric dihydroxylation of heterodimeric alkene *E*- and *Z*-**262**, using standard Sharpless protocol, with AD mix α.

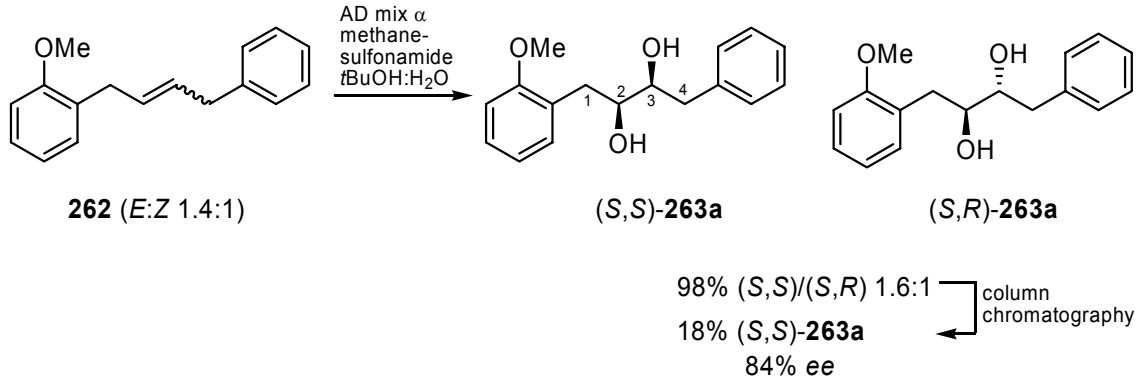

The ^{1}H NMR spectrum of diol (*S*,*S*)-**263a** displayed a peak at 2.92 ppm, assigned to the methylene H1 protons, while the peak at 2.89 ppm was assigned to the methylene H4 protons. The peak at 35.2 and 40.0 ppm in the ^{13}C NMR spectrum were assigned to C1 and C4 respectively. The assignment of H1 and C1 were made through gHMBC ^{1}H-^{13}C correlations to the peak at 157.4 ppm in the ^{13}C NMR spectrum assigned to the methoxy substituted *ipso* carbon. Through further gHMBC correlations, the peaks at 73.5 and 74.1 ppm in the ^{13}C NMR were assigned to C2 and C3 respectively. Two doublets at 2.38 and 2.46 ppm in the ^{1}H NMR spectrum were assigned to the two hydroxy protons, and the singlet of integration 3H at 3.82 ppm was assigned to the methoxy protons. MS (ES, +ve) analysis showed a peak at *m/z* 273 assigned to the M+H ion.

A mixture of alkene **262** (*E*:*Z*, 2.4:1) was subjected to standard Sharpless conditions using AD mix β (**Scheme 5.15**). A diastereomeric mixture (5.7:1) the (*R*,*R*) and (*R*,*S*) diols **263** was obtained in 90% yield. Due to the difficulty in obtaining the (*S*,*S*) isomer via column chromatography, recrystallisation of the mixture was attempted from DCM/hexanes. The ratio was increased to 10.5:1, which was sufficiently pure for determination of the *ee* via HPLC analysis which revealed that the *ee* was 84%.

Scheme 5.15: Conditions for the asymmetric dihydroxylation of alkene **262** using AD mix β.

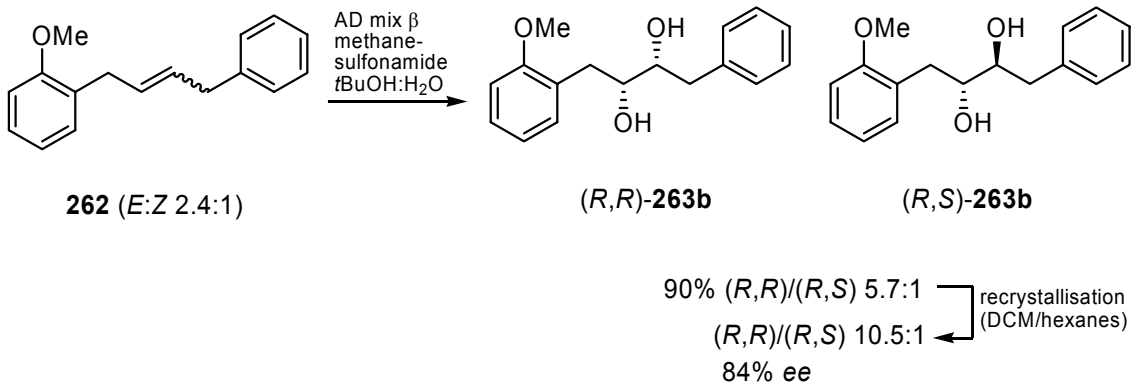

The improved outcome of the AD reaction of the heterodimer **263** showed that the lack of an *ortho* substituent on one of the aromatic rings allowed the approach of the substrate to the OsO_4, resulting in good enantioselection. The enantioselectivity of the reaction was better than that of the OMe homodimer **202** (34-40% *ee*), although not as good as that obtained from the AD reaction of the unsubstituted alkene **170** (93-95% *ee*). Therefore, the removal of one sterically imposing group allows entry of the 1,2-disubstituted alkene system to fit into the binding pocket of the chiral ligand. Conversely, the presence of *ortho* substituents on both aromatic rings in these types of systems results in poor selectivity, due to steric interactions between the alkene and the biscinchona ligand.

5.8 Conclusion

The results obtained from this study show that the synthetic strategy proposed in **Figure 4.1** via the phenol-based derivatives or in **Figure 4.5** by the nitrogen-based derivatives cannot be improved by the modification of the *O*- or *N*-protecting group. It is the very presence of this group that is causing the poor result. Modification of the protecting group was found to alter the result by changing the level of interaction between substrate and the ligand (e.g. when R = OAc, NHAc the corresponding diols were not formed), however, the only improvements made were via the reduction in the effective size of the substituent (R = Me), shifting of the substituent to the *meta*- or *para*-positions (R = *m*-OMe, *p*-OMe), or ultimately, complete removal of the aromatic substitution (R = H); all of which cannot be incorporated into the synthetic strategy.

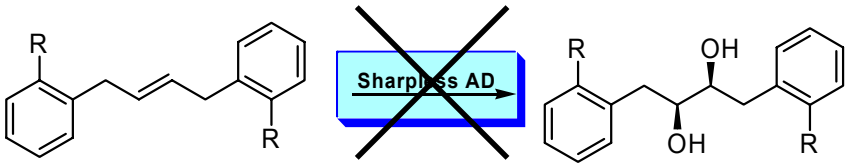

228 **234**

The exact position of the steric interaction between the alkene substrate and the biscinchona ligands was not determined. To determine which part of the ligand is experiencing the interaction the structure of the ligand-OsO_4-alkene would need to be examined through extensive computer modelling. Additionally, modelling studies would provide information regarding the structure adopted by the alkene within the ligand binding pocket, and therefore limitations on the size of the substrates for potential reaction feasibility. Computer modelling studies, in combination with the synthetic results obtained would also give a more complete understanding of the, still debated,[153,182] mechanism of the Sharpless asymmetric dihydroxylation.

It was therefore concluded that the presence of *ortho*-substituents in the aromatic rings of dimeric allylic aromatic alkenes prevented access of the substrate to the ligand bound OsO_4, thereby minimising chemical yield and enantioselection.

CHAPTER 6
Conclusions and Future Directions

6.1 Ligand design

The Suzuki reaction using a chiral catalyst offers many advantages as an enantioselective method for the stereoselective synthesis of axially chiral biaryls. The incorporation of a chiral ligand provides the source of chirality in catalytic quantities, and additionally positions the ligand in close proximity to the site of bond formation. There are currently no programs, however, for the design of chiral ligands for use in the stereoselective synthesis of sterically hindered systems, in particular atropisomeric biaryls.

A new design concept utilising helical-sense discrimination was investigated, for use in Pd-based Suzuki coupling reactions. A new set of design principles was established for chiral ligands for use in these reactions;

1. The ligand must contain a defined helical twist enclosed at each by donor atoms, such as N, P or As.
2. The ligand must be bidentate, to best transfer the helical aspect of the ligand to the Pd reaction site
3. The substituents of the donor atoms should be tied back in ring systems to minimise steric hindrance of the already demanding reaction site.
4. The helical twist should be in close proximity to the Pd reaction site.

The first two target scaffolds which would incorporate the above principles were based on chiral 2,2'-bispyrrolidine and 2,2'-bisindoline.

6.2 2,2'-Bispyrrolidine synthesis

A new strategy was devised for the enantioselective synthesis of chiral 2,2'-bispyrrolidines (*R*,*R*)-**92a** and (*S*,*S*)-**92b**. The keys steps of the synthesis were the metathesis dimerisation and subsequent Sharpless asymmetric dihydroxylation (AD) from achiral starting materials. Boc protected bispyrrolidine (*R*,*R*)-**92a** was synthesised in 13% yield, over 10 steps, from commercially available 4-penten-1-ol. The metathesis reaction gave the desired benzyl protected alkene **129** as a mixture of geometric isomers (4:1) which could not be separated using column chromatography. The AD reaction using AD mix α gave the diol (*S*,*S*)-**107a** with an *ee* of 80%, which was converted to 2,2'-bispyrrolidines (*R*,*R*)-**92a** via the known procedure.[164] The synthesis was repeated using the PMB protected derivatives, to give (*R*,*R*)-**92a** in overall 9% yield. The presence of the PMB group aided in the separation of *E* and *Z* isomers from the starting material and side metathesis products. The AD reaction of the PMB protected alkene **150** using AD mix α gave the corresponding diol (*S*,*S*)-**153a** in 92% *ee*. The AD reaction of the same alkene **150** using AD mix β gave the enantiomeric diol (*R*,*R*)-**153b** in 88% *ee*, which was converted to bispyrrolidine (*S*,*S*)-**92b** in 24% overall yield.

Attempts were made to reduce the total number of steps to the derivatised 2,2'-bispyrrolidine **92** by changing the nitrogen nucleophile. Further attempts were made to derivatise the chiral diol via the cyclic sulfate, in order to separate the *meso* and chiral diastereomers, and to allow incorporate of two different heteroatoms, via sequential nucleophilic substitution reactions. The cyclic sulfite however, could not be oxidised efficiently to the desired sulfate.

6.3 2,2'-Bisindoline synthesis

The new strategy was applied to the synthesis of the chiral 2,2'-bisindoline **112** (**Scheme 6.1**). The AD reaction of the benzyl protected *ortho* substituted dimeric aromatic allylic alkene **165** however, gave the diol (*S*,*S*)-**166a** in poor chemical (15%) and stereochemical yield (64% *ee*). The yield was increased to 60% by using modified Sharpless conditions, however the enantiopurity decrease to 36% *ee*. This poor outcome was also realised in concurrent studies which required the AD reaction of the Boc-protected anilino derivative **188**, which gave the desired diols **189** in 31-34% yield and

50-56% *ee*.[185] Therefore, an extensive study was undertaken to improve the outcome of the AD reaction. The AD reaction was performed on a total of 9 protected phenolic and nitrogen-based derivatives. Each of the alkenes was synthesised via dimerisation of protected monomeric *ortho*-allyl substituted phenols, or the N-based analogues, using the metathesis reaction. Grubbs 2 was found to provide the *E* alkenes in higher selectivity, however separation of the desired alkene from the secondary metathesis products was difficult, and in most cases not possible.

Scheme 6.1: The proposed synthesis of 2,2'-bisindoline **112** via the key steps of **metathesis** and **Sharpless AD** was limited by the poor outcome of the AD reaction.

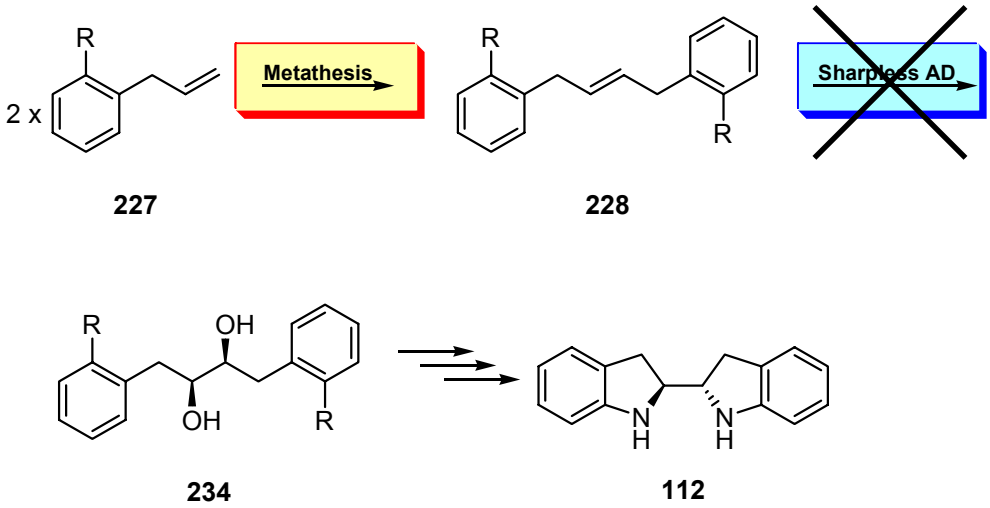

Modification of the protecting group of the phenolic and nitrogen-based derivatives did not improve the outcome of the AD, with yields of 0-58% and enantioselectivities of 1-58%. This lead to further investigation into the size and position of the *ortho*-substituent. The outcome of the AD was improved by reduction in the effective bulk of the entire substituent (R = Me, 62-70% *ee*), removal of the substituent from the *ortho* position (R = *m*-OMe, 73-76% *ee*; R = *p*-OMe, 85-87% *ee*), removal from one aromatic ring (84% *ee*), or ultimately, removal from both aromatic rings (R = H, 93-95% *ee*). It was therefore concluded that the presence of *ortho*-substituents on the aromatic rings of dimeric allylic aromatic alkenes of the type **228** was preventing access of the substrate to the ligand bound OsO_4, thereby causing the poor chemical yield and poor *ee*. Consequently, 2,2'-bisindoline **112** would not be attained in sufficient enantiomeric purity via this synthetic strategy, using the AD mix ligands $(DHQ)_2PHAL$ and $(DHDQ)_2PHAL$.

6.3.1 Improvement of the AD reaction

The synthetic strategy could be improved by modification of the AD mix ligands, by using a ligand such as the 9-anthracenylmethyl quaternary ammonium salt derivative (**265**, **Figure 6.1**) which has been reported to show improved facial selectivity in the dihydroxylation of substrates containing remotely positioned functional groups, presumably due the deeper binding pocket of the ligand.[153,222]

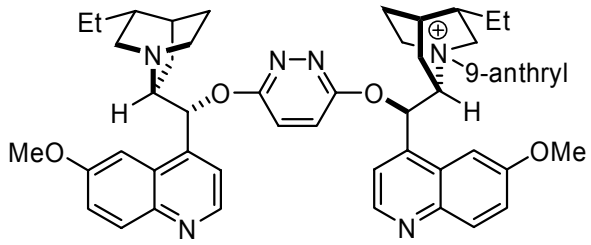

265

Figure 6.1: The 9-anthracenylmethyl quaternary ammonium salt derivative of the biscinchona ligands.

Alternatively, based on our design principle, the use of 2,2'-bispyrrolidine derivatives should remove the steric problems resulting from the sterically hindered substrate. 2,2'-Bispyrrolidine derivatives have been reported as ligands for use in asymmetric dihydroxylations (see **Figure 2.8**).[154,155] The method is limited however; as OsO_4 is used stoichiometrically. Modification to a catalytic mechanism would be required in order for the method to be synthetically viable.

6.3.2 Alternative approach to 2,2'-bisindoline

As a result of this thesis, an alternate strategy which avoids the AD of dimeric aromatic alkenes was proposed. The synthesis outlined in **Scheme 6.2** is currently under investigation.[192] Alkene *E*-**266** is subjected to AD conditions to give chiral diol (*R*,*R*)-**267b** in 94% *ee*.[3] The diol is converted to the diepoxide (*R*,*R*)-**268b** with subsequent S_N2 reaction with *ortho*-substituted aryl Grignard reagents **269** giving the diol (*R*,*R*)-**234b**, which in turn would provide 2,2'-bisindoline (*S*,*S*)-**112b**.

Scheme 6.2: The proposed alternate strategy towards chiral 2,2'-bisindoline (*S*,*S*)-**112b**, via ring-opening of epoxide (*R*,*R*)-**268b**. The enantioselectivity of the AD reaction of alkene **266** is reported to be 94%.[3]

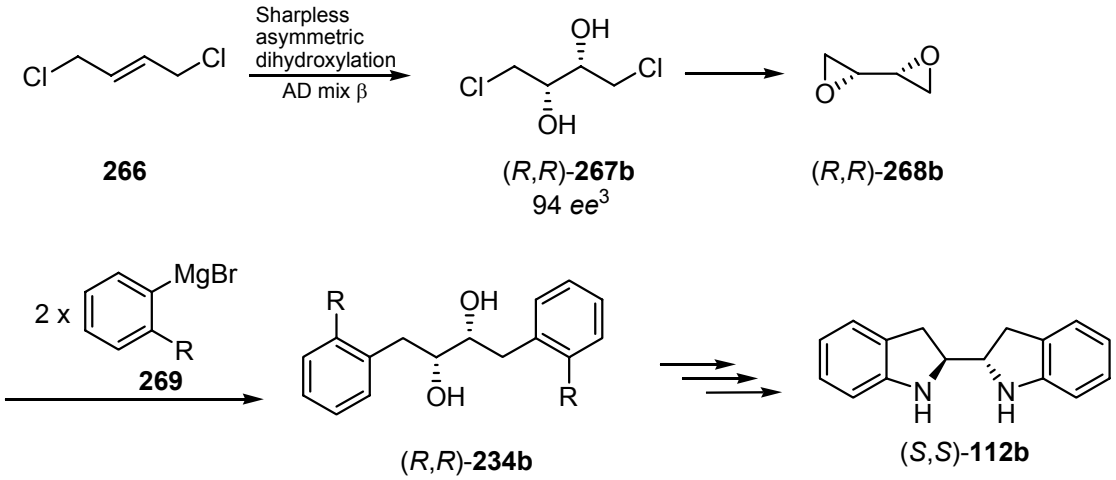

6.4 Biaryl coupling reactions

The concept of helical-sense discrimination for the stereoselective synthesis of axially chiral biaryls was not tested. The diamines **86** and **112** were not expected to be utilised in Pd-based reactions, since the ligands used for such reactions are generally phosphine- or arsine-based. The new concept using helicity can be tested however, using the dibenzyl bispyrrolidine **160** in Cu catalysed oxidative homocouplings. Therefore, the optimisation of the deprotection of Boc-protected 2,2'-bispyrrolidine **92** and subsequent derivatisation is required. The Cu^{I}-diamine complexes can be obtained and used for the stereoselective couplings of 2-naphthols, according to the literature procedure for similar chiral diamines (**Scheme 6.3**).[110-114]

Scheme 6.3: The proposed application of the chiral bispyrrolidines **86** or **160** in the stereoselective oxidative biaryl coupling of 2-naphthol **54** to give binaphthol (*M*)- or (*P*)-**3**.

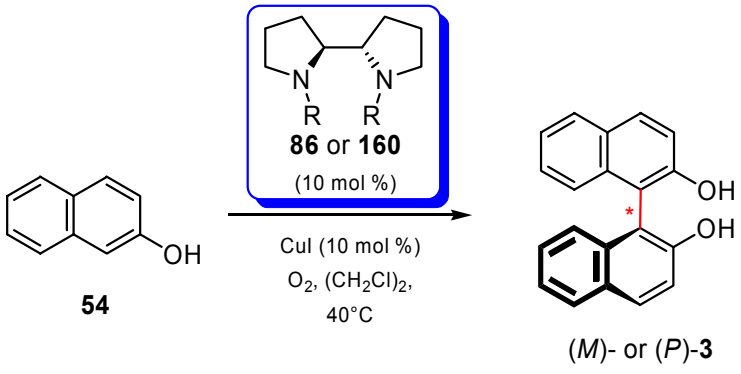

The synthetic strategy towards 2,2'-bispyrrolidine can be modified to synthesise the diarsine derivative and the mixed N, As derivative, from cyclic sulfate **158**. For example the proposed synthesis shown in **Scheme 6.4** involves monoazidation of (*S*,*S*)-**158a** followed by hydrolysis and mesylation to give (*R*,*S*)-**270a**. Displacement of the mesylate group via reaction with $AsPh_3$[223] gives (*R*,*R*)-**271a** which can be converted to the mixed N, As derivative (*R*,*R*)-**272a**. This ligand can then be tested in Pd and Cu based coupling reactions.

Scheme 6.4: Proposed synthesis of the mixed N, As derivative (*R*,*R*)-**272a** via stepwise nucleophilic substitution of cyclic sulfate (*S*,*S*)-**158a**.

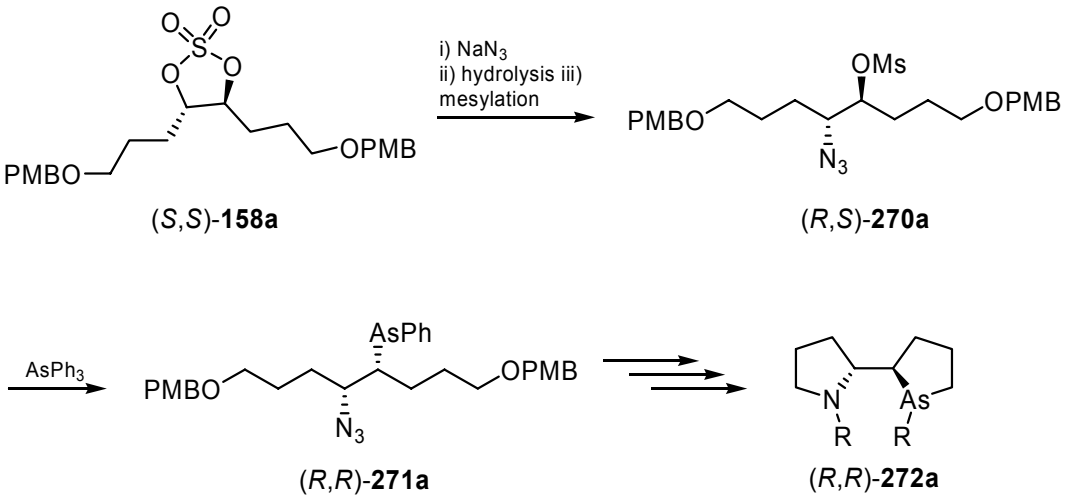

(*S*,*S*)-**158a** (*R*,*S*)-**270a**

(*R*,*R*)-**271a** (*R*,*R*)-**272a**

CHAPTER 7
Experimental

7.1 General experimental procedure

All glassware was acetone washed and oven dried, unless otherwise stated. All air sensitive reactions were performed under a positive pressure of argon or nitrogen gas. All air and moisture sensitive compounds were introduced into the reaction vessel through a rubber septum and syringe. THF and Et_2O were distilled from sodium/benzophenone and DCM was distilled from CaH_2. All other reagents were used as purchased without further purification, unless otherwise stated.

Thin Layer Chromatography (TLC) was performed using Merck Silica Gel F_{254} precoated aluminium plates. Gravity column chromatography was performed using Merck Silica Gel 60 (230-400 mesh) under gravity. All flash column chromatography was performed using Merck Silica Gel 60 (63-200 mesh) under the pressure of a hand pump. Eluents are expressed in volume to volume (v:v) proportions. All excess solvent was removed under reduced pressure.

High Performance Liquid Chromatography (HPLC) was performed using a Waters 1515 pump and a Daicel Chiralcel OD-H column with a flow rate of 0.5 mL/min and a detection wavelength of 254 nm, unless otherwise stated. Enantiomeric excesses (*ee*) were determined by analysis of analyte peak area.

Proton (^1H) and carbon (^{13}C) nuclear magnetic resonance (NMR) spectra were recorded at 300 MHz and 75 MHz respectively on a Varian Mercury 300MHz spectrometer. Alternatively, ^1H and ^{13}C spectra were recorded at 500 MHz and 125 MHz on a Varian Inova 500 MHz spectrometer. NMR spectra were acquired in $CDCl_3$ unless otherwise

noted, and are reported in parts per million (δ) relative to TMS (δ = 0 ppm) or $CDCl_3$ (δ = 77.0 ppm) as an internal standard. Coupling constants (*J*) are reported in Hertz (Hz). Multiplicities are reported as singlet (s), broad singlet (bs), doublet (d), triplet (t), quartet (q), multiplet (m), and doublet of doublets (dd).

Chemical ionization (CI) and electron impact (EI) mass spectra (MS) were obtained using a Shimadzu QP-5000 GC-MS spectrometer by direct insertion technique with a 70 eV electron beam and high resolution (HR) on a VG Autospec spectrometer. Electrospray (ES) MS were recorded on a Micromass Platform LCZ spectrometer and HR on a Micromass QTOF2 spectrometer. Ion mass to charge (*m/z*) values are stated and their relative abundances as a percentage in parentheses.

Melting points (m.p.) were determined using a GallenKamp (Griffin) melting point apparatus. Temperatures are expressed in degrees Celsius (^oC) and are uncorrected. Optical rotations were measured using a Jasco polarimeter with a 10 mm path length. Concentrations are expressed as *c* (10 mg/mL). Infrared (IR) spectra were recorded on a Nicolet Avatar 360 FT-IR spectrometer fitted with a Smart Omni-Sampler germanium crystal accessory. All IR spectra were recorded on neat samples.

Grubbs 1st generation catalyst is benzylidene-bis(tricyclohexylphosphine)dichloro-ruthenium. Grubbs 2nd generation catalyst is benzylidene[1,3-bis(2,4,6-trimethyl-phenyl)-2-imidazolidinylidene]dichloro(tricyclohexylphosphine)ruthenium. AD mix α contains chiral ligand $(DHQ)_2PHAL$, $K_3Fe(CN)_6$, K_2CO_3 and $K_2OsO_4.2H_2O$. AD mix β contains chiral ligand $(DHQD)_2PHAL$, $K_3Fe(CN)_6$, K_2CO_3 and $K_2OsO_4.2H_2O$.

Compound names for previously synthesised compounds are underlined.

NMR assignments

Protons and carbons of symmetrical molecules are assigned as follows;

- Integrations are given for total number of protons.
- Assignments are given once for both chemically equivalent atoms.

For example, in the symmetrical molecule **129** (**Figure 7.1**), H1 is equivalent to H8. Therefore, the assignment is ^{1}H NMR δ 3.45 (t, 4H, *J* = 6.5 Hz, OC<u>H</u>$_2$CH$_2$). That is, a total of 4H (H1 and H8), assigned to the CH_2 adjacent to the benzyl ether.

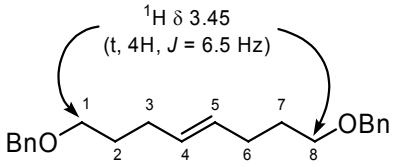

***E*-129**

Figure 7.1: NMR assignments of symmetrical molecules, for e.g. alkene **129**.

Where separation of diastereomeric (e.g. *E*/*Z* or chiral/*meso*) mixtures was not possible, yields are expressed as total overall yield, with diastereomeric ratios given in parentheses. The peaks arising in the ^{1}H and ^{13}C NMR due to the *Z* or *meso* impurities are marked with an asterix (*). For example, the peak at 3.46 ppm in the ^{1}H NMR of *E*/*Z*-**129** is assigned to the H1 proton of the *Z* isomer and is therefore marked with an asterix (**Figure 7.2**). Coupling constants and assignments are given where applicable, however integrations are not.

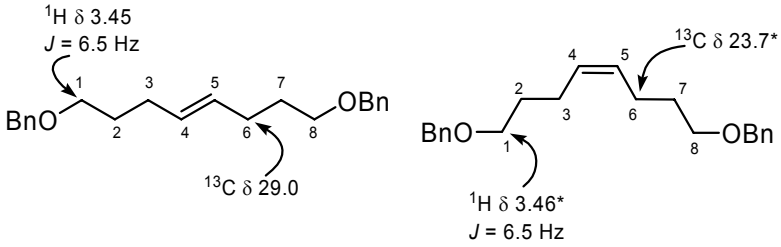

***E*-129** ***Z*-129**

Figure 7.2: NMR assignments for diastereomeric mixtures, e.g. the peaks arising from *Z*-**129** are marked with an asterix.

7.2 Bispyrrolidine synthesis

1-Benzyloxy-4-pentene 128[224,225]

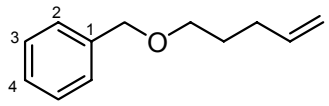

4-Penten-1-ol (0.24 mL, 2.32 mmol) was added dropwise to a stirred suspension of NaH (60% dispersion in oil; 250 mg, 6.25 mmol) in THF (6 mL) at 0 °C. Benzyl bromide (0.28 mL, 2.32 mmol) was added after 30 min, and the reaction was allowed to warm to RT with stirring for 23 h. The reaction was quenched with water, extracted with EtOAc (3 x 20 mL), the combined organic layers washed with sat. NaCl, dried ($MgSO_4$) and concentrated. The crude oil was subjected to gravity silica gel column chromatography to afford the protected alkene **128** as a volatile, colourless oil (409 mg, 99%).‡ ^{1}H NMR (300 MHz) δ 1.71 (tt (app. p), 2H, *J* = 6.8, 7.7 Hz, $OCH_2C\underline{H}_2$), 2.15 (dt (app. q), 2H, *J* = 7.1, 7.4 Hz, $C\underline{H}_2CH{=}CH_2$), 3.48 (t, 2H, *J* = 6.5 Hz, $OC\underline{H}_2CH_2$), 4.50 (s, 2H, $PhCH_2$), 4.93-4.98 (m, 1H, CH=C<u>H</u>H), 4.99-5.05 (m, 1H, CH=CH<u>H</u>), 5.82 (ddt, 1H, *J* = 6.6, 12.2, 16.9 Hz, $C\underline{H}{=}CH_2$), 7.24-7.34 (m, 5H, ArH); ^{13}C NMR (75 MHz) δ 28.9 ($OCH_2\underline{C}H_2$), 30.3 ($\underline{C}H_2CH{=}CH_2$), 69.7 ($O\underline{C}H_2CH_2$), 72.9 ($PhCH_2$), 114.7 ($CH{=}\underline{C}H_2$), 127.5 (ArC4), 127.6 (ArC2), 128.3 (ArC3), 138.3 ($\underline{C}H{=}CH_2$), 138.6 (ArC1); FTIR *v* 1721 (w), 1640 (w), 1554 (w), 1363 (w), 1101 (s), 1075 (m), 1028 (w), 994 (w), 913 (m), 737 (s); MS (CI, +ve) *m/z* 177 (82, M+H), 159 (100%, M-18).

***E*-5-Benzyloxy-1-phenyl-1-pentene 130**[226] **and *E*-1,8-Di(benzyloxy)-4-octene 129**[179]

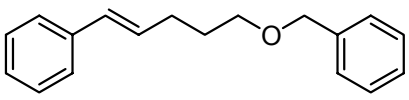

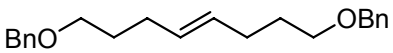

Grubbs 1 catalyst (246 mg, 0.30 mmol, 5 mol %) was added to a solution of alkene **128** (1.053 g, 5.98 mmol) in DCM (15 mL) and the solution was heated at reflux for 5 h. The reaction mixture was filtered through Celite and the solvent evaporated *in vacuo*. The crude oil was subjected to flash silica gel column chromatography (hexanes to 2% EtOAc:hexanes) to yield the pentene **130** (78 mg, 5%) as a colourless oil, which was spectroscopically identical to that reported in the literature.[226] ^{1}H NMR (300 MHz) δ 1.75-1.84 (m, 2H, $C\underline{H}_2CH_2O$), 2.31 (dddd, 2H, *J* = 1.04, 7.5, 7.8, 7.8 Hz, $CH{=}CHC\underline{H}_2$),

‡ No physical or spectral data reported in reference 224 or 225.

3.48 (ddd, 2H, *J* = 0.8, 6.4, 6.3 Hz, $CH_2C\underline{H}_2O$), 4.51 (s, 2H, $PhCH_2$), 6.20 (ddd, 1H, *J* = 6.8, 6.8, 15.8 Hz, PhCH=C<u>H</u>), 6.38 (d, 1H, *J* = 15.8 Hz, PhC<u>H</u>=CH), 7.25-7.35 (m, 10H, ArH).

Further elution afforded the octene **129** (1.728 g, 75%, *E*:*Z* 5:1) as a colourless oil.‡ ^{1}H NMR (300 MHz) δ 1.66 (tt (app. p), 4H, *J* = 6.7, 7.3 Hz, $OCH_2C\underline{H}_2$), 2.04-2.10 (m, 4H, $CH=CHC\underline{H}_2$), 2.12-2.16*, 3.45 (t, 4H, *J* = 6.5 Hz, $OC\underline{H}_2CH_2$), 3.46* (t, *J* = 6.5 Hz), 4.48 (s, 4H, $PhCH_2$), 5.38-5.41 (m, 2H, C<u>H</u>=C<u>H</u>), 7.28-7.41 (m, 10H, ArH); ^{13}C NMR (75 MHz) δ 23.7*, 29.0 ($\underline{C}H_2CH=CH$), 29.5 ($OCH_2\underline{C}H_2$), 29.6*, 69.65 ($O\underline{C}H_2CH_2$), 69.74*, 72.78 ($PhCH_2$), 72.82*, 127.4 (ArC4), 127.5 (ArC2), 128.3 (ArC3), 129.8*, 130.0 (<u>C</u>H=<u>C</u>H), 138.6 (ArC1); MS (CI, +ve) *m/z* 325 (16, M+H), 233 (10), 181 (20), 127 (100%).

(4*S*,5*S*)-1,8-Dibenzyloxy-4,5-octanediol 107a[164]

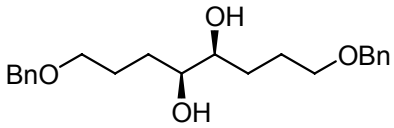

General Procedure A:[3] A suspension of AD mix α (1.88 g, 5.4 μmol osmium) and methanesulfonamide (128 mg, 1.35 mmol) was stirred at RT in a 1:1 mixture of *t*BuOH and water (7 mL) until completely dissolved. The mixture was cooled in an ice bath until a precipitate formed, and alkene **129** (436 mg, 1.35 mmol, *E*:*Z* 4.4:1) was added. The mixture was stirred vigorously at 0 ^{o}C for 1 h and a further 23 h at RT. The mixture was cooled in an ice bath and sodium sulfite (1.74 g) was added. After 1 h at 0 ^{o}C, the reaction mixture was returned to RT, partitioned between water (50 mL) and DCM (50 mL), and the aqueous layer back extracted with a further 3 portions of DCM (3 x 50 mL). The combined organic layers were washed with 2M KOH (2 x 30 mL), then sat. NaCl (1 x 50 mL), dried ($MgSO_4$) and concentrated *in vacuo*. The crude oil was subjected to gravity silica column chromatography (20% to 100% EtOAc:hexanes) which afforded the diol (*R*,*R*)-**107a** as a colourless oil (416 mg, 86%) as a mixture of chiral:*meso* diastereomers (4.9:1), which was spectroscopically identical to that reported in the literature.[164] HPLC analysis (10% to 40% 2-propanol:hexane, retention times (*R*,*R*)-diol **107b** 30.8 min (minor), (*S*,*S*)-diol **107a** 33.9 min (major)) showed the *ee* of the (*S*,*S*)-diol **107a** was 80%. $[\alpha]_D^{25}$ = –13.8^{o} (*c* 0.08, chiral:*meso*, 3.4:1, $CHCl_3$). ^{1}H

‡ No physical or spectral data reported in reference 179.

NMR (300 MHz) δ 1.44-1.56 (m, 2H, CHHCHOH), 1.60-1.73 (m, 2H, CHHCHOH), 1.75-1.82 (m, 4H, OCH_2CH_2), 3.00*, 3.07 (bs, 2H, OH), 3.40 (d, 2H, *J* = 5.7 Hz, CHOH), 3.51 (t, 4H, *J* = 5.9 Hz, OCH_2CH_2), 4.51 (s, 4H, $PhCH_2$), 7.25-7.35 (m, 10H, ArH); ^{13}C NMR (75 MHz) δ 26.0 (OCH_2CH_2), 26.5*, 28.9*, 30.8 (CH_2CHOH), 70.4 (OCH_2CH_2), 70.5*, 73.0 ($PhCH_2$), 74.1 (CHOH), 74.3*, 127.6 (ArC4), 127.7 (ArC2), 128.4 (ArC3), 138.1 (ArC1); MS (CI, +ve) *m/z* 359 (100%, M+H); MS (ES, +ve) *m/z* 381 (100%, M+Na), 376 (60, $M+NH_4$), 359 (30, M+H); HRMS (ES, +ve) calcd for $C_{22}H_{31}O_4$ 359.2222, found 359.2210.

(4*R*,5*R*)-1,8-Dibenzyloxy-4,5-octanediol 107b[164]

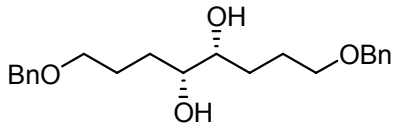

The diol (*R*,*R*)-**107b** was synthesised by *General Procedure A* using alkene **129** (265 mg, 0.82 mmol, *E*:*Z* 4:1), AD mix β (1.14 g), methanesulfonamide (78 mg, 0.82 mmol), *t*BuOH (4.1 mL), water (4.1 mL) and sodium sulfite (733 mg). The diol (*R*,*R*)-**107b** (231 mg, 80%) was isolated as a colourless oil, as a mixture of chiral:*meso* diastereomers (4:1), which had identical spectroscopic properties to the (*S*,*S*) enantiomer. HPLC analysis (10% to 40% 2-propanol:hexane, retention times (*R*,*R*)-diol **107b** 30.5 min (major), (*S*,*S*)-diol **107a** 34.7 min (minor)) showed the *ee* of the (*R*,*R*)-diol **107b** was 98%.

(4*S*,5*S*)-1,8-Dibenzyloxy-4,5-dimethanesulfonyloctane 144a[164]

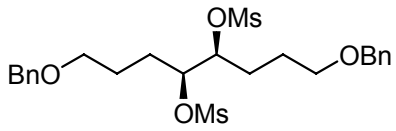

To a stirred solution of (*S*,*S*)-diol **166a** (700 mg, 1.97 mmol, chiral:*meso* 7:1) and Et_3N (2.18 mL, 15.6 mmol) in DCM (35 mL) at 0 ^{o}C was added MsCl (0.95 mL, 9.78 mmol). The reaction mixture was returned to RT and after 20 min was diluted with DCM (50 mL), washed sequentially with 5% $CuSO_4$, sat. $NaHCO_3$, sat. NaCl, and dried ($MgSO_4$). The crude oil was subjected to gravity silica gel column chromatography (10% to 100% EtOAc:hexanes) to afford the dimesylate (*S*,*S*)-**144a** as a colourless, viscous oil (766 mg, 76%) as a mixture of the chiral:*meso* diastereomers (7:1).‡ ^{1}H NMR (300 MHz) δ 1.67-1.77 (m, 4H, CH_2CH_2CHOMs), 1.79-2.01 (m, 4H,

‡ No physical or spectral data reported in reference 164.

C<u>H</u>$_2$CHOMs), 3.02 (s, 6H, SO_2CH_3), 3.05*, 3.49 (t, 4H, *J* = 5.5 Hz, OC<u>H</u>$_2$CH$_2$), 4.47 (s, 4H, PhCH$_2$), 4.48*, 4.83-4.89 (m, 2H, C<u>H</u>OMs), 7.23-7.36 (m, 10H, ArH); ^{13}C NMR (75 MHz) δ 24.9 (<u>C</u>H$_2$CH$_2$CHOMs), 25.5*, 26.7*, 27.6 (C<u>H</u>$_2$CHOMs), 38.7 (SO_2CH_3), 69.2*, 69.3 (O<u>C</u>H$_2$CH$_2$), 72.99 (PhCH$_2$), 73.04*, 80.6 (<u>C</u>HOMs), 82.6*, 127.6 (ArC4), 127.7 (ArC2), 128.4 (ArC3), 138.2 (ArC1); FTIR *v* 1357 (s), 1168 (s), 1101 (m), 906 (br, s); MS (CI, +ve) *m/z* 515 (7, M+H), 513 (7, M-H), 359 (26), 329 (46), 233 (100%); HRMS (EI, +ve) calcd for $C_{24}H_{33}O_8S_2$ 513.1617, found 513.1608.

(4*R*,5*R*)-1,8-Dibenzyloxy-4,5-diazidooctane 108a[164]

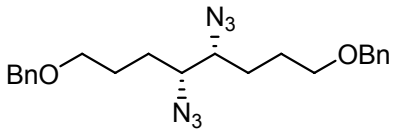

Sodium azide (253 mg, 3.89 mmol) was added to a solution of dimesylate (*S*,*S*)-**144a** (500 mg, 0.973 mmol, chiral:*meso* 2.5:1) in DMF (6 mL) and the reaction mixture was stirred at 80 ^{o}C for 2 h. The mixture was then poured into sat. NaCl, extracted with EtOAc (3 x 30 mL) and the combined organic layers were concentrated *in vacuo*. The crude oil was subjected to gravity silica gel column chromatography (20% EtOAc:hexanes) to afford the diazido (*R*,*R*)-**108a** (281 mg, 71%) as a colourless, viscous oil, as a mixture of chiral:*meso* diastereomers (4:1), which was spectroscopically identical to that reported in the literature.[164] ^{1}H NMR (300 MHz) δ 1.62-1.83 (m, 8H, C<u>H</u>$_2$CHN$_3$ and C<u>H</u>$_2$CH$_2$CHN$_3$), 3.30 (t, 2H, *J* = 4.2 Hz, CHN$_3$), 3.37-3.41*, 3.45-3.51 (m, 4H, OC<u>H</u>$_2$CH$_2$), 4.48 (s, 4H, PhCH$_2$), 7.25-7.36 (m, 10H, ArH); ^{13}C NMR (75 MHz) δ 26.3 (<u>C</u>H$_2$CH$_2$CHN$_3$), 26.4*, 27.2*, 28.2 (C<u>H</u>$_2$CHN$_3$), 65.0 (<u>C</u>HN$_3$), 65.6*, 69.4 (O<u>C</u>H$_2$CH$_2$), 72.9 (PhCH$_2$), 127.56 (ArC4), 127.59 (ArC2), 128.3 (ArC3), 138.2 (ArC1); FTIR *v* 2101 (s), 1711 (w), 1454 (w), 1276 (w), 1101 (s), 1030 (w); MS (CI, +ve) *m/z* 409 (3, M+H), 381 (100%), 353 (100%); HRMS (ES, +ve) calcd for $C_{22}H_{29}N_6O_2$ 409.2352, found 409.2341.

(4*R*,5*R*)-1,8-dibenzyloxy-4,5-diaminooctane 145a[164]

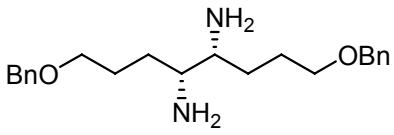

A 2-necked flask containing diazido (*R*,*R*)-**108a** (187 mg, 0.46 mmol, chiral:*meso* 5:1) and a catalytic amount of Pd/C in abs. EtOH (6 mL) was placed under vacuum. A balloon filled with H_2(g) was added and the reaction mixture was stirred at RT for 2 h. The mixture was then filtered through Celite, and concentrated under

reduced pressure. The crude mixture was redissolved in Et_2O, acidified (HCl) and extracted with water (4 x 20 mL). The combined aqueous layers were basified (NaOH) and extracted with DCM (4 x 20 mL). The combined organic layers were dried ($MgSO_4$) and concentrated to yield the diamine (*R*,*R*)-**145a** (163 mg, 100%) as a white solid, as a mixture of chiral:*meso* diastereomers (5:1).‡ ^{1}H NMR (300 MHz) δ 1.26-1.38 (m, 2H, C<u>H</u>HCHNH$_2$), 1.35 (s, 4H, NH$_2$), 1.49-1.66 (m, 4H, C<u>H$_2$</u>CH$_2$CHNH$_2$), 1.68-1.84 (m, 2H, CH<u>H</u>CHNH$_2$), 2.55 (bs, 2H, C<u>H</u>NH$_2$), 2.62-2.65*, 3.49 (t, 4H, *J* = 6.2 Hz, OC<u>H$_2$</u>CH$_2$), 4.50 (s, 4H, PhCH$_2$), 7.25-7.34 (m, 10H, ArH); ^{13}C NMR (75 MHz) δ 26.7 (OCH$_2$<u>C</u>H$_2$), 26.9*, 29.2*, 31.5 (OCH$_2$CH$_2$<u>C</u>H$_2$), 55.0 (<u>C</u>HNH$_2$), 55.9*, 70.3 (O<u>C</u>H$_2$CH$_2$), 72.8 (PhCH$_2$), 127.4 (ArC4), 127.5 (ArC2), 128.3 (ArC3), 138.4 (ArC1); MS (CI, +ve) *m/z* 357 (100%, M+H).

<u>(4*R*,5*R*)-1,8-Dibenzyloxy-4,5-di(*N*-*tert*-butoxycarbonylamino)octane 109a</u>[164] **and (4*R*,5*S*)-1,8-Dibenzyloxy-4,5-di(*N*-*tert*-butoxycarbonylamino)octane 109meso**

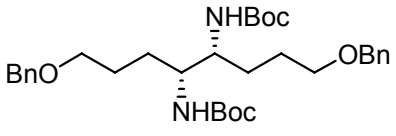

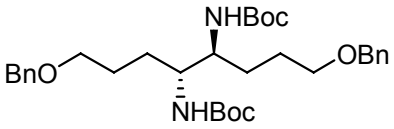

Di-*tert*-butyldicarbonate (618 mg, 2.82 mmol) in Et_2O (5 mL) was added to a stirred solution of diamine **145a** (168 mg, 0.47 mmol, chiral:*meso* 9:1) and Et_3N (0.26 mL, 1.88 mmol) in Et_2O (6 mL). The reaction was stirred at RT for 4 h and the solvent was evaporated under reduced pressure. The crude oil was subjected to gravity silica gel column chromatography (5% to 50% EtOAc:hexanes) to yield the chiral diBoc (*R*,*R*)-**109a** (168 mg, 64%) as a white solid, m.p. 78-80 ^{o}C, which was spectroscopically identical to that reported in the literature.[164] $[\alpha]_D^{25}$ = +31.1^o (*c* 0.31, $CHCl_3$).^{1}H NMR (300 MHz) δ 1.42 (bs, 20H, C(C<u>H$_3$</u>)$_3$ and C<u>H</u>HCHNH), 1.67 (bs, 6H, C<u>H$_2$</u>CH$_2$CHNH and CH$_2$CH<u>H</u>CHNH), 3.46-3.47 (m, 4H, OC<u>H$_2$</u>CH$_2$), 3.52-3.55 (m, 2H, C<u>H</u>NH), 4.48 (s, 4H, PhCH$_2$), 4.65 (d, 2H, ^4J = 8.7 Hz, NHBoc), 7.24-7.33 (m, 10H, ArH); ^{13}C NMR (75 MHz) δ 26.2 (<u>C</u>H$_2$CH$_2$CHNH), 28.3 (C(<u>C</u>H$_3$)$_3$), 29.6 (CH$_2$<u>C</u>H$_2$CHNH), 54.3 (CHNH), 69.9 (O<u>C</u>H$_2$CH$_2$), 72.8 (PhCH$_2$), 79.1 (<u>C</u>(CH$_3$)$_3$), 127.4 (ArC4), 127.6 (ArC2),

‡ No physical or spectral data reported in reference 164.

128.3 (ArC3), 138.5 (ArC1), 156.4 (C=O); MS (CI, +ve) *m/z* 557 (41, M+H), 458 (30), 457 (100%); HRMS (ES, +ve) calcd for $C_{32}H_{48}N_2O_6Na$ 579.3410, found 579.3376.

Further elution gave the corresponding *meso*-**109** compound (19 mg, 7%) as a white solid, m.p. 126 ^oC. $[\alpha]_D^{25}$ = + 2.5^o (*c* 0.12, $CHCl_3$). ^1H NMR (300 MHz) δ 1.42-1.49 (m, 2H, C<u>H</u>HCHNH), 1.42 (s, 18H, C(C<u>H</u>$_3$)$_3$), 1.53-1.77 (m, 6H, C<u>H</u>$_2$CH$_2$CHNH and CH$_2$CH<u>H</u>CHNH), 3.47 (t, 4H, *J* = 5.6 Hz, OC<u>H</u>$_2$CH$_2$), 3.61 (t, 2H, *J* = 9.0 Hz, C<u>H</u>NH), 4.49 (s, 4H, PhCH$_2$), 4.61 (bs, 2H, NHBoc), 7.28-7.33 (m, 10H, ArH). ^{13}C NMR (125 MHz) δ 26.4 (<u>C</u>H$_2$CH$_2$CHNH), 28.2 (CH$_2$<u>C</u>H$_2$CHNH), 28.4 (C(<u>C</u>H$_3$)$_3$), 54.3 (CHNH), 69.9 (O<u>C</u>H$_2$CH$_2$), 72.9 (PhCH$_2$), 79.2 (<u>C</u>(CH$_3$)$_3$), 127.4 (ArC4), 127.6 (ArC2), 128.3 (ArC3), 138.5 (ArC1), 156.0 (C=O); FTIR *v* 3355 (w), 1279 (s), 1527 (s), 1455 (w), 1368 (w), 1299 (w), 1242 (w), 1164 (m), 1120 (m), 991 (w), 866 (w), 741 (s) cm^{-1}; MS (ES, +ve) *m/z* 579 (100%, M+Na), 557 (10, M+H); HRMS (ES, +ve) calcd for $C_{32}H_{49}N_2O_6$ 557.3591, found 557.3590.

(4*R*,5*R*)-4,5-Di(3-benzyloxypropyl)-1-*tert*-butoxycarbonyl-2-imidazolidinone 147

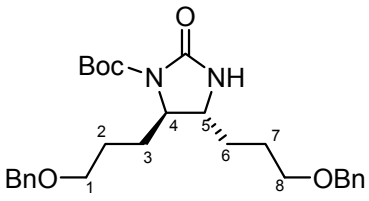

A 2-necked flask containing diazido **108a** (200 mg, 0.49 mmol, chiral:*meso* 2:1) and a catalytic amount of Pd/C in abs. EtOH (6 mL) was placed under vacuum. A balloon filled with H_2(g) was added and the reaction mixture was stirred at RT for 3.5 h. The mixture was then filtered through Celite and concentrated under reduced pressure. To a stirred solution of the crude diamine (*R*,*R*)-**145a** in Et_2O (10 mL) was added Et_3N (0.2 ml, 1.44 mmol) and Boc_2O (500 mg, 2.28 mmol) and the mixture was heated at reflux for 15 h. The solvent was removed *in vacuo* and the crude oil was subjected to gravity silica gel column chromatography (2% to 20% EtOAc:hexanes) to give the cyclic urea **147** (26 mg, 12%) as a colourless oil. ^1H NMR (300 MHz) δ 1.42 (s, 9H, C(C<u>H</u>$_3$)$_3$), 1.56-1.77 (m, 8H, H2, H3, H6 and H7), 3.46-3.50 (m, 5H, H1, H8 and H5), 3.70-3.75 (m, 1H, NH), 4.47-4.52 (m, 1H, H4), 4.50 (s, 4H, 2 x PhCH$_2$), 7.25-7.34 (m, 10H, ArH); MS (CI, +ve) *m/z* 483 (50, M+H), 383 (100%).

Further elution gave (*R*,*R*)-**109a** (70 mg, 26%) and further elution gave *meso*-**109** (40 mg, 14%).

(4*S*,5*S*)-4,5-Di(*N*-*tert*-butoxycarbonylamino)-1,8-octanediol 110b[164]

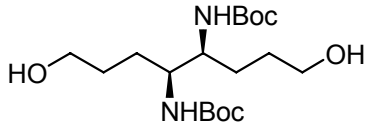

A flask containing a solution of diBoc **157b**† (91 mg, 0.15 mmol) and Pd/C (17 mg) in abs. EtOH (3 mL) was placed under vacuum. A balloon filled with H_2(g) was inserted, and the reaction was stirred at RT for 5 h. The reaction was filtered through Celite and the solvent was removed under reduced pressure to yield the diol (*S*,*S*)-**110b** (53 mg, 95%) as a white solid, m.p. 133-136 ^oC, which was spectroscopically identical to that reported in the literature.[164] ^1H NMR (300 MHz, CD_3OD) δ 1.44 (s, 18H, $C(CH_3)_3$), 1.44-1.47 (m, 2H, C<u>H</u>HCHNH), 1.56-1.60 (m, 6H, CH<u>H</u>CHNH and $HOCH_2C\underline{H}_2$), 3.53-3.57 (m, 6H, $HOC\underline{H}_2$ and C<u>H</u>NH), 4.85 (bs, 2H, NH); ^{13}C NMR (75 MHz, CD_3OD) δ 28.8 ($C(\underline{C}H_3)_3$), 29.9 ($HOCH_2\underline{C}H_2$), 30.3 ($\underline{C}H_2CHNH$), 55.2 (CHNH), 62.7 ($HO\underline{C}H_2$), 80.0 ($\underline{C}(CH_3)_3$), 158.6 (C=O); FTIR *v* 3319 (br), 1707 (s), 1681 (s), 1532 (s), 1446 (w), 1368 (m), 1278 (m), 1249 (s), 1165 (s), 1068 (m), 1044 (m), 996 (w), 864 (w); MS (ES, +ve) *m/z* 399 (100%, M+Na), 377 (40, M+H), 277 (10); HRMS (ES, +ve) calcd for $C_{18}H_{36}N_2O_6Na$ 399.2471, found 399.2461.

(4*R*,5*R*)-4,5-Di(*N*-*tert*-butoxycarbonylamino)-1,8-octanediol 110a[164]

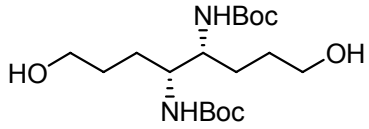

A 2-necked flask containing diBoc **109a** (200 mg, 0.36 mmol) and Pd/C (173 mg) in abs. EtOH (8.7 mL) was placed under vacuum. A balloon filled with H_2(g) was inserted and the reaction mixture was stirred at RT for 1.5 h. The mixture was filtered through Celite twice and the solvent was evaporated under reduced pressure to afford the (*R*,*R*)-diol **110a** (115 mg, 85%) as a white solid, m.p. 136-138 ^oC, which exhibited identical spectral properties to the (*S*,*S*)-**110b** enantiomer.

(4*S*,5*S*)-4,5-Di(*N*-*tert*-butoxycarbonylamino)-1,8-dimethanesulfonyloctane 119b[164]

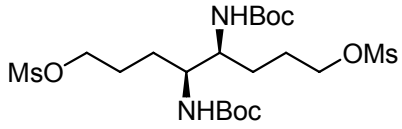

To a stirred solution of (*S*,*S*)-**110b** (53 mg, 0.14 mmol) and Et_3N (0.16 mL, 1.13 mmol) in DCM (2.5 mL) was added MsCl (0.043 mL, 0.56 mmol). The reaction mixture was diluted with DCM (20 mL) after 10 min, washed sequentially with sat.

† Experimental procedure for the synthesis of (*S*,*S*)-**157b** given in *Section 7.2.1*.

$NaHCO_3$ (2 x 30 mL), sat. NaCl (2 x 30 mL) and dried ($MgSO_4$). The solvent was removed under reduced pressure to afford the dimesylate (*S*,*S*)-**119b** (75 mg, 100%) as a viscous oil.‡ ^{1}H NMR (300 MHz) δ 1.41 (s, 18H, $C(CH_3)_3$), 1.45-1.65 (m, 4H, CH_2CHNH), 1.80-1.82 (m, 4H, $MsOCH_2CH_2$), 2.99 (s, 6H, SO_2CH_3), 3.56 (bs, 2H, CHNH), 4.22 (t, 4H, *J* = 5.8 Hz, $MsOCH_2$), 4.71 (bs, 2H, NH); ^{13}C NMR (75 MHz) δ 25.7 ($MsOCH_2CH_2$), 28.3 ($C(CH_3)_3$), 28.8 (CH_2CHNH), 37.2 (SO_2CH_3), 53.5 (CHNH), 69.6 ($MsOCH_2$), 79.5 ($C(CH_3)_3$), 158.3 (C=O); MS (ES, +ve) *m/z* 555 (100%, M+Na), 550 (30, M+NH_4); HRMS (ES, +ve) calcd for $C_{20}H_{40}N_2O_{10}Na$ 555.2022, found 555.2052.

(4*R*,5*R*)-4,5-Di(*N*-*tert*-butoxycarbonylamino)-1,8-dimethanesulfonyloctane 119a[164]

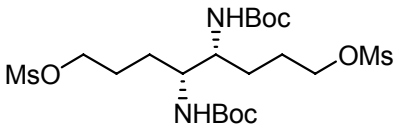

To a stirred solution of (*R*,*R*)-**110a** (115 mg, 0.31 mmol) and Et_3N (0.34 mL, 2.45 mmol) in DCM (6.2 mL) was added MsCl (0.15 mL, 1.53 mmol). The reaction was diluted with DCM (20 mL) after 20 min, washed sequentially with 5% $CuSO_4$ (2 x 20 mL), water (2 x 30 mL), sat. $NaHCO_3$ (2 x 30 mL) and sat. NaCl (2 x 30 mL) and dried ($MgSO_4$). The solvent was removed *in vacuo* to afford the dimesylate (*R*,*R*)-**119a** (140 mg, 86%) as a viscous oil, which had identical spectral properties to the (*S*,*S*)-**119b** enantiomer.

(2*S*,2'*S*)-*N*,*N*'-Di-*tert*-butoxycarbonyl-2,2'-bispyrrolidine 92b[160,164]

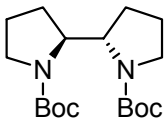

A stirred suspension of NaH (60% dispersion in oil, 41 mg, 1.012 mmol, washed with Et_2O (x 3)) in THF (1.5 mL) was placed in an ice bath. A solution of dimesylate (*S*,*S*)-**119b** (77 mg, 0.14 mmol) in THF (3 mL) was added dropwise. The ice bath was removed, and stirring was continued at RT for 3 h. The reaction was quenched with sat. ammonium chloride (5 mL) and the organic solvent was removed under reduced pressure. The mixture was partitioned between DCM and water, and the aqueous layer was extracted with DCM (3 x 40 mL). The combined organic layers were dried ($MgSO_4$) and concentrated *in vacuo*. The crude mixture was subjected to flash silica gel column chromatography (10% to 20% EtOAc:hexanes) to yield the chiral bispyrrolidine (*S*,*S*)-**92b** (37 mg, 76%) as a

‡ No physical or spectral data reported in reference 164.

colourless oil, which was spectroscopically identical to that reported in the literature.[160,164] $[\alpha]_D^{23}$ = -43.7° (*c* 0.198, $CHCl_3$). ^{1}H NMR (300 MHz) δ 1.44 (s, 9H, $C(CH_3)_3$), 1.47 (s, 9H, $C(CH_3)_3$), 1.55-1.63 (m, 2H, CHC<u>H</u>H), 1.83-1.86 (m, 6H, CHCH<u>H</u> and $CHCH_2C\underline{H}_2$), 3.30-3.54 (m, 4H, NCH_2), 3.80-3.90 (m, 2H, CH); ^{13}C NMR (75 MHz) δ 22.4, 22.8, 23.3 ($CHCH_2\underline{C}H_2$), 28.4 ($C(\underline{C}H_3)_3$), 28.9, 29.2 ($CH\underline{C}H_2$), 46.4, 46.5, 47.0 (NCH_2), 58.7, 59.0, 59.4, 59.6 (CH), 78.4, 78.8, 79.2 ($\underline{C}(CH_3)_3$), 154.8 (C=O); MS (EI, +ve) *m/z* 340 (3, M^+), 240 (4), 170 (8), 114 (100%); HRMS (EI, +ve) calcd for $C_{18}H_{32}N_2O_4$ 340.2362, found 340.2356.

(2*R*,2'*R*)-*N*,*N*'-Di-*tert*-butoxycarbonyl-2,2'-bispyrrolidine 92a[160,164]

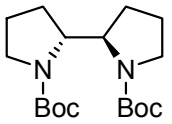

A stirred suspension of NaH (60% dispersion in oil, 87 mg, 2.15 mmol, washed with Et_2O (x 3)) in DMF (3.2 mL) was placed in an ice bath. A solution of dimesylate (*R*,*R*)-**119a** (115 mg, 0.31 mmol) in DMF (6.6 mL) was added dropwise. The ice bath was removed, and stirring was continued at RT for 2 h. The reaction was quenched with sat. NH_4Cl (5 mL) and reaction mixture was extracted with DCM (3 x 40 mL). The combined organic layers were dried ($MgSO_4$) and concentrated *in vacuo*. The crude mixture was subjected to flash silica gel column chromatography (5% to 20% EtOAc:hexanes) to yield the chiral bispyrrolidine (*R*,*R*)-**92a** (55 mg, 62%) as a colourless oil, which was spectroscopically identical to the (*S*,*S*) enantiomer **92b**. $[\alpha]_D^{23}$ = +45.9° (*c* 0.155, $CHCl_3$).

7.2.1 Bispyrrolidine synthesis using the PMB protecting group

5-(4-Methoxybenzyloxy)-1-pentene 149[227-229]

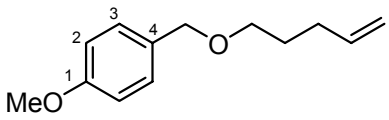

4-Methoxybenzyl alcohol (4.30 mL, 34.8 mmol) was dissolved in HBr (10 mL, 45% solution in glacial acetic acid) and stirred for 20 min at RT. The mixture was diluted with Et_2O (50 mL) and the organic layer was washed with sat. $NaHCO_3$ (3 x 60 mL) and water (50 mL). The organic layer was dried ($MgSO_4$), filtered and concentrated *in vacuo* to yield the crude 4-methoxybenzyl bromide. A suspension of washed NaH (1.022 g, 25.5 mmol) in dry THF (20 mL) was cooled to 0 °C and treated with 4-penten-1-ol (2.40 mL, 23.2 mmol). After stirring for 20 min at 0 °C, the crude 4-methoxybenzyl bromide was slowly added as a solution in THF (10 mL), and the

mixture was allowed to warm to RT. The reaction mixture was quenched after 20 h with glacial acetic acid (10 mL), followed by water (150 mL). The aqueous layer was extracted with EtOAc (3 x 80 mL). The combined organic layers were washed with sat. $NaHCO_3$ (5 x 50 mL), water (1 x 50 mL), then dried ($MgSO_4$). The crude oil was subjected to flash silica gel column chromatography (hexanes to 2% EtOAc:hexanes) to yield the protected alkene **149** (3.473 g, 73%) as a colourless oil.‡ ^{1}H NMR (300 MHz) δ 1.69 (tt, 2H, *J* = 5.9, 6.5, 6.9, 7.9 Hz, $OCH_2C\underline{H}_2$), 2.12 (dt, 2H, *J* = 6.7, 7.8 Hz, $C\underline{H}_2CH{=}CH_2$), 3.45 (t, 2H, *J* = 6.5 Hz, $OC\underline{H}_2CH_2$), 3.79 (s, 3H, OCH_3), 4.42 (s, 2H, $PhCH_2$), 4.95 (dddd, 1H, $^4J_{HH}$ = 0.4 Hz, $^4J_{HH}$ = 1.3 Hz, $^3J_{HH}$ = 10.2 Hz, $^2J_{HH}$ = 3.3 Hz, CH=C$\underline{H}$H), 5.01 (dddd, 1H, $^4J_{HH}$ = 0.5 Hz, $^4J_{HH}$ = 1.6 Hz, $^3J_{HH}$ = 17.6 Hz, $^2J_{HH}$ = 3.4 Hz, CH=CH$\underline{H}$), 5.81 (ddt, 1H, $^3J_{HH}$ = 6.6, 10.2, 16.9 Hz, C$\underline{H}$=CH_2), 6.87 (d, 2H, *J* = 8.7 Hz, ArH2), 7.27 (d, 2H, *J* = 8.8 Hz, ArH3); ^{13}C NMR (75 MHz) δ 28.9 ($OCH_2\underline{C}H_2$), 30.3 ($\underline{C}H_2CH{=}CH_2$), 55.2 ($OCH_3$), 69.4 ($O\underline{C}H_2CH_2$), 72.5 ($PhCH_2$), 113.7 (ArC2), 114.6 (CH=$\underline{C}H_2$), 129.2 (ArC3), 130.6 (ArC4), 138.3 ($\underline{C}H{=}CH_2$), 159.0 (ArC1); FTIR *v* 1613 (w), 1513 (s), 1464 (w), 1363 (w), 1247 (s), 1173 (w), 1099 (s), 1037 (s), 913 (w), 820 (m).

_E_-1,8-Di(4-methoxybenzyloxy)-4-octene 150

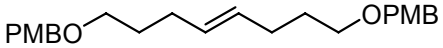

Grubbs 1 catalyst (141 mg, 0.17 mmol, 2.5 mol %) was added to a solution of alkene **149** (1.413g, 6.87 mmol) in DCM (25 mL) and the solution was heated at reflux for 20 h. The reaction mixture was washed with water (2 x 25 mL), and the solvent was evaporated *in vacuo*. The crude oil was subjected to flash silica gel column chromatography (4% to 50% EtOAc:hexanes) to yield the octene **150** (1.132g, 86%, *E*:*Z* 3.5:1) as a colourless oil. ^{1}H NMR (500 MHz) δ 1.59-1.68 (m, 4H, $OCH_2C\underline{H}_2$), 2.03-2.07 (m, 4H, CH=CHC$\underline{H}_2$), 2.09-2.15*, 3.42 (t, 4H, J = 6.5 Hz, $OC\underline{H}_2CH_2$), 3.79 (s, 6H, OCH_3), 4.41 (s, 4H, $PhCH_2$), 5.38-5.40 (m, 2H, C$\underline{H}$=C$\underline{H}$), 6.87 (d, 4H, *J* = 8.6 Hz, ArH2), 7.25 (d, 4H, *J* = 8.5 Hz, ArH3); ^{13}C NMR (75 MHz) δ 23.8*, 29.1 (CH=CH$\underline{C}H_2$), 29.5 ($OCH_2\underline{C}H_2$), 29.7*, 55.2 (OCH_3), 69.4 ($O\underline{C}H_2CH_2$), 69.5*, 72.46 ($PhCH_2$), 72.50*, 113.7 (ArC2), 129.2 (ArC3), 129.6*, 130.0 ($\underline{C}H{=}\underline{C}H$), 130.7 (ArC4), 159.0 (ArC1); MS (ES, +ve) *m/z*

‡ No physical or spectral data reported in references 227-229.

407 (20, M+Na), 402 (100%, M+NH_4); HRMS (ES, +ve) calcd for $C_{24}H_{32}O_4Na$ 407.2198, found 407.2259.

(4*R*,5*R*)-1,8-Di(4-methoxybenzyloxy)-4,5-octanediol 153b

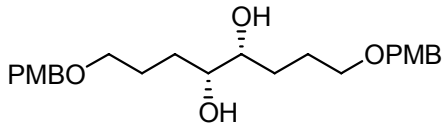

The diol (*R*,*R*)-**153b** was synthesised by *General Procedure A* using alkene **150** (960 mg, 2.5 mmol, *E*:*Z* 4:1), AD mix β (3.482 g), methanesulfonamide (237 mg, 2.5 mmol), sodium sulfite (3.731 g), *t*BuOH (12.5 mL) and water (12.5 mL). The crude solid was subjected to flash silica gel column chromatography (50% EtOAc:hexanes to 100% EtOAc) to give the diol (*R*,*R*)-**153b** (971 mg, 93%) as a white solid as a mixture of chiral:*meso* diastereomers (2.9:1), m.p. 58-70 ^oC. HPLC analysis (20% to 60% 2-propanol:hexane, retention times (*R*,*R*)-diol **153b** 24.2 min (major), (*S*,*S*)-diol **153a** 28.1 min (minor)) showed the *ee* of the (*R*,*R*)-diol **153b** was 70%. ^1H NMR (500 MHz) δ 1.45-1.53 (m, 2H, C<u>H</u>HCHOH), 1.63-1.68 (m, 2H, CH<u>H</u>CHOH), 1.72-1.78 (m, 4H, C<u>H</u>$_2$CH$_2$CHOH), 3.04*, 3.10 (bs, 2H, OH), 3.39 (d, 2H, *J* = 5.8 Hz, C<u>H</u>OH), 3.49 (t, 4H, *J* = 5.9 Hz, OC<u>H</u>$_2$CH$_2$), 3.80 (s, 6H, OCH_3), 4.44 (s, 4H, $PhCH_2$), 6.87 (d, 4H, *J* = 8.5 Hz, ArH2), 7.25 (d, 4H, *J* = 8.5 Hz, ArH3); ^{13}C NMR (125 MHz) δ 26.1 (<u>C</u>H$_2$CH$_2$CHOH), 26.5*, 29.0*, 30.9 (<u>C</u>H$_2$CHOH), 55.2 (OCH_3), 70.2 (O<u>C</u>H$_2$CH$_2$), 70.3*, 72.7 ($PhCH_2$), 74.2 (<u>C</u>HOH), 74.3*, 113.8 (ArC2), 129.3 (ArC3), 130.2 (ArC4), 159.2 (ArC1); FTIR *v* 1607 (w), 1512 (w), 1246 (w), 1172 (w), 1099 (w), 1034 (w), 811 (w), 681 (w), 649 (w), 645 (w); MS (ES, +ve) *m/z* 441 (40, M+Na), 419 (100%, M+H); HRMS (ES, +ve) calcd for $C_{24}H_{35}O_6$ 419.2434, found 419.2432.

(4*S*,5*S*)-1,8-Di(4-methoxybenzyloxy)-4,5-octanediol 153a

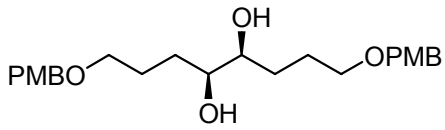

The diol (*S*,*S*)-**153a** was synthesised by *General Procedure A* using alkene **150** (1.104 g, 2.87 mmol, *E*:*Z* 3.4:1), AD mix α (4.02 g), methanesulfonamide (273 mg, 2.87 mmol), sodium sulfite (4.30 g), *t*BuOH (14.5 mL) and water (14.5 mL). The crude solid was subjected to column chromatography to yield the diol **153a** (1.078 g, 90%) as a white powder, as a 3.7:1 mixture of chiral:*meso* diastereomers, which exhibited identical spectral properties to the (*R*,*R*)-diol. HPLC analysis (20% to 60% 2-propanol:hexane, retention times (*R*,*R*)-diol **153b** 24.3 min

(minor), (*S*,*S*)-diol **153a** 28.1 min (major)) showed the *ee* of the (*S*,*S*)-diol **153a** was 92%.

(4*R*,5*R*)-1,8-Di(4-methoxybenzyloxy)-4,5-dimethanesulfonyloctane 154b

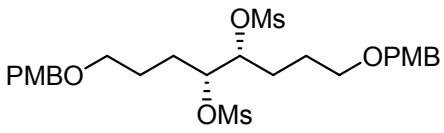

A solution of diol (*R*,*R*)-**153b** (320 mg, 0.77 mmol, chiral:*meso* 5.7:1) in DCM (15 mL) was treated with Et_3N (0.85 mL, 6.12 mmol) and was stirred on an ice bath. MsCl (0.37 mL, 3.83 mmol) was added neat and the mixture was stirred at RT for 20 min. The reaction was diluted with DCM (40 mL), washed sequentially with 5% $CuSO_4$ (3 x 30 mL), sat. $NaHCO_3$ (2 x 50 mL) and sat. NaCl (2 x 50 mL). The organic layer was dried ($MgSO_4$) and concentrated *in vacuo*. The crude oil was subjected to flash silica gel column chromatography (40% to 50% EtOAc:hexanes) to yield the dimesylate (*R*,*R*)-**154b** (440 mg, 95%) as a colourless oil, as a mixture of chiral:*meso* diastereomers (5:1), which solidified upon standing. ^{1}H NMR (500 MHz) δ 1.69-1.74 (m, 4H, $OCH_2C\underline{H}_2$), 1.75-1.83 (m, 2H, MsOCHC$\underline{H}$H), 1.90-1.97 (m, 2H, MsOCHCH$\underline{H}$), 3.02 (s, 6H, SO_2CH_3), 3.47-3.48 (m, 4H, $OC\underline{H}_2CH_2$), 3.79 (s, 6H, OCH_3), 4.40 (s, 4H, $PhCH_2$), 4.84-4.87 (m, 2H, MsOC$\underline{H}$), 6.86 (d, 4H, *J* = 8.6 Hz, ArH2), 7.24 (d, 4H, *J* = 8.5 Hz, ArH3); ^{13}C NMR (125 MHz) δ 24.8 ($OCH_2\underline{C}H_2$), 25.5*, 26.7*, 27.5 (MsOCH$\underline{C}H_2$), 38.7 (SO_2CH_3), 55.2 (OCH_3), 68.9*, 69.0 (O-$\underline{C}H_2CH_2$), 72.6 ($PhCH_2$), 72.7*, 80.7 (MsO$\underline{C}$H), 82.6*, 113.7 (ArC3), 113.8*, 129.3 (ArC2), 130.3 (ArC4), 159.1 (ArC1); MS (ES, +ve) *m/z* 597 (100%, M+Na), 592 ($M+NH_4$); HRMS (ES, +ve) calcd for $C_{26}H_{38}O_{10}S_2Na$ 597.1804, found 597.1813.

(4*S*,5*S*)-1,8-Di(4-methoxybenzyloxy)-4,5-dimethanesulfonyloctane 154a

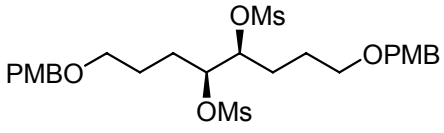

A solution of diol (*S*,*S*)-**153a** (430 mg, 1.03 mmol, chiral:*meso* 4:1) in DCM (20 mL) was treated with Et_3N (1.15 mL, 8.23 mmol) and was stirred on an ice bath. MsCl (0.50 mL, 5.12 mmol) was added neat and the mixture was stirred at RT for 25 min. The reaction was diluted with DCM (50 mL), washed sequentially with 5% $CuSO_4$ (2 x 50 mL), sat. $NaHCO_3$ (2 x 50 mL) and sat. NaCl (2 x 50 mL). The organic layer was dried ($MgSO_4$) and concentrated *in vacuo*. The crude oil was subjected to flash silica gel column chromatography (40% EtOAc:hexanes) to yield the dimesylate

(*S*,*S*)-**154b** (582 mg, 99%) as a colourless oil, as a mixture of chiral:*meso* diastereomers (3.3:1), which solidified upon standing and was spectroscopically identical to the (*R*,*R*)-diol.

(4*S*,5*S*)-1,8-Di(4-methoxybenzyloxy)-4,5-diazidooctane 155b

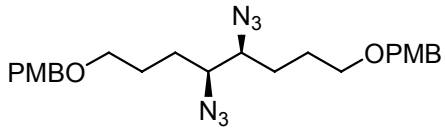

A stirred solution of dimesylate (*R*,*R*)-**154b** (397 mg, 0.691 mmol, chiral:*meso* 5:1) in DMF (4.7 mL) was heated to 80 ^{o}C. Sodium azide (270 mg, 4.15 mmol) was added, and stirring was continued at 80 ^{o}C for 18 h. The reaction mixture was poured into sat. NaCl, and extracted with EtOAc (3 x 50 mL). The organic layers were combined, washed with water (8 x 50 mL), dried ($MgSO_4$) and concentrated under reduced pressure. Flash silica gel column chromatography (20% EtOAc:hexanes) afforded diazido (*S*,*S*)-**155b** (179 mg) as a colourless oil, as a mixture of chiral:*meso* diastereomers (4.9:1). Further elution afforded the chiral diastereomer (68 mg), to give a total overall yield of 76%. ^{1}H NMR (500 MHz) δ 1.71-1.73 (m, 8H, $OCH_2C\underline{H}_2CH_2$ and $OCH_2CH_2C\underline{H}_2$), 3.29 (bs, 2H, CHN_3), 3.46-3.48 (m, 4H, $OC\underline{H}_2CH_2$), 3.79 (s, 6H, OCH_3), 4.43 (s, 4H, $PhCH_2$), 6.87 (dd, 4H, *J* = 8.5, 1.7 Hz, ArH2), 7.25 (dd, 4H, *J* = 8.5, 1.6 Hz, ArH3); ^{13}C NMR (125 MHz) δ 26.3 ($OCH_2\underline{C}H_2$), 28.3 ($OCH_2CH_2\underline{C}H_2$), 55.2 ($OCH_3$), 65.0 ($\underline{C}HN_3$), 69.1 ($O\underline{C}H_2CH_2$), 72.6 ($PhCH_2$), 113.7 (ArC3), 129.3 (ArC2), 130.3 (ArC4), 159.1 (ArC1); MS (ES, +ve) *m/z* 491 (70, M+Na), 486 (100%, $M+NH_4$); HRMS (ES, +ve) calcd for $C_{24}H_{32}N_6O_4Na$ 491.2383, found 491.2393.

(4*R*,5*R*)-1,8-Di(4-methoxybenzyloxy)-4,5-diazidooctane 155a

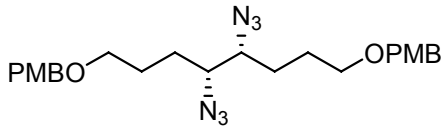

A stirred solution of dimesylate (*S*,*S*)-**154a** (566 mg, 0.986 mmol, chiral:*meso* 3.3:1) in DMF (6.8 mL) was heated to 60 ^{o}C. Solid sodium azide (384 mg, 5.91 mmol) was added, and the reaction was stirred at 80 ^{o}C for 23 h. The reaction mixture was poured into sat. NaCl and extracted with EtOAc (4 x 50 mL). The organic layers were combined and washed with water (6 x 30 mL), dried ($MgSO_4$) and concentrated under reduced pressure. The crude oil was subjected to flash silica gel column chromatography (20% to 30% EtOAc:hexanes) to give the diazido (*R*,*R*)-**155a**

(336 mg, 73%) as a mixture of chiral:*meso* diastereomers (3.2:1), which had identical spectral properties to (*S*,*S*)-**155b**.

(4*S*,5*S*)-3,4-Diamino-1,8-di(4-methoxybenzyloxy)octane 156b

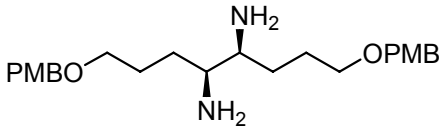

To a solution of (*S*,*S*)-**155b** (170 mg, 0.363 mmol, chiral:*meso* 4.9:1) in abs. EtOH (4 mL) was added Pd/C (38 mg, 0.018 mmol). The reaction vessel was placed under vacuum, and a balloon filled with H_2(g) was inserted. The reaction mixture was stirred for 3.5 h, then filtered through Celite. The solvent was removed *in vacuo* to yield the diamine **156b** (151 mg, 100%) as a white solid. ^{1}H NMR (300 MHz, $CO(CD_3)_2$) δ 1.27-1.75 (m, 8H, C$\underline{H}_2$CH$_2$CHNH$_2$ and C$\underline{H}_2$CHNH$_2$), 2.70 (bs, 6H, C$\underline{H}$NH$_2$ and NH$_2$), 3.45 (t, 4H, *J* = 5.9 Hz, OC$\underline{H}_2$CH$_2$), 3.77 (s, 6H, OCH$_3$), 4.40 (s, 4H, PhCH$_2$), 6.89 (d, 4H, *J* = 8.6 Hz, ArH2), 7.26 (d, 4H, *J* = 8.4 Hz, ArH3); ^{13}C NMR (75 MHz, $CO(CD_3)_2$) δ 28.1 (C$\underline{H}_2$CH$_2$CHNH$_2$), 31.6 (C$\underline{H}_2$CHNH$_2$), 54.8 (OCH$_3$), 65.0 (C$\underline{H}$NH$_2$), 70.0 (OC$\underline{H}_2$), 72.2 (PhCH$_2$), 113.8 (ArC2), 129.3 (ArC3), 131.4 (ArC4), 159.4 (ArC1); MS (ES, +ve) *m/z* 417 (100%, M+H); HRMS (ES, +ve) calcd for $C_{24}H_{37}N_2O_4$ 417.2753, found 417.2759.

(4*R*,5*R*)-3,4-Diamino-1,8-di(4-methoxybenzyloxy)octane 156a

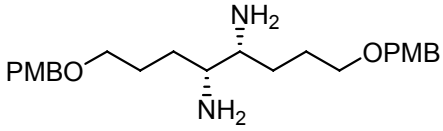

To a solution of (*R*,*R*)-**155a** (973 mg, 2.08 mmol, chiral:*meso* 3.9:1) in abs. EtOH (25 mL) was added Pd/C (50 mg, 0.52 mmol). The reaction vessel was placed under vacuum and a balloon filled with H_2(g) was inserted. The reaction mixture was stirred at RT for 6 h, filtered through Celite and concentrated under reduced pressure, to yield the diamine (*R*,*R*)-**156a** (861 mg, 100%) as a white solid which had identical spectral properties to the (*S*,*S*)-diamine.

(4*S*,5*S*)-1,8-Di(4-methoxybenzyloxy)-4,5-di(*N*-*tert*-butoxycarbonylamino)octane 157b

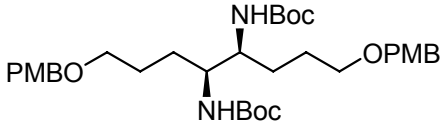

To a stirred solution of diamine (*S*,*S*)-**156b** (192 mg, 0.46 mmol) and Et_3N (0.26 mL, 1.84 mmol) in

THF (10 mL) was added di-*tert*-butyldicarbonate (604 mg, 2.77 mmol). The reaction mixture was heated at 35 ^{o}C for 15 h. The solvent was removed under reduced pressure and the crude mixture was subjected to flash silica gel column chromatography (10% to 30% EtOAc:hexanes) to yield the Boc-protected diamine (*S*,*S*)-**157b** (213 mg, 75%) as a viscous oil. ^{1}H NMR (300 MHz) δ 1.48 (s, 18H, C(CH$_3$)$_3$), 1.35-1.49 (m, 2H, CHHCHNH), 1.60-1.71 (m, 6H, CH$_2$CH$_2$CHNH and CHHCHNH), 3.41-3.47 (m, 4H, OCH$_2$CH$_2$), 3.48-3.53 (m, 2H, CHNH), 3.79 (s, 6H, OCH$_3$), 4.41 (s, 4H, PhCH$_2$), 4.61 (d, 2H, *J* = 7.7 Hz, NH), 6.86 (d, 4H, *J* = 8.5 Hz, ArH2), 7.24 (d, 4H, *J* = 8.5 Hz, ArH3); ^{13}C NMR (75 MHz) δ 26.2 (CH$_2$CHNH), 28.4 (C(CH$_3$)$_3$), 29.6 (OCH$_2$CH$_2$), 54.3 (CHNH), 55.2 (OCH$_3$), 69.6 (OCH$_2$CH$_2$), 72.5 (PhCH$_2$), 79.1 (C(CH$_3$)$_3$), 113.7 (ArC3), 129.2 (ArC2), 130.6 (ArC4), 156.4 (C=O), 159.1 (ArC1); FTIR *v* 2920 (br), 1693 (m), 1513 (m), 1367 (w), 1247 (m), 1217 (w), 1171 (m), 1097 (w), 752 (s); MS (ES, +ve) *m/z* 639 (100%, M+Na), 634 (30, M+NH$_4$), 617 (15, M+H); HRMS (ES, +ve) calcd for $C_{34}H_{53}N_2O_8$ 617.3802, found 617.3826.

(4*R*,5*R*)-1,8-Di(4-methoxybenzyloxy)-4,5-di(*N*-*tert*-butoxycarbonylamino)octane 157a and

***meso*-1,8-di(4-methoxybenzyloxy)-4,5-di(*N*-*tert*-butoxycarbonylamino)octane 157**

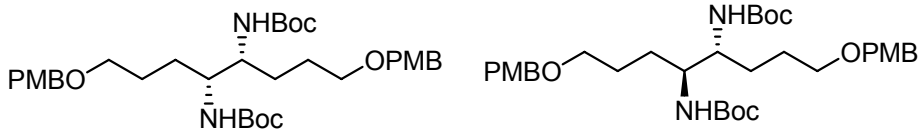

To a stirred solution of diamine (*R*,*R*)-**156a** (865 mg, 2.08 mmol, chiral:*meso* 3.9:1) and Et$_3$N (1.2 mL, 8.31 mmol) in THF (40 mL) was added di-*tert*-butyldicarbonate (2.710 g, 12.5 mmol). The reaction mixture was heated at 35 ^{o}C for 17 h. The solvent was removed *in vacuo* and the crude mixture was subjected to flash silica gel column chromatography (10% to 50% EtOAc:hexanes) to yield the Boc-protected diamine as a colourless, viscous oil, as a mixture of chiral:*meso* diastereomers. The mixture was recrystallised (DCM/hexanes) to yield the diastereomer *meso*-**157** (92 mg, 7%) as a white solid, m.p. 124-125 ^{o}C. ^{1}H NMR δ ^{1}H NMR (500 MHz) δ 1.30 (bs, 2H, CHHCHNH), 1.43 (s, 18H, C(CH$_3$)$_3$), 1.60-1.70 (m, 6H, CH$_2$CH$_2$CHNH and CHHCHNH), 3.43-3.45 (m, 4H, OCH$_2$CH$_2$), 3.60-3.65 (m, 2H, CHNH), 3.79 (s, 6H, OCH$_3$), 4.41 (s, 4H, PhCH$_2$), 4.63 (d, 2H, *J* = 6.7 Hz, NH), 6.87 (d, 4H, *J* = 8.6 Hz,

ArH2), 7.24 (d, 4H, *J* = 8.5 Hz, ArH3); ^{13}C NMR (125 MHz) δ 26.4 ($OCH_2\underline{C}H_2$), 28.2 ($\underline{C}H_2CHNH$), 28.4 ($C(\underline{C}H_3)_3$), 54.3 (CHNH), 55.2 (OCH_3), 69.6 ($O\underline{C}H_2CH_2$), 72.5 ($PhCH_2$), 79.2 ($\underline{C}(CH_3)_3$), 113.7 (ArC3), 129.2 (ArC2), 130.6 (ArC4), 156.0 (C=O), 159.1 (ArC1); MS (ES, +ve) *m/z* 639 (100%, M+Na), 617 (90, M+H), 603 (35), 517 (10); HRMS (ES, +ve) calcd for $C_{34}H_{53}N_2O_8$ 617.3802, found 617.3082.

The filtrate was concentrated under reduced pressure and subjected to flash silica gel column chromatography (10% to 50% EtOAc:hexanes) to afford the chiral (*R*,*R*)-**157a** (512 mg, 40%) as a colourless, viscous oil, which had identical spectral properties to the (*S*,*S*)-**157b** enantiomer.

(4*R*,5*R*)-4,5-Di(3-(4-methoxybenzyloxy)-propyl)[1,3,2]dioxathiolane-2-dioxide 159b and *meso*-4,5-Di(3-(4-methoxybenzyloxy)propyl)[1,3,2]dioxathiolane-2-dioxide 159

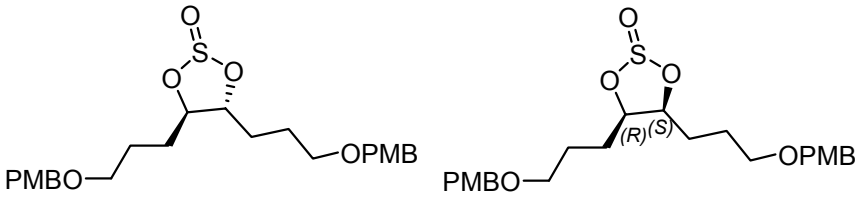

To a solution of diol (*R*,*R*)-**153b** (79 mg, 0.189 mmol) and Et_3N (61 μL, 0.434 mmol) at 0 ^oC was added $SOCl_2$ (17.2 μL, 0.233 mmol). The reaction was stirred for 30 min at 0 ^oC and quenched with water (8 mL). The reaction mixture was extracted with DCM (4 x 20 mL), and the combined organic layers were dried ($MgSO_4$). The crude oil was subjected to flash silica gel column chromatography (hexanes to 20% EtOAc:hexanes) to afford the cyclic sulfite (*R*,*R*)-**159** (19 mg, 22%) as a colourless oil. HPLC analysis (20% to 60% 2-propanol:hexane, retention times sulfite (*R*,*R*)-**159b** 26.7 min (major), (*S*,*S*)-**159a** 39.5 min (minor)) showed the *ee* of the (*R*,*R*)-sulfite **159b** was 75%. ^{1}H NMR (300 MHz) δ 1.67-1.95 (m, 8H, 2 x $C\underline{H}_2CHOS$ and 2 x $C\underline{H}_2CH_2CHOS$), 3.42-3.56 (m, 4H, 2 x $OC\underline{H}_2CH_2$), 3.80 (s, 6H, 2 x OCH_3), 4.07 (ddd, 1H, *J* = 3.7, 7.9, 7.6 Hz, $C\underline{H}OS$), 4.425 (s, 2H, $PhCH_2$), 4.430 (s, 2H, $PhCH_2$), 4.60 (ddd, 1H, *J* = 2.7, 8.2, 8.0 Hz, $C\underline{H}OS$), 6.88 (d, 4H, *J* = 8.7 Hz, ArH2), 7.25 (d, 4H, *J* = 8.6 Hz, ArH3); ^{13}C NMR (75 MHz) δ 26.0 and 26.1 (2 x $\underline{C}H_2CHOS$), 28.5 and 30.5 (2 x $\underline{C}H_2CH_2CHOS$), 55.3 (OCH_3), 68.9 and 69.0 (2 x $O\underline{C}H_2CH_2$), 72.6 ($PhCH_2$), 83.2 and 87.7 (2 x $\underline{C}HOS$),

113.8 (ArC2), 129.3 (ArC3), 130.4 (ArC4), 159.2 (ArC1); MS (ES, +ve) *m/z* 487 (20, M+Na), 482 (100%, M+NH_4); HRMS (ES, +ve) calcd for $C_{24}H_{36}O_7SN$ 482.2212, found 482.2225.

Further elution gave the title compound as a mixture of chiral:*meso* diastereomers (31 mg, 35%). Further elution gave *meso*-**159** (11 mg, 13%) as a colourless oil. ^{1}H NMR (300 MHz) δ 1.62-1.93 (m, 8H, C$\underline{H}_2$CHOS and C$\underline{H}_2$CH_2CHOS), 3.42-3.54 (m, 4H, OC$\underline{H}_2$CH_2), 3.80 (s, 6H, OCH_3), 4.43 (s, 4H, PhCH_2), 4.81-4.88 (m, 2H, C$\underline{H}$OS), 6.88 (d, 4H, *J* = 8.7 Hz, ArH2), 7.25 (d, 4H, *J* = 8.6 Hz, ArH3); ^{13}C NMR (75 MHz) δ 25.4 (C$\underline{H}_2$CHOS), 28.9 (C$\underline{H}_2$CH_2CHOS), 55.2 (OCH_3), 68.4 (OC$\underline{H}_2$CH_2), 72.7 (PhCH_2), 87.3 (C$\underline{H}$OS), 113.8 (ArC2), 129.3 (ArC3), 130.1 (ArC4), 159.2 (ArC1); MS (ES, +ve) *m/z* 487 (100%, M+Na), 482 (20, M+NH_4); HRMS (ES, +ve) calcd for $C_{24}H_{32}O_7SNa$ 487.1766, found 482.1774.

(4*R*,5*R*)-4,5-Di(3-(4-methoxybenzyloxy)propyl)[1,3,2]dioxathiolane-2,2-dioxide 158b

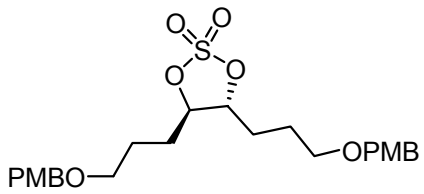

To a stirred solution of (*R*,*R*)-**159b** (30 mg, 0.065 mmol) in CCl_4 (0.5 mL), CH_3CN (0.5 mL) and water (0.75 mL) was added $RuCl_3.3H_2O$ (1.5 mg, 2.7 μmol) and $NaIO_4$ (44 mg, 0.21 mmol). After stirring for 2.5 h, the reaction was diluted with Et_2O (20 mL) and water (20 mL). The organic layer was washed sequentially with sat. $NaHCO_3$ (3 x 20 mL) and sat. NaCl (3 x 20 mL), dried ($MgSO_4$) and concentrated under reduced pressure. The crude oil was subjected to flash silica gel column chromatography (20% EtOAc:hexanes) to give the cyclic sulfate (*R*,*R*)-**158b** (1 mg, 3%) as a colourless oil. ^{1}H NMR (300 MHz) δ 1.64-2.02 (m, 8H, C$\underline{H}_2$CHOS and C$\underline{H}_2$CH_2CHOS), 3.38-3.54 (m, 4H, OC$\underline{H}_2$CH_2), 3.80 (s, 6H, OCH_3), 4.42 (s, 4H, PhCH_2), 4.57-4.59 (m, 2H, C$\underline{H}$OS), 6.88 (d, 4H, *J* = 8.3 Hz, ArH2), 7.23 (d, 4H, *J* = 8.3 Hz, ArH3); ^{13}C NMR (75 MHz) δ 25.4 (C$\underline{H}_2$CHOS), 29.0 (C$\underline{H}_2$CH_2CHOS), 55.3 (OCH_3), 68.4 (OC$\underline{H}_2$CH_2), 72.7 (PhCH_2), 87.3 (C$\underline{H}$OS), 113.8 (ArC2), 129.3 (ArC3), 130.1 (ArC4), 159.2 (ArC1); MS (ES, +ve) *m/z* 503 (100%, M+Na).

(2*S*,2'*S*)-*N*,*N*'-Dibenzyl-2,2'-bispyrrolidine 160b

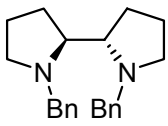

To a stirred solution of (*S*,*S*)-**92b** (30 mg, 0.089 mmol) in DCM (0.5 mL) at 0 °C was added dropwise TFA (0.06 mL, 0.78 mmol). The reaction was stirred at RT for 12 h, diluted with DCM (20 mL), basified (2M NaOH) and extracted with DCM (3 x 20 mL). The combined organic layers were dried ($MgSO_4$) and concentrated *in vacuo*. The crude bispyrrolidine was redissolved in DCM (1 mL), and Et_3N (0.05 mL, 0.35 mmol) and benzyl bromide (0.03 mL, 0.22 mmol) were added. The reaction mixture was stirred for 15 h, quenched with water, extracted with DCM (3 x 15 mL) and concentrated to give the dibenzyl bispyrrolidine **160b** (8 mg, 28%) as a colourless oil. ^{1}H NMR (500 MHz) δ 1.86-1.90 (m, 4H, $NCH_2C\underline{H}_2$), 2.10-2.18 (m, 4H, $NCHC\underline{H}_2$), 2.68-2.72 (m, 2H, $NC\underline{H}H$), 3.29-3.33 (m, 2H, $NCH\underline{H}$), 3.35-3.38 (m, 2H, $NC\underline{H}$), 3.98 (d, 2H, J = 13.5 Hz, $PhC\underline{H}H$), 4.26 (d, 2H, J = 13.0 Hz, $PhCH\underline{H}$), 7.34-7.46 (m, 10H, ArH); MS (ES, +ve) *m/z* 321 (100%, M+H), 317 (30); HRMS (ES, +ve) calcd for $C_{22}H_{29}N_2$ 321.2331, found 321.2310.

7.3 Attempted bisindoline synthesis

2-Allyl-1-benzyloxybenzene 164[190]

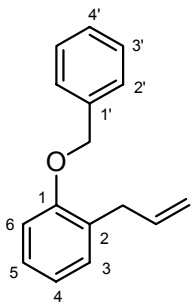

2-Allylphenol (1.74 mL, 13.41 mmol) was added dropwise to a stirred suspension of NaH (645 mg, 60% dispersion in oil, 16.11 mmol) in THF (45 mL) at 0 °C. Benzyl bromide (1.59 mL, 13.41 mmol) was added after 1 h, the reaction was allowed to warm to RT and stirring was continued for 20 h. The reaction was quenched with isopropyl alcohol and water, and extracted with EtOAc (3 x 50 mL). The combined organic layers were washed with NaOH (2M) and water then dried ($MgSO_4$). The crude oil was subjected to gravity silica gel column chromatography (1% EtOAc:hexanes) to afford the protected phenol **164** (2.85 mg, 95%) as a volatile, colourless oil.‡ ^{1}H NMR (300 MHz) δ 3.45 (d, 2H, $^3J_{HH}$ = 6.6 Hz, $C\underline{H}_2CH=CH_2$), 5.02-5.09 (m, 2H, $CH=C\underline{H}_2$), 5.07 (s, 2H, $PhCH_2$), 6.02 (ddt, 1H, $^3J_{HH}$ = 6.7 Hz, $^3J_{HH}$ = 10.1 Hz, $^3J_{HH}$ = 16.8 Hz, $C\underline{H}=CH_2$), 6.89-6.94 (m, 2H, ArH4 and ArH6), 7.14-7.21 (m, 2H, ArH3 and ArH5), 7.28-7.44 (m, 5H, 5 x ArH'); ^{13}C NMR (75 MHz) δ 34.4

‡ No physical or spectral data reported in reference 190.

(CH_2CH=CH_2), 69.9 (PhCH_2), 111.7 (ArC6), 115.4 (CH=CH_2), 120.8 (ArC4), 127.1 (ArC2'), 127.3 (ArC5), 127.7 (ArC4'), 128.5 (ArC3'), 129.0 (ArC2), 129.9 (ArC3), 137.0 (CH=CH_2), 137.4 (ArC1'), 156.3 (ArC1); FTIR *v* 1600 (w), 1492 (m), 1452 (m), 1240 (s), 1126 (w), 1024 (w), 913 (w), 750 (s), 735 (s); MS (CI, +ve) *m/z* 225 (100%, M+H), 147 (33), 131 (43); HRMS (EI, +ve) calcd for $C_{16}H_{16}O$ 224.1201, found 224.1192.

_E_-1,4-Di(2-benzyloxy)phenyl-2-butene 165

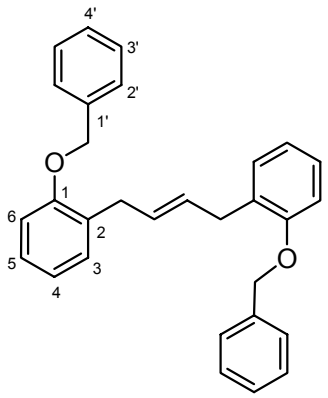

Grubbs 1 catalyst (195 mg, 0.237 mmol, 6.7 mol %) was added to a solution of alkene **164** (820 mg, 3.68 mmol) in DCM (20 mL) and the solution was heated at reflux for 4.5 h. The reaction mixture was concentrated *in vacuo* and subjected to gravity silica column chromatography (1% EtOAc:hexanes) yielding the dimer **165** (629 mg, 81%, *E*:*Z* 5.2:1) as a white solid, m.p. 68-70 ^{o}C. ^{1}H NMR (300 MHz) δ 3.42 (d, 4H, *J* = 4.9 Hz, CH_2), 3.54* (d, *J* = 5.1 Hz), 5.05 (s, 4H, PhCH_2), 5.07*, 5.68-5.70 (m, 2H, CH=CH), 6.86-6.91 (m, 4H, ArH4 and ArH6), 7.12-7.17 (m, 4H, ArH3 and ArH5), 7.28-7.43 (m, 10H, 10 x ArH'); ^{13}C NMR (75 MHz) δ 27.9*, 33.1 (CH_2), 67.9 (PhCH_2), 111.7 (ArC6), 120.8 (ArC4), 127.1 (ArC2'), 127.2 (ArC1'), 127.6 (ArC5), 128.5 (ArC3'), 129.6 (ArC3), 129.8 (CH=CH), 129.9 (ArC2), 137.4 (ArC1'), 156.3 (ArC1); MS (CI, +ve) *m/z* 421 (47, M+H), 237 (72), 147 (100%); MS (EI, +ve) 420 (10, M^{+}), 329 (30), 313 (10), 237 (30), 223 (40), 197 (40), 107 (100); HRMS (EI, +ve) calcd for $C_{30}H_{28}O_2$ 420.2089, found 420.2087.

(2*R*,3*R*)-Di(2-benzyloxyphenyl)-2,3-butanediol 166b

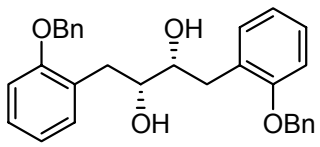

The diol (*R*,*R*)-**166b** was synthesised by *General Procedure A* using alkene **165** (80 mg, 0.19 mmol, *E*:*Z* 8.5:1), AD mix β (267 mg), methanesulfonamide (18 mg, 0.19 mmol), sodium sulfite (238 mg) in *t*BuOH (1.5 mL), water (1 mL) and THF (0.45 mL), for 37 h. The crude residue was subjected to gravity silica column chromatography (10% to 20% EtOAc:hexanes) to yield the chiral diol (*R*,*R*)-**166b** (60 mg, 69%) as a white solid, m.p. 57-59 ^{o}C, as a mixture of chiral:*meso* diastereomers

(7.2:1). HPLC analysis (20% to 70% 2-propanol:hexane, retention times (*R*,*R*)-diol **166b** 24.0 min (major), (*S*,*S*)-diol **166a** 33.7 min (minor) showed the *ee* of the (*R*,*R*)-diol **166b** was 91%. ^{1}H NMR (300 MHz) δ 2.24 (bs, 2H, OH), 2.75 (dd, 2H, $^{2}J_{HH}$ = 13.5 Hz, $^{3}J_{HH}$ = 7.7 Hz, CHH), 2.87 (dd, 2H, $^{2}J_{HH}$ = 13.5 Hz, $^{3}J_{HH}$ = 5.2 Hz, CHH), 2.99* (dd, $^{2}J_{HH}$ = 13.7 Hz, $^{3}J_{HH}$ = 2.4 Hz), 3.66 (dd, 2H, *J* = 5.7, 5.7 Hz, CHOH), 3.76* (d, *J* = 8.1 Hz), 4.90 (s, 4H, $PhCH_2$), 5.98*, 6.78-6.85 (m, 4H, ArH4 and ArH6), 7.05-7.10 (m, 4H, ArH3 and ArH5), 7.23-7.29 (m, 10H, 10 x ArH'); ^{13}C NMR (75 MHz) δ 33.3*, 35.1 (CH_2), 70.1 ($PhCH_2$), 70.2*, 73.1 (CHOH), 74.4*, 111.8 (ArC6), 111.9*, 121.0 (ArC4), 121.1*, 127.2 (ArC2'), 127.6 (ArC4'), 127.9 (ArC5), 128.6 (ArC3'), 131.5 (ArC3), 131.7*, 136.8 (ArC1'), 156.6 (ArC1); MS (CI, +ve) *m/z* 455 (100%, M+H), 419 (84); MS (ES, +ve) *m/z* 477 (100%, M+Na); HRMS (ES, +ve) calcd for $C_{30}H_{30}O_4Na$ 477.2042, found 477.2044.

(2*S*,3*S*)-Di(2-benzyloxyphenyl)-2,3-butanediol 166a

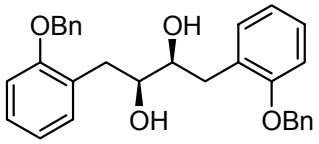

Procedure 1: The diol (*S*,*S*)-**166a** was synthesised by *General Procedure A* using alkene **165** (376 mg, 0.90 mmol, *E*:*Z* 3.1:1), AD mix α (1.253 g), methanesulfonamide (85 mg, 0.90 mmol), sodium sulfite (1.120 g) in *t*BuOH (4.5 mL), water (4.5 mL) and THF (1.2 mL), for 91 h. Purification via gravity silica column chromatography (2% to 50% EtOAc:hexanes) isolated the diol (*S*,*S*)-**166a** as a white solid (280 mg, 64%) as a mixture of chiral:*meso* diastereomers (15:1), m.p. 58-59 ^{o}C, which exhibited identical spectral properties to the (*R*,*R*)-diol. HPLC analysis (20% to 70% 2-propanol:hexane, retention times (*R*,*R*)-diol **166b** 23.4 min (minor), (*S*,*S*)-diol **166a** 32.4 min (major)) showed the *ee* of the (*S*,*S*)-diol **166a** was 33%.

Procedure 2: The diol (*S*,*S*)-**166a** was synthesised by *General Procedure A* using alkene **165** (171 mg, 0.41 mmol, *E*:*Z* 3.9:1), AD mix α (0.54 g), methanesulfonamide (39 mg, 0.41 mmol), sodium sulfite (0.552 g) in *t*BuOH (2 mL), water (2 mL), for 24 h. Purification via gravity silica column chromatography (10% to 20% EtOAc:hexanes) isolated the diol (*S*,*S*)-**166a** as a white solid (27 mg, 15%) as a mixture of chiral:*meso* diastereomers (4.8:1). HPLC analysis (20% to 70% 2-propanol:hexane, retention times (*R*,*R*)-diol **166b** 24.3 min (minor), (*S*,*S*)-diol **166a** 33.0 min (major)) showed the *ee* of the (*S*,*S*)-diol **166a** was 64%.

(2*S*,3*S*)-1,4-Di(2-benzyloxy)phenyl-2,3-dimethanesulfonylbutane 174a

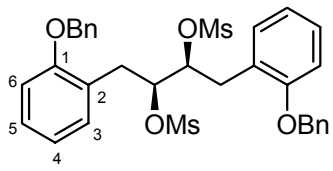

MsCl (0.065 mL, 0.66 mmol) was added to a solution of diol (*R*,*R*)-**166a** (60 mg, 0.132 mmol) and Et_3N (0.15 mL, 1.05 mmol) in DCM (2.5 mL) at 0 ^oC. The reaction mixture was stirred at RT for 30 min and diluted with DCM (20 mL). The diluted reaction mixture was washed sequentially with 5% $CuSO_4$ (2 x 50 mL), sat. $NaHCO_3$ (2 x 50 mL), sat. NaCl (2 x 50 mL) and dried ($MgSO_4$). The solvent was removed *in vacuo*, and the crude product was subjected to gravity silica gel column chromatography (20% EtOAc:hexanes) to yield the dimesylate (*R*,*R*)-**174a** (80 mg, 99%) as a white solid as a mixture of chiral:*meso* diastereomers (14:1). The mixture of isomers was recrystallised from DCM/hexanes, filtered, crushed and washed with EtOH to give the chiral dimesylate (70 mg, 88%). ^1H NMR (500 MHz) δ 3.22 (s, 6H, SO_2CH_3), 2.98 (dd, 2H, $^2J_{HH}$ = 14.0 Hz, $^3J_{HH}$ = 9.5 Hz, C<u>H</u>HCH(OMs)), 3.26 (dd, 2H, $^2J_{HH}$ = 14.0 Hz, $^3J_{HH}$ = 3.3 Hz, CH<u>H</u>CH(OMs)), 5.06 (s, 4H, $PhCH_2$), 5.23 (dd, 2H, $^3J_{HH}$ = 8.5 Hz, $^3J_{HH}$ = 2.4 Hz, C<u>H</u>(OMs)), 6.88-6.90 (m, 4H, ArH), 7.19-7.22 (m, 4H, ArH), 7.27-7.29 (m, 2H, ArH), 7.33-7.36 (m, 4H, ArH), 7.41-7.42 (m, 4H, ArH); ^{13}C NMR (75 MHz) δ 32.8 (CH_2), 37.5 (SO_2CH_3), 70.2 ($PhCH_2$), 81.3 (<u>C</u>HOMs), 111.8 (ArC6), 120.7 (ArC4), 124.5 (ArC2), 127.6 (ArC2'), 128.0 (ArC5), 128.7 (ArC3'), 128.8 (ArC4'), 132.3 (ArC3), 136.8 (ArC1'), 156.9 (ArC1); MS (ES, +ve) *m/z* 633 (40, M+Na), 105 (100%); HRMS (ES, +ve) calcd for $C_{32}H_{34}O_8NaS_2$ 633.1593, found 633.1588.

(3*R*,1*E*)-3-Azido-1,4-di(2-benzyloxy)phenyl-1-butene 175 and (2*S*,3*R*)-3-azido-1,4-di(2-benzyloxy)phenyl-2-methanesulfonylbutane 176

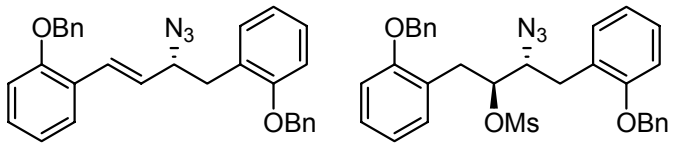

175 **176**

To a solution of dimesylate (*S*,*S*)-**174a** (80 mg, 0.13 mmol) in DMF (1 mL) was added sodium azide (52 mg, 0.79 mmol) and the reaction mixture was heated to 50 ^oC and stirred for 3 h. The reaction mixture was stirred for a further 13 h at 80 ^oC. Sodium azide (52 mg, 0.79 mmol) was added and stirring was continued for 7 h at 80 ^oC. The

mixture was poured into sat. NaCl (20 mL) and extracted with EtOAc (3 x 30 mL). The combined organic layers were washed with sat. NaCl (4 x 30 mL), dried ($MgSO_4$) and the solvent removed *in vacuo*. The crude oil was subjected to gravity silica gel column chromatography (5% to 20% EtOAc:hexanes) to yield the alkene **175** (12 mg, 20%) as a colourless oil. ^{1}H NMR (500 MHz) δ 2.86-2.98 (m, 2H, CH_2), 4.32 (ddd, 1H, *J* = 7.7, 7.7, 7.7 Hz, CHN_3), 5.01-5.02 (m, 4H, $PhCH_2$ x 2), 6.14 (dd, 1H, *J* = 8.1, 15.9 Hz, ArCH=C<u>H</u>), 6.82 (d, 1H, *J* = 16.2 Hz, ArC<u>H</u>=CH), 6.77-7.34 (m, 18H, ArH).

Further elution afforded the monoazido **176** (11 mg, 15%) as a colourless oil. ^{1}H NMR (500 MHz) δ 2.17 (s, 3H, SO_2CH_3), 2.67 (dd, 1H, *J* = 9.5, 13.7 Hz, $N_3CHC\underline{H}H$), 2.89 (dd, 1H, *J* = 6.8, 13.8 Hz, $N_3CHCH\underline{H}$), 2.90 (dd, 1H, *J* = 1.2, 13.0 Hz, C<u>H</u>HCHOMs), 3.08 (dd, 1H, *J* = 3.7, 14.0 Hz, CH<u>H</u>CHOMs), 4.15 (ddd, 1H, *J* = 2.8, 4.6, 9.2 Hz, CHN_3), 4.99 (s, 4H, $PhCH_2$ x 2), 5.00-5.06 (m, 1H, CHOMs), 6.80-7.36 (m, 18H, ArH).

Further elution recovered the dimesylate **174a** (23 mg, 29%).

7.4 Phenolic-based derivatives

*7.4.1 Phenolic-based derivatives (**Monomers**)*

<u>1-(4-Methoxybenzyloxy)-2-allylbenzene 193</u>[193]

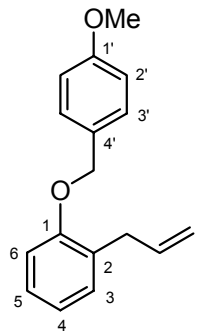

4-Methoxybenzyl alcohol (0.28 mL, 2.26 mmol) was dissolved in HBr (0.6 mL, 45% solution in glacial acetic acid) and stirred for 30 min at RT. The mixture was diluted with Et_2O (20 mL) and washed with sat. $NaHCO_3$ (4 x 20 mL), followed by sat. NaCl (3 x 25 mL). The organic layer was dried ($MgSO_4$), filtered and concentrated *in vacuo* to yield the crude 4-methoxybenzyl bromide. A suspension of NaH (60% dispersion in oil, 66 mg, 1.65 mmol, washed with hexanes (x 1), Et_2O (x 3)) in dry THF (5 mL) was cooled to 0 ^oC and treated with 2-allylphenol (0.20 mL, 1.5 mmol). After stirring for 50 min at 0 ^oC, the crude 4-methoxybenzyl bromide was slowly added as a solution in THF (2 mL), and the mixture was allowed to warm to RT. The reaction mixture was quenched after 23 h with glacial acetic acid (2 mL), followed by water (20 mL). The aqueous layer was extracted with EtOAc (3 x 20 mL). The

combined organic layers were washed with sat. $NaHCO_3$ (3 x 20 mL) and dried ($MgSO_4$). The crude mixture was subjected to flash silica gel column chromatography (hexanes to 1% EtOAc:hexanes) to yield the protected allylic phenol **193** (344 mg, 90%) as a colourless oil, which was spectroscopically identical to that reported in the literature.[193] ^{1}H NMR (300 MHz) δ 3.42 (d, 2H, $^3J_{HH}$ = 6.7 Hz, C<u>H</u>$_2$CH=CH$_2$), 3.81 (s, 3H, OCH_3), 5.00 (s, 2H, $PhCH_2$), 5.01-5.08 (m, 2H, CH=C<u>H</u>$_2$), 6.00 (tdd, 1H, $^3J_{HH}$ = 16.9, $^3J_{HH}$ = 10.2, $^3J_{HH}$ = 6.7 Hz, C<u>H</u>=CH$_2$), 6.88-6.92 (m, 4H, ArH), 7.15-7.20 (m, 2H, ArH), 7.35 (d, 2H, $^3J_{HH}$ = 8.8 Hz, ArH3'); ^{13}C NMR (75 MHz) δ 34.4 (<u>C</u>H$_2$CH=CH$_2$), 55.3 (OCH_3), 69.7 ($PhCH_2$), 111.8 (ArC6), 113.9 (ArC2'), 115.4 (CH=<u>C</u>H$_2$), 120.7 (ArC4), 127.2 (ArC5), 128.8 (ArC3'), 129.0 (ArC4'), 129.4 (ArC2), 129.8 (ArC3), 137.0 (<u>C</u>H=CH$_2$), 156.4 (ArC1), 159.3 (ArC1'); MS (EI, +ve) *m/z* 254 (4, M^+), 121 (100); HRMS (EI, +ve) calcd for $C_{17}H_{18}O_2$ 254.1307, found 254.1307.

<u>2-Allylphenyl acetate 194</u>[194,230]

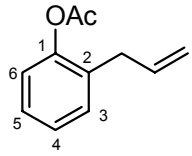

Acetic anhydride (5 mL) was added to a stirred solution of 2-allylphenol (200 mg, 0.49 mmol) in Et_3N (5 mL) at RT for 25 h. The reaction was quenched with water and extracted with DCM (4 x 20 mL). The combined organic layers were washed with sodium hydroxide (3 x 20 mL) and concentrated *in vacuo*. The crude product was subjected to gravity silica gel column chromatography (5% EtOAc:hexanes) to afford the acetylated phenol **194** (262 mg, 99%) as a colourless, volatile liquid.‡ ^{1}H NMR (300 MHz) δ 2.30 (s, 3H, CH_3), 3.30 (d, 2H, $^3J_{HH}$ = 6.6 Hz, C<u>H</u>$_2$CH=CH$_2$), 5.04-5.07 (m, 1H, CH=CH<u>H</u>), 5.09-5.10 (m, 1H, CH=C<u>H</u>H), 5.84-5.98 (m, 1H, C<u>H</u>=CH$_2$), 7.02-7.05 (m, 1H, ArH), 7.16-7.28 (m, 3H, ArH); ^{13}C NMR (75 MHz) δ 20.9 (CH_3), 34.6 (<u>C</u>H$_2$CH=CH$_2$), 116.2 (CH=<u>C</u>H$_2$), 122.3 (ArC6), 126.2 (ArC4), 127.4 (ArC5), 130.4 (ArC3), 131.9 (ArC2), 135.9 (<u>C</u>H=CH$_2$), 148.9 (ArC1), 169.3 (C=O); FTIR *v* 1760 (s), 1639 (w), 1488 (w), 1453 (w), 1370 (w), 1202 (s), 1170 (s), 1118 (w), 1010 (w), 915 (w), 751 (w); MS (EI, +ve) *m/z* 176 (20, M^+), 147 (33), 134 (100%), 133 (67), 132 (21), 131 (79), 119 (53); HRMS (EI, +ve) calcd for $C_{11}H_{12}O_2$ 176.0837, found 176.0837.

‡ No physical or spectral data reported in reference 194 or 230.

2-Allyl-1-trifluoromethanesulfonylbenzene 195[231]

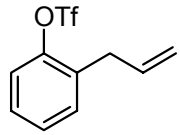

2-Allylphenol (1.00 g, 7.46 mmol) was added to a stirred mixture of *N*-phenyltriflimide (3.4 g, 11.18 mmol) and K_2CO_3 (2.06 g, 14.9 mmol) in THF (50 mL). The reaction mixture was heated at reflux and after 48 h was partitioned between DCM and sat. NaCl. The aqueous layer was extracted with DCM (3 x 20 mL) and the combined organic layers were washed with brine (2 x 20 mL), dried ($MgSO_4$) and concentrated under reduced pressure. The crude product was subjected to gravity silica gel column chromatography (1% EtOAc:hexanes) to afford the triflated phenol **195** (1.648 g, 83%) as a colourless, volatile liquid, which was spectroscopically identical to that reported in the literature.[231] ^{1}H NMR (300 MHz) δ 3.40 (dd, 1H, $^2J_{HH}$ = 1.4, $^3J_{HH}$ = 1.4 Hz, C<u>H</u>HCH=CH_2), 3.42 (dd, 1H, $^2J_{HH}$ = 1.4, $^3J_{HH}$ = 1.4 Hz, CH<u>H</u>CH=CH_2), 5.06 (ddd, 1H, $^4J_{HH}$ = 1.4, $^2J_{HH}$ = 2.9, $^3J_{HH}$ = 17.0 Hz, CH=CH<u>H</u>), 5.08 (ddd, 1H, $^4J_{HH}$ = 1.4, $^2J_{HH}$ = 2.8, $^3J_{HH}$ = 10.2 Hz, CH=C<u>H</u>H), 5.85 (ddt, 1H, $^3J_{HH}$ = 6.0, $^3J_{HH}$ = 10.2, $^3J_{HH}$ = 16.8 Hz, C<u>H</u>=CH_2), 7.26-7.33 (m, 4H, ArH); ^{13}C NMR (75 MHz) δ 34.0 (<u>C</u>H_2CH=CH_2), 112.2, 116.5, 120.7, 125.0 (118.6, q, *J* = 320 Hz, CF_3), 117.5 (CH=<u>C</u>H_2), 121.3 (ArC6), 128.1 (ArC4), 128.4 (ArC5), 131.4 (ArC3), 132.8 (ArC2), 134.6 (<u>C</u>H=CH_2), 147.9 (ArC1); FTIR *v* 1483 (w), 1420 (m), 1250 (w), 1210 (s), 1138 (s), 1073 (w), 889 (s), 766 (m); MS (EI, +ve) *m/z* 266 (9, M^+), 265 (59), 131 (99), 115 (100%), 103 (63); HRMS (EI, +ve) calcd for $C_{10}H_9F_3O_S$ 266.0225, found 266.0225.

1-*tert*-Butyldimethylsilyloxy-2-allylbenzene 196[196]

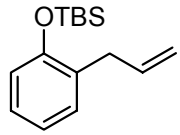

2-Allylphenol (0.20 mL, 3.0 mmol) was added to a stirred suspension of imidazole (246 mg, 3.6 mmol) in DCM (10 mL). *tert*-Butyldimethylsilyl chloride (520 mg, 3.45 mmol) was added as a solid and stirring was continued at RT for 18 h. The reaction mixture was partitioned between DCM and water, and the aqueous layer was extracted with DCM (3 x 25 mL). The organic layers were combined and washed with water, dried ($MgSO_4$) and the solvent was removed under reduced pressure. The crude mixture was subjected to a flash silica gel plug (100% hexanes) to afford the TBS protected phenol **196** (740 mg, 99%) as a colourless, volatile liquid, which was spectroscopically identical to that reported in the literature.[196] ^{1}H NMR (500 MHz) δ 0.24 (s, 6H, $Si(CH_3)_2$), 1.02 (s, 9H, $C(CH_3)_3$), 3.37 (d, 2H, *J* =

6.5 Hz, C<u>H</u>$_2$CH=CH$_2$), 4.99-5.03 (m, 1H, CH=CH<u>H</u>), 5.05-5.06 (m, 1H, CH=C<u>H</u>H), 5.90-6.04 (m, 1H, C<u>H</u>=CH$_2$), 6.79 (d, 1H, *J* = 8 Hz, ArH6), 6.89 (t, 1H, *J* = 7.4 Hz, ArH4), 7.08 (t, 1H, *J* = 7.7 Hz, ArH5), 7.14 (d, 1H, *J* = 7.5 Hz, ArH3); ^{13}C NMR (75 MHz) δ -4.1 (Si(CH$_3$)$_2$), 18.3 (<u>C</u>(CH$_3$)$_3$, 25.8 (C(<u>C</u>H$_3$)$_3$), 34.4 (<u>C</u>H$_2$CH=CH$_2$), 115.4 (CH=<u>C</u>H$_2$), 118.4 (ArC6), 121.1 (ArC4), 127.0 (ArC5), 130.1 (ArC3), 130.7 (ArC2), 137.0 (<u>C</u>H=CH$_2$), 153.3 (ArC1); MS (EI, +ve) *m/z* 247 (39, M-H), 237 (42), 221 (47), 205 (55), 193 (63), 179 (100%), 161 (71), 131 (92), 121 (92), 115 (79); HRMS (EI, +ve) calcd for $C_{15}H_{23}OSi$ 247.1518, found 247.1516.

<u>2-Allyl-1-methoxybenzene 197</u>[197]

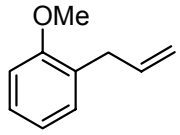

2-Allylphenol (507 mg, 3.73 mmol) was dissolved in acetone (40 mL) and K_2CO_3 (2.063 g, 14.9 mmol) was added, followed by a few drops of water. The reaction vessel was heated to 40 ^{o}C and methyl iodide (0.94 mL, 14.9 mmol) was added. After 20 h the solvent was removed under reduced pressure, the crude mixture dissolved in EtOAc and washed with water (3 x 30 mL). The organic layer was dried ($MgSO_4$) and adsorbed onto silica gel. After flash silica gel column chromatography (hexanes), the protected allylphenol **197** (482 mg, 87%) was obtained as a colourless, volatile liquid, which was spectroscopically identical to that reported in the literature.[197] ^{1}H NMR (500 MHz) δ 3.38 (d, 2H, *J* = 6.2 Hz, CH$_2$), 3.81 (s, 3H, OCH$_3$), 5.02-5.06 (m, 2H, CH=C<u>H</u>$_2$), 5.95-6.03 (m, 1H, C<u>H</u>=CH$_2$), 6.84 (d, 1H, *J* = 8.1 Hz, ArH6), 6.89 (t, 1H, *J* = 7.4 Hz, ArH4), 7.13 (d, 1H, *J* = 7.3 Hz, ArH3), 7.19 (t, 1H, *J* = 7.7 Hz, ArH5); ^{13}C NMR (125 MHz) δ 34.2 (CH$_2$), 55.3 (OCH$_3$), 110.3 (ArC6), 115.3 (CH=<u>C</u>H$_2$), 120.5 (ArC4), 127.3 (ArC5), 128.6 (ArC2), 129.7 (ArC3), 137.0 (<u>C</u>H=CH$_2$), 157.3 (ArC1); FTIR *v* 1600 (w), 1493 (m), 1464 (w), 1243 (s), 1050 (w), 1031 (m), 912 (w), 751 (s); MS (EI, +ve) *m/z* 148 (17, M^{+}), 147 (90, M-H), 131 (100%), 121 (78), 105 (55); HRMS (EI, +ve) calcd for $C_{10}H_{12}O$ 148.0888, found 148.0888.

*7.4.2 Phenolic-based derivatives (**Dimers**)*

***E*-1,4-Di(2-(4-methoxybenzyloxy)phenyl)-2-butene 198**

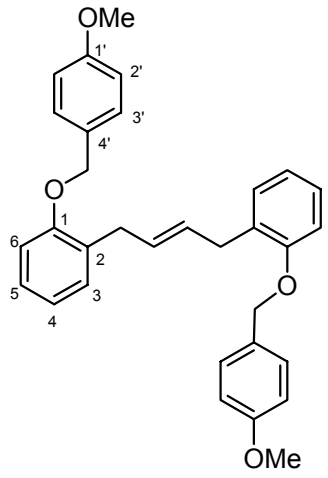

Grubbs 2 catalyst (34 mg, 0.039 mmol, 5 mol %) was added to a solution of alkene **193** (180 mg, 0.708 mmol) in DCM (6 mL) and the solution was heated at reflux for 23 h. The reaction mixture was concentrated *in vacuo* and subjected to flash silica gel column chromatography (2% EtOAc:hexanes) to yield the dimer **198** (27 mg, *E*:*Z* 3:1) as a white solid. Further elution (2% to 50% EtOAc:hexanes) yielded 5 more portions of **198**, with a total mass of 121 mg (71%) and an increasing *E*:*Z* ratio (5:1 to 20:1). The fractions were combined and recrystallisation from DCM/hexanes gave the pure *E* isomer as a white solid (80 mg, 47%), m.p. 132-133 ^{o}C. ^{1}H NMR (300 MHz) δ 3.39 (d, 4H, *J* = 4.8 Hz, C$\underline{H}_2$CH=CH_2), 3.80 (s, 6H, OCH_3), 4.98 (s, 4H, $PhCH_2$), 5.66 (m, 2H, C$\underline{H}$=C$\underline{H}$), 6.84-6.90 (m, 8H, ArH), 7.13-7.20 (m, 4H, ArH), 7.28-7.38 (m, 4H, ArH3'); ^{13}C NMR (75 MHz) δ 33.1 (CH_2), 55.3 (OCH_3), 69.7 ($PhCH_2$), 111.7 (ArC6), 113.8 (ArC2'), 120.7 (ArC4), 127.0 (ArC5), 128.7 (ArC3'), 129.4 (ArC4'), 129.5 (C$\underline{H}$=C$\underline{H}$), 129.7 (ArC3), 129.8 (ArC2), 156.4 (ArC1), 159.2 (ArC1'); FTIR *v* 1614 (w), 1587 (w), 1515 (w), 1489 (w), 1451 (w), 1378 (w), 1252 (w), 1230 (w), 1106 (w), 1032 (w), 998 (w); MS (EI, +ve) *m/z* 480 (5, M^+), 241 (12), 121 (100%); HRMS (EI, +ve) calcd for $C_{32}H_{32}O_4$ 480.2301, found 480.2291.

***E*-1,4-Di(2-acetyloxyphenyl)-2-butene 199**

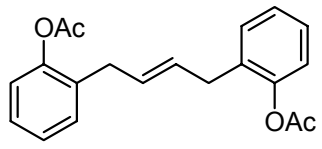

Grubbs 1 catalyst (61 mg, 0.074 mmol, 5 mol %) was added to a solution of alkene **194** (262 mg, 1.49 mmol) in DCM (12 mL) and the solution was heated at reflux for 15 h. The reaction mixture was adsorbed onto silica gel and subjected to gravity silica gel column chromatography (5% to 7% EtOAc:hexanes) to yield the dimer **199** (204 mg, 85%, *E*:*Z* 4:1) as a colourless oil. ^{1}H NMR (300 MHz) δ 2.24 (s, 6H, CH_3), 2.28*, 3.26 (dd, 4H, *J* = 1.4, 3.7 Hz, CH_2), 3.38* (d, *J* = 5.3 Hz, CH_2), 5.56-5.59 (m, 2H, C$\underline{H}$=C$\underline{H}$), 5.62-5.65*, 7.00-7.05 (m, 2H, ArH), 7.14-7.26 (m, 6H, ArH);

^{13}C NMR (75 MHz) δ 20.8 (CH_3), 27.9*, 33.3 (CH_2), 122.3 (ArC6), 126.1 (ArC4), 126.2*, 127.3 (ArC5), 128.2*, 129.2 (CH=CH), 129.9*, 130.3 (ArC3), 132.3 (ArC2), 132.4*, 148.8 (ArC1), 169.3 (C=O); MS (EI, +ve) *m/z* 324 (11, M^+), 282 (16), 264 (11), 176 (10), 147 (33), 133 (100%), 131 (68), 107 (75); HRMS (EI, +ve) calcd for $C_{20}H_{20}O_4$ 324.1362, found 324.1354.

_E_-1,4-Di(2-trifluoromethanesulfonylphenyl)-2-butene 200

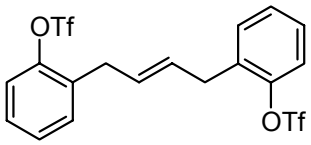

Grubbs 1 catalyst (23 mg, 0.028 mmol, 5 mol %) was added to a solution of alkene **195** (151 mg, 0.568 mmol) in DCM (6 mL) and the solution was heated at reflux for 15 h. The reaction mixture was adsorbed onto silica gel and subjected to gravity silica gel column chromatography (0.5% to 1% EtOAc:hexanes) to afford the dimer **200** (126 mg, 88%, *E*:*Z* 3.8:1) as a colourless oil. ^{1}H NMR (300 MHz) δ 3.48 (dd, 4H, *J* = 1.5, 3.6 Hz, CH_2), 3.59* (dd, *J* = 0.9, 4.6 Hz, CH_2), 5.65 (ddd, 2H, *J* = 1.5, 3.6, 5.1 Hz, CH=CH), 5.73* (ddd, *J* = 0.9, 4.6, 5.5 Hz, CH=CH), 7.23-7.34 (m, 8H, ArH); ^{13}C NMR (75 MHz) δ 27.6*, 32.8 (CH_2), 112.2, 116.5, 120.7, 124.9 (118.6, q, *J* = 320 Hz, CF_3), 121.3 (ArC6), 128.1 (ArC4), 128.2* (CH=CH), 128.4 (ArC5), 128.5*, 129.3 (CH=CH), 131.0*, 131.3 (ArC3), 133.0 (ArC2), 147.9 (ArC1); MS (EI, +ve) *m/z* 504 (27, M^+), 359 (13), 281 (33), 265 (100%), 239 (80), 131 (100%), 115 (93), 109 (67); HRMS (ES, +ve) calcd for $C_{18}H_{14}F_6O_6S_2$ 504.0136, found 504.0127.

_E_-1,4-Di(2- *tert*-butyldimethylsilyloxy)phenyl-2-butene 201

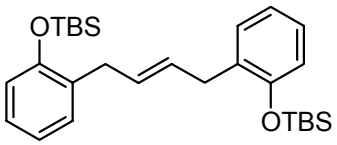

Grubbs 2 catalyst (34 mg, 0.040 mmol, 5 mol %) was added to a solution of alkene **196** (200 mg, 0.805 mmol) in DCM (8 mL) and the solution was heated at reflux for 3 d. The reaction mixture was adsorbed onto silica gel and subjected to flash silica gel column chromatography (hexanes) yielding the dimer **201** as a pale yellow semi-solid (97 mg, *E*:*Z* 12:1). Further elution yielded 2 more portions of **201**, with a total mass of 180 mg (95%) and a decreasing *E*:*Z* ratio (6:1 and 4:1). ^{1}H NMR (500 MHz) δ 0.20 (s, 12H, $Si(CH_3)_2$), 0.24*, 0.99 (s, 18H, $C(CH_3)_3$), 1.02*, 3.34 (d, 4H, *J* = 3.9 Hz, CH_2), 3.47* (d, *J* = 4.8 Hz, CH_2), 5.61-5.62 (m, 2H, CH=CH), 5.70* (t, *J* = 4.6 Hz, CH=CH), 6.77 (d, 2H, *J* = 8.1 Hz, ArH6), 6.87 (t, 2H, *J* = 7.4 Hz, ArH4), 7.06 (t, 2H, *J* = 7.6 Hz,

ArH5), 7.13 (d, 2H, J = 7.4 Hz, ArH3); ^{13}C NMR (125 MHz) δ -4.2 (Si(CH_3)$_2$), -4.1*, 18.25 (C(CH_3)$_3$, 18.29*, 25.81 (C(CH_3)$_3$), 25.82*, 27.8*, 33.1 (CH_2), 118.34 (ArC6), 118.39*, 121.0 (ArC4), 121.1*, 126.78*, 126.80 (ArC5), 128.7* (CH=CH), 129.6 (CH=CH), 129.7*, 130.1 (ArC3), 131.5 (ArC2), 153.3 (ArC1); MS (EI, +ve) *m/z* 468 (8, M^+), 411 (92), 295 (18), 281 (91), 247 (42), 221 (87), 203 (45), 179 (78), 165 (100%), 115 (92); HRMS (EI, +ve) calcd for $C_{28}H_{44}O_Si_2$ 468.2880, found 468.2866.

_E_-1,4-Di(2-methoxyphenyl)-2-butene 202

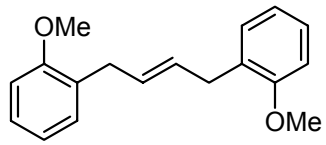

Grubbs 1 catalyst (51 mg, 0.062 mmol, 5 mol %) was added to a solution of alkene **197** (183 mg, 1.236 mmol) in DCM (10 mL) and the solution was heated at reflux for 7 h. The reaction mixture was adsorbed onto silica gel and subjected to flash silica gel column chromatography (1% EtOAc:hexanes) to afford the dimer **202** (151 mg, 91%, *E*:*Z* 4.5:1) as a colourless oil. ^{1}H NMR (300 MHz) δ 3.35 (d, 4H, J = 4.2 Hz, CH_2), 3.50* (d, J = 4.9 Hz), 3.81 (s, 6H, OCH_3), 5.64-5.68 (m, 2H, CH=CH), 6.83 (d, 2H, J = 8.1 Hz, ArH6), 6.88 (dt, J = 1.1, 7.4, 7.5 Hz, ArH4), 7.14-7.21 (m, 4H, ArH3 and ArH5); ^{13}C NMR (75 MHz) δ 32.9 (CH_2), 55.3 (OCH_3), 110.2 (ArC6), 120.4 (ArC4), 123.8 (ArC2), 127.0 (ArC5), 129.5 (CH=CH), 129.6 (ArC3), 157.2 (ArC1); MS (EI, +ve) *m/z* 268 (25, M^+), 147 (100%), 121 (75); HRMS (EI, +ve) calcd for $C_{18}H_{20}O_2$ 268.1463, found 268.1464.

_E_-1,4-Di(2-hydroxyphenyl)-2-butene 203

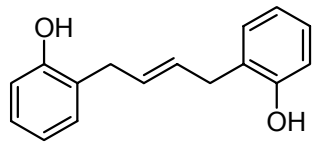

Tetrabutylammonium fluoride (2.6 mL, 1 M solution in THF) was added to **201** (310 mg, 0.661 mmol, *E*:*Z* 15.6:1) under N_2(g) and the reaction mixture was stirred at RT for 21 h. The solvent was removed *in vacuo*, and the crude solid was dissolved in DCM and washed with water. The alkene **203** (21 mg, 13%, *E*:*Z* 27:1) was recrystallised from DCM/hexanes as a white solid, m.p. 126-128 ^{o}C. Two additional crops of **203** (123 mg, 79%) were obtained by recrystallisation from the filtrate to give a total yield of 92% (144 mg). ^{1}H NMR (300 MHz, CD_3OH) δ 3.30 (dd, 4H, $^2J_{HH}$ = 1.4, $^3J_{HH}$ = 3.5 Hz, CH_2CH=CH_2), 4.89 (bs, 2H, OH), 5.61-5.65 (m, 2H, CH=CH), 6.70-6.75 (m, 4H, ArH), 6.95-7.05 (m, 4H, ArH); ^{13}C NMR (75 MHz, CD_3OH) δ 33.9 (CH_2),

115.8 (ArC6), 120.6 (ArC4), 128.0 (ArC5), 128.6 (ArC2), 130.6 (CH=CH), 130.8 (ArC3), 156.0 (ArC1); FTIR *v* 3084 (w), 2395 (w), 1711 (w), 1369 (w), 1230 (w), 1073 (s); MS (ES, -ve) *m/z* 275 (23, M+Cl), 239 (100%, M-H); HRMS (ES, -ve) calcd for $C_{16}H_{15}O_2$ 239.1072, found 239.1080.

*7.4.3 Phenolic-based derivatives (**Diols**)*

(2*R*,3*R*)-1,4-Di(2-trifluorosulfonylphenyl)-2,3-butandiol 206b

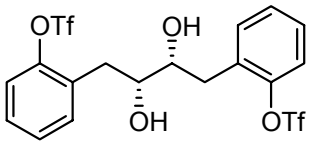

The diol (*R*,*R*)-**206b** was synthesised by *General Procedure A* using alkene **200** (120 mg, 0.238 mmol, *E*:*Z* 9.1:1), AD mix β (333 mg), methanesulfonamide (23 mg, 0.238 mmol), sodium sulfite (211 mg) in *t*BuOH (1.2 mL) and water (1.2 mL). The crude residue was subjected to gravity silica gel column chromatography (10% to 50% EtOAc:hexanes) to yield the diol **206b** (74 mg, 58%) as a white solid as a mixture of chiral:*meso* diastereomers (27:1). Recrystallisation of the mixture from DCM/hexanes removed the *meso* isomer. The filtrate was concentrated *in vacuo* to give the chiral diol (*R*,*R*)-**206b** (60 mg, 47%), m.p. 114-115 ^{o}C. HPLC analysis (20% 2-propanol:hexane, retention times (*R*,*R*)-diol **206b** 8.73 min (major), (*S*,*S*)-diol **206a** 9.39 min (minor)) showed the *ee* of the (*R*,*R*)-diol **206b** was 8%. ^{1}H NMR (300 MHz) δ 2.21 (d, 2H, J = 6.4 Hz, OH), 2.96 (dd, 2H, $^{2}J_{HH}$ = 13.5 Hz, $^{3}J_{HH}$ = 7.5 Hz, CHH), 3.03 (dd, 2H, $^{2}J_{HH}$ = 13.5 Hz, $^{3}J_{HH}$ = 4.2 Hz, CHH), 3.73-3.90 (m, 2H, CHOH), 7.23-7.45 (m, 8H, ArH); ^{13}C NMR (300 MHz) δ 34.8 ($CH_2CH=CH_2$), 72.8 (CHOH), 112.1, 116.4, 120.6, 124.8 (118.5, q, J = 320 Hz, CF_3), 121.5 (ArC6), 128.5 (ArC4), 128.6 (ArC5), 131.1 (ArC2), 132.5 (ArC3), 148.3 (ArC1); FTIR *v* 3268 (w), 1483 (w), 1416 (w), 1228 (w), 1207 (w), 1134 (w), 1096 (w), 903 (w), 809 (w), 772 (w), 635 (w); MS (ES, +ve) *m/z* 561 (100%, M+Na), 556 (15, M+NH_4); HRMS (ES, +ve) calcd for $C_{18}H_{20}F_6O_8S_2N$ 556.0535, found 556.0535.

(2*S*,3*S*)-1,4-Di(2-trifluorosulfonylphenyl)-2,3-butandiol 206a

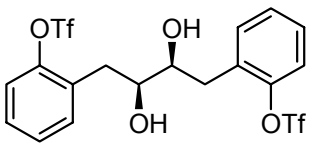

The diol (*S*,*S*)-**206a** was synthesised by *General Procedure A* using alkene **200** (110 mg, 0.523 mmol, *E*:*Z* 3.6:1), AD mix α (333 mg), methanesulfonamide (23 mg, 0.238 mmol) and

sodium sulfite (211 mg) in *t*BuOH (1.2 mL) and water (1.2 mL). The crude residue was subjected to gravity silica gel column chromatography (10% to 50% EtOAc:hexanes) to yield the diol **206a** (32 mg, 25%) as a white solid, m.p. 110-112 ^{o}C, as a mixture of chiral:*meso* diastereomers (24:1), which had identical spectral properties to the (*R*,*R*)-**206b** enantiomer. HPLC analysis (20% 2-propanol:hexane, retention times (*R*,*R*)-diol **206b** 8.76 min (minor), (*S*,*S*)-diol **206a** 9.42 min (major)) showed the *ee* of the (*S*,*S*)-diol **206a** was 1.4%.

(2*S*,2*R*)-1,4-Di(2- *tert*-butyldimethylsilyloxyphenyl)-2,3-butandiol 207 and (2*R*,3*R*)-1,4-di(2- *tert*-butyldimethylsilyloxyphenyl)-2,3-butandiol 207b

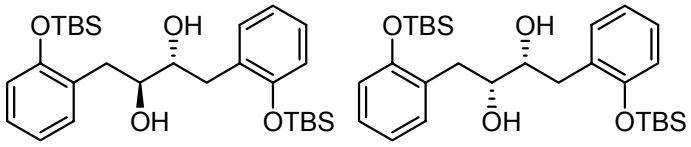

The diol (*R*,*R*)-**207** was synthesised by *General Procedure A* using alkene **201** (88 mg, 0.188 mmol, *E*:*Z* 6:1), AD mix β (263 mg), methanesulfonamide (18 mg, 0.188 mmol), sodium sulfite (166 mg) in *t*BuOH (1 mL) and water (1 mL). The crude residue was subjected to gravity silica gel column chromatography (1% to 100% EtOAc:hexanes) to yield the *meso* diol **207meso** (4 mg, 4%) as a white solid. ^{1}H NMR (300 MHz) δ 0.25 (d, 12H, *J* = 3.8 Hz, Si(CH$_3$)$_2$), 1.01 (s, 18H, C(CH$_3$)$_3$), 2.56 (d, 2H, *J* = 3.0 Hz, OH), 2.84 (dd, 2H, $^{2}J_{HH}$ = 13.7 Hz, $^{3}J_{HH}$ = 8.6 Hz, CHH), 3.04 (dd, 2H, $^{2}J_{HH}$ = 13.7 Hz, $^{3}J_{HH}$ = 2.6 Hz, CHH), 3.76-3.83 (m, 2H, CHOH), 6.83 (dd, 2H, *J* = 0.9, 8.0 Hz, ArH6), 6.92 (dt, 2H, *J* = 1.0, 7.4 Hz, ArH4), 7.11 (dt, 2H, *J* = 1.7, 7.8 Hz, ArH5), 7.21 (dd, 2H, *J* = 1.7, 7.5 Hz, ArH3); ^{13}C NMR (75 MHz) δ –4.1 and –4.0 ((Si(CH$_3$)$_2$), 18.2 (C(CH$_3$)$_3$), 25.8 (C(CH$_3$)$_3$), 33.4 (CH$_2$), 74.7 (CHOH), 118.7 (ArC6), 121.5 (ArC4), 127.5 (ArC5), 129.1 (ArC2), 131.8 (ArC3), 153.8 (ArC1); MS (ES, +ve) *m/z* 1027 (100%, 2M+Na), 525 (25, M+Na), 503 (5%, M+H); HRMS (ES, +ve) calcd for $C_{28}H_{47}O_{S}i_2$ 503.3013, found 503.3020.

Further elution gave the chiral diol (*R*,*R*)-**207b** (25 mg, 27%) as a viscous oil. HPLC analysis (2.5% 2-propanol:hexane, retention times (*R*,*R*)-diol **207b** 13.3 min (major), (*S*,*S*)-diol **207a** 12.1 min (minor)) showed the *ee* of the (*R*,*R*)-diol **207b** was 14%. ^{1}H NMR (300 MHz) δ 0.20 (s, 12H, Si(CH$_3$)$_2$), 0.97 (s, 18H, C(CH$_3$)$_3$), 2.47 (d, 2H, *J* = 5.7

Hz, OH), 2.82 (dd, 2H, $^2J_{HH}$ = 13.5 Hz, $^3J_{HH}$ = 5.6 Hz, CHH), 2.93 (dd, 2H, $^2J_{HH}$ = 13.3 Hz, $^3J_{HH}$ = 7.9 Hz, CHH), 3.67-3.73 (m, 2H, CHOH), 6.78 (dd, 2H, *J* = 1.1, 8.0 Hz, ArH6), 6.88 (dt, 2H, *J* = 1.2, 7.4 Hz, ArH4), 7.09 (dt, 2H, *J* = 1.8, 8.6 Hz, ArH5), 7.14 (d, 2H, *J* = 1.7, 7.4 Hz, ArH3); ^{13}C NMR (75 MHz) δ –4.2 and –4.1 ((Si(CH$_3$)$_2$), 18.2 (C(CH$_3$)$_3$), 25.8 (C(CH$_3$)$_3$), 35.2 (CH$_2$), 73.2 (CHOH), 118.6 (ArC6), 121.4 (ArC4), 127.5 (ArC5), 128.9 (ArC2), 131.6 (ArC3), 153.7 (ArC1) MS (ES, +ve) *m/z* 1027 (100%, 2M+Na), 525 (45, M+Na), 503 (6%, M+H); HRMS (ES, +ve) calcd for $C_{28}H_{47}OSi_2$ 503.3013, found 503.3008.

(2*S*,3*S*)-1,4-Di(2- *tert*-butyldimethylsilyloxyphenyl)-2,3-butandiol 207a

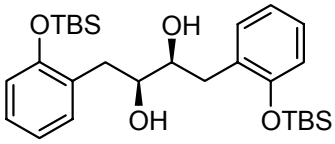

The diol (*S*,*S*)-**207a** was synthesised by *General Procedure A* using alkene **201** (97 mg, 0.207 mmol, *E*:*Z* 12:1), AD mix α (290 mg), methanesulfonamide (18 mg, 0.188 mmol) and sodium sulfite (166 mg) in *t*BuOH (1 mL) and water (1 mL). Flash silica gel column chromatography (1% to 100% EtOAc:hexanes) isolated the diol **207a** (15 mg, 13%) as an oil as a mixture of chiral:*meso* diastereomers (12:1), which exhibited identical spectral properties to the (*R*,*R*)-diol. HPLC analysis (2.5% 2-propanol:hexane, retention times (*R*,*R*)-diol **207b** 13.4 min (minor), (*S*,*S*)-diol **207a** 12.3 min (major)) showed the *ee* of the (*S*,*S*)-diol **207a** was 23%.

(2*S*,3*S*)-1,4-Di(2-methoxyphenyl)-2,3-butandiol 208a[232]

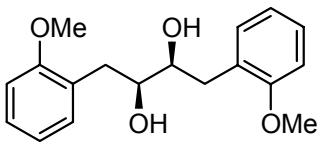

The diol (*S*,*S*)-**208a** was synthesised by *General Procedure A* using alkene **202** (75 mg, 0.28 mmol), AD mix α (392 mg), methanesulfonamide (27 mg, 0.28 mmol), sodium sulfite (420 mg) in a 1:1 mixture of *t*BuOH and water (2.8 mL). The crude solid was subjected to flash silica gel column chromatography (10% EtOAc:hexanes to 100% EtOAc) to yield the diol **208a** (44 mg, 52%) as a viscous, colourless oil, as a mixture of chiral:*meso* diastereomers (6:1), which was spectroscopically identical to that reported in the literature.[232] HPLC analysis (20% to 40% 2-propanol:hexane, retention times (*R*,*R*)-diol **208b** 22.8 min (minor), (*S*,*S*)-diol **208a** 26.7 min (major)) showed the *ee* of the (*S*,*S*)-diol **208a** was 34%. ^{1}H NMR (500 MHz) δ 2.66 (bs, 2H, OH), 2.89 (dd, 2H, $^2J_{HH}$ = 13.2 Hz, $^3J_{HH}$ = 7.4 Hz, CHH), 2.92 (dd, 2H, $^2J_{HH}$ = 13.2 Hz, $^3J_{HH}$ = 4.6 Hz,

CHH), 3.05* (dd, $^{2}J_{HH}$ = 13.8 Hz, $^{3}J_{HH}$ = 2.1 Hz, CHH), 3.72-3.73 (m, 2H, CHOH), 3.78 (s, 6H, OCH_3), 3.83*, 6.85 (d, 2H, *J* = 8.2 Hz, ArH6), 6.89 (t, 2H, *J* = 7.3 Hz, ArH4), 7.16 (d, 2H, *J* = 7.3 Hz, ArH3), 7.20 (t, 2H, *J* = 8.5 Hz, ArH5); ^{13}C NMR (125 MHz) δ 33.1*, 34.9 (CH_2), 55.3 (OCH_3), 73.4 (CHOH), 74.3*, 110.4 (ArC6), 120.8 (ArC4), 126.9 (ArC2), 127.7 (ArC5), 131.3 (ArC3), 157.4 (ArC1); FTIR *v* 1496 (w), 1265 (w), 1245 (w), 1055 (w), 853 (w), 828 (w), 815 (w), 753 (s), 745 (s); MS (ES, +ve) *m/z* 325 (50, M+Na), 320 (28, M+NH_4), 303 (100%, M+H), 285 (45, M-H_2O); HRMS (ES, +ve) calcd for $C_{18}H_{23}O_4$ 303.1596, found 303.1595.

(2*R*,3*R*)-1,4-Di(2-methoxyphenyl)-2,3-butandiol 208b[232]

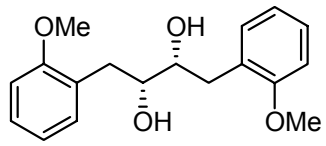

The diol (*R*,*R*)-**208b** was synthesised by *General Procedure A* using alkene **202** (75 mg, 0.28 mmol), AD mix β (392 mg), methanesulfonamide (27 mg, 0.28 mmol), sodium sulfite (420 mg) in a 1:1 mixture of *t*BuOH and water (2.8 mL). Flash silica gel column chromatography (10% to 20% EtOAc:hexanes) yielded the diol (*R*,*R*)-**208b** (31 mg, 37%) as a viscous, colourless oil, which had identical spectral properties to the diol (*S*,*S*)-**208a**. HPLC analysis (20% to 40% 2-propanol:hexane, retention times (*R*,*R*)-diol **208b** 22.4 min (major), (*S*,*S*)-diol **208a** 26.6 min (minor)) showed the *ee* of the (*R*,*R*)-diol **208b** was 40%.

7.5 Nitrogen-based derivatives

*7.5.1 Nitrogen-based derivatives (**Monomers**)*

2-Allylaniline 219[198]

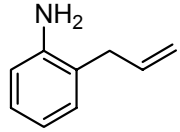

To a stirred solution of *N*-allylaniline (2.0 mL, 14.7 mmol) in xylenes (12 mL) was added $BF_3.Et_2O$ (1.8 mL, 17.0 mmol), and the mixture was heated at reflux for 49 h. The reaction mixture was poured into 2M NaOH (20 mL) and extracted with DCM (3 x 20 mL). The combined organic layers were washed with sat. NaCl (3 x 20 mL), dried ($MgSO_4$), and concentrated under reduced pressure. The crude brown oil was subjected to gravity silica gel column chromatography (hexanes to 10% EtOAc:hexanes) to yield the aniline **219** (634 mg, 32%) as a colourless oil, which turned brown when exposed to air, and was

spectroscopically identical to that reported in the literature.[198] ^{1}H NMR (500 MHz) δ 3.35 (d, 2H, $^3J_{HH}$ = 6.2 Hz, C$\underline{H}_2$CH=CH$_2$), 3.63 (bs, 2H, NH$_2$), 5.13-5.19 (m, 2H, CH=C$\underline{H}_2$), 5.95-6.05 (m, 1H, C$\underline{H}$=CH$_2$), 6.71 (d, 1H, *J* = 7.8 Hz, ArH6), 6.81 (t, 1H, *J* = 7.4 Hz, ArH4), 7.08-7.13 (m, 2H, ArH3 and 5); ^{13}C NMR (75 MHz) δ 36.3 (C$\underline{H}_2$CH=CH$_2$), 115.7 (ArC6), 116.0 (CH=C$\underline{H}_2$), 118.8 (ArC4), 123.9 (ArC2), 127.4 (ArC5), 130.1 (ArC3), 135.9 (C$\underline{H}$=CH$_2$), 144.7 (ArC1); MS (ES, +ve) *m/z* 134 (18, M+H), 105 (125), 83 (100); HRMS (ES, +ve) calcd for $C_9H_{12}N$ 134.0970, found 134.0945.

_N_-trifluoromethanesulfonyl-2-allylaniline 221

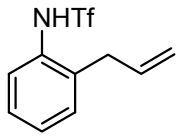

To a mixture of *N*-phenyltriflimide (806 mg, 2.25 mmol) and K_2CO_3 (416 mg, 3.01 mmol) in THF (30 mL) was added 2-allylaniline **219** (187 mg, 1.41 mmol) and the mixture was heated at reflux for 6 d. The mixture was partitioned between DCM and water, and the aqueous layer was extracted with DCM (3 x 20 mL). The combined organic layers were washed with sat. NaCl (3 x 20 mL), dried ($MgSO_4$) and the solvent removed under reduced pressure. The crude solid was subjected to gravity silica gel column chromatography (2% to 10% EtOAc:hexanes) to afford the triflate **221** (6 mg, 2%) as a white solid, m.p. 190 ^{o}C. ^{1}H NMR (300 MHz) δ 3.28 (dd, 1H, $^2J_{HH}$ = 1.6, $^3J_{HH}$ = 6.0 Hz, ArC$\underline{H}$H), 3.30 (dd, 1H, $^2J_{HH}$ = 1.6, $^3J_{HH}$ = 6.0 Hz, ArCH$\underline{H}$), 4.76 (dddd, 1H, $^4J_{HH}$ = 1.7 Hz, $^4J_{HH}$ = 1.7 Hz, $^2J_{HH}$ = 1.8 Hz, $^3J_{HH}$ = 17.2 Hz, CH=CH$\underline{H}$), 4.92 (dddd, 1H, $^4J_{HH}$ = 1.6 Hz, $^4J_{HH}$ = 1.6 Hz, $^2J_{HH}$ = 1.6 Hz, $^3J_{HH}$ = 10.2 Hz, CH=C$\underline{H}$H), 5.78 (dddd, 1H, $^3J_{HH}$ = 6.1, $^3J_{HH}$ = 6.1, $^3J_{HH}$ = 10.2, $^3J_{HH}$ = 17.1, C$\underline{H}$=CH$_2$), 6.25 (bs, 1H, NH), 7.13-7.22 (m, 2H, ArH3 and ArH4), 7.26-7.31 (1H, m, ArH5), 7.66 (d, 1H, *J* = 7.9, ArH6); ^{13}C NMR (75 MHz) δ 36.4 (CH$_2$), 116.4 (CH=C$\underline{H}_2$), 119.7 (CF_3), 125.3 (ArC6), 125.9 (ArC4), 127.7 (ArC5), 130.5 (ArC3), 135.6 (C$\underline{H}$=CH$_2$), 135.9 (ArC2), 154.1 (ArC1).

_N_-Acetyl-2-allylaniline 222[199]

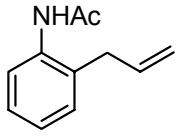

Acetic anhydride (5 mL) was added to a stirred solution of 2-allylaniline **219** (153 mg, 1.149 mmol) in Et_3N (0.4 mL) at RT. The reaction was quenched after 3 d with water and extracted with DCM (4 x 20 mL). The combined organic layers were washed with 2M NaOH (3 x 20 mL) and

concentrated *in vacuo*. The crude product was subjected to gravity silica gel column chromatography (20% to 40% EtOAc:hexanes) to afford the acetylated aniline **222** (128 mg, 65%) as a white solid, m.p. 90-91 ^{o}C, which was spectroscopically identical to that reported in the literature.[199] ^{1}H NMR (300 MHz) δ 1.81 (bs, 1H, NH), 2.07 (CH_3), 3.30 (dt, 2H, $^{2}J_{HH}$ = 1.4, $^{3}J_{HH}$ = 6.1 Hz, C<u>H</u>$_2$CH=CH$_2$), 5.02 (dd, 1H, $^{2}J_{HH}$ = 1.3 Hz, $^{3}J_{HH}$ = 17.2 Hz, CH$_2$CH=CH<u>H</u>), 5.10 (dd, 1H, $^{2}J_{HH}$ = 1.0 Hz, $^{3}J_{HH}$ = 10.0 Hz, CH$_2$CH=C<u>H</u>H), 5.90 (ddt, 1H, $^{3}J_{HH}$ = 6.1, $^{3}J_{HH}$ = 10.3, $^{3}J_{HH}$ = 16.4 Hz, C<u>H</u>=CH$_2$), 7.04-7.21 (m, 3H, ArH), 7.74 (d, 1H, *J* = 8.0 Hz, ArC6); ^{13}C NMR (75 MHz) δ 24.2 (CH_3), 36.9 (<u>C</u>H$_2$CH=CH$_2$), 116.5 (CH=<u>C</u>H$_2$), 123.8 (ArC6), 125.3 (ArC4), 127.4 (ArC5), 129.9 (ArC2), 130.2 (ArC3), 136.0 (ArC1), 136.3 (<u>C</u>H=CH$_2$), 168.3 (C=O); FTIR *v* 3273 (w), 1656 (s), 1586 (w), 1535 (m), 1450 (w), 1370 (w), 1298 (w), 917 (w), 753 (s), 716 (w); MS (ES, +ve) *m/z* 239 (5, M+K), 176 (3, M+H), 146 (80), 105 (100%); HRMS (ES, +ve) calcd for $C_{11}H_{14}NO$ 176.1075, found 176.1072.

<u>1-Allyl-2-nitrobenzene 215</u>[209]

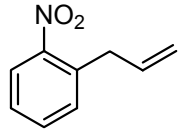

1-Iodo-2-nitrobenzene (776 mg, 3.11 mmol) was dissolved in THF (5 mL) in a 25 mL flask flushed with Ar(g) and fitted with a rubber septum. The flask was placed in a slush bath of acetonitrile and N_2(l) (–40 ^{o}C). Phenylmagnesium bromide (3.44 mL, 1.0 M solution in THF) was added dropwise and stirring continued a further 10 min. A solution of copper (I) cyanide (276 mg, 3.11 mmol) and lithium chloride (264 mg, 6.22 mmol) in THF (2 mL) was added and stirring was continued for a further 10 min. Allyl bromide (0.32 mL, 3.42 mmol) was then added neat and after 2 h the reaction was quenched with sat. NH_4Cl, partitioned between water and Et_2O and extracted with Et_2O (3 x 50 mL). The organic layers were combined and washed with sat. NaCl (4 x 30 mL), and filtered after addition of charcoal. The filtered solution was dried ($MgSO_4$) and the crude residue was subjected to flash silica gel column chromatography (hexanes) to afford the allylated product **215** (415 mg, 82%) as a colourless oil, which was spectroscopically identical to that reported in the literature.[209] ^{1}H NMR (300 MHz) δ 3.72 (dt, 2H, *J* = 1.4, 6.3 Hz, C<u>H</u>$_2$CH=CH$_2$), 5.11 (ddd, 1H, $^{4}J_{HH}$ = 1.6, $^{2}J_{HH}$ = 2.8, $^{3}J_{HH}$ = 16.8 Hz, CH=CH<u>H</u>), 5.15 (ddd, 1H, $^{4}J_{HH}$ = 1.4, $^{2}J_{HH}$ = 2.9, $^{3}J_{HH}$ = 10.2 Hz, CH=C<u>H</u>H), 6.01 (ddt, 1H, $^{3}J_{HH}$ = 6.4, $^{3}J_{HH}$ = 10.2, $^{3}J_{HH}$ = 16.7 Hz, C<u>H</u>=CH$_2$), 7.37-7.43 (m, 2H, ArH3 and 5), 7.57 (dt, 1H, *J* = 1.4, 7.6 Hz, ArH4), 7.94 (dd, 1H, *J* = 1.4, 8.5 Hz, ArH6); ^{13}C NMR (75 MHz) δ 36.9

(CH_2), 117.1 (CH=<u>C</u>H_2), 124.6 (ArC6), 127.3 (ArC5), 131.9 (ArC3), 133.0 (ArC4), 134.8 (ArC2), 135.0 (<u>C</u>H=CH_2), 150.0 (ArC1); MS (ES, +ve) *m/z* 186 (5, M+Na), 146 (5), 135 (10), 121 (5), 94 (18), 83 (100%).

*7.5.2 Nitrogen-based derivatives (**Dimers**)*

***E*-1,4-Di(2-*N*-acetylaniline)-2-butene 229**

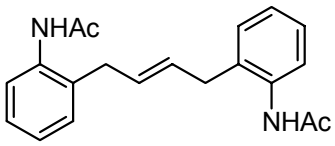

Grubbs 2 catalyst (15 mg, 0.035 mmol, 10 mol %) was added to a solution of *N*-acetyl-2-allylaniline **222** (67 mg, 0.35 mmol) in DCM (6 mL). The mixture was heated at reflux for 17 h then filtered to collect the metathesis product **229** (45 mg, 73%) as a white powder, decomp. 220 ^{o}C. ^{1}H NMR (300 MHz, DMSO) δ 1.99 (s, 6H, CH_3), 3.31 (d, 4H, *J* = 4.2 Hz, CH_2), 5.50 (t, 2H, *J* = 3.3 Hz, C<u>H</u>=C<u>H</u>), 7.04-7.17 (m, 6H, ArH), 7.37 (d, 2H, *J* = 7.7 Hz, ArH6), 9.21 (bs, 2H, NH); ^{13}C NMR (75 MHz,) δ 23.2 (CH_3), 34.0 (CH_2), 125.2 (ArC6), 125.7 (ArC4), 126.2 (ArC5), 129.2 (ArC3), 129.3 (ArC2), 134.2 (ArC1), 135.9 (<u>C</u>H=<u>C</u>H), 169.3 (C=O); FTIR *v* 3275 (w), 1655 (s), 1587 (w), 1534 (m), 1449 (w), 1369 (w), 1296 (s), 1272 (w), 973 (w), 849 (w), 750 (s), 706 (w); MS (ES, +ve) *m/z* 345 (5, M+Na), 323 (5, M+H), 146 (100%), 105 (40); HRMS (ES, +ve) calcd for $C_{20}H_{22}N_2O_2Na$ 345.1579, found 345.1584.

***E*-1,4-Di(2-nitrophenyl)-2-butene 216**

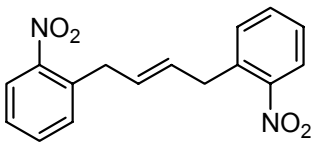

Grubbs 2 catalyst (48 mg, 0.057 mmol, 5 mol %) was added to a solution of 2-allylnitrobenzene **215** (185 mg, 1.14 mmol) in DCM (5 mL), and the flask was flushed with Ar(g) and heated at reflux for 7 h. The reaction mixture was washed with water, and the aqueous layer was extracted with DCM (3 x 20 mL). Charcoal was added to the combined organic layers and filtered. Hexane was added to the filtrate, and a brown solid was crystallised and collected. The brown solid was subjected to gravity silica gel column chromatography (3% EtOAc:hexanes) to yield the homo-coupled product **216** (44 mg, 26%, *E*:*Z* 43:1) as a white solid, m.p. 78 ^{o}C. ^{1}H NMR (500 MHz) δ 3.65-3.66 (m, 4H, CH_2), 3.82*, 5.70 (ddd, 2H, *J* = 1.5, 3.5, 5.0 Hz, C<u>H</u>=C<u>H</u>), 7.34-7.38 (m, 4H, ArH3 and 5), 7.53 (t, 2H, *J* = 7.6 Hz, ArH4), 7.89 (d, 2H, *J* = 8.1 Hz, ArCH6); ^{13}C NMR (125

MHz) δ 35.7 (CH_2), 124.6 (ArC6), 127.3 (ArC5), 129.5 (CH=CH), 131.8 (ArC3), 133.0 (ArC4), 135.1 (ArC2), 149.2 (ArC1); MS (ES, +ve) *m/z* 321 (28, M+Na), 299 (2, M+H), 297 (2), 146 (5), 105 (100%), 64 (40); HRMS (ES, +ve) calcd for $C_{16}H_{14}N_2O_4Na$ 321.0851, found 321.0854.

_E_-1,4-Di(2-nitrophenyl)-2-butene 216, _E_-1,5-di(2-nitrophenyl)-2-pentene 233, _E_-1,4-di(2-nitrophenyl)-1-butene 232 and _E_-1-phenyl-3-(2nitrophenyl)propene 231[233]

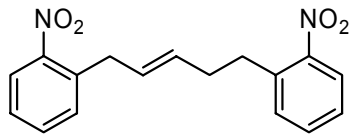

233

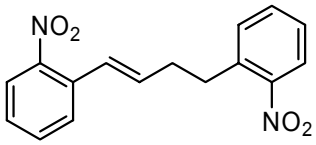

232

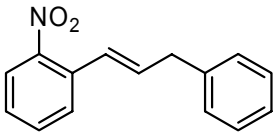

231

Grubbs 2 catalyst (88 mg, 0.103 mmol, 5 mol %) was added to a solution of 2-allylnitrobenzene **215** (337 mg, 2.067 mmol) in DCM (5 mL) and the flask was flushed with Ar(g) and heated at reflux for 19.5 h. The reaction mixture was adsorbed onto silica gel and subjected to flash silica gel column chromatography (2% EtOAc:hexanes) to yield a mixture of **233** (4 mg, 1.3%) and *E* and *Z*-**216** (27 mg, 9%, *E*:*Z* 8.8:1), as a white solid (total mass 31 mg, **233**:**216** 1:6). **233**: ^{1}H NMR (300 MHz) δ 2.34-2.41 (m, 2H, CH_2CH_2Ar), 2.93-2.98 (m, 2H, CH_2CH_2Ar), 3.60 (d, 2H, $^3J_{HH}$ = 4.6 Hz, $ArCH_2CH=CH$), 5.52-5.57 (m, 2H, CH=CH), 7.27-7.94 (m, 4H, ArCH).

Further elution yielded a mixture of *E*-**216**:*Z*-**216**:**233**:**232**:**231** (11.8:1.1:1:2.4:1.2, determined by ^{1}H NMR analysis) with a total mass of 60 mg. **216** (44 mg, 14%, *E*:*Z* 11:1); **233** (3.4 mg, 1%); **232** (8 mg, 3%): ^{1}H NMR (300 MHz) δ 2.67 (dddd, 2H, *J* = 1.4, 7.2, 7.2, 7.2, $CH=CHCH_2$), 3.14 (dd, 2H, *J* = 6.7, 8.5 Hz, CH_2CH_2Ar), 6.25 (ddd, 1H, *J* = 7.0, 7.0, 15.6 Hz, $CH=CHCH_2$), 6.88 (ddd, 1H, *J* = 1.4, 1.4, 15.6 Hz, $CH=CHCH_2$), 7.27-7.94 (m, 8H, ArH); **231** (4 mg, 1%): ^{1}H NMR (300 MHz) δ 3.91 (dd, 2H, *J* = 1.4, 6.7 Hz, CH_2), 6.39 (ddd, 1H, J = 6.7, 6.7, 15.6 Hz, $CH=CHCH_2$), 6.97 (ddd, 1H, *J* = 1.5, 1.5, 15.6 Hz, $CH=CHCH_2$), 7.27-7.94 (m, 9H, ArH).

7.5.3 Nitrogen-based derivatives (**Diols**)

(2*R*,3*R*)-1,4-Di(2-nitrophenyl)-2,3-butandiol 217b

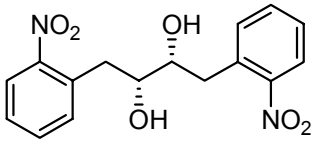

(*R*,*R*)-**217b** was synthesised using *General Procedure A*, alkene **216** (20 mg, 0.067 mmol, *E*:*Z* 18:1), AD mix β (94 mg), methanesulfonamide (6 mg, 0.067 mmol), sodium sulfite (100 mg) and a 1:1 mixture of *t*BuOH and water (0.7 mL), The crude solid was subjected to flash silica gel column chromatography (20% to 30% EtOAc:hexanes) to afford the diol **217b** (10 mg, 45%) as a white solid, m.p. 132-134 ^{o}C, as a mixture of chiral:*meso* diastereomers (16:1). HPLC analysis (35% 2-propanol:hexane, retention times (*R*,*R*)-diol **217b** 19.4 min (major), (*S*,*S*)-diol **217a** 31.0 min (minor)) showed the *ee* of the (*R*,*R*)-diol **217b** was 58%. ^{1}H NMR (300MHz) δ 2.48 (bs, 2H, OH), 3.13 (dd, 2H, $^{2}J_{HH}$ = 13.5 Hz, $^{3}J_{HH}$ = 8.5 Hz, CHH), 3.27 (dd, 2H, $^{2}J_{HH}$ = 13.3 Hz, $^{3}J_{HH}$ = 3.3 Hz, CHH), 3.90 (dd, 2H, $^{3}J_{HH}$ = 3.0 Hz, $^{3}J_{HH}$ = 7.0 Hz, CHOH), 7.41 (t, 2H, $^{3}J_{HH}$ = 7.0 Hz, ArH5), 7.46 (d, 2H, $^{3}J_{HH}$ = 7.7 Hz, ArH3), 7.57 (t, 2H, $^{3}J_{HH}$ = 7.5 Hz, ArH4), 7.94 (d, 2H, $^{3}J_{HH}$ = 8.2 Hz, ArH6); ^{13}C NMR (75 MHz) δ 37.3 (CH_2), 74.1 (CHOH), 124.9 (ArC6), 127.8 (ArC5), 133.1 (ArC4), 133.3 (ArC3), 133.4 (ArC2), 149.9 (ArC1); FTIR *v* 1513 (w), 1344 (w), 1255 (m), 1077 (w), 1023 (m, br), 797 (m), 660 (s), 673 (s), 626 (s); MS (ES, +ve) *m/z* 355 (28, M+Na), 350 (8, M+NH_4), 233 (10), 211 (12), 146 (70), 105 (100%); HRMS (ES, +ve) calcd for $C_{16}H_{16}N_2O_6Na$ 355.0906, found 355.0904.

(2*S*,3*S*)-1,4-Di(2-nitrophenyl)-2,3-butandiol 217a

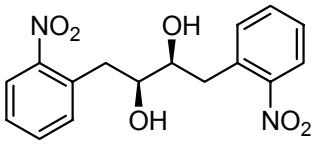

The diol (*S*,*S*)-**217a** was synthesised by *General Procedure A* using alkene **216** (20 mg, 0.067 mmol, *E*:*Z* 18:1), AD mix α (94 mg), methanesulfonamide (6 mg, 0.067 mmol), sodium sulfite (100 mg) and a 1:1 mixture of *t*BuOH and water (0.68 mL). The crude mixture was subjected to flash silica gel column chromatography (20% to 30% EtOAc: hexanes) to yield the diol (*S*,*S*)-**217a** (4 mg, 18%) as a mixture of chiral:*meso* diastereomers (4:1), which was spectroscopically identical to the (*R*,*R*)-**217b** enantiomer. HPLC analysis (35% 2-propanol:hexane, retention times (*R*,*R*)-diol **217b** 19.4 min (minor), (*S*,*S*)-diol **217a** 30.6 min (major)) showed the *ee* of the (*S*,*S*)-diol **217a** was 44%.

(2*S*,3*S*)-1,5-Di(2-nitrophenyl)-2,3-pentandiol 236a

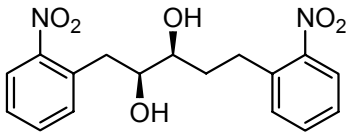

The diol (*R*,*R*)-**236b** was synthesised by *General Procedure A* using a mixture of alkenes **216** and **233** (31 mg, *E*-**216**:*Z*-**216**:**233** 8.5:1:1.4), AD mix α (0.146 g), methanesulfonamide (10 mg, 0.104 mmol), sodium sulfite (155 mg) and a 1:1:0.1 mixture of *t*BuOH:H_2O:THF (1.1 mL). The crude solid was adsorbed onto silica gel, and subsequent separation via flash column chromatography (5% to 20% EtOAc:hexanes) yielded a mixture of diols *meso*-**217m**:(*S*,*S*)-**217a**:(*S*,*S*)-**236a** (4 mg, 1:5.3:3.2). (*S*,*S*)-**236a** (1.4 mg, 30%) was recrystallised from the mixture, as a white solid. HPLC analysis (20% 2-propanol:hexane, retention times (*R*,*R*)-diol **236b** 14.4 min (minor), (*S*,*S*)-diol **236a** 16.6 min (major)) showed the *ee* of the (*S*,*S*)-diol **236a** was 94%. ^{1}H NMR (500MHz) δ 1.89-2.02 (m, 2H, $CH_2C\underline{H}_2Ar$), 2.03 (d, 1H, J = 5.4 Hz, $ArCH_2CH(OH)CH(O\underline{H})$), 2.31 (d, 1H, J = 4.7 Hz, $ArCH_2CH(O\underline{H})$), 2.99 (dd, 1H, $^3J_{HH}$ = 9.7 Hz, $^2J_{HH}$ = 13.2 Hz, $ArC\underline{H}HCH(OH)$), 3.03 (dd, 1H, $^2J_{HH}$ = 13.8 Hz, $^3J_{HH}$ = 9.2 Hz, $C\underline{H}HCH_2Ar$), 3.13 (ddd, 1H, $^3J_{HH}$ = 5.5 Hz, $^3J_{HH}$ = 9.9 Hz, $^2J_{HH}$ = 13.7 Hz, $CH\underline{H}CH_2Ar$), 3.22 (dd, 1H, $^2J_{HH}$ = 13.6 Hz, $^3J_{HH}$ = 3.8 Hz, $ArCH\underline{H}CH(OH)$), 3.59 (ddd, 1H, $^3J_{HH}$ = 10.2 Hz, $^3J_{HH}$ = 8.6 Hz, $^3J_{HOH}$ = 4.3 Hz, $ArCH_2CH(OH)C\underline{H}(OH)$), 3.83 (dt, 1H, $^3J_{HH}$ = 9.4 Hz, $^3J_{HOH}$ = 4.2 Hz, $ArCH_2C\underline{H}(OH)$), 7.35-7.47 (m, 4H, ArH), 7.54 (t, 1H, J = 7.4 Hz, ArH), 7.56 (t, 1H, J = 7.4 Hz, ArH), 7.93 (t, 2H, J = 7.7 Hz, ArCH); MS (ES, +ve) *m/z* 369 (4, M+Na), 329 (2), 233 (20), 211 (12), 170 (11), 148 (10), 106 (100%), 83 (10), 64 (20); HRMS (ES, +ve) calcd for $C_{17}H_{18}N_2O_6Na$ 369.1063, found 369.1048.

The remaining filtrate solidified as **217a** (3 mg, 9%) as a mixture of chiral:*meso* diastereomers (5.3:1). HPLC analysis (20% 2-propanol:hexane, retention times (*R*,*R*)-diol **217b** 13.9 min (minor), (*S*,*S*)-diol **217a** 24.6 min (major)) showed the *ee* of the (*S*,*S*)-diol **217a** was 14%.

7.6 Non-coordinating derivatives

*7.6.1 Non-coordinating derivatives (**Monomers**)*

2-Allyl-1-bromobenzene 239[214]

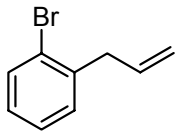

Magnesium turnings (105 mg, 4.32 mmol) were washed sequentially with 1M HCl, EtOH and Et_2O, oven-dried and added to THF (2 mL) in a two-necked flask equipped with a condenser. Isopropyl bromide (0.37 mL, 3.88 mmol), which had been distilled from CaH_2, was added. After 5 min, the reaction mixture began to boil. After 15 min, the clear solution turned grey, and a white precipitate formed. Stirring was continued for a further 30 min, at which time 0.5 mL of the solution was drawn out, and added to a solution of 2-bromoiodobenzene (0.1 mL, 0.778 mmol) in THF (5 mL) on a NaCl/ice bath. Allyl bromide (0.08 mL, 0.855 mmol) was added after 30 min. The reaction was stirred under N_2(g) and allowed to return to RT (18 ^oC). The reaction was quenched after 22 h with sat. NH_4Cl (5 mL), and partitioned between Et_2O and water. The aqueous layer was extracted with Et_2O (3 x 20 mL), and the combined organic layers were washed with sat. NaCl and dried ($MgSO_4$). The crude oil was subjected to gravity silica column chromatography (1% EtOAc:hexanes) to afford the bromide **239** (144 mg, 94%) as a volatile, colourless liquid, which was spectroscopically identical to that reported in the literature.[214] ^1H NMR (500 MHz) δ 3.54 (dd, 1H, J = 1.3, 1.3 Hz, C<u>H</u>HCH=CH_2), 3.56 (dd, 1H, J = 1.3, 1.3 Hz, CH<u>H</u>CH=CH_2), 5.11 (dddd, 1H, J = 1.7, 1.7, 1.7, 17.0 Hz, CH=CH<u>H</u>$_E$), 5.15 (dddd, 1H, J = 1.5, 1.5, 1.4, 10.1 Hz, CH=C<u>H</u>$_Z$H), 6.01 (dddd, 1H, J = 6.5, 6.5, 10.2, 16.7 Hz, C<u>H</u>=CH_2), 7.20-7.31 (m, 3H, ArH), 7.58 (d, 1H, J = 8.5 Hz, ArH6); ^{13}C NMR (125 MHz) δ 40.2 (CH_2), 116.5 (CH=<u>C</u>H_2), 124.5 (ArC1), 127.4 (ArC4), 127.8 (ArC5), 130.4 (ArC3), 132.7 (ArC6), 135.5 (<u>C</u>H=CH_2), 139.4 (ArC2).

2-Allyltoluene 241[234]

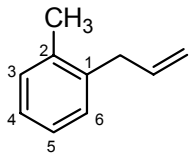

Magnesium turnings (217 mg, 12.0 mmol) were crushed and washed sequentially with 1M HCl, EtOH and Et_2O, and were placed in an oven-dried flask. The flask and magnesium were flame-dried under a N_2(g) purge. THF (8 mL) was added, followed by 2-bromotoluene that had been distilled from CaH_2 (0.2 mL, 1.67 mmol). One crystal of iodine was added,

and the flask was heated in an oil bath (50 ^{o}C). The remaining 2-bromotoluene (0.7 mL, 2.8 mmol) was added portionwise over 1 h, and the reaction was stirred for a further 30 min, at which time allyl bromide (1.26 mL, 14.8 mmol) was added. The reaction was stirred under N_2(g) and was quenched after 15 h with sat. NH_4Cl (5 mL). The reaction mixture was extracted with Et_2O (3 x 25 mL), the combined organic layers were dried ($MgSO_4$) and the solvent was evaporated *in vacuo*. The crude mixture was subjected to flash silica gel column chromatography and elution with hexanes gave the bromide **241** (458 mg, 35%) as a volatile, colourless liquid, which was spectroscopically identical to that reported in the literature.[234] ^{1}H NMR (500 MHz) δ 2.33 (s, 3H, CH_3), 3.41 (d, 2H, *J* = 6.5 Hz, C$\underline{H}_2$CH=CH$_2$), 5.03 (d, 1H, *J* = 17 Hz, *E* CH=CH$\underline{H}$), 5.09 (d, 1H, *J* = 10 Hz, *Z* CH=C$\underline{H}$H), 5.96-6.02 (m, 1H, C$\underline{H}$=CH$_2$), 7.17 (s, 4H, ArH); ^{13}C NMR (125 MHz) δ 19.3 (CH_3), 37.7 ($\underline{C}H_2$CH=CH$_2$), 115.6 (CH=$\underline{C}H_2$), 126.0 (ArC4 or ArC5), 126.3 (ArC4 or ArC5), 129.1 (ArC3 or ArC6), 130.1 (ArC3 or ArC6), 136.3 (ArC2), 136.6 ($\underline{C}$H=CH$_2$), 138.0 (ArC1); FTIR *v* 2360 (w), 1459 (w), 995 (w), 910 (w), 739 (m), 661 (s); MS (EI +ve) *m/z* 132 (56, M^+), 131 (100%, M-H), 115 (33), 103 (58); HRMS (ES, +ve) calcd for $C_{10}H_{12}$ 132.0939, found 132.0934.

*7.6.2 Non-coordinating derivatives (**Dimers**)*

<u>*E*-1,4-Diphenyl-2-butene 170</u>[235]

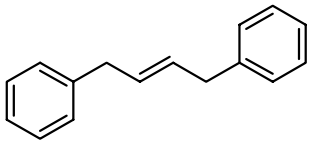

Grubbs 1 catalyst (45 mg, 2.5 mol %, 0.11 mmol) was added to a solution of allylbenzene (260 mg, 2.20 mmol) in DCM (10 mL) and flushed with Ar(g). The solution was heated at reflux for 18 h under an Ar(g) atmosphere. The solvent was removed *in vacuo*, and the crude mixture was subjected to flash silica gel column chromatography. Elution with hexanes gave the homo-coupled product **170** (204 mg, 89%, *E*:*Z* 4.7:1) as a colourless, volatile oil, which was spectroscopically identical to that reported in the literature.[235] ^{1}H NMR (500 MHz) δ 3.36 (d, 4H, *J* = 5.1 Hz, C$\underline{H}_2$), 3.51* (d, *J* = 5.5 Hz, C$\underline{H}_2$), 5.65-5.73 (m, 2H, C$\underline{H}$=C$\underline{H}$), 7.17-7.31 (m, 10H, ArH); ^{13}C NMR (125 MHz) δ 33.5*, 38.9 ($\underline{C}H_2$CH=CH$_2$), 125.9 (ArC4), 128.3 (ArC3), 128.4 (ArC2), 130.4 ($\underline{C}$H=$\underline{C}$H), 140.7 (ArC1); FTIR *v* 3026 (w), 2362 (w), 1602 (w), 1494 (m), 1452 (w), 969 (w), 737 (w), 697 (s); MS (EI, +ve) *m/z* 208 (49, M^+), 130 (48), 117 (100%), 104 (50); HRMS (EI, +ve) calcd for $C_{16}H_{16}$ 208.1252, found 208.1257.

_E_-1,4-Di-(2-tolyl)-2-butene 242[236]

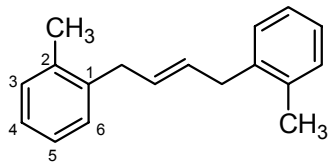

Grubbs 1 catalyst (31 mg, 0.038 mmol, 2.5 mol %) was added to a solution of alkene **241** (200 mg, 1.515 mmol) in DCM (6 mL) and the solution was heated at reflux for 27 h. The solvent was evaporated and the crude mixture was subjected to flash silica gel column chromatography and eluted with hexanes to give the dimer **242** (73 mg, *E*:*Z* 6:1) as a colourless oil. Further elution yielded a second portion of **242** (64 mg, *E*:*Z* 3:1), giving a total yield of 77%, which was spectrscopically identical to that reported in the literature.[236] ^{1}H NMR (500 MHz) δ 2.27 (s, 6H, CH_3), 2.32*, 3.33 (d, 4H, *J* = 3.5 Hz, CH_2), 3.48*, 5.56 (m, 2H, C<u>H</u>=C<u>H</u>), 5.65*, 7.11-7.14 (m, 8H, ArH); ^{13}C NMR (500 MHz) δ 19.3 (CH_3), 31.3*, 36.4 (CH_2), 125.9 (ArC4 or ArC5), 126.0*, 126.1 (ArC4 or ArC5), 128.5*, 128.9 (ArC3 or ArC6), 129.4 (<u>C</u>H=<u>C</u>H), 130.0 (ArC3 or ArC6), 130.1*, 136.2 (ArC2), 138.8 (ArC1); MS (EI, +ve) *m/z* 236 (7, M^+), 119 (100%); HRMS (EI, +ve) calcd for $C_{18}H_{20}$ 236.1565, found 236.1565.

_E_-1,4-Di(2-bromophenyl)-2-butene 234, _Z_-1,4-di(2-bromophenyl)-2-butene 234, _E_-1,4-di(2-bromophenyl)-1-butene 244, _E_-1,5-di(2-bromophenyl)-2-pentene 245, _E_-3-(2-bromophenyl)-1-phenylpropene 246[237] **and _E_-1-(2-bromophenyl)-3-phenylpropene 247**

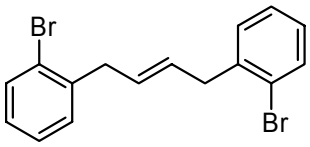

***E*-243**

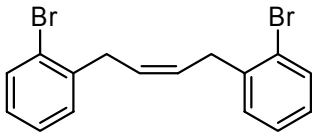

***Z*-243**

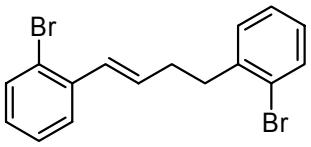

244

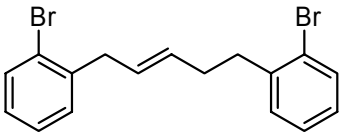

245

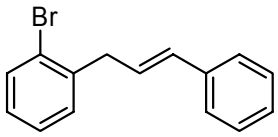

246

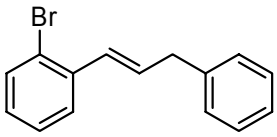

247

To a solution of **239** (140 mg, 0.71 mmol) in DCM (5 mL) was added Grubbs 2 catalyst (30 mg, 0.036 mmol, 5 mol %) and the reaction was heated at reflux for 23 h. The solvent was removed *in vacuo* and the crude mixture was subjected to flash silica gel

column chromatography (hexanes) to give a mixture of alkenes *E*-**234**:*Z*-**234**:**244**:**245**:**246**:**247** (6.3:1:1.2:1.1:1:1.2, determined by ^{1}H NMR analysis), with a total mass of 34 mg. *E*-**234** (18 mg, 14%): ^{1}H NMR (500 MHz) δ 3.49 (dd, 4H, *J* = 1.6, 3.4 Hz, CH_2), 5.65-5.67 (m, 2H, CH=CH), 7.04-7.57 (m, 8H, ArH). *Z*-**234** (3 mg, 2%): ^{1}H NMR (500 MHz) δ 3.63 (d, 4H, *J* = 5.3 Hz, CH_2), 5.61-5.63 (m, 2H, CH=CH), 7.04-7.57 (m, 8H, ArH). **244** (3.5 mg, 3%): ^{1}H NMR (500 MHz) δ 2.55-2.60 (m, 2H, CH=CHC$\underline{H}_2$), 2.92-2.95 (m, 2H, CH_2Ar), 6.20 (dt, 1H, *J* = 6.9, 6.9, 15.6 Hz, ArCH=C$\underline{H}$), 6.74 (d, 1H, *J* = 15.7 Hz, ArC$\underline{H}$=CH), 7.04-7.57 (m, 8H, ArH). **245** (3.2 mg, 2%): ^{1}H NMR (500 MHz) δ 2.31-2.37 (m, 2H, C$\underline{H}_2$CH_2Ar), 2.79-2.82 (m, 2H, CH_2C$\underline{H}_2$Ar), 3.43-3.45 (m, 2H, ArC$\underline{H}_2$CH=CH), 5.55-5.58 (m, 2H, C$\underline{H}$=C$\underline{H}$), 7.04-7.57 (m, 8H, ArH). **246** (3 mg, 2%): ^{1}H NMR (500 MHz) δ 3.71 (dd, 2H, *J* = 1.3, 7.0 Hz, CH_2), 6.34 (dt, 1H, *J* = 6.7, 6.7, 15.8 Hz, CH_2C$\underline{H}$=CH), 6.45 (d, 1H, *J* = 15.9 Hz, CH_2CH=C$\underline{H}$), 7.04-7.57 (m, 9H, ArH). **247** (3.5 mg, 3%): ^{1}H NMR (500 MHz) δ 3.66 (dd, 2H, *J* = 0.9, 6.7 Hz, CH_2), 6.27 (dt, 1H, *J* = 6.9, 6.9, 15.6 Hz, CH=C$\underline{H}$$CH_2$), 6.82 (d, 1H, *J* = 15.7 Hz, C$\underline{H}$=CHCH_2), 7.04-7.57 (m, 9H, ArH).

*7.6.3 Non-coordinating derivatives (**Diols**)*

(2*S*,3*S*)-1,4-Diphenyl-2,3-butandiol 171a[238]

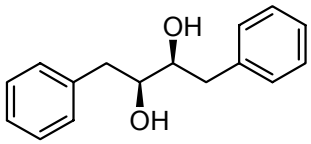

The diol (*S*,*S*)-**171a** was synthesised by *General Procedure A* using alkene **170** (83 mg, 0.398 mmol, *E*:*Z* 5:1), AD mix α (558 mg), methanesulfonamide (38 mg, 0.398 mmol), sodium sulfite (594 mg) in *t*BuOH (2 mL) and water (2 mL). The crude residue was subjected to flash silica gel column chromatography (5% to 50% EtOAc:hexanes) to yield the diol **171a** (85 mg, 88%) as a white solid, m.p. 132-134 ^{o}C, as a mixture of chiral:*meso* diastereomers (4:1), which was spectroscopically identical to that reported in the literature.[238] HPLC analysis (hexane to 50% 2-propanol:hexane, retention times (*R*,*R*)-diol **171b** 18.6 min (minor), (*S*,*S*)-diol **171a** 20.0 min (major)) showed the *ee* of the (*S*,*S*)-diol **171a** was 93%. ^{1}H NMR (500 MHz) δ 1.91*, 2.03 (bs, 2H, OH), 2.81* (dd, $^2J_{HH}$ = 13.9 Hz, $^3J_{HH}$ = 8.9 Hz, *meso* C$\underline{H}$H), 2.85 (dd, 2H, $^2J_{HH}$ = 13.7 Hz, $^3J_{HH}$ = 8.4 Hz, C$\underline{H}$H), 2.92 (dd, 2H, $^2J_{HH}$ = 13.7 Hz, $^3J_{HH}$ = 4.3 Hz, CH$\underline{H}$), 3.01 (dd, $^2J_{HH}$ = 13.8 Hz, $^3J_{HH}$ = 2.9 Hz, *meso* CH$\underline{H}$), 3.74-3.78 (m, 2H, C$\underline{H}$OH), 3.86-3.91*, 7.17-7.39 (m, 10H, ArH); ^{13}C NMR (125 MHz) δ 38.3*, 40.3 (CH_2), 74.0 (CHOH), 74.7* (CHOH), 126.5

(ArC4), 126.6*, 128.6 (ArC3), 128.7*, 129.4 (ArC2), 138.0 (ArC1); FTIR *v* 3335 (b), 1491 (w), 1454 (w), 1213 (w), 1106 (w), 1045 (m), 1013 (w), 948 (w), 753 (s), 702 (s); MS (ES, +ve) *m/z* 265 (5, M+Na), 260 (5, M+NH_4), 146 (100%), 105 (100%); HRMS (ES, +ve) calcd for $C_{16}H_{18}O_2Na$ 265.1204, found 265.1205.

(2*R*,3*R*)-1,4-Diphenyl-2,3-butandiol 171b[238]

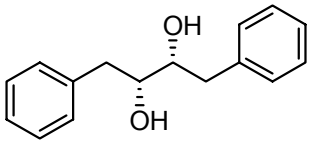

The diol (*R*,*R*)-**171b** was synthesised by *General Procedure A* using alkene **170** (110 mg, 0.523 mmol, *E*:*Z* 5:1), methanesulfonamide (50 mg, 0.528 mmol), *t*BuOH (2.6 mL), water (2.6 mL), sodium sulfite (788 mg) and AD mix β (739 mg). The crude residue was subjected to flash silica gel column chromatography (10% to 50% EtOAc:hexanes) to give the diol (*R*,*R*)-**171b** (107 mg, 84%) as a white solid, m.p. 132-134 ^oC, as a mixture of chiral:*meso* diastereomers (7.5:1), with spectral properties identical to the (*S*,*S*)-**171a** diol. HPLC analysis (5% to 50% 2-propanol:hexane, retention times (*R*,*R*)-diol **171b** 18.2 min (major), (*S*,*S*)-diol **171a** 20.1 min (minor)) showed the *ee* of the (*R*,*R*)-diol **171b** was 95%.

(2*S*,3*S*)-1,4-Di-(2-tolyl)-2,3-butandiol 248a

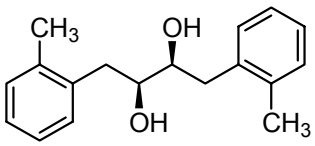

The diol (*S*,S)-**248a** was synthesised by *General Procedure A* using alkene **242** (62 mg, 0.263 mmol, *E*:*Z* 6:1), AD mix α (356 mg), methanesulfonamide (24 mg, 0.263 mmol), sodium sulfite (381 mg) in a 1:1 mixture of *t*BuOH and water (2.6 mL). The diol **248a** (46 mg, 65%) was isolated using flash silica gel column chromatography (hexanes to 50% EtOAc:hexanes) as a white solid, m.p. 66-68 ^oC, as a mixture of chiral:*meso* diastereomers (10:1). HPLC analysis (20% to 40% 2-propanol:hexane, retention times (*R*,*R*)-diol **248b** 13.5 min (minor), (*S*,*S*)-diol **248a** 19.0 min (major)) showed the *ee* of the (*S*,*S*)-diol **248a** was 62%. ^1H NMR (300 MHz) δ 2.34 (d, 2H, *J* = 4.8 Hz, OH), 2.37 (s, 6H, CH_3), 2.83 (d, 2H, *J* = 2.7 Hz, C<u>H</u>H), 2.97 (s, 2H, CH<u>H</u>), 3.82-3.84 (m, 2H, C<u>H</u>OH), 7.19-7.26 (m, 8H, ArH); ^{13}C NMR (75 MHz) δ 19.58 (CH_3), 19.64*, 35.4*, 37.5 (CH_2), 73.0 (CHOH), 74.0*, 126.0 (ArC5), 126.6 (ArC4), 130.0 (ArC6), 130.4 (ArC3), 136.3 (ArC2), 136.6 (ArC1); FTIR *v* 3388 (w), 2500 (w), 1491 (w), 1448 (w), 1099 (w), 1030 (w), 742 (m), 669 (s); MS (ES, +ve) *m/z* 293 (12, M+Na), 288 (13,

M+NH_4), 143 (10), 105 (100%, Ph(CH_3)CH_2^+), 102 (38), 84 (30); HRMS (ES, +ve) calcd for $C_{18}H_{22}O_2Na$ 293.1517, found 293.1517.

(2*R*,3*R*)-1,4-Di-(2-tolyl)-2,3-butandiol 248b

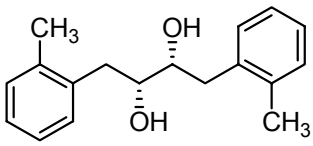

The diol (*R*,*R*)-**248b** was synthesised by *General Procedure A* using alkene **242** (60 mg, 0.254 mmol, *E*:*Z* 3:1), AD mix β (356 mg), methanesulfonamide (24 mg, 0.263 mmol) and sodium sulfite (381 mg) in a 1:1 mixture of *t*BuOH and water (2.6 mL) to yield **248b** (31 mg, 45%) as a white solid, m.p. 67-69 °C, as a mixture of chiral:*meso* diastereomers (8:1), which had identical spectroscopic properties to (*S*,*S*)-**248a**. HPLC analysis (20% to 40% 2-propanol:hexane, retention times (*R*,*R*)-diol **248b** 13.3 min (major), (*S*,*S*)-diol **248a** 19.7 min (minor)) showed the *ee* of the (*R*,*R*)-diol **248b** was 70%.

7.7 *Meta* and *para* substituted derivatives

*7.7.1 Meta and para substituted derivatives (**Monomers**)*

3-Allyl-1-methoxybenzene 251[216]

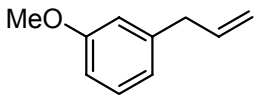

Magnesium turnings (292 mg, 12.0 mmol) were washed sequentially with 1M HCl, EtOH and Et_2O and placed in an oven-dried flask. The flask and magnesium were then flame-dried under a N_2(g) purge. THF (10 mL) was added and 3-bromoanisole (0.27 mL, 2.13 mmol) was slowly added. One crystal of iodine was added, and the reaction vessel was warmed in an oil bath (25 °C). The remaining 3-bromoanisole (1.0 mL, 7.87 mmol) was slowly added in 4 portions, over 1 h. The reaction was stirred for a further 1 h; some residual magnesium remained, and a grey precipitate was observed. Allylbromide (1.7 mL, 20.0 mmol) was slowly added, and stirring was continued at 25 °C for 20 h. The mixture was partitioned between Et_2O and sat. NH_4Cl. The aqueous layer was extracted with a Et_2O (3 x 25 mL), the combined organic layers dried ($MgSO_4$) and the solvent was evaporated under reduced pressure. The crude oil was subjected to flash silica gel column chromatography (hexanes) to afford the protected phenol **251** (855 mg, 58%) as a colourless oil, which was spectroscopically identical to that reported in the literature.[216] ^{1}H NMR (500 MHz) δ 3.35 (d, 2H, *J* = 6.6 Hz, CH_2), 3.77 (s, 3H, OCH_3),

5.05-5.10 (m, 2H, CH=C<u>H</u>$_2$), 5.95 (tdd, 1H, *J* = 6.7, 9.9, 13.5 Hz, C<u>H</u>=CH$_2$), 6.73-6.75 (m, 2H, ArH2 and ArH6), 6.77 (d, 1H, *J* = 7.5 Hz, ArH4), 7.19 (t, 1H, *J* = 8.2 Hz, ArH5); ^{13}C NMR (125 MHz) δ 40.2 (CH$_2$), 55.0 (OCH$_3$), 111.4 (ArC6), 114.2 (ArC2), 115.8 (CH=<u>C</u>H$_2$), 120.9 (ArC4), 129.3 (ArC5), 137.2 (<u>C</u>H=CH$_2$), 141.6 (ArC3), 159.7 (ArC1); FTIR *v* 1600 (m), 1585 (m), 1489 (m), 1455 (w), 1436 (w), 1259 (s), 1162 (w), 1149 (m), 1049 (m), 914 (m), 877 (w), 778 (m), 748 (m); MS (EI, +ve) *m/z* 148 (12, M$^+$), 147 (20, M-H), 131 (59), 120 (100%), 109 (83); HRMS (EI, +ve) calcd for $C_{10}H_{12}O$ 148.0888, found 148.0890.

*7.7.2 Meta and para substituted derivatives (**Dimers**)*

<u>*E*-1,4-Di(3-methoxyphenyl)-2-butene 255</u>[239]

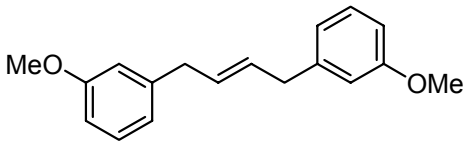

1-Methoxy-3-allylbenzene **251** (500 mg, 3.37 mmol) was added to a solution of Grubbs 1 catalyst (70 mg, 2.5 mol %) in DCM (10 mL) and the flask was flushed with N_2(g). The reaction mixture was heated at reflux for 15 h and subjected to flash silica gel column chromatography (1% EtOAc:hexanes) to yield the homo-coupled product **255** (283 mg, 63%, *E*:*Z* 4.5:1) as a colourless oil.‡ ^{1}H NMR (500 MHz) δ 3.34 (d, 4H, *J* = 4.3 Hz, CH$_2$), 3.48* (d, *J* = 5.1 Hz, CH$_2$), 3.76*, 3.77 (s, 6H, OCH$_3$), 5.66-5.67 (m, 2H, <u>C</u>H=<u>C</u>H), 5.70-5.72*, 6.74 (s, 2H, ArH2), 6.72-6.81 (m, 4H, ArH4 and ArH6), 7.17-7.21 (m, 2H, ArH5); ^{13}C NMR (125 MHz) δ 33.5*, 38.9 (CH$_2$), 55.1 (OCH$_3$), 111.3 (ArC6), 113.4*, 114.0*, 114.1 (ArC2), 120.7*, 120.9 (ArC4), 129.0* (<u>C</u>H=<u>C</u>H), 129.3 (ArC5), 129.4*, 130.3 (<u>C</u>H=<u>C</u>H), 142.3 (ArC3), 159.7 (ArC1); MS (EI, +ve) *m/z* 268 (58, M$^+$), 147 (100%), 134 (47), 122 (57); HRMS (EI, +ve) calcd for $C_{18}H_{20}O_2$ 268.1463, found 268.1464.

<u>*E*-1,4-Di(4-methoxyphenyl)-2-butene 256</u>[240]

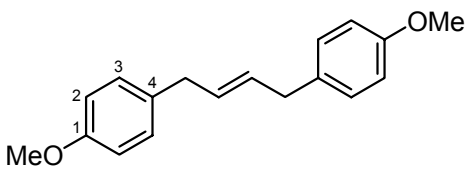

4-Allyl-2-methoxybenzene (500 mg, 3.374 mmol) was added to a solution of Grubbs 1 catalyst (69 mg, 2.5 mol %) in DCM (10 mL)

‡ No physical or spectral data reported in reference 239.

and the flask was flushed with Ar(g). The reaction mixture was heated at reflux for 4.5 hours and subjected to flash silica gel column chromatography (1% EtOAc:hexanes) to yield the homo-coupled product **256** (440 mg, 97 %, *E*:*Z* 6.2:1) as a white solid, m.p. 61-64 ^{o}C, which was spectroscopically identical to that reported in the literature.[240] ^{1}H NMR (300MHz) δ 3.20-3.22 (m, 4H, CH_2), 3.35-3.36*, 3.676 (s, 6H, OCH_3), 3.682*, 5.51-5.56 (m, 2H, C<u>H</u>=C<u>H</u>), 5.57-5.59*, 6.71-6.77 (m, 4H, ArH2), 6.99-7.02 (m, 4H, ArH3); ^{13}C NMR (75 MHz) δ 32.5*, 38.0 (CH_2), 55.2 (OCH_3), 113.8 (ArC2), 113.9*, 129.2* (<u>C</u>H=<u>C</u>H), 129.4 (ArC3), 130.5 (<u>C</u>H=<u>C</u>H), 132.8 (ArC4), 157.9 (ArC1); MS (EI, +ve) *m/z* 268 (71, M^+), 160 (62), 147 (100%), 134 (54), 121 (86); HRMS (EI, +ve) calcd for $C_{18}H_{20}O_2$ 268.1463, found 268.1469.

*7.7.3 Meta and para substituted derivatives (**Diols**)*

(2*S*,3*S*)-1,4-Di(3-methoxyphenyl)-2,3-butandiol 257a

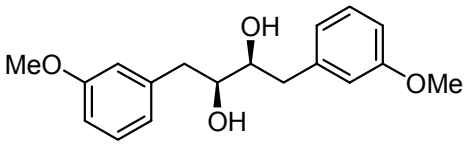

The diol (*S*,*S*)-**257a** was synthesised by *General Procedure A* using alkene **255** (98 mg, 0.366 mmol, *E*:*Z* 4.3:1), AD mix α (512 mg), methanesulfonamide (35 mg, 0.366 mmol) and sodium sulfite (549 mg) in a 1:1 mixture of *t*BuOH and water (3.7 mL). The crude diol was subjected to flash silica gel column chromatography to give (*S*,*S*)-**257a** (85 mg, 77%) a white solid, m.p. 52-54 ^{o}C. HPLC analysis (40% 2-propanol:hexane, retention times (*R*,*R*)-diol **257b** 13.1 min (minor), (*S*,*S*)-diol **257a** 16.1 min (major)) showed the *ee* of the (*S*,*S*)-diol **257a** was 73%. ^{1}H NMR (500 MHz) δ 2.05 (bs, 2H, OH), 2.83 (dd, 2H, $^{2}J_{HH}$ = 13.6 Hz, $^{3}J_{HH}$ = 8.3 Hz, C<u>H</u>H), 2.89 (dd, 2H, $^{2}J_{HH}$ = 13.6 Hz, $^{3}J_{HH}$ = 4.3 Hz, CH<u>H</u>), 3.75-3.82 (m, 2H, C<u>H</u>OH), 3.79 (s, 6H, OCH_3), 6.77 (s, 2H, ArH2), 6.79-6.82 (m, 4H, ArH4 and ArH6), 7.23 (t, 2H, *J* = 7.8 Hz, ArH5); ^{13}C NMR (125 MHz) δ 40.4 (CH_2), 55.2 (OCH_3), 74.0 (CHOH), 111.9 (ArC6), 115.1 (ArC2), 121.7 (ArC4), 129.6 (ArC5), 139.6 (ArC3), 159.8 (ArC1); FTIR *v* 3329 (br), 1611 (w), 1583 (m), 1487 (m), 1454 (w), 1264 (m), 1104 (w), 1043 (s), 930 (w), 763 (w); MS (ES, +ve) *m/z* 325 (100%, M+Na), 320 (90, M+NH_4); HRMS (ES, +ve) calcd for $C_{18}H_{22}O_4Na$ 325.1416, found 325.1403.

(2*R*,3*R*)-1,4-Di(3-methoxyphenyl)-2,3-butandiol 257b

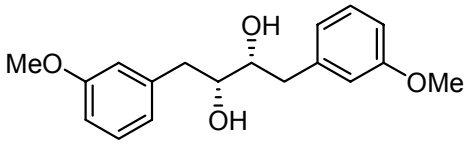

The diol (*R*,*R*)-**257b** was synthesised by *General Procedure A* using alkene **255** (98 mg, 0.366 mmol, *E*:*Z* 4.3:1), AD mix α (512 mg), methanesulfonamide (35 mg, 0.366 mmol) and sodium sulfite (549 mg) in a 1:1 mixture of *t*BuOH and water (3.7 mL). The diol (*R*,*R*)-**257a** (94 mg, 85%) was purified via flash silica gel column chromatography as a white solid, m.p. 52-56 ^{o}C, which had identical spectral properties to the diol (*S*,*S*)-**257a**. HPLC analysis (40% 2-propanol:hexane, retention times (*R*,*R*)-diol **257b** 12.8 min (major), (*S*,*S*)-diol **257a** 16.2 min (minor)) showed the *ee* of the (*R*,*R*)-diol **208b** was 76%.

(2*S*,3*S*)-1,4-Di(4-methoxyphenyl)-2,3-butandiol 258a[240]

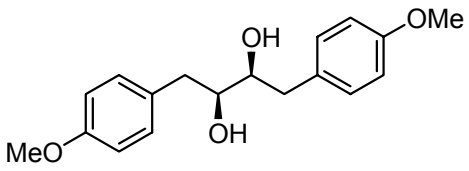

The diol (*S*,*S*)-**258a** was synthesised by *General Procedure A* using alkene **256** (200 mg, 0.745 mmol, *E*:*Z* 6.2:1), AD mix α (1.043 g), methanesulfonamide (71 mg, 0.745 mmol) and sodium sulfite (1.113 g) in a 1:1 mixture of *t*BuOH and water (7.4 mL). The diol (*S*,*S*)-**258a** was recrystallised from DCM/hexanes as a white powder (202 mg, 90%) as a mixture of chiral:*meso* diastereomers (8.8:1), m.p. 100-102 ^{o}C, which was spectroscopically identical to that reported in the literature.[240] HPLC analysis (40% isopropanol:hexane, retention times (*R*,*R*)-diol **258b** 12.3 min (minor), (*S*,*S*)-diol **258a** 13.8 min (major)) showed the *ee* of the (*S*,*S*)-diol **258a** was 85%. ^{1}H NMR (500 MHz) δ 2.01 (bs, 2H, OH), 2.77 (dd, 2H, $^{2}J_{HH}$ = 13.8 Hz, $^{3}J_{HH}$ = 8.1 Hz, CHH), 2.84 (dd, 2H, $^{2}J_{HH}$ = 13.8 Hz, $^{3}J_{HH}$ = 4.2 Hz, CHH), 2.92* (dd, $^{2}J_{HH}$ = 13.9 Hz, $^{3}J_{HH}$ = 2.6 Hz, CHH), 3.67-3.69 (m, 2H, CHOH), 3.79 (s, 6H, OCH_3), 6.84 (d, 4H, *J* = 8.5 Hz, ArH2), 7.13 (d, 4H, *J* = 8.4 Hz, ArH3); ^{13}C NMR (125 MHz) δ 37.4*, 39.4 (CH_2), 55.2 (OCH_3), 74.0 (CHOH), 74.7* (CHOH), 114.0 (ArC2), 114.1*, 130.0 (ArC4), 130.3 (ArC3), 158.3 (ArC1); FTIR *v* 3352 (br), 1614 (w), 1512 (s), 1468 (w), 1248 (s), 1178 (m), 1032 (s), 1021 (s), 804 (s); MS (ES, +ve) *m/z* 325 (100%, M+Na), 320 (90, M+H); HRMS (ES, +ve) calcd for $C_{18}H_{22}O_4Na$ 325.1416, found 325.1407.

(2*R*,3*R*)-1,4-Di(4-methoxyphenyl)-2,3-butandiol 258b[240]

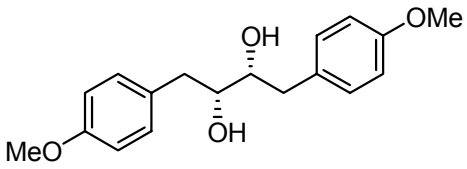

The diol (*R*,*R*)-**258b** was synthesised by *General Procedure A* using alkene **256** (200 mg, 0.745 mmol, *E*:*Z* 6.2:1), AD mix β (1.043 g), methanesulfonamide (71 mg, 0.745 mmol) and sodium sulfite (1.113 g) in a 1:1 mixture of *t*BuOH and water (7.4 mL). The diol (*R*,*R*)-**258b** (217 mg, 96%) was recrystallised from DCM/hexanes as a white powder as a mixture of chiral:*meso* diastereomers (9.1:1), m.p. 104-105 °C, which had identical spectral properties to the (*S*,*S*)-**258a** diol. HPLC analysis (40% isopropanol:hexane, retention times (*R*,*R*)-diol **258b** 12.0 min (major), (*S*,*S*)-diol **258a** 14.1 min (minor)) showed the *ee* of the (*R*,*R*)-diol **258b** was 87%.

7.8 AD reaction of terminal alkenes

(2*S*)-3-(2-Methoxyphenyl)-1,2-propandiol 259a[217,218]

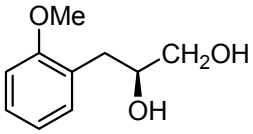

General Procedure B:[3] AD mix α (804 mg) was dissolved in *t*BuOH (2.9 mL) and water (2.9 mL). The reaction vessel was placed on an icebath, and alkene **197** (85 mg, 0.574 mmol) was added. The reaction was stirred vigorously and allowed to return to RT after 1 h. After 24 h the reaction was returned to the ice bath and sodium sulfite was added (861 mg). Stirring was continued for 1 h, before the mixture was returned to RT and partitioned between EtOAc and water. The aqueous layer was extracted with EtOAc (3 x 20 mL), the combined organic layers were dried ($MgSO_4$), the solvent was evaporated *in vacuo* and the crude solid was subjected to flash silica gel column chromatography (50% EtOAc:hexanes) to afford the diol (*S*)-**259a** (102 mg, 97%) as a white solid, m.p. 48 °C. Immediately after isolation, the flask was stored at -15 °C [freezer] under Ar(g).‡ $[\alpha]_D^{23}$ = –3.8° (*c* 0.045, $CHCl_3$). ^{1}H NMR (500 MHz) δ 2.75 (bs, 1H, OH), 2.80 (bs, 1H, OH), 2.78 (dd, 1H, $^2J_{HH}$ = 13.5 Hz, $^3J_{HH}$ = 7.4 Hz ArC<u>H</u>H), 2.84 (dd, 1H, $^2J_{HH}$ = 13.5 Hz, $^3J_{HH}$ = 5.7 Hz, ArCH<u>H</u>), 3.46 (dd, 1H, $^2J_{HH}$ = 11.3 Hz, $^3J_{HH}$ = 6.5 Hz C<u>H</u>HOH), 3.59 (dd, 1H, $^2J_{HH}$ = 11.4 Hz, $^3J_{HH}$ = 2.1 Hz, CH<u>H</u>OH), 3.82 (s, 3H, OCH_3), 3.92-3.93 (m,

‡ Synthesis of the racemic mixture was reported in reference 217, however no physical or spectral data was given. ^{1}H NMR of (2*R*)-**259b** reported in reference 218.

1H, CHOH), 6.86 (d, 1H, *J* = 8.2 Hz, ArH6), 6.91 (t, 1H, *J* = 7.4 Hz, ArH4), 7.15 (d, 1H, *J* = 7.3 Hz, ArH5), 7.21 (t, 1H, *J* = 7.8 Hz, ArH3); ^{13}C NMR (125 MHz) δ 34.4 ($ArCH_2$), 55.3 (OCH_3), 66.0 (CH_2OH), 72.2 (CHOH), 110.4 (ArC6), 120.8 (ArC4), 126.1 (ArC2), 127.9 (ArC3), 131.3 (ArC5), 157.4 (ArC1); MS (ES, +ve) *m/z* 200 (35, $M+NH_4$), 183 (30, M+H); HRMS (ES, +ve) calcd for $C_{10}H_{14}O_3Na$ 205.0841, found 205.0826.

(2*R*)-3-(2-Methoxyphenyl)-1,2-propandiol 259b[217,218]

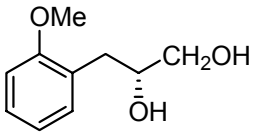

The diol (*R*)-**259b** was prepared by *General Procedure B* using alkene **197** (85 mg, 0.574 mmol), AD mix β (804 mg), sodium sulfite (861 mg) and a 1:1 mixture of *t*BuOH and water (5.8 mL). The crude mixture was subjected to flash silica gel column chromatography (0.5% to 1% EtOAc:hexanes) to afford the diol (*R*)-**259b** (103 mg, 98%) as a white solid, which had identical spectroscopic properties to the diol (*R*)-**259a**. $[\alpha]_D^{23}$ = +5.9° (*c* 0.053, $CHCl_3$).

2-((2*S*)-2,3-dihydroxypropyl)phenyl acetate 260a

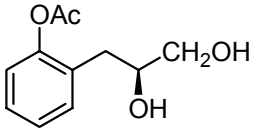

The diol (*S*)-**260a** was prepared by *General Procedure B* using alkene **194** (202 mg, 1.146 mmol), AD mix α (1.590 g), sodium sulfite (1.704 g) and a 1:1 mixture of *t*BuOH and water (11.4 mL). The crude oil was subjected to flash silica gel column chromatography (20% to 30% EtOAc:hexanes) to afford the chiral diol (*S*)-**260a** (18 mg, 7%) as a colourless oil. ^{1}H NMR (500 MHz) δ 2.10 (s, 3H, OCH_3), 2.85 (dd, 1H, $^2J_{HH}$ = 14.7 Hz, $^3J_{HH}$ = 7.1 Hz ArCHH), 2.91 (dd, 1H, $^2J_{HH}$ = 14.7 Hz, $^3J_{HH}$ = 2.9 Hz, ArCHH), 3.38 (bs, 1H, OH), 3.98 (dd, 1H, $^2J_{HH}$ = 12.2 Hz, $^3J_{HH}$ = 8.4 Hz, CHHOH), 4.19-4.24 (m, 2H, CHHOH and CHOH), 6.85 (t, 1H, *J* = 7.4 Hz, ArH4), 6.91 (d, 1H, *J* = 8.0 Hz, ArH6), 7.04 (d, 1H, *J* = 7.4 Hz, ArH3), 7.16 (t, 1H, *J* = 7.7, ArH5), 7.90 (bs, 1H, OH); ^{13}C NMR (125 MHz) δ 20.8 (CH_3), 35.5 ($ArCH_2$), 68.3 (CH_2OH), 72.0 (CHOH), 117.3 (ArC6), 120.6 (ArC4), 123.9 (ArC2), 128.7 (ArC5), 131.4 (ArC3), 155.4 (ArC1), 171.4 (C=O); FTIR *v* 3366 (br), 2972 (m), 1460 (w), 1379 (w), 1162 (w), 1129 (w), 951 (s), 817 (w); MS (ES, +ve) *m/z* 211 (100%, M+H).

2-((2*R*)-2,3-dihydroxypropyl)phenyl acetate 260b

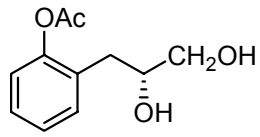

The diol (*R*)-**260b** was prepared by *General Procedure B* using alkene **194** (204 mg, 1.158 mmol), AD mix β (1.590 g), sodium sulfite (1.704 g) in a 1:1 mixture of *t*BuOH and water (11.4 mL). The crude oil was subjected to flash silica gel column chromatography (20% to 30% EtOAc:hexanes) to afford the chiral diol (*R*)-**260b** (23 mg, 9%) as a colourless oil, which had identical spectral properties to the diol (*S*)-**260a**.

7.9 Heterodimeric alkenes

<u>*E*-1-(2-Methoxyphenyl)-4-phenyl-2-butene 262</u>[241] **and 1-(2-Methoxyphenyl)-4-phenylbut-3-en-2-ol 264**

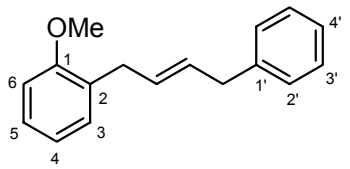

262

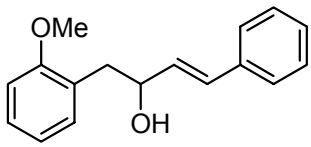

264

Grubbs 1 catalyst (40 mg, 0.047 mmol, 5 mol %) was added to a solution of 2-allylanisole **197** (140 mg, 0.95 mmol) and allylbenzene (1.145 g, 9.69 mmol) in DCM (10 mL) and the solution was heated at reflux for 21 h. The solvent was evaporated and the crude mixture was subjected to flash silica gel column chromatography (1% EtOAc:hexanes) yielding the homo-coupled allylbenzene dimer **170** (878 mg) and the cross-metathesis product **262** (67 mg, *E*:*Z* 1.4:1) as a colourless oil. Further elution gave a second portion of alkene **262** (145 mg, *E*:*Z* 4.2:1) to give a total yield of 94%.‡ ^{1}H NMR (300 MHz) δ 3.35-3.37 (m, 4H, 2 x CH_2), 3.49-3.54* (m, 2 x CH_2), 3.81 (s, 3H, OCH_3), 3.82* (s, OCH_3), 5.58-5.67 (m, 2H, *E* and *Z* C<u>H</u>=C<u>H</u>), 6.83-6.92 (m, 2H, ArH), 7.14-7.28 (m, 7H, ArH); ^{13}C NMR (75 MHz) δ 27.8* (MeOPh<u>C</u>H_2), 33.0 (MeOPh<u>C</u>H_2), 33.5* ($PhCH_2$), 39.0 ($PhCH_2$), 55.3 (OCH_3), 110.3 (ArC6), 120.4 (ArC4), 125.8 (ArC4'), 127.2 (ArC5), 128.3 (ArC3'), 128.5 (ArC2'), 129.2 (ArC2), 129.6 (ArC3), 129.9 (<u>C</u>H=<u>C</u>H), 141.0 (ArC1'), 157.2 (ArC1); MS (EI, +ve) *m/z* 238 (21, M^+), 207

‡ No physical or spectral data reported in reference 241.

(19), 147 (77), 130 (58), 121 (100%); HRMS (EI, +ve) calcd for $C_{17}H_{18}O$ 238.1358, found 238.1360.

The alkene **233** (145 mg) was stored in the freezer for 4 d. The sample had degraded and was subjected to column chromatography (20% EtOAc:hexanes) to give the major product alkenol **264** (95 mg) as a colourless oil. ^{1}H NMR (300 MHz) δ 3.07 (dd, 1H, *J* = 1.2, 2.1 Hz, CHHCH(OH)), 3.09 (dd, 1H, *J* = 1.4, 1.4 Hz, CHHCH(OH)), 3.89 (d, 3H, *J* = 1.5 Hz, OCH_3), 4.78 (dd, 1H, *J* = 6.5, 13.3 Hz, CH_2CH(OH)), 6.25 (ddd, 1H, $^4J_{HH}$ = 1.6 Hz, $^3J_{HH}$ = 7.5 Hz, $^3J_{HH}$ = 16.1 Hz, CH(OH)CH=CH), 6.62 (d, 1H, $^3J_{HH}$ = 16.0 Hz, CH=CHPh), 6.86-6.99 (m, 2H, ArH4 and ArH6), 7.16-7.39 (m, 7H, ArH3, 5, 2', 3' and 4'), 8.78 (bs, 1H, OH); ^{13}C NMR (75 MHz) δ 33.3 (CH_2CH(OH)), 55.7 (OCH_3), 86.0 (CH_2CH(OH)), 110.6 (ArC6), 120.9 (ArC4), 125.5 (ArC2), 126.6 (ArC2'), 127.3 (CH=CHPh), 127.9 (ArC5 or ArC4'), 128.0 (ArC5 or ArC4'), 128.5 (ArC3'), 131.6 (ArC3), 133.6 (CH=CHPh), 136.3 (ArC1'), 157.5 (ArC1); MS (EI, +ve) *m/z* 253 (8, M-H), 252 (11), 237 (8, M-OH), 202 (8), 179 (19), 163 (25), 131 (100%), 121 (100%).

(2*R*,3*R*)-1-(2-Methoxyphenyl)-4-phenylbutandiol 263b

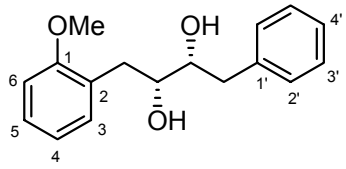

The diol (*R*,*R*)-**263b** was synthesised by *General Procedure A* using alkene **262** (77 mg, 0.324 mmol, *E*:*Z* 2.4:1), AD mix β (453 mg), methanesulfonamide (31 mg, 0.324 mmol), sodium sulfite (485 mg) in a 1:1 mixture of *t*BuOH and water (3.2 mL). The diol (*R*,*R*)-**263b** (77 mg, 90%) was purified using flash silica gel column chromatography (20% EtOAc:hexanes) as a white solid as a mixture of (*R*,*R*)/(*S*,*S*):(*R*,*S*)/(*S*,*R*) diastereomers (5.7:1). Recrystallisation from DCM/hexanes increased the ratio of diastereomers (10.5:1). HPLC analysis (20% 2-propanol:hexane, retention times (*R*,*R*)-diol **263b** 23.5 min (major), (*S*,*S*)-diol **263a** 29.0 min (minor)) showed the *ee* of the (*R*,*R*)-diol **263b** was 84%. ^{1}H NMR (300 MHz) δ 2.38 (d, 1H, *J* = 4.9 Hz, $PhCH_2CHOH$), 2.46 (d, 1H, *J* = 5.7 Hz, $MeOPhCH_2CHOH$), 2.89 (dd, 2H, *J* = 4.9, 6.7 Hz, $PhCH_2$), 2.92 (dd, 2H, *J* = 3.5, 6.9 Hz, $MeOPhCH_2$), 3.67-3.79 (m, 2H, CH(OH)CH(OH)), 3.82 (s, 3H, OCH_3), 6.86-6.94 (m, 2H, ArH4 and ArH6), 7.14-7.32 (m, 7H, ArH3, 5, 2', 3' and 4'); ^{13}C NMR (125 MHz) δ 35.2 ($MeOPhCH_2$), 40.0 ($PhCH_2$), 55.4 (OCH_3), 73.5 ($MeOPhCH_2CH$), 74.1 ($PhCH_2CH$), 110.6 (ArC6), 121.0

(ArC4), 126.3 (ArC5), 126.4 (ArC2), 128.0 (ArC4'), 128.4 (ArC2'), 129.4 (ArC3'), 131.4 (ArC3), 138.6 (ArC1'), 157.4 (ArC1); MS (ES +ve) *m/z* 273 (100%, M+H), 255 (60, M-OH), 237 (45); HRMS (ES, +ve) calcd for $C_{17}H_{21}O_3$ 273.1491, found 273.1497.

(2*S*,3*S*)-1-(2-Methoxyphenyl)-4-phenylbutandiol 263a

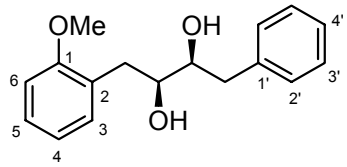

The diol (*S*,*S*)-**263a** was synthesised by *General Procedure A* using alkene **262** (50 mg, 0.210 mmol, *E*:*Z* 1.4:1), AD mix α (294 mg), methanesulfonamide (20 mg, 0.210 mmol), sodium sulfite (315 mg) in a 1:1 mixture of *t*BuOH and water (2.1 mL). The diol (*S*,*S*)-**263a** (56 mg, 98%) was purified using flash silica gel column chromatography (20% EtOAc:hexanes) as a white solid as a mixture of (*S*,*S*)/(*R*,*R*):(*S*,*R*)/(*R*,*S*) diastereomers (1.6:1). Further purification via flash silica gel column chromatography (10% to 20% EtOAc:hexanes) isolated the diol (*S*,*S*)-**263a** (10 mg, 18%) as a white solid, m.p. 58 ^{o}C. The diol had identical spectral properties to the (*R*,*R*)-**263b** diol. HPLC analysis (20% 2-propanol:hexane, retention times (*R*,*R*)-diol **263b** 23.9 min (minor), (*S*,*S*)-diol **263a** 29.0 min (major)) showed the *ee* of the (*S*,*S*)-diol **263a** was 84%.

CHAPTER 8
References

1. Bringmann, G.; Mortimer, A. J. P.; Keller, P. A.; Gresser, M. J.; Garner, J.; Breuning, M. *Angew. Chem. Int. Ed.* **2005**, *44*, 5384-5427.

2. Crepy, K. V. L.; Imamoto, T. *Adv. Synth. Cat.* **2003**, *345*, 79-101.

3. Kolb, H. C.; VanNieuwenhze, M. S.; Sharpless, K. B. *Chem. Rev.* **1994**, *94*, 2483-2547.

4. Sawamura, M.; Ito, Y. *Chem. Rev.* **1992**, *92*, 857-871.

5. Bolm, C.; Hildebrand, J. P.; Muniz, K.; Hermanns, N. *Angew. Chem. Int. Ed.* **2001**, *40*, 3285-3308.

6. Bringmann, G.; Walter, R.; Weirich, R. *Angew. Chem. Int. Ed.* **1990**, *29*, 977-991.

7. Yin, J. J.; Buchwald, S. L. *J. Am. Chem. Soc.* **2000**, *122*, 12051-12052.

8. Oki, M. In *Topics in Stereochemistry*; Allinger, N. L.;Eliel, E. L.;Wilen, S. H., Eds.; Wiley Interscience: New York, **1983**; *14*, 1-76.

9. Clayden, J. *Angew. Chem. Int. Ed.* **1997**, *36*, 949-951.

10. Charlton, J. L.; Oleschuk, C. J.; Chee, G.-L. *J. Org. Chem.* **1996**, *61*, 3452-3457.

11. Kuhn, R. In *Stereochemie*; Freudenberg, K., Ed.; Franz Deuticke: Leipzig, **1933**, 803-824.

12. Bott, G.; Field, L. D.; Sternhell, S. *J. Am. Chem. Soc.* **1980**, *102*, 5618-5626.

13. Baker, R. W.; Brkic, Z.; Sargent, M. V.; Skelton, B. W.; White, A. H. *Aust. J. Chem.* **2000**, *53*, 925-938.

14. Meyers, A. I.; Himmelsbach, R. J. *J. Am. Chem. Soc.* **1985**, *107*, 682-685.

15. Cooke, A. S.; Harris, M. M. *J. Chem. Soc.* **1963**, 2365-2373.

16. Wolf, C.; Koenig, W. A.; Roussel, C. *Liebigs Ann.* **1995**, 781-786.

17. Miura, K.; Inagaki, T.; Nakatani, N. *Chem. Pharm. Bull.* **1989**, *37*, 1816-1819.

18. Colter, A. K.; Clemens, L. M. *J. Phys. Chem.* **1964**, *68*, 651-654.

19. Fleischhauer, J.; Koslowski, A.; Kramer, B.; Zobel, E.; Bringmann, G.; Gulden, K. P.; Ortmann, T.; Peter, B. *Z. Naturforsch. B* **1993**, *48*, 140-148.

20. Meca, L.; Reha, D.; Havlas, Z. *J. Org. Chem.* **2003**, *68*, 5677-5680.

21. Bringmann, G.; Gunther, C.; Ochse, M.; Schupp, O.; Tasler, S. In *Progress in the Chemistry of Organic Natural Products*; Herz, W.;Falk, H.;Kirby, G. W.;Moore, R. E., Eds.; Springer: Vienna, **2001**; *82*, 1-249.

22. Bringmann, G.; Menche, D. *Acc. Chem. Res.* **2001**, *34*, 615-624.

23. Bringmann, G.; Tasler, S. *Tetrahedron* **2001**, *57*, 331-343.

24. Hubbard, B. K.; Walsh, C. T. *Angew. Chem. Int. Ed.* **2003**, *42*, 730-765.

25. Williams, D. H.; Bardsley, B. *Angew. Chem. Int. Ed.* **1999**, *38*, 1173-1193.

26. Nicolaou, K. C.; Boddy, C. N. C.; Brase, S.; Winssinger, N. *Angew. Chem. Int. Ed.* **1999**, *38*, 2097-2152.

27. Fukuyama, Y.; Asakawa, Y. *J. Chem. Soc., Perkin Trans. 1* **1991**, 2737-2741.

28. Manfredi, K. P.; Blunt, J. W.; Cardellina, J. H., 2nd; McMahon, J. B.; Pannell, L. L.; Cragg, G. M.; Boyd, M. R. *J. Med. Chem.* **1991**, *34*, 3402-3405.

29. Bringmann, G.; Pokorny, F. In *The Alkaloids*; Cordell, G. A., Ed.; Academic Press: San Diego, **1995**; *46*, 127-271.

30. Boyd, M. R.; Hallock, Y. F.; Cardellina, J. H., II; Manfredi, K. P.; Blunt, J. W.; McMahon, J. B.; Buckheit, R. W., Jr.; Bringmann, G.; Schaeffer, M.; et al. *J. Med. Chem.* **1994**, *37*, 1740-1745.

31. McCarthy, M.; Guiry, P. J. *Tetrahedron* **2001**, *57*, 3809-3844.

32. Rosini, C.; Franzini, L.; Raffaelli, A.; Salvadori, P. *Synthesis* **1992**, 503-517.

33. Noyori, R. *Acta Chem. Scand.* **1996**, *50*, 380-390.

34. Noyori, R.; Takaya, H. *Acc. Chem. Res.* **1990**, *23*, 345-350.

35. Miyashita, A.; Yasuda, A.; Takaya, H.; Toriumi, K.; Ito, T.; Souchi, T.; Noyori, R. *J. Am. Chem. Soc.* **1980**, *102*, 7932-7934.

36. Sasaki, H.; Irie, R.; Hamada, T.; Suzuki, K.; Katsuki, T. *Tetrahedron* **1994**, *50*, 11827-11838.

37. Khanbabaee, K. *Nachr. Chem.* **2003**, *51*, 163-166.

38. Bringmann, G.; Menche, D. *Acc. Chem. Res.* **2001**, *34*, 615-624.

39. Bringmann, G.; Tasler, S.; Pfeifer, R.-M.; Breuning, M. *J. Organomet. Chem.* **2002**, *661*, 49-65.

40. Bringmann, G.; Breuning, M.; Pfeifer, R.-M.; Schenk, W. A.; Kamikawa, K.; Uemura, M. *J. Organomet. Chem.* **2002**, *661*, 31-47.

41. Bringmann, G.; Tasler, S. In *Current Trends in Organic Synthesis*; Scolastico, C.;Nicotra, F., Eds.; Plenum Publishing Corporation: New York, **1999**, 105-116.

42. Bringmann, G.; Breuning, M.; Tasler, S. *Synthesis* **1999**, 525-558.

43. Lloyd-Williams, P.; Giralt, E. *Chem. Soc. Rev.* **2001**, *30*, 145-157.

44. Hassan, J.; Sevignon, M.; Gozzi, C.; Schulz, E.; Lemaire, M. *Chem. Rev.* **2002**, *102*, 1359-1469.

45. Kamikawa, K.; Uemura, M. *Synlett* **2000**, 938-949.

46. Shibata, T.; Fujimoto, T.; Yokota, K.; Takagi, K. *J. Am. Chem. Soc.* **2004**, *126*, 8382-8383.

47. Gutnov, A.; Heller, B.; Fischer, C.; Drexler, H.-J.; Spannenberg, A.; Sundermann, B.; Sundermann, C. *Angew. Chem. Int. Ed.* **2004**, *43*, 3795-3797.

48. Nishii, Y.; Wakasugi, K.; Koga, K.; Tanabe, Y. *J. Am. Chem. Soc.* **2004**, *126*, 5358-5359.

49. Anderson, J. C.; Cran, J. W.; King, N. P. *Tetrahedron Lett.* **2003**, *44*, 7771-7774.

50. Hattori, T.; Date, M.; Sakurai, K.; Morohashi, N.; Kosugi, H.; Miyano, S. *Tetrahedron Lett.* **2001**, *42*, 8035-8038.

51. Vorogushin, A. V.; Wulff, W. D.; Hansen, H.-J. *J. Am. Chem. Soc.* **2002**, *124*, 6512-6513.

52. Wanjohi, J. M.; Yenesew, A.; Midiwo, J. O.; Heydenreich, M.; Peter, M. G.; Dreyer, M.; Reichert, M.; Bringmann, G. *Tetrahedron* **2005**, *61*, 2667-2674.

53. Bao, J.; Wulff, W. D.; Fumo, M. J.; Grant, E. B.; Heller, D. P.; Whitcomb, M. C.; Yeung, S.-M. *J. Am. Chem. Soc.* **1996**, *118*, 2166-2181.

54. Hayashi, T.; Niizuma, S.; Kamikawa, T.; Suzuki, N.; Uozumi, Y. *J. Am. Chem. Soc.* **1995**, *117*, 9101-9102.

55. Kamikawa, T.; Uozumi, Y.; Hayashi, T. *Tetrahedron Lett.* **1996**, *37*, 3161-3164.

56. Kamikawa, T.; Hayashi, T. *Tetrahedron* **1999**, *55*, 3455-3466.

57. Capozzi, G.; Ciampi, C.; Delogu, G.; Menichetti, S.; Nativi, C. *J. Org. Chem.* **2001**, *66*, 8787-8792.

58. Imai, Y.; Zhang, W.; Kida, T.; Nakatsuji, Y.; Ikeda, I. *J. Org. Chem.* **2000**, *65*, 3326-3333.

59. Imai, Y.; Zhang, W.; Kida, T.; Nakatsuji, Y.; Ikeda, I. *Tetrahedron Lett.* **1997**, *38*, 2681-2684.

60. Mikami, K.; Aikawa, K.; Yusa, Y.; Jodry, J. J.; Yamanaka, M. *Synlett* **2002**, 1561-1578.

61. Mikami, K.; Yamanaka, M. *Chem. Rev.* **2003**, *103*, 3369-3400.

62. Mikami, K.; Korenaga, T.; Terada, M.; Ohkuma, T.; Pham, T.; Noyori, R. *Angew. Chem. Int. Ed.* **1999**, *38*, 495-497.

63. Korenaga, T.; Aikawa, K.; Terada, M.; Kawauchi, S.; Mikami, K. *Adv. Synth. Catal.* **2001**, *343*, 284-288.

64. Bringmann, G.; Hartung, T. *Liebigs Ann. Chem.* **1994**, 313-316.

65. Bringmann, G.; Breuning, M.; Henschel, P.; Hinrichs, J. *Org. Synth.* **2003**, *79*, 72-83.

66. Bringmann, G.; Hinrichs, J.; Pabst, T.; Henschel, P.; Peters, K.; Peters, E.-M. *Synthesis* **2001**, 155-167.

67. Bringmann, G.; Pabst, T.; Henschel, P.; Kraus, J.; Peters, K.; Peters, E.-M.; Rycroft, D. S.; Connolly, J. D. *J. Am. Chem. Soc.* **2000**, *122*, 9127-9133.

68. Bringmann, G.; Menche, D. *Angew. Chem. Int. Ed.* **2001**, *40*, 1687-1690.

69. Bringmann, G.; Ochse, M. *Synlett* **1998**, 1294-1296.

70. Bringmann, G.; Holenz, J.; Weirich, R.; Rubenacker, M.; Funke, C.; Boyd, M. R.; Gulakowski, R. J.; Francois, G. *Tetrahedron* **1998**, *54*, 497-512.

71. Bringmann, G.; Menche, D.; Muhlbacher, J.; Reichert, M.; Saito, N.; Pfeiffer, S. S.; Lipshutz, B. H. *Org. Lett.* **2002**, *4*, 2833-2836.

72. Molander, G. A.; George, K. M.; Monovich, L. G. *J. Org. Chem.* **2003**, *68*, 9533-9540.

73. Abe, H.; Takeda, S.; Fujita, T.; Nishioka, K.; Takeuchi, Y.; Harayama, T. *Tetrahedron Lett.* **2004**, *45*, 2327-2329.

74. Bringmann, G.; Breuning, M.; Tasler, S.; Endress, H.; Ewers, C. L. J.; Gobel, L.; Peters, K.; Peters, E.-M. *Chem. Eur. J.* **1999**, *5*, 3029-3038.

75. Bringmann, G.; Breuning, M.; Walter, R.; Wuzik, A.; Peters, K.; Peters, E.-M. *Eur. J. Org. Chem.* **1999**, 3047-3055.

76. Miyano, S.; Tobita, M.; Hashimoto, H. *Bull. Chem. Soc. Jpn.* **1981**, *54*, 3522-3526.

77. Miyano, S.; Handa, S.; Shimizu, K.; Tagami, K.; Hashimoto, H. *Bull. Chem. Soc. Jpn.* **1984**, *57*, 1943-1947.

78. Miyano, S.; Fukushima, H.; Handa, S.; Ito, H.; Hashimoto, H. *Bull. Chem. Soc. Jpn.* **1988**, *61*, 3249-3254.

79. Lipshutz, B. H.; Siegmann, K.; Garcia, E.; Kayser, F. *J. Am. Chem. Soc.* **1993**, *115*, 9276-9282.

80. Lipshutz, B. H.; Kayser, F.; Liu, Z.-P. *Angew. Chem. Int. Ed.* **1994**, *33*, 1842-1844.

81. Kyasnoor, R. V.; Sargent, M. V. *Chem. Commun.* **1998**, 2713-2714.

82. Sugimura, T.; Yamada, H.; Inoue, S.; Tai, A. *Tetrahedron: Asymmetry* **1997**, *8*, 649-655.

83. Meyers, A. I.; Nelson, T. D.; Moorlag, H.; Rawson, D. J.; Meier, A. *Tetrahedron* **2004**, *60*, 4459-4473.

84. Meyers, A. I. *J. Heterocycl. Chem.* **1998**, *35*, 991-1002.

85. Wilson, J. M.; Cram, D. J. *J. Am. Chem. Soc.* **1982**, *104*, 881-884.

86. Wilson, J. M.; Cram, D. J. *J. Org. Chem.* **1984**, *49*, 4930-4943.

87. Suzuki, T.; Hotta, H.; Hattori, T.; Miyano, S. *Chem. Lett.* **1990**, 807-810.

88. Hattori, T.; Koike, N.; Miyano, S. *J. Chem. Soc., Perkin Trans. 1* **1994**, 2273-2282.

89. Baker, R. W.; Pocock, G. R.; Sargent, M. V.; Twiss, E. *Tetrahedron: Asymmetry* **1993**, *4*, 2423-2426.

90. Baker, R. W.; Sargent, M. V. *Pure Appl. Chem.* **1994**, *66*, 2143-2150.

91. Baker, R. W.; Hockless, D. C. R.; Pocock, G. R.; Sargent, M. V.; Skelton, B. W.; Sobolev, A. N.; Twiss, E.; white, A. H. *J. Chem. Soc., Perkin Trans. 1* **1995**, 2615-2629.

92. Meyers, A. I.; Meier, A.; Rawson, D. J. *Tetrahedron Lett.* **1992**, *33*, 853-856.

93. Moorlag, H.; Meyers, A. I. *Tetrahedron Lett.* **1993**, *34*, 6989-6992.

94. Moorlag, H.; Meyers, A. I. *Tetrahedron Lett.* **1993**, *34*, 6993-6996.

95. Meyers, A. I.; Flisak, J. R.; Aitken, R. A. *J. Am. Chem. Soc.* **1987**, *109*, 5446-5452.

96. Warshawsky, A. M.; Meyers, A. I. *J. Am. Chem. Soc.* **1990**, *112*, 8090-8099.

97. Uemura, M.; Kamikawa, K. *J. Chem. Soc., Chem. Comm.* **1994**, 2697-2698.

98. Kamikawa, K.; Watanabe, T.; Uemura, M. *J. Org. Chem.* **1996**, *61*, 1375-1384.

99. Kamikawa, K.; Uemura, M. *Tetrahedron Lett.* **1996**, *37*, 6359-6362.

100. Hattori, T.; Hotta, H.; Suzuki, T.; Miyano, S. *Bull. Chem. Soc. Jpn.* **1993**, *66*, 613-622.

101. Uemura, M.; Nishimura, H.; Kamikawa, K.; Nakayama, K.; Hayashi, Y. *Tetrahedron Lett.* **1994**, *35*, 1909-1912.

102. Watanabe, T.; Kamikawa, K.; Uemura, M. *Tetrahedron Lett.* **1995**, *36*, 6695-6698.

103. Kamikawa, K.; Watanabe, T.; Uemura, M. *Synlett* **1995**, 1040-1042.

104. Tanaka, Y.; Sakamoto, T.; Kamikawa, K.; Uemura, M. *Synlett* **2003**, 519-521.

105. Kamikawa, K.; Sakamoto, T.; Tanaka, Y.; Uemura, M. *J. Org. Chem.* **2003**, *68*, 9356-9363.

106. Kamikawa, K.; Sakamoto, T.; Uemura, M. *Synlett* **2003**, 516-518.

107. Watanabe, T.; Shakadou, M.; Uemura, M. *Inorg. Chim. Acta* **1999**, *296*, 80-85.

108. Kamikawa, K.; Watanabe, T.; Daimon, A.; Uemura, M. *Tetrahedron* **2000**, *56*, 2325-2337.

109. Bromley, L. A.; Davies, S. G.; Goodfellow, C. L. *Tetrahedron: Asymmetry* **1991**, *2*, 139-156.

110. Li, X.; Yang, J.; Kozlowski, M. C. *Org. Lett.* **2001**, *3*, 1137-1140.

111. Li, X.; Hewgley, J. B.; Mulrooney, C. A.; Yang, J.; Kozlowski, M. C. *J. Org. Chem.* **2003**, *68*, 5500-5511.

112. Kozlowski, M. C.; Li, X.; Carroll, P. J.; Xu, Z. *Organomet.* **2002**, *21*, 4513-4522.

113. Nakajima, M.; Kanayama, K.; Miyoshi, I.; Hashimoto, S.-i. *Tetrahedron Lett.* **1995**, *36*, 9519-9520.

114. Nakajima, M.; Miyoshi, I.; Kanayama, K.; Hashimoto, S.-i.; Noji, M.; Koga, K. *J. Org. Chem.* **1999**, *64*, 2264-2271.

115. Irie, R.; Masutani, K.; Katsuki, T. *Synlett* **2000**, 1433-1436.

116. Luo, Z.; Liu, Q.; Gong, L.; Cui, X.; Mi, A.; Jiang, Y. *Angew. Chem. Int. Ed.* **2002**, *41*, 4532-4535.

117. Luo, Z.; Liu, Q.; Gong, L.; Cui, X.; Mi, A.; Jiang, Y. *Chem. Commun.* **2002**, 914-915.

118. Chu, C.-Y.; Uang, B.-J. *Tetrahedron: Asymmetry* **2003**, *14*, 53-55.

119. Barhate, N. B.; Chen, C.-T. *Org. Lett.* **2002**, *4*, 2529-2532.

120. Chu, C.-Y.; Hwang, D.-R.; Wang, S.-K.; Uang, B.-J. *Chem. Commun.* **2001**, 980-981.

121. Hon, S.-W.; Li, C.-H.; Kuo, J.-H.; Barhate, N. B.; Liu, Y.-H.; Wang, Y.; Chen, C.-T. *Org. Lett.* **2001**, *3*, 869-872.

122. Tamao, K.; Minato, A.; Miyake, N.; Matsuda, T.; Kiso, Y.; Kumada, M. *Chem. Lett.* **1975**, 133-136.

123. Tamao, K.; Yamamoto, H.; Matsumoto, H.; Miyake, N.; Hayashi, T.; Kumada, M. *Tetrahedron Lett.* **1977**, 1389-1392.

124. Hayashi, T. *J. Organomet. Chem.* **2002**, *653*, 41-45.

125. Hayashi, T.; Hayashizaki, K.; Kiyoi, T.; Ito, Y. *J. Am. Chem. Soc.* **1988**, *110*, 8153-8156.

126. Suzuki, A. *J. Organomet. Chem.* **1999**, *576*, 147-168.

127. Anastasia, L.; Negishi, E.-i. In *Handbook of Organopalladium Chemistry for Organic Synthesis*; Negishi, E.-i.;de Meijere, A., Eds.; Wiley: New York, **2002**; *1*, 311-334.

128. Miyaura, N.; Yanagi, T.; Suzuki, A. *Synth. Commun.* **1981**, *11*, 513-519.

129. Walker, S. D.; Barder, T. E.; Martinelli, J. R.; Buchwald, S. L. *Angew. Chem. Int. Ed.* **2004**, *43*, 1871-1876.

130. Barder, T. E.; Buchwald, S. L. *Org. Lett.* **2004**, *6*, 2649-2652.

131. Yin, J.; Rainka, M. P.; Zhang, X.-X.; Buchwald, S. L. *J. Am. Chem. Soc.* **2002**, *124*, 1162-1163.

132. Wolfe, J. P.; Buchwald, S. L. *Angew. Chem. Int. Ed.* **1999**, *38*, 2413-2416.

133. Wolfe, J. P.; Singer, R. A.; Yang, B. H.; Buchwald, S. L. *J. Am. Chem. Soc.* **1999**, *121*, 9550-9561.

134. Jutand, A.; Mosleh, A. *J. Org. Chem.* **1997**, *62*, 261-274.

135. Chaumeil, H.; Signorella, S.; Le Drian, C. *Tetrahedron* **2000**, *56*, 9655-9662.

136. Cammidge, A. N.; Crepy, K. V. L. *Chem. Commun.* **2000**, 1723-1724.

137. Cammidge, A. N.; Crepy, K. V. L. *Tetrahedron* **2004**, *60*, 4377-4386.

138. Jensen, J. F.; Johannsen, M. *Org. Lett.* **2003**, *5*, 3025-3028.

139. Yin, J.; Buchwald, S. L. *J. Am. Chem. Soc.* **2000**, *122*, 12051-12052.

140. Yin, J. J.; Rainka, M. P.; Zhang, X. X.; Buchwald, S. L. *J. Am. Chem. Soc.* **2002**, *124*, 1162-1163.

141. Alexakis, A.; Tomassini, A.; Chouillet, C.; Roland, S.; Mangeney, P.; Bernardinelli, G. *Angew. Chem. Int. Ed.* **2000**, *39*, 4093-4095.

142. Denmark, S. E.; Fu, J.; Lawler, M. J.; Lee, S.; Huntsman, E.; Grabowski, E. J. J. *Org. Synth.* **2006**, *83*, 121-130.

143. Bennani, Y. L.; Hanessian, S. *Chem. Rev.* **1997**, *97*, 3161-3195.

144. Lucet, D.; Le Gall, T.; Mioskowski, C. *Angew. Chem. Int. Ed.* **1998**, *37*, 2580-2627.

145. Wu, J.; Chan, A. S. C. *Acc. Chem. Res.* **2006**, *39*, 711-720.

146. Figge, A.; Altenbach, H. J.; Brauer, D. J.; Tielmann, P. *Tetrahedron: Asymmetry* **2002**, *13*, 137-144.

147. McCarthy, M.; Goddard, R.; Guiry, P. J. *Tetrahedron: Asymmetry* **1999**, *10*, 2797-2807.

148. Buchwald, S. L.; Fox, J. M. *The Strem Chemiker*, **2000**.

149. Bringmann, G.; Gotz, R.; Keller, P. A.; Walter, R.; Boyd, M. R.; Lang, F. R.; Garcia, A.; Walsh, J. J.; Tellitu, I.; Bhaskar, K. V.; Kelly, T. R. *J. Org. Chem.* **1998**, *63*, 1090-1097.

150. Cammidge, A. N.; Crepy, K. V. L. *Chem. Commun.* **2000**, 1723-1724.

151. Alcock, N. W.; Brown, J. M.; Perez-Torrente, J. J. *Tetrahedron Lett.* **1992**, *33*, 389-392.

152. Glaser, R. *Chirality* **1993**, *5*, 272-276.

153. Noe, M. C.; Letavic, M. A.; Snow, S. L. *Org. React.* **2005**, *66*, 109-625.

154. Hirama, M.; Oishi, T.; Ito, S. *J. Chem. Soc., Chem. Commun.* **1989**, 665-666.

155. Oishi, T.; Hirama, M. *J. Org. Chem.* **1989**, *54*, 5834-5835.

156. Oishi, T.; Hirama, M.; Sita, L. R.; Masamune, S. *Synthesis* **1991**, 789-792.

157. Denmark, S. E.; Fu, J.; Lawler, M. J. *J. Org. Chem.* **2006**, *71*, 1523-1536.

158. Denmark, S. E.; Fu, J. P. *J. Am. Chem. Soc.* **2001**, *123*, 9488-9489.

159. Li, S.; Dieter, R. K. *J. Org. Chem.* **2003**, *68*, 969-973.

160. Dieter, R. K.; Li, S.; Chen, N. *J. Org. Chem.* **2004**, *69*, 2867-2870.

161. Neumann, W. L.; Rogic, M. M.; Dunn, T. J. *Tetrahedron Lett.* **1991**, *32*, 5865-5868.

162. Alvaro, G.; Grepioni, F.; Savoia, D. *J. Org. Chem.* **1997**, *62*, 4180-4182.

163. Tom Dieck, H.; Dietrich, J. *Chem. Ber.* **1984**, *117*, 694-701.

164. Kotsuki, H.; Kuzume, H.; Gohda, T.; Fukuhara, M.; Ochi, M.; Oishi, T.; Hirama, M.; Shiro, M. *Tetrahedron: Asymmetry* **1995**, *6*, 2227-2236.

165. Kohra, S.; Hayashida, H.; Tominaga, Y.; Hosomi, A. *Tetrahedron Lett.* **1988**, *29*, 89-92.

166. Gresser, M. J. *Honours Thesis*, University of Wollongong, **2002**.

167. Naarmann, H.; Zdenek, J.; Viehe, H. G.; Beaujean, M.; Merenyi, R.; Application: DE; 79-2934131; **1981**; 10 pp.

168. Kwong, F. Y.; Buchwald, S. L. *Org. Lett.* **2003**, *5*, 793-796.

169. Zhang, H.; Cai, Q.; Ma, D. *J. Org. Chem.* **2005**, *70*, 5164-5173.

170. Blackwell, H. E.; O'Leary, D. J.; Chatterjee, A. K.; Washenfelder, R. A.; Bussmann, D. A.; Grubbs, R. H. *J. Am. Chem. Soc.* **2000**, *122*, 58-71.

171. Forman, G. S.; McConnell, A. E.; Tooze, R. P.; Van Rensburg, W. J.; Meyer, W. H.; Kirk, M. M.; Dwyer, C. L.; Serfontein, D. W. *Organomet.* **2005**, *24*, 4528-4542.

172. Chatterjee, A. K.; Choi, T.-L.; Sanders, D. P.; Grubbs, R. H. *J. Am. Chem. Soc.* **2003**, *125*, 11360-11370.

173. Breitmaier, E.; Voelter, W. *Carbon-13 NMR Spectroscopy, High Resolution Methods and Applications in Organic Chemistry and Biochemistry*; 3rd ed.; VCH: New York, **1987**.

174. Dominique, R.; Das, S. K.; Roy, R. *Chem. Commun.* **1998**, 2437-2438.

175. Pavia, D. L.; Lampman, G. M.; Kriz, G. S. *Introduction to Spectroscopy*; 2nd ed.; Saunders College Publishing: Orlando, Florida, **1996**.

176. Trnka, T. M.; Grubbs, R. H. *Acc. Chem. Res.* **2001**, *34*, 18-29.

177. Grubbs, R. H. *Tetrahedron* **2004**, *60*, 7117-7140.

178. Grubbs, R. H. *Handbook of Metathesis - Catalyst Development*; Wiley-VCH: Weinheim, **2003**; Vol. 1.

179. Crowe, W. E.; Zhang, Z. J. *J. Am. Chem. Soc.* **1993**, *115*, 10998-10999.

180. Cadot, C.; Dalko, P. I.; Cossy, J. *Tetrahedron Lett.* **2002**, *43*, 1839-1841.

181. Schroeder, M. *Chem. Rev.* **1980**, *80*, 187-213.

182. Kolb, H. C.; Sharpless, K. B. In *Transition Metals for Organic Synthesis (2nd Edition)*; Beller, M., Ed.; Wiley-VCH: Weinheim, **2004**; *2*, 275-298.

183. Clayden, J.; Greeves, N.; Warren, S.; Wothers, P. *Organic Chemistry*; Oxford University Press: New York, **2006**.

184. The same conditions applied to the formation of the 2,2'-bisindoline system produced <1% yield of the undesired 6,6'-fused heterocycle.

185. Wales, S. M. *Honours Thesis*, University of Wollongong, **2004**.

186. Huang, J.; Stevens, E. D.; Nolan, S. P.; Petersen, J. L. *J. Am. Chem. Soc.* **1999**, *121*, 2674-2678.

187. Scholl, M.; Trnka, T. M.; Morgan, J. P.; Grubbs, R. H. *Tetrahedron Lett.* **1999**, *40*, 2247-2250.

188. Fuerstner, A.; Thiel, O. R.; Ackermann, L.; Schanz, H.-J.; Nolan, S. P. *J. Org. Chem.* **2000**, *65*, 2204-2207.

189. Tang, M.; Pyne, S. G. *Tetrahedron* **2004**, *60*, 5759-5767.

190. Pitsinos, E. N.; Wascholowski, V.; Karaliota, S.; Rigou, C.; Couladouros, E. A.; Giannis, A. *ChemBioChem* **2003**, *4*, 1223-1225.

191. Andersson, P. G.; Johansson, F.; Tanner, D. *Tetrahedron* **1998**, *54*, 11549-11566.

192. Wales, S. M. *unpublished results*, University of Wollongong, **2006**.

193. Shah, S. T. A.; Khan, K. M.; Hussain, H.; Anwar, M. U.; Fecker, M.; Voelter, W. *Tetrahedron* **2005**, *61*, 6652-6656.

194. Phukan, P. *Tetrahedron Lett.* **2004**, *45*, 4785-4787.

195. Echavarren, A. M.; Stille, J. K. *J. Am. Chem. Soc.* **1987**, *109*, 5478-5486.

196. Ikawa, T.; Hattori, K.; Sajiki, H.; Hirota, K. *Tetrahedron* **2004**, *60*, 6901-6911.

197. Ueno, M.; Wheatley, A. E. H.; Kondo, Y. *Chem. Commun.* **2006**, 3549-3550.

198. Yip, K.-T.; Yang, M.; Law, K.-L.; Zhu, N.-Y.; Yang, D. *J. Am. Chem. Soc.* **2006**, *128*, 3130-3131.

199. Bender, C. F.; Widenhoefer, R. A. *Chem. Commun.* **2006**, 4143-4144.

200. Zabawa, T. P.; Kasi, D.; Chemler, S. R. *J. Am. Chem. Soc.* **2005**, *127*, 11250-11251.

201. Sherman, E. S.; Chemler, S. R.; Tan, T. B.; Gerlits, O. *Org. Lett.* **2004**, *6*, 1573-1575.

202. Cooper, M. A.; Francis, C. L.; Holman, J. W.; Kasum, B.; Taverner, T.; Tiekink, E. R. T.; Ward, A. D. *Aust. J. Chem.* **2000**, *53*, 123-129.

203. Knight, P. D.; Munslow, I.; O'Shaughnessy, P. N.; Scott, P. *Chem. Commun.* **2004**, 894-895.

204. Michael, F. E.; Cochran, B. M. *J. Am. Chem. Soc.* **2006**, *128*, 4246-4247.

205. Gajare, A. S.; Jensen, R. S.; Toyota, K.; Yoshifuji, M.; Ozawa, F. *Synlett* **2005**, 144-148.

206. Littke, A. F.; Schwarz, L.; Fu, G. C. *J. Am. Chem. Soc.* **2002**, *124*, 6343-6348.

207. Kayaki, Y.; Koda, T.; Ikariya, T. *Eur. J. Org. Chem.* **2004**, 4989-4993.

208. Newcomb, M.; Vieta, R. S. *J. Org. Chem.* **1980**, *45*, 4793-4795.

209. Sapountzis, I.; Dube, H.; Lewis, R.; Gommermann, N.; Knochel, P. *J. Org. Chem.* **2005**, *70*, 2445-2454.

210. Sapountzis, I.; Knochel, P. *Angew. Chem. Int. Ed.* **2002**, *41*, 1610-1611.

211. Knochel, P. In *Metal-Catalyzed Cross-Coupling Reactions*; Diederich, F.;Stang, P. J., Eds.; Wiley-VCH: Weinheim, **1998**, 387-419.

212. Dunn, M. J.; Jackson, R. F. W.; Pietruszka, J.; Wishart, N.; Ellis, D.; Wythes, M. J. *Synlett* **1993**, 499-500.

213. Sun, C.; Bittman, R. *J. Org. Chem.* **2006**, *71*, 2200-2202.

214. Boymond, L.; Rottlander, M.; Cahiez, G.; Knochel, P. *Angew. Chem. Int. Ed.* **1998**, *37*, 1701-1703.

215. Dragoli, D. R.; Burdett, M. T.; Ellman, J. A. *J. Am. Chem. Soc.* **2001**, *123*, 10127-10128.

216. Yan, B.; Spilling, C. D. *J. Org. Chem.* **2004**, *69*, 2859-2862.

217. Dalla, V.; Cotelle, P.; Catteau, J. P. *Tetrahedron Lett.* **1997**, *38*, 1577-1580.

218. Nishiyama, H.; Ohgaki, M.; Yamanishi, R.; Hara, T.; 93-JP286 9319053; **1993**; 118 pp.

219. Ashimori, A.; Bachand, B.; Overman, L. E.; Poon, D. J. *J. Am. Chem. Soc.* **1998**, *120*, 6477-6487.

220. Malaise, G.; Bonrath, W.; Breuninger, M.; Netscher, T. *Helv. Chim. Act.* **2006**, *89*, 797-812.

221. O'Leary, D. J.; Blackwell, H. E.; Washenfelder, R. A.; Grubbs, R. H. *Tetrahedron Lett.* **1998**, *39*, 7427-7430.

222. Corey, E. J.; Noe, M. C.; Ting, A. Y. *Tetrahedron Lett.* **1996**, *37*, 1735-1738.

223. Doak, G. O.; Freedman, L. D. *Synthesis* **1974**, 328-338.

224. Suzuki, T.; Oriyama, T. *Synlett* **2000**, 859-861.

225. Henningsen, M. C.; Jeropoulos, S.; Smith, E. H. *J. Org. Chem.* **1989**, *54*, 3015-3018.

226. Namiki, T.; Nishikawa, M.; Itoh, Y.; Uchida, I.; Hashimoto, M. *J. Antibiot.* **1987**, *40*, 1400-1407.

227. Vedrenne, E.; Dupont, H.; Oualef, S.; Elkaim, L.; Grimaud, L. *Synlett* **2005**, 670-672.

228. Hartley, J. P.; Pyne, S. G. *Synlett* **2004**, 2209-2211.

229. Okada, M.; Kitagawa, O.; Fujita, M.; Taguchi, T. *Tetrahedron* **1996**, *52*, 8135-8142.

230. Kawamura, K.; Ohta, T.; Otani, G. *Chem. Pharm. Bull.* **1990**, *38*, 2088-2091.

231. Ganton, M. D.; Kerr, M. A. *Org. Lett.* **2005**, *7*, 4777-4779.

232. De March, P.; Figueredo, M.; Font, J.; Medrano, J. *Tetrahedron* **1999**, *55*, 7907-7914.

233. Hurd, C. D.; Jenkins, W. W. *J. Org. Chem.* **1957**, *22*, 1418-1423.

234. Franz, J. A.; Barrows, R. D.; Camaioni, D. M. *J. Am. Chem. Soc.* **1984**, *106*, 3964-3967.

235. Chevalier, P.; Sinou, D.; Descotes, G. *Bull. Soc.Chim. Fr.* **1975**, 2254-2258.

236. Taylor, S. K.; Clark, D. L.; Heinz, K. J.; Schramm, S. B.; Westermann, C. D.; Barnell, K. K. *J. Org. Chem.* **1983**, *48*, 592-596.

237. Srogl, J.; Allred, G. D.; Liebeskind, L. S. *J. Am. Chem. Soc.* **1997**, *119*, 12376-12377.

238. Pelz, N. F.; Morken, J. P. *Org. Lett.* **2006**, *8*, 4557-4559.

239. Giger, T.; Wigger, M.; Audetat, S.; Benner, S. A. *Synlett* **1998**, 688-691.

240. Crotti, P.; Ferretti, M.; Macchia, F.; Stoppinoni, A. *J. Org. Chem.* **1986**, *51*, 2759-2766.

241. Yamaguchi, J.; Takagi, Y.; Nakayama, A.; Fujiwara, T.; Takeda, T. *Chem. Lett.* **1991**, 133-136.